

CCS2022-2024 WP1: The Thorning structure

Seismic data and interpretation to mature
potential geological storage of CO₂

Morten Bjerager, Tanni Abramovitz, Henrik Vosgerau,
Ulrik Gregersen, Florian W.H. Smit, Tomi A. Jusri, Anders Mathiesen,
Finn Mørk, Niels H. Schovsbo, Henrik I. Petersen,
Lars Henrik Nielsen, Bodil W. Lauridsen, Emma Sheldon,
Karen Dybkjær, Shahjahan Laghari,
Lasse M. Rasmussen & Marie Keiding

CCS2022-2024 WP1: The Thorning structure

Seismic data and interpretation to mature
potential geological storage of CO₂

Morten Bjerager, Tanni Abramovitz, Henrik Vosgerau, Ulrik Gregersen,
Florian W.H. Smit, Tomi A. Jusri, Anders Mathiesen, Finn Mørk,
Niels H. Schovsbo, Henrik I. Petersen, Lars Henrik Nielsen, Bodil W. Lauridsen,
Emma Sheldon, Karen Dybkjær, Shahjahan Laghari,
Lasse M. Rasmussen & Marie Keiding

Preface

A new Danish Climate Act was decided by the Danish Government and a large majority of the Danish Parliament on June 26th, 2020. It includes the aim of reducing the Danish greenhouse gas emissions with 70% by 2030 compared to the level of emissions in 1990. The first part of a new Danish CCS Strategy of June 30th, 2021 includes a decision to continue the initial investigations of sites for potential geological storage of CO₂ in Denmark. GEUS has therefore from 2022 commenced seismic acquisition and investigations of potential sites for geological storage of CO₂ in Denmark.

The structures decided for maturation by the authorities are some of the largest structures onshore Zealand, Jutland and Lolland and in the eastern North Sea (Fig. 1.1). The onshore structures include the Gassum, Havnsø, Rødby, and Thorning structures, and in addition the small Stenlille structure. The offshore structures include the Inez, Jammerbugt and Lisa structures. A GEUS Report is produced for the Stenlille, Havnsø, Rødby, Gassum, and the Jammerbugt structures to mature the structure as part of the CCS2022–2024 project towards potential geological storage of CO₂.

The intension with the project reporting for each structure is to provide a knowledge-based maturation with improved database and solid basic descriptions to improve the understanding of the formation, composition, and geometry of the structure. Each report includes a description overview and mapping of the reservoir and seal formations, the largest faults, the lowermost closure (spill-point) and structural top point of the reservoir, estimations of the overall closure area and gross-rock volume. In addition, the database will be updated, where needed with rescanning of some of the old seismic data, and acquisition of new seismic data in a grid over the structures, except for the Inez and Lisa structures.

The reports will provide an updated overview of the database, geology, and seismic interpretation for all with interests in the structures and will become public available. Each reporting is a first step toward geological maturation and site characterization of the structures. A full technical evaluation of the structures to cover all site characterization aspects related to CO₂ storage including risk assessment is recommended for the further process.

Contents

Preface	3
Dansk sammendrag	6
1. Summary	9
2. Introduction	16
3. Geological setting	17
4. Database	24
4.1 Seismic data	24
4.2 New seismic data acquired in this project	34
4.3 Reprocessed seismic data applied in this project	42
4.4 Well data	49
5. Methods	50
6. Results of seismic and well-tie interpretation	63
6.1 Stratigraphy of the structure	63
6.2 Structure description and tectonostratigraphic evolution	74
6.3 Summary of the structural evolution – The Thorning structure	108
7. Geology and parameters of the reservoirs and seals	109
7.1 Reservoirs – Summary of geology and parameters	115
7.2 Seals – Summary of geology and parameters	141
8. Discussion of storage and potential risks	161
8.1 Volumetrics and Storage Capacity	161
8.2 Volumetric input parameters	163
8.3 Storage efficiency	166
8.4 Summary of input factors	167
8.5 Storage capacity results	168
8.6 Potential risks	170

9.	Conclusions	174
10.	Recommendations for further work	176
11.	Acknowledgement – The new seismic data	178
12.	References	
	Appendix A	
	Appendix B	

Dansk sammendrag

Regeringen og et bredt flertal i Folketinget vedtog i juni 2021 en køreplan for lagring af CO₂, der inkluderer undersøgelser af potentielle lagringslokaliteter i den danske undergrund. Der er derfor udvalgt fire store strukturer på land med dataindsamling og kortlægning til videre modning: Gassum, Havnsø, Rødby og Thorning, samt den mindre Stenlille struktur (Fig. 1.1). Derudover indsamles nye data til kortlægning og modning for den kystnære Jammerbugt struktur.

Thorning strukturen er en stor struktur, der ligger i det centrale Midtjylland, mellem Viborg, Herning og Silkeborg. Tidligere og nye seismiske data viser strukturens form, og de nye seismiske data afslører desuden tilstedeværelsen af flere større forkastninger i den sydvestlige del af strukturen, samt et antal mindre forkastninger omkring toppen af strukturen. Thorning strukturen adskiller sig fra flere af de andre strukturer ved ikke at være gennemboret af dybe borer. Korrelation af de seismiske data til gennemborede geologiske data er derfor foretaget til omkringliggende borer i en afstand på 30–40 km fra Thorning strukturen for at belyse geologien af reservoir og segl.

Dette sammendrag opsummerer forundersøgelsen og den initiale vurdering af lagringsmuligheden i Thorning strukturen. Vurderingen bygger på tolkning af eksisterende samt nye geologiske og geofysiske data og viden (Kapitel 3–5) og belyser undergrundens geologiske opbygning i og omkring Thorning strukturen (Kapitel 6–7). Vurderingen har fokus på strukturens form, størrelse, overordnede opdeling inklusive reservoir- og seglforhold, geologiske risikofaktorer, især større forkastninger og segl, og der foretages en vurdering af statisk lagringskapacitet for det primære reservoir (Kapitel 8). Desuden opsummeres anbefalinger til yderligere modning af strukturen hen imod en mulig CO₂-lagring (Kapitel 9–10).

Datagrundlag

Thorning strukturen er dækket af ældre reflektionsseismiske data med 2D profiler af sparsom tæthed og kvalitet indsamlet i 1960'erne, 1970'erne og 1980'erne, 2010 samt et tættere netværk af nye reflektionsseismiske data indsamlet i 2023 for dette projekt (Fig. 4.1.1). De ældre datasæt er generelt af dårlig kvalitet med meget støj (Tabel 4.1). For at forbedre datakvaliteten blev der i august til oktober 2023 indsamlet otte nye 2D reflektionsseismiske profiler på i alt 133 km ved hjælp af vibroseis-lastbiler som seismisk kilde, og et dobbelt optagesystem bestående af en landstreamer med geofoner trukket bag lastbilerne og trådløse geofoner i vejsiden. Disse data har markant forbedret dækning og kvaliteten af data samt tolkningsmulighederne hen over strukturen og ned ad flankerne. Uppsala Universitet gennemførte indsamlingen og processeringen på vegne af GEUS, med vibroseis-lastbiler fra polske Geopartner Geofizyka og med feltassistance fra universitetsstuderende fra København, Århus og Uppsala universiteter. COWI varetog ansøgninger om tilladelser, logistik, dele af kommunikationen og den løbende borgerkontakt. Der blev i forbindelse med indsamlingen informeret på to informationsmøder for borgere, via projekt-webside, informationsbreve og flyers, samt på to besøgsdage.

Det nye 2D seismiske indsamling (GEUS2023-THORNING) har markant forbedret datagrundlaget over toppen og flankerne af Thorning strukturen, hvilket muliggør en væsentlig forbedret kortlægning af strukturens geometri, og særligt af forkastninger i toppen af reservoir og segl.

Tolkning

Thorning strukturen er en geologisk struktur, som er opstået som følge af dannelsen af en dybtliggende saltpude i det underliggende Zechstein salt. Saltpudens vækst nedefra, opløftede de overliggende lag, op gennem millioner af år i perioderne Trias, Jura, Kridt og Kænozoikum, hvorved der blev dannet en stor antiklinal i form af en tre-vejs-lukning, afgrænset mod sydvest af en forkastningszone. Det primære reservoir-segl-par i Thorning strukturen anses for at være Gassum-Fjerritslev formationerne (Kapitel 6, 7). Beskrivelser fra omkringliggende borer i området viser, at Gassum Formationen kan indeholde gode reservoirintervaller, og Fjerritslev Formationen forventes at indeholde gode seglintervaller. Derudover kan der være et sekundært, højereliggende reservoir-segl-par i Frederikshavn-Vedsted formationerne samt et dybereliggende reservoir-segl-par i form af Skagerrak Formationen og den overliggende Ørslev Formation. Der kan være et yderligere potentielt reservoir i strukturen i form af Tønder Formationen.

Strukturen lukker på flere stratigrafiske niveauer fra Trias til Jura. Særligt vigtigt er tre-vejs-lukningen på toppen af Gassum Formation (tidlig Jura alder), som er det primære reservoir. Gassum Formationen har en estimeret tykkelse på c. 100 m hen over Thorning strukturen baseret på seismisk tolkning forbundet til de omkringliggende borer og efterfølgende dybdekonvertering. Korrelation imellem de omkringliggende borer viser, at Gassum Formationen er lateralt udbredt over et stort område og består af vekslende lag af sandsten og lersten. Nettotykkelsen af potentielle gode reservoirsandsten varierer imellem 11–63 m i borerne Nøvling-1, Mejrup-1, Kvovls-1, Hobro-1, Gassum-1, Voldum-1 og Horsens-1. Der er ingen dybe borer beliggende i Thorning strukturen. Der er derfor regnet på tre scenarier baseret på to reference borer (Gassum-1 og Nøvling-1) og geologiske antagelser, som angiver sandsynlige nettotykkelser på gode reservoirsandsten mellem 20,5 og 35 m i Thorning strukturen. Et reservoir i Gassum Formationen defineres som en sandsten, der har et lerindhold <0,5% og porøsitet >10%. Estimerer på reservoir parametre i de tre scenarier angiver porøsiteter for reservoirsandsten på 25,6–28,8% og permeabiliteter på 1004–1531 mD. En middel lagringskapacitet på 125 Mt CO₂ er beregnet baseret på Scenarie 3 med antagelse af 35 m reservoir sand i hele Gassum Formationen.

Der er gennemført en opdateret tolkning af Thorning strukturen på baggrund af eksisterende data kombineret med de nye seismiske data (Kapitel 6). Der anvendes boringskorrelation og seismiske profiler for at identificere seismiske refleksioner og intervaller, der kan korreleres med de geologiske formationer. Tolkningen viser, at toppen af reservoiret, som er kortlagt ved Top Gassum Formationen i Thorning strukturen, er veldefineret med tre-vejs-lukning og et areal på 235 km² i 1950 m dybde under havniveau.

De nye seismiske data viser forskellige typer af forkastninger på reservoirniveauet af Top Gassum Formation henover og langs med Thorning strukturen. Mindre nord-syd gående ekstensionsforkastninger er kortlagt langs toppen af strukturen, og er givetvis dannet ved strækning af lagene forårsaget af bevægelserne i den dybe saltpude. Forkastningerne er identificeret på flere af de seismiske profiler og strækker sig fra Tønder Formationen op i Fjerritslev Formationen. De forskyder toppen af Gassum Formationen med 34–35 m. Et tilsvarende sæt forkastninger er kortlagt fra Top Fjerritslev Fm til den ovenliggende Kridt pakke (Chalk Group), med mindre forskydninger på op til 20 ms. Det sandsynliggøres af de to forkastningssystemer ikke er forbundet gennem det primære Fjerritslev Formation segl til Gassum Formationen, men dette anbefales undersøgt nærmere med tættere seismisk dækning.

Et markant forkastningssystem og mindre gravsænkning er kortlagt langs den sydvestlige flanke af Thorning strukturen. Gravsænknningen blev dannet i Trias med hovedpart af bevægelse i Tidlig Jura; gravsænknningen er lokal ca. 5 km bred og orienteret NNV–SSØ. Den nordøstlige hovedforkastning forskyder Gassum Formationen langs lukningen af Thorning strukturen, som dermed defineres af en tre-vejs-lukning. Seglintegriteten af denne forkastning bør undersøges nærmere i forhold til vurdering af forseglende egenskaber af forkastningen og den overliggende Fjerritslev Formation.

Samlet set observeres forkastninger i og omkring toppen af strukturen med betydelige forskydninger og laterale udstrækning i Gassum Formationen (primære reservoir) og Fjerritslev Formationen (primære segl). Det anbefales derfor, at der foretages en nærmere undersøgelse af forkastningerne i forbindelse med yderligere modning af strukturen. Grundet afstanden mellem de 2D seismiske profiler er det nuværende datagrundlag stadigvæk ikke tilstrækkeligt til en fyldestgørende undersøgelse af segl-integriteten og eventuel risiko for lækage af CO₂, samt hvorvidt nogle forkastninger kan danne barrierer i reservoiret (*compartments*) ifm. CO₂-lagring. En yderligere modning af strukturen bør derfor baseres på nye tætliggende seismiske (3D) data og yderligere geologiske og tekniske vurderinger.

1. Summary

The subsurface in Denmark has many deep structures offshore and onshore, and some of these are suited for CO₂ storage. Eight structures named in Fig. 1.1 were selected for initial investigation and maturation through seismic acquisition, geological analyses, and renewed mapping during 2022–2024 by GEUS, with cooperating partners on acquisition and processing (see chapter 4).

New 2D seismic data were acquired across the Thorning structure to improve the database with more dense, good quality seismic data. The improved seismic database is used in this report – together with ties to well logs from deep boreholes situated in the perimeter of 30–40 km from the Thorning structure – to improve the understanding of the structure in terms of its geological development, the lowermost closure (spill-point) and top point at the top of the reservoir, the overall closure area and potential static storage capacity, the largest faults, and details of reservoir and seal successions for this initial maturation. The new seismic data and grids in two-way time of key seismic horizons are available at the [GEUS CCS data webpage](#). There are no deep wells situated within the Thorning structure.

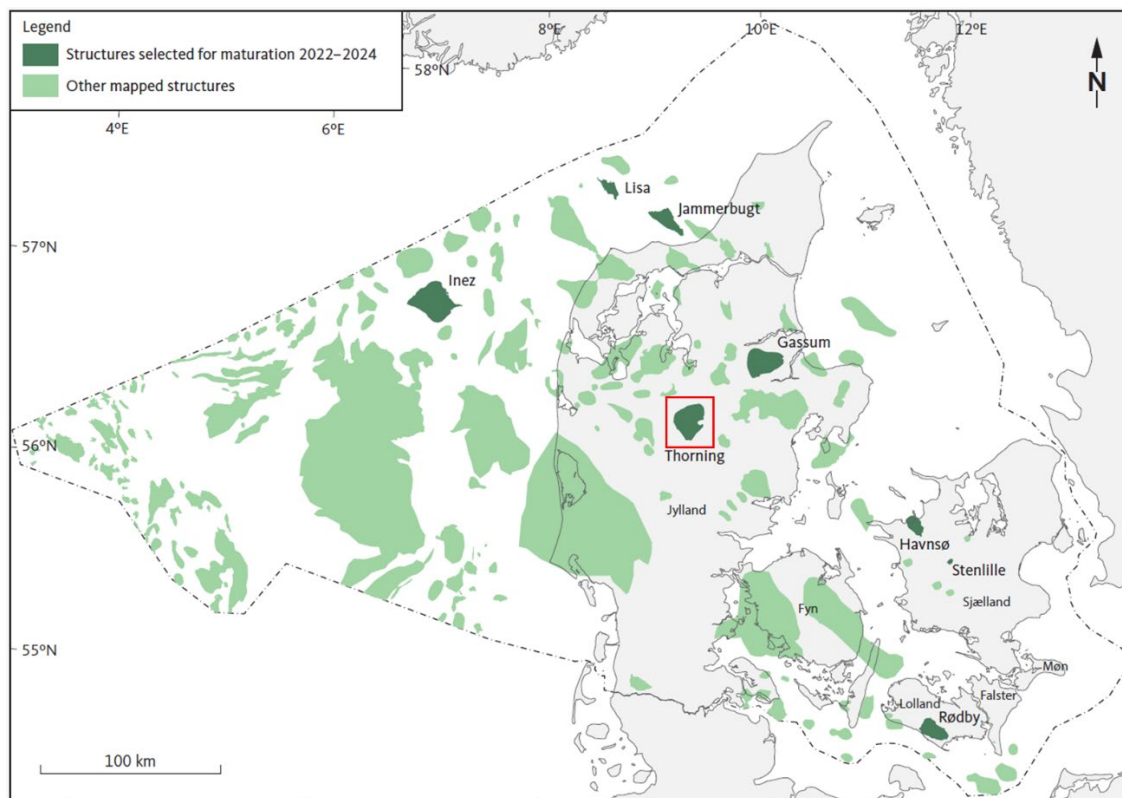


Figure 1.1. Map of Danish structures with potential for geological storage of CO₂. The named dark green structures (Gassum, Havnsø, Jammerbugt, Rødby, Stenlille and Thorning) are currently investigated with acquisition of new data and updated mapping in GEUS' CCS project during 2022–2024. This reporting is for the Thorning structure, and the study area is marked with a red rectangle.

The new 2D seismic survey (GEUS2023-THORNING) included in the present reporting was acquired in the summer and autumn 2023 and consists of eight seismic lines with a total line length of c. 133 km across the structure (Fig. 1.2, Chapter 4).

The Thorning structure is a geological three-way dip structure, bounded by a fault zone at its southwest side. The structure has an extent of around 235 km² (Fig. 1.2). The main reservoir-seal couple of the Thorning structure is suggested to be the Gassum Formation and Fjerritslev Formation, which are shown in Figure 1.3. Descriptions of well logs in the area show that the Gassum Formation and large parts of the Fjerritslev Formation contain suitable reservoir and seal intervals, respectively. In addition, a secondary, shallower reservoir-seal couple may be provided by the Frederikshavn Formation and the Vedsted Formation, and a deeper situated reservoir-seal couple of the Bunter Sandstone Formation / Skagerrak Formation and the Ørslev and Falster formations. In addition, the Tønder Formation may possibly form an additional reservoir in the structure. See Chapter 7.1 for more details on the reservoirs.

There are no deep wells penetrating the Gassum Formation in the Thorning structure which cause significant uncertainty on the presence and quality of reservoir and seal units. The thickness estimate of the Gassum Formation across the structure is c. 100 m based on the mapped seismic reflectors with well ties in vicinity of the structure and seismic depth conversion. Seismic mapping and correlation to the Nøvling-1, Vinding-1, Mejrup-1 and Kvols-1 wells shows a large lateral continuity of the Gassum Formation, see Chapter 5. The Gassum Formation is expected to comprise sandstones with interbedded claystones, and in the wells surrounding the Thorning structure the range of net sand thickness is 11–63 m and the range of Net to Gross ratio is 0.13–0.57. Three modelled scenarios of the Thorning structure based on two reference wells (Gassum-1 and Nøvling-1) and seismic geological assumptions has been carried out to calculate a potential range of net reservoir sand thickness of 20.5–35 m in the Thorning structure.

A reservoir is defined as a sandstone containing a volume of shale <0.5% and with porosities >10%. The Gassum Formation reservoir sandstones in the surrounding wells have porosity range of 12.8–24.3% and average of 20.9% providing good reservoir properties. The modelled values are between 25.6–28.8%.

The primary seal for the Gassum Formation in the structure is the Fjerritslev Formation, which is up to a few hundred-meter-thick mudstone succession of Early Jurassic age and is expected to include good to very good sealing mudstone intervals. In the Stenlille structure on Sjælland, safe storage of natural gas in the Gassum Formation and monitoring for potential leakage through many years has proven that the Fjerritslev Formation seal is efficient. The same stratigraphic seal interval is also expected to be present in the Thorning structure. See also Section 7.2 for more details on the seals.

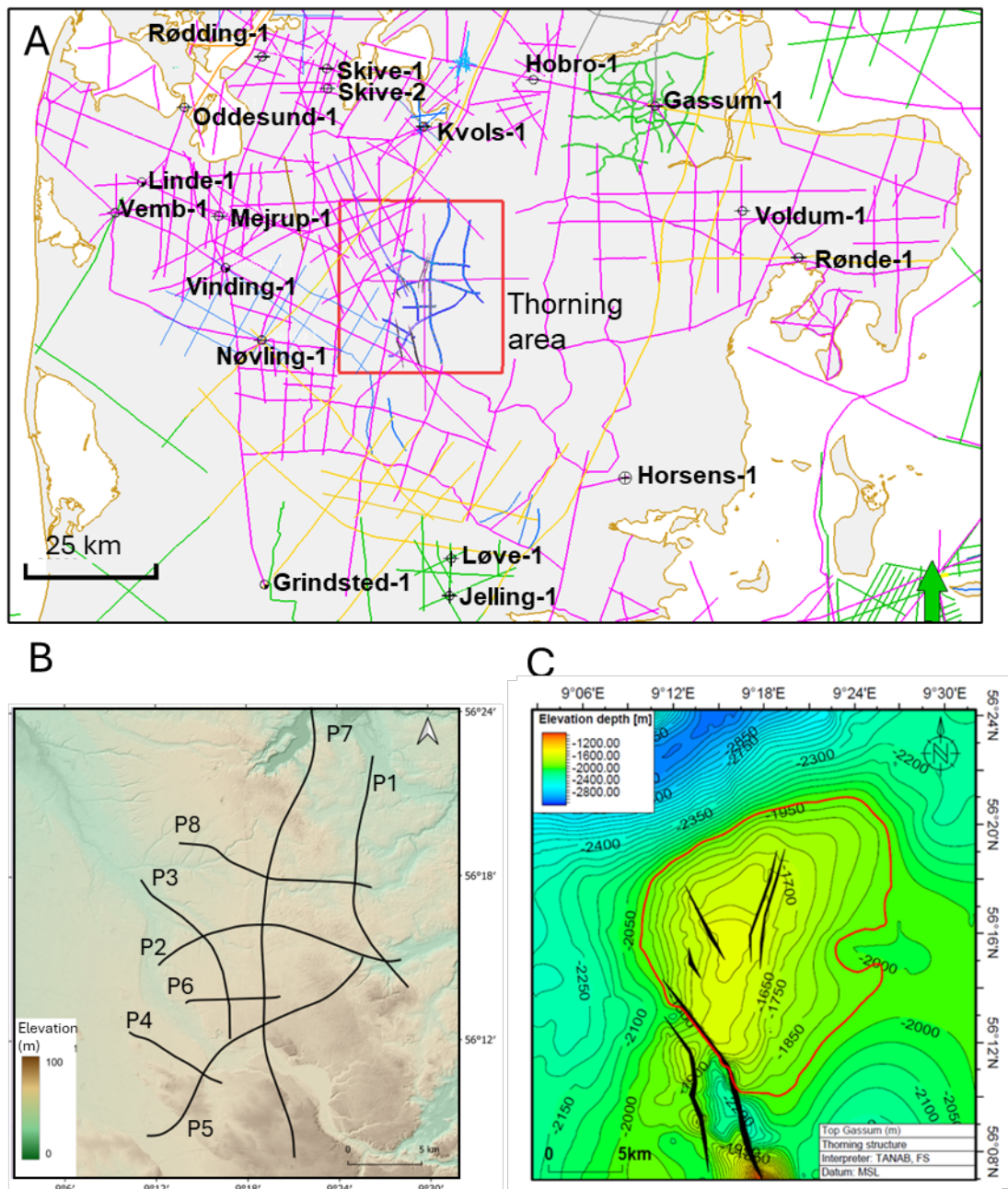


Figure 1.2. A: Map of central Jylland with deep wells and legacy seismic lines (purple, yellow, light blue and green). The new seismic lines are shown at Thorning (Bold dark blue) and at Gassum (Bold green). B: Topographic map of the Thorning study area, with outlines of new seismic lines P1–P8. C: Depth-structure map of the Top Gassum Formation reflector meters (m) below mean sea level (b. msl) shown with the largest faults as black, filled polygons. The map is produced with a 100x100 m grid and mildly smoothed (iteration x1; filter width 3). The outline of the Thorning structure is shown with red polygon at top Gassum Fm level with spill point at 1950 m below mean sea level. Faults indicated with black polygons.

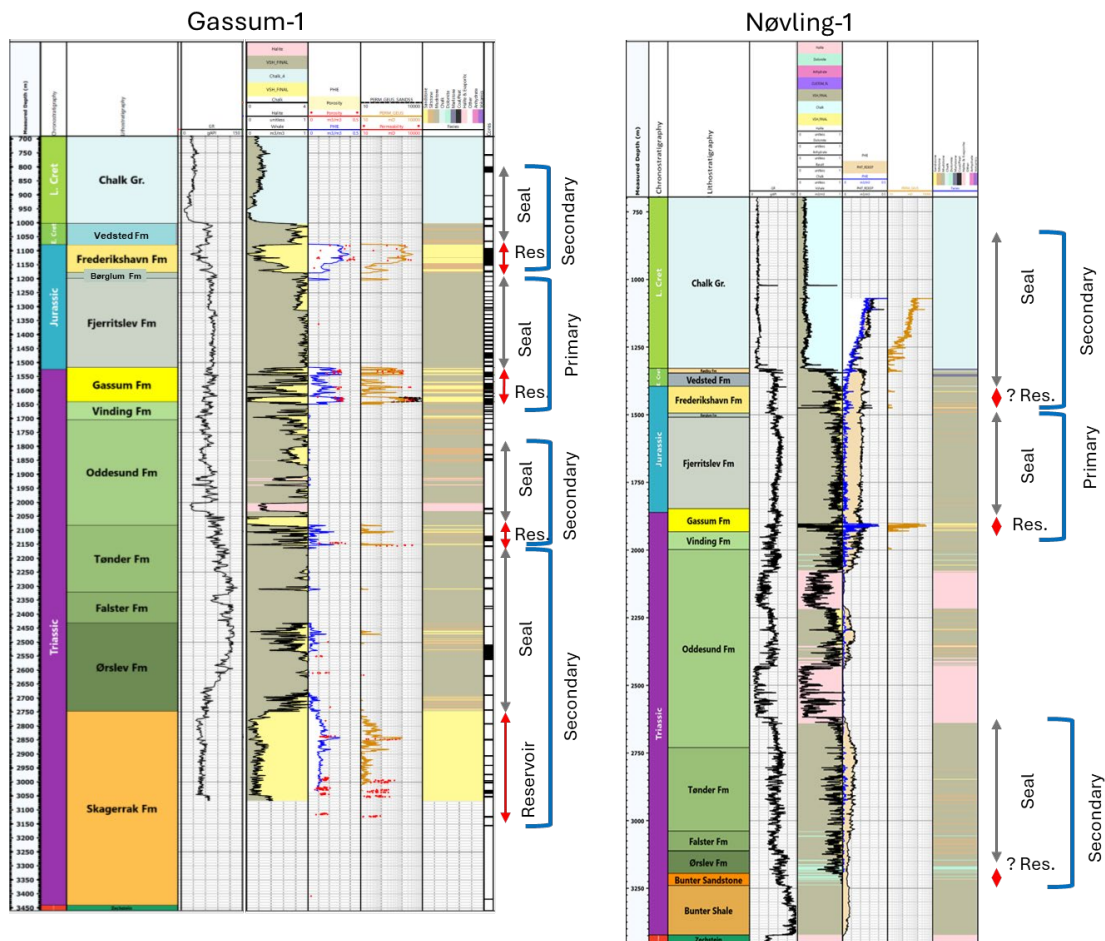


Figure 1.3. Two reference wells for the Thorning structure; Gassum-1 and Nøvling-1 with petrophysical logs displaying the potential primary and secondary reservoir-seal pairs. Note the apparent lack of reservoir sand within the Frederikshavn Fm, Tønder Fm and Bunters Sandstone Fm in the Nøvling-1 well. Location of wells are shown in Figure 1.2A.

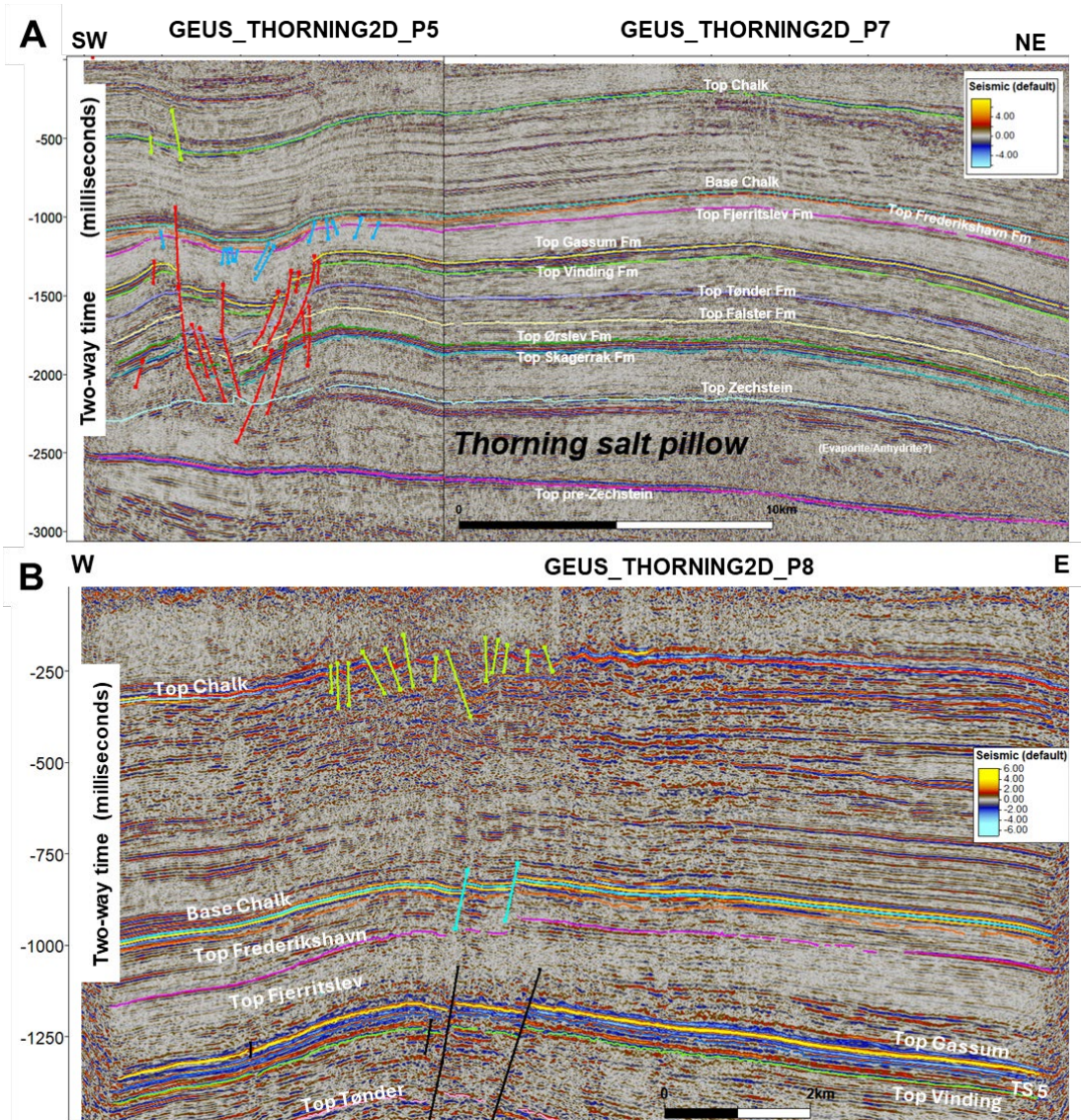


Figure 1.4. A: Composite 2D seismic line P5 and P7 from GEUS2023_THORNING-RE2023 showing the Thorning structure from Top-Zechstein level, with the salt pillow and overlying stratigraphic units incl. Gassum Fm and Fjerritslev Fm. The interpreted faults occur at different levels and are shown with red, blue, and green lines. Horizontal scale bar is 10 km (black–white). B: Profile 8 from GEUS2023_THORNING-RE2023 including the interpreted horizons. The black faults are normal faults active during the Early Jurassic offsetting the top Gassum Fm with up to 21–23 msec TWT at the northeastern crest of the structure. The Base Cretaceous–Upper Jurassic faults are shown by light blue lines. Faults at Top Chalk are shown by green lines. Horizontal scale bar is 2 km (black–white).

The new data and mapping confirm that the Thorning structure has closures at the Top Gassum Formation and at shallower levels including the top of the secondary reservoir with potential sandstone intervals of the Frederikshavn Formation, as well as deeper levels with potential sandstones of the Skagerrak / Bunter Sandstone Formation. The area of the lowermost closure on the Top Gassum depth-structure map is c. 235 km² at the closing contour of c. 1950 m depth below mean sea level (Fig. 1.2). The top of the structure at the Top Gassum map is at c. 1520 m below mean sea level corresponding to c. 1580 m below terrain, and the

relief of the structure at Top Gassum is thus c. 430 m. The calculations on storage capacity in this study is based on Scenario 3 with a net reservoir sand of 35 m in the entire Gassum Formation, which results in a static storage capacity of the Gassum Formation of 125 Mt CO₂ (Chapter 8).

A marked fault zone is present on the southwest slope of the Thorning structure (seen in Fig. 1.4A), which also marks the southwest closure of the Thorning structure at the primary reservoir level. The fault zone is observed on two of the new seismic profiles, (P4 and P5) and represents a c. 5 km wide significant fault zone with graben-like, listric normal (synthetic and antithetic) faults offsetting the entire Triassic section from the Gassum Fm horizon to the Skagerrak (former Bunter Sandstone) Formation horizon (red lines in Fig. 1.4A). The graben structure probably formed as a mini-basin due to salt withdrawal and collapse resulting in a marked thickening of the Fjerritslev Formation in the fault zone. The large throws at the Top Gassum to Top Falster horizons indicate faulting during deposition of the Fjerritslev Formation. The salt has migrated either northeastwards to the Thorning salt pillow or southwards to the Bording salt diapir located south of the study area. The southern main listric boundary fault plane is dipping to the northeast and downfaults the Top Gassum horizon with a throw of >100 msec TWT, corresponding to c. 150–170 m offset. The main listric boundary fault is the only visible fault that extends upwards and offsets the Top Fjerritslev to Base Chalk horizons, with a throw of 11 msec at Base Chalk, corresponding to c. 15–20 m offset. The opposite boundary fault, the northern-most Triassic fault of the graben-like structure is southwest-dipping and located along the boundary of the closing contour for the Top Gassum Fm horizon at the 1270 msec TWT-contour curve and follows the spill point of the structure. The northward continuation of this fault is poorly defined due to lack of seismic data coverage, and this is a potential critical issue for defining the closure of the Thorning structure. Another suite of younger normal faults is observed overlying the graben structure with minor faulting of the Top Fjerritslev to Top Frederikshavn Fm horizons (shown by blue lines in Fig. 1.4A). The present seismic data show no indications for direct connection or upward continuation of the deeper Triassic fault planes linking them to the younger overlying fault zones (see Fig. 6.1.4), however, possible fault connection cannot be ruled out.

Few faults are present over the Thorning structure itself (Fig 1.4A). These extensional faults are mapped at the northeastern crest of the structure on the E–W striking profiles P2 and P8 that demonstrate W-dipping, normal faults that offset the top Gassum Formation horizon (black lines in Fig. 1.4B) with throws up-to 21–23 msec TWT, corresponding to 34–35 m offset assuming an average seismic velocity of 3000 m/s for the Gassum Fm interval at 1160–1170 msec TWT depth. It is not known if the faults continue up through the Fjerritslev Formation, but a similar set of younger, W-dipping fault planes (cyan lines in Fig. 1.4B) are observed offsetting the interpreted Base Chalk and the Fjerritslev Fm horizons with throws up-to 20 msec TWT. These two fault systems appear to be isolated (i.e. not directly linked) as the Triassic–Jurassic faults seem to terminate up-ward within the (more than 250 msec) thick Fjerritslev Fm. A connectivity between the over- and underlying fault systems can however not be ruled out based on the present seismic data coverage. A third set of minor faults are recorded at Top Chalk level (Bright green).

The new 2D seismic data has significantly improved the seismic database with good quality seismic data. However, it is still a rather open seismic grid with relatively large distances between the lines. Therefore, additional seismic acquisition, in particular of 3D data over the Thorning structure and the potential CO₂ injection and storage areas is recommended. This can improve site-specific evaluation with more details on the faults, reservoir and seal and

provide input to modelling of CO₂ migration and analyses of geological and other technical uncertainties and risks. Repeated seismic surveys in same place can subsequently contribute to monitor the extent of the CO₂ migration, together with other monitoring techniques (e.g., well logging, downhole seismics, micro seismicity, surface deformation, etc).

The present assessment of the investigated Thorning structure will be included in the further work of the authorities to reveal opportunities and requirements towards further maturation for potential geological CO₂ storage in this structure.

2. Introduction

Carbon capture and storage (CCS) is an important instrument for considerably lowering atmospheric CO₂ emissions (IPCC 2022). Geological storage of CO₂ is known from more than 30 sites situated in many countries, including Norway (Sleipner), Canada (Weyburn) and Germany (Ketzin), since the first started more than 25 years ago (e.g., Chadwick et al. 2004) and more than 190 facilities are in the project pipeline (Global CCS Institute 2022).

The Danish subsurface is highly suited for CO₂ storage, and screening studies document an enormous geological storage potential that is widely distributed below the country and adjacent sea areas (Larsen et al. 2003; Anthonsen et al. 2014; Hjelm et al. 2022; Mathiesen et al. 2022). The significant Danish storage potential is based on the favorable geology that includes excellent and regionally distributed reservoirs, tight seals, large structures, and a relatively quiescent tectonic environment. The largest storage potential is contained within saline aquifers, and the Danish onshore and nearshore areas contain a number of these structures with a potentially significant CO₂ storage potential (Hjelm et al. 2022).

The Thorning structure is one of these structures and is a relatively large structure geographically located in central part of Jutland (Fig. 1.1), and geologically also in the central part of the Danish Basin (Fig. 3.1). The structure was only covered by a limited number of old, poor quality 2D seismic lines, acquired in the 1960s, 1970s, 1980s and 2010. However, in 2023 new seismic data for this project was acquired (see Chapter 4). The new seismic lines can be tied with old seismic profiles and thereby to the wells surrounding the Thorning structure, which document the geology. The Thorning structure is expected to have storage potential for resources such as CO₂, and this structure with the Gassum Formation as the main focus of this study, but also a shallower and two deeper reservoir-seal couples of the structure are described.

Earlier screening projects by GEUS for structures relevant for CCS have also evaluated the Thorning structure for potential CO₂ storage. A comprehensive summary with an evaluation of the CO₂ storage potential in Denmark, including an initial evaluation of the Thorning structure, was provided by Hjelm et al. (2022).

In this study, the Thorning structure is investigated further based on evaluation of the integrated database of old and new seismic data, with correlation to wells, to characterize its tectonic and depositional evolution, composition with reservoir-seal couples, faults and geometry towards maturation for potentially geological storage of CO₂.

3. Geological setting

The Thorning structure is located in the Danish Basin which forms the eastern part of the WNW–ESE trending Norwegian–Danish Basin (Vejbæk 1997, Nielsen 2003). To the south the Danish Basin is separated from the North German Basin by the Ringkøbing–Fyn High, and to the north and northeast by the Sorgenfrei–Tornquist Zone which further north is limited by the Skagerrak–Kattegat Platform (Figs. 3.1, 3.2). Both the Norwegian–Danish Basin and the North German Basin are intracratonic basins formed by stretching of the lithosphere which caused Carboniferous–Permian rifting with extension and normal faulting followed by basin subsidence. The Ringkøbing–Fyn High probably formed at the same time due to less stretching than the basin areas (Vejbæk 1997). The tectonism led to large, rotated fault blocks, intrusive volcanism, extensive erosion, and mostly coarse siliciclastic deposition (Rotliegende) affecting large parts of the basin (Vejbæk 1997; Michelsen & Nielsen 1991, 1993; Nielsen 2003).

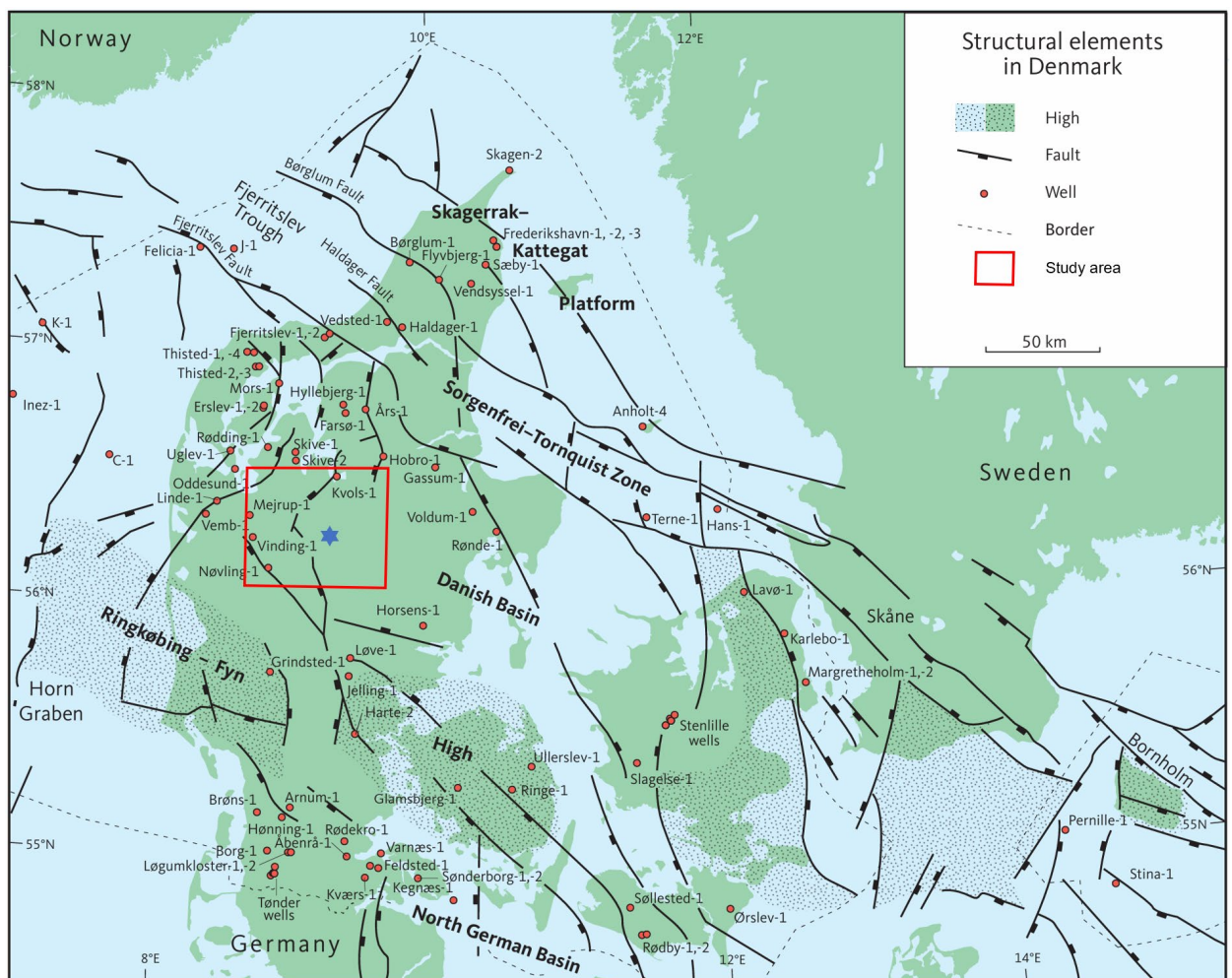


Figure 3.1. Map of the main structural elements including highs, basins, and main faults onshore and offshore Denmark. The elements include the Danish Basin, the Sorgenfrei–Tornquist Zone, the Skagerrak–Kattegat Platform, the Ringkøbing–Fyn High, and the northern part of the North German Basin. The study area is marked with a red square and the approximately location of the Thorning structure with a blue star. Positions of deep wells are also marked. Modified from Nielsen (2003).

After mainly evaporites (Zechstein Group) developed in shallow basin areas during late Permian time, the region subsided and thick Triassic clay and mud-dominated successions formed with a few sandstones and minor carbonate and salt deposits (Bunter Shale, Bunter Sandstone, Skagerrak, Ørslev, Falster, Tønder, Oddesund, Vinding formations; Figs 3.3, 3.4, 3.5A, B). Sandstones are in particular known from the Bunter Sandstone Formation in the North German Basin and the Skagerrak Formation in the Danish Basin (Bertelsen 1978, 1980). During latest Triassic (Rhaetian) and into the earliest Jurassic (Hettangian–early Sinemurian) times the coastal to continental areas were repeatedly overstepped by the sea depositing the Gassum Formation (Fig. 3.6). The relative sea-level rise resulted during the Early Jurassic in the deposition of thick claystone-dominated successions with some silty and sandy layers (Fjerritslev Formation), which have been correlated basin wide in several depositional sequences and members (Nielsen 2003; Michelsen et al. 2003).

Mainly Middle–Late Jurassic regional uplift and salt mobilization led to formation of structures, associated faults, and major erosion in large parts of the basins, with a hiatus expanding towards the Ringkøbing–Fyn High (Fig. 3.3) (Nielsen 2003). However, fault-related subsidence continued in the Sorgenfrei-Tornquist Zone, where sand and mud were deposited (Middle Jurassic Haldager Sand Formation). Regional subsidence occurred again during the late Middle Jurassic and generally continued until Late Cretaceous–Paleogene time, when subsidence was replaced by uplift and erosion related to the Alpine deformation and the opening of the North Atlantic. The deposits from the last period of subsidence consist of Upper Jurassic–Lower Cretaceous mudstones and sandstones (Flyvbjerg, Børglum, Frederikshavn, Vedsted and Rødby formations) followed by thick Upper Cretaceous carbonate and calcareous deposits (Chalk Group), which were formed throughout the Danish Basin. Finally, Cenozoic including Quaternary successions were deposited in the Danish Basin, with episodic uplift (Japsen & Bidstrup 1999; Japsen et al. 2007). Deposits of sandstones in the Late Jurassic–Early Cretaceous interval are mainly known from the Flyvbjerg and Frederikshavn formations.

The significant amounts of sediments deposited throughout the Mesozoic period caused underlying deposits of Zechstein salt to be plastically deformed and in some places to move upwards along zones of weakness. This resulted in uplift of the underlying layers in some places (salt pillows) or breaching by the rising salt (salt diapirs). Above the salt structures, the layers may be absent or partly absent due to non-deposition or erosion, whereas increased subsidence along/in the flanks of the salt structures (in the synclines) may have led to corresponding layers being extra thick in these areas.

Several formations with sandstone reservoirs may potentially be present in the Thorning structure. However, since the structure has not been drilled the lithological composition of the formations is associated with uncertainty as discussed in Chapter 7. Based on interpretations of the available seismic data and by analogue to other structures presented in Chapter 6 and 7, the Gassum Formation is considered the prime reservoir for CO₂ storage as it is overlain by a several hundred meters thick mudstone-dominated succession of the Fjerritslev Formation, which in general is considered as having good seal properties.

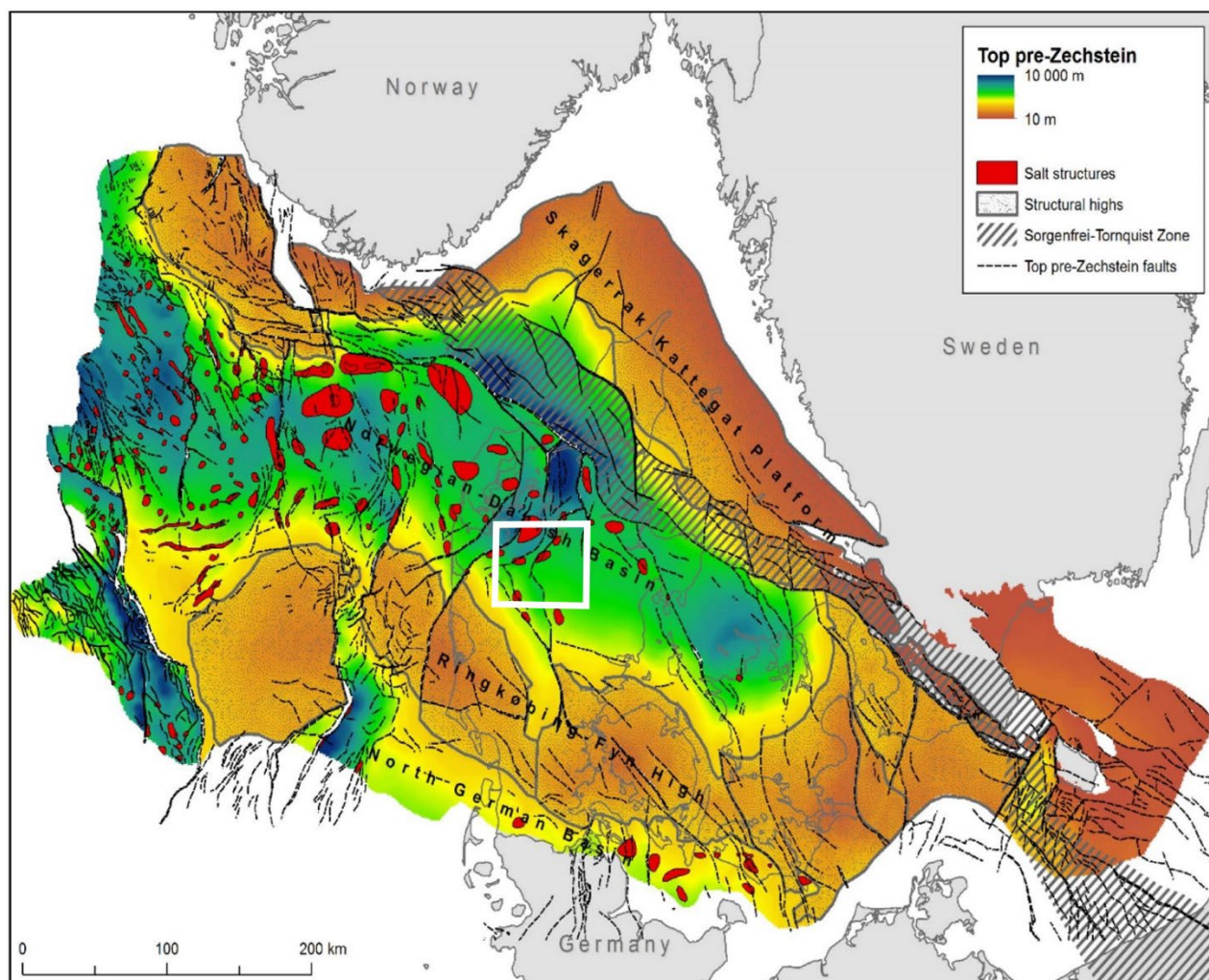


Figure 3.2. Map of the main structural elements onshore and offshore Denmark, including highs, basins, and main faults. The location of the study area around the Thorning structure is marked with a white square. The elements include the Norwegian–Danish Basin (of which the eastern part in Denmark is the Danish Basin), the Sorgenfrei-Tornquist Zone, the Skagerrak-Kattegat Platform, the Ringkøbing-Fyn High, and the northern part of the North German Basin. Modified from Vejrbæk & Britze (1994).

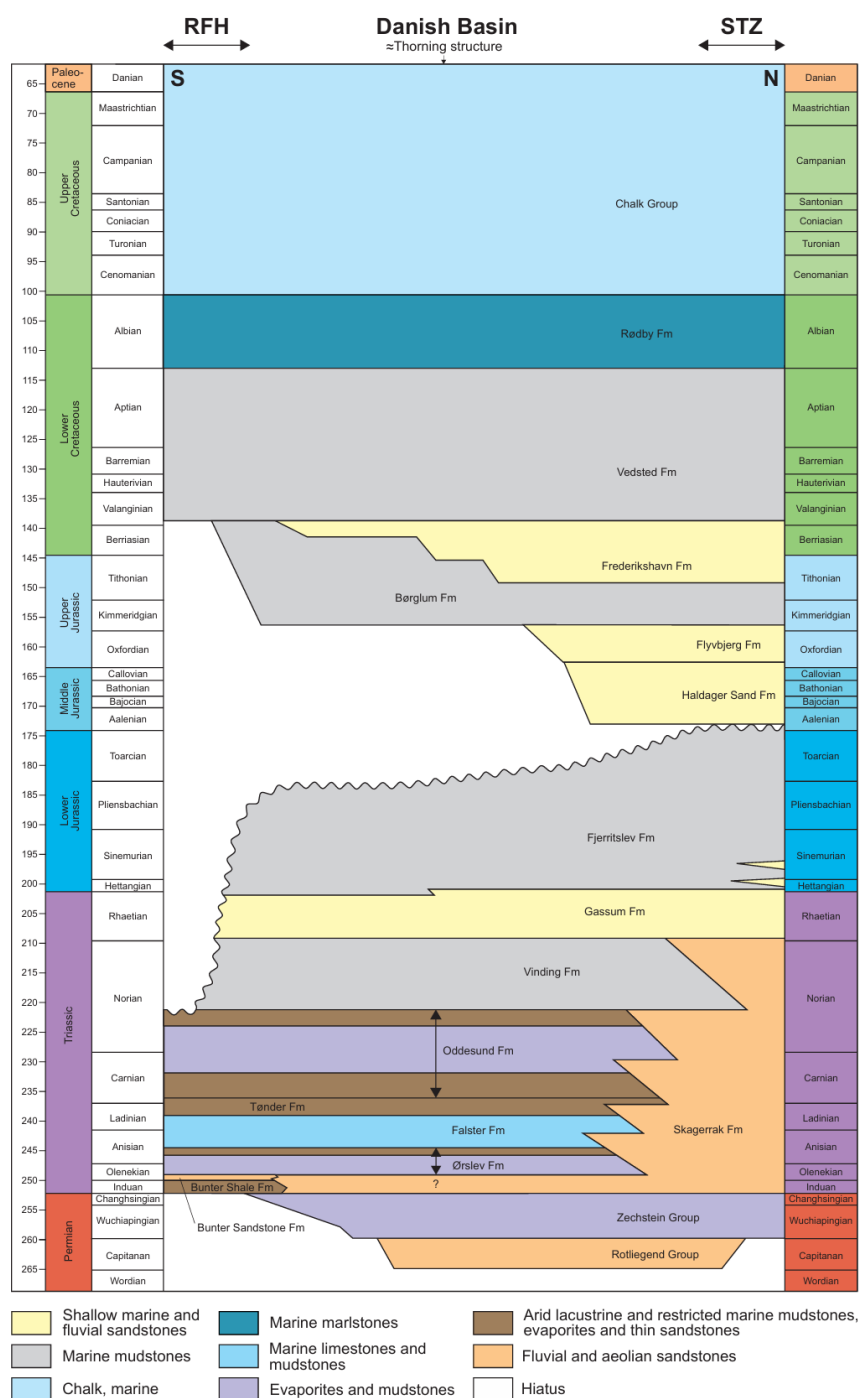


Figure 3.3. Generalized stratigraphy from south to north in the Danish Basin. To the south the basin is limited by the Ringkøbing–Fyn High (RFH) and to the north by the Sorgenfrei–Tornquist Zone (STZ) (Fig. 3.2). The schematic position of the Thorning structure in the basin is indicated at the top of the stratigraphic scheme to indicate which lithostratigraphic units are presumed to be present in the structure. This is based on the seismic mapping and interpretation in addition to information from the nearest wells. Sandstone reservoirs of the Haldager Sand and Flyvbjerg fms are thus not considered to present in the structure. Also, although the Frederikshavn and Skagerrak fms may be present, their large sandstone content in the northwestern part of the basin may largely have been replaced by mudstones in the central part of the Danish Basin where the Thorning structure is located (this is discussed in chapter 7). The stratigraphic scheme is based on Bertelsen (1980) and Nielsen (2003).

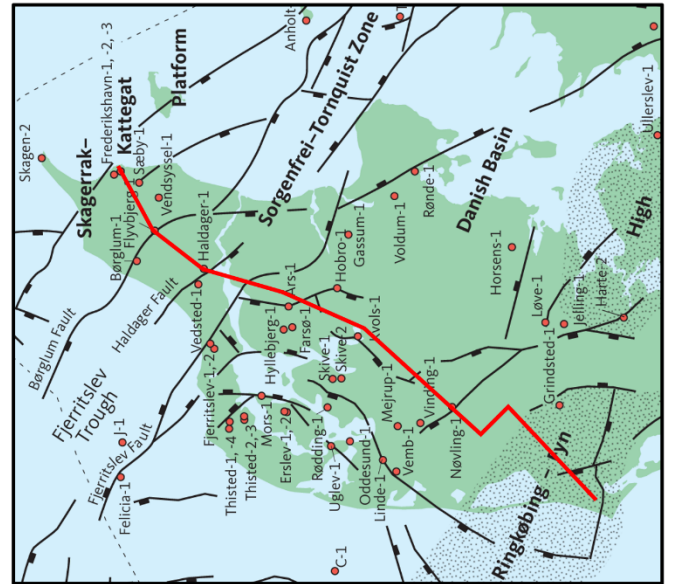
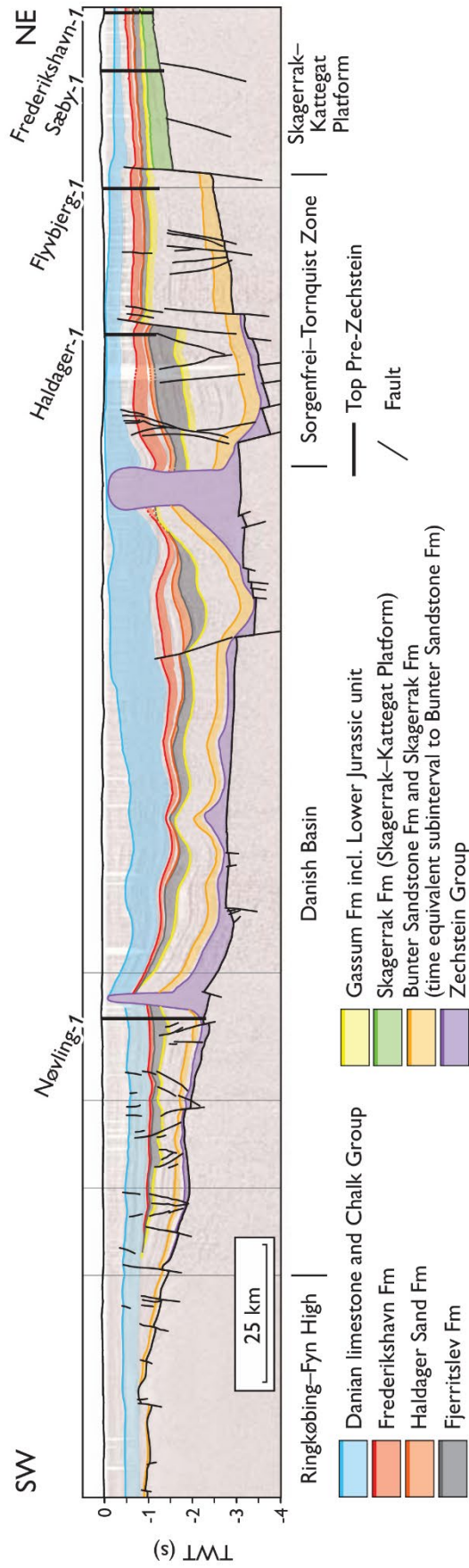


Figure 3.4. Regional S-N profile through eastern Jylland, extending over the Ringkøbing-Fyn High, Danish Basin, Sorgenfrei-Tornquist Zone and the Skagerrak-Kattegat Platform (approximate location of profile is shown with red line on map). Shown wells are projected onto the profile. From Vosgerau (2016).

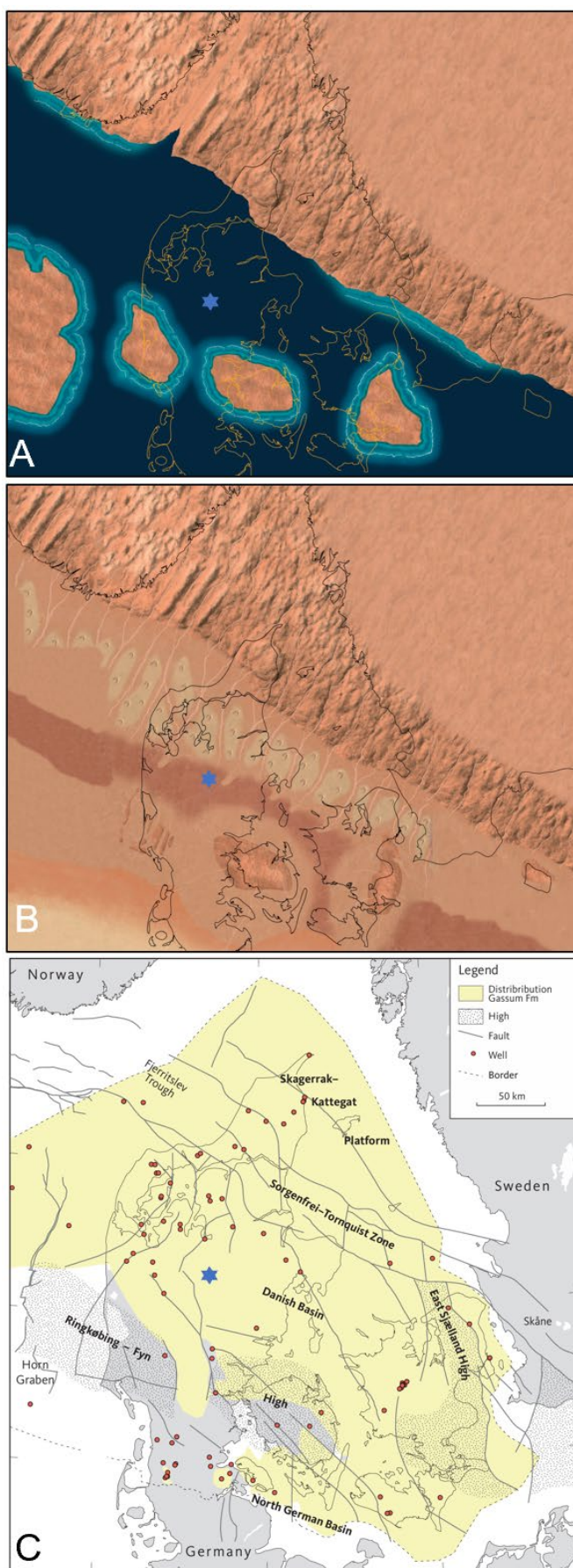


Figure 3.5. Paleogeographic maps of Denmark and southern Scandinavia illustrating the possible distribution of general depositional environments. The approximately location of the Thorning structure area is indicated with a blue star.

(A) Late Permian (Zechstein) sea (dark blue), coastal near areas (light blue) and onshore areas (orange red). From Rasmussen & Nielsen (2020).

(B) Early – Middle Triassic (incl. the Bunter Sandstone and Skagerrak fms) dominated by desert with local sand dunes, lakes and sabkhas. From Rasmussen & Nielsen (2020).

(C) Late Triassic (Rhaetian) to earliest Jurassic (Hettangian–early Sinemurian) Gassum Fm distribution in Denmark. The formation is composed of several depositional sequences with regressions–transgression cycles and deposition in onshore, near-shore, and shallow marine environments (Nielsen 2003, Vosgerau et al. 2020, see also Section 7.1)

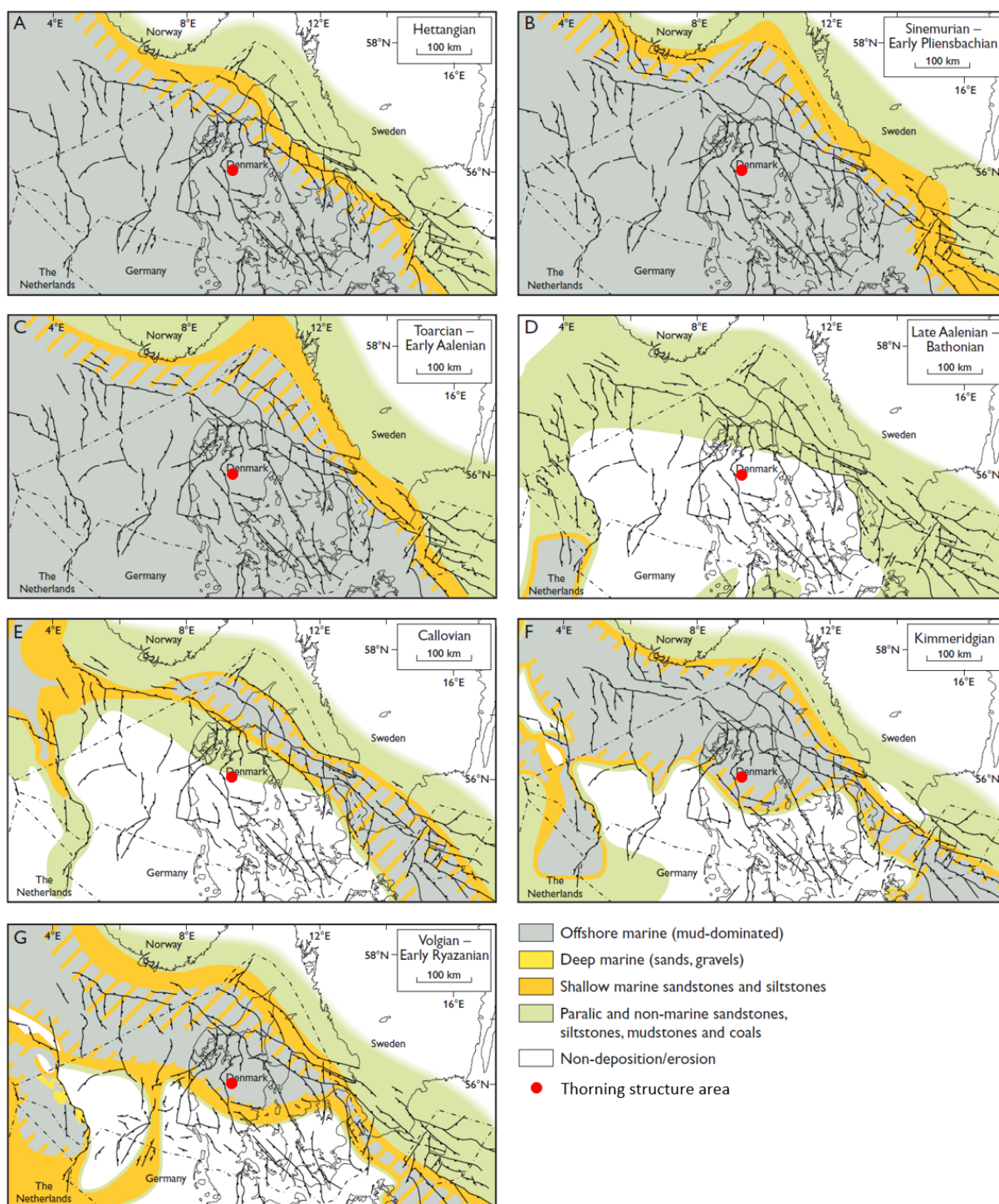


Figure 3.6. Paleogeographic maps of Denmark showing the inferred distribution of general depositional environments during the Jurassic time, when the primary seal of the Fjerritslev Formation was deposited (A–C). The central part of the Danish Basin, incl. the Thorning structure area (red circle), is dominated by deposition of marine clays with possibly some minor layers/beds of silt to sand, from Hettangian to Toarcian/Aalenian (A–C). Some of these sediments were probably removed by erosion due to regional uplift in the early Middle Jurassic (D). Subsequently deposition of various paralic sediments (Haldager Sand and Flyvbjerg fms), marine clays (Børglum Fm) and shallow marine silt and sand (Frederikshavn Fm) took over (E–F). From Petersen et al. (2008), modified from Michelsen et al. (2003).

4. Database

4.1 Seismic data

The geophysical database in the Thorning area comprises three decades of mostly old (1960s to 1980s) poor to medium quality 2D seismic lines, some younger lines from 2010's and the new 2D seismic data from 2023 (GEUS2023-THORNING survey) acquired for this project (Fig. 4.1.1).

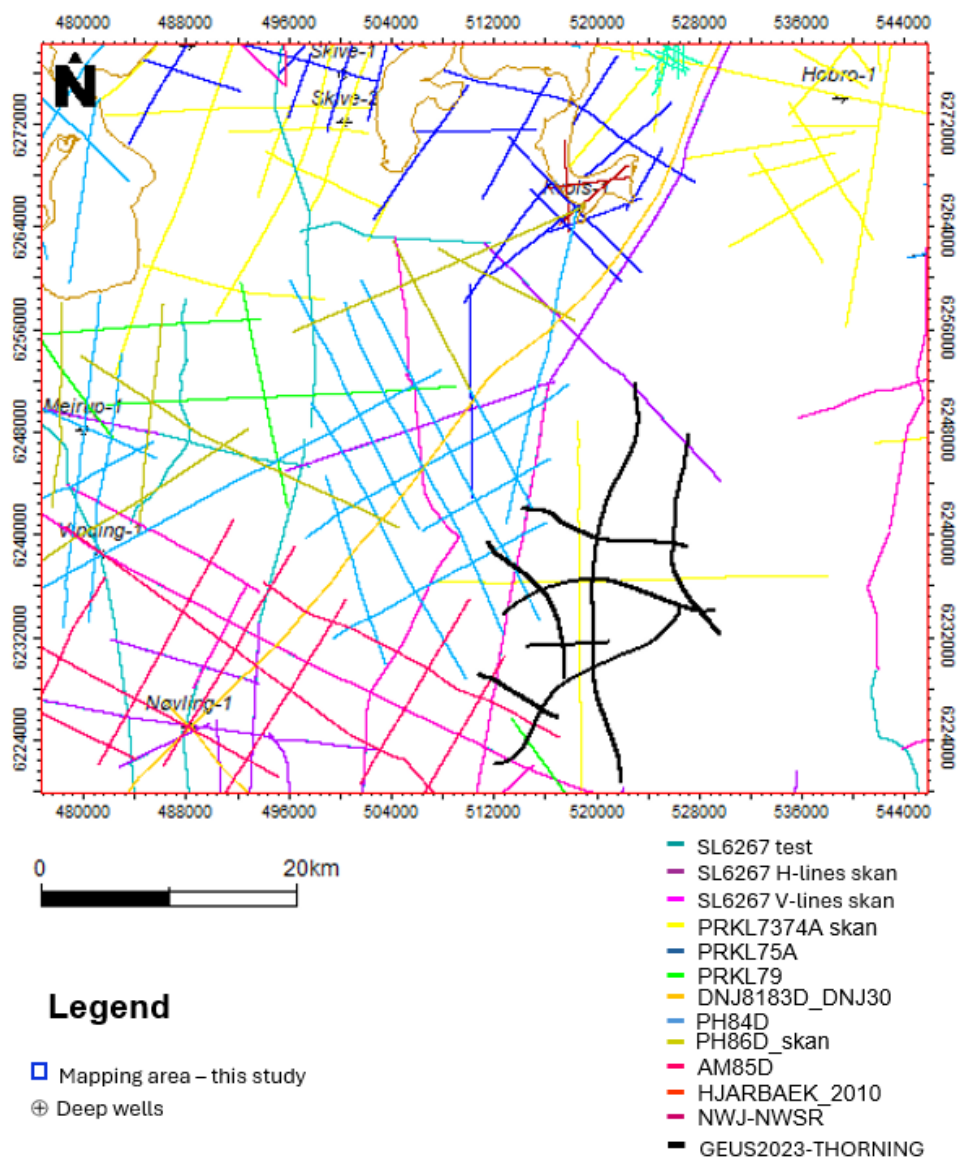


Figure 4.1.1. Project database of the Greater Thorning area with the new 2023 Thorning 2D seismic survey (GEUS2023- THORNING), older onshore 2D legacy data and deep onshore wells in the area.

There are no deep wells directly at the Thorning structure, and the nearest well, Nøvling-1, is located c. 33 km to the west. However, numerous wells exist in a circle around the greater Thorning area with wells such as Nøvling-1, Vinding-1 (no logs), Mejrup-1 and Kvols-1.

Additional wells located outside the main study area have been used for tying the seismic marker horizons, such as Vemb-1, Linde-1 and Oddesund-1 to the west; the Rødding-1, Skive-1 and Skive-2 to the north, and the Hobro-1 well to the northeast. In addition, the wells Gassum-1 to the northeast (no sonic log), Horsens-1 to the southeast, Grindsted-1 to the southwest, Jelling-1 and Løve-1 to the south situated outside the map are included.

This chapter will focus on the new data of the GEUS2023-THORNING survey integrated with the old legacy data for mapping and interpretation of the Thorning structure as described below. The seismic database used is shown in Figures 4.1.1 and Table 4.1.1. Seismic surveys, and acquisition and processing reports are available through GEUS (www.geus.dk), or by requests to the GEUS Subsurface Archive: info-data@geus.dk.

The legacy 2D data in Central Jutland

The quality of the seismic data in the study area is highly variable from very good to very poor (Table 4.1.1 and Fig. 4.1.2). The majority of the oldest 2D seismic surveys from the 1960s and 1970s are generally very poor to poor in quality and represented by digitalised versions of old paper sections, whereas the more recent 2D and 3D seismic data are generally of good to excellent quality and in digital format.

The oldest seismic datasets in the mapped area are the scanned 2D seismic surveys SSL6267-test, SSL6267_H-lines and SSL6267_S, V-lines, which were acquired in 1962–67 by Gulf Oil Co. Denmark and Shell for DUC, and selected lines were used for interpretation in the area, although they are mostly of very poor quality (Table 4.1.1 and see example on Fig. 4.1.2.A-C).

The 2D seismic survey PRKL73A was acquired in 1973–74 by Gulf Oil Co. Denmark on behalf of DUC in the license *DUC Eneret 1962 B*. Most of these scanned 2D profiles with poor to moderate data quality were used for interpretation in the study area, see example on Figure 4.1.2D.

The 2D seismic survey PRKL75A was acquired in 1975 by Dansk Boresekskab A/S on behalf of Mærsk Olie og Gas in the license *DUC Eneret 1962 B*. Thirteen seismic lines with poor to moderate data quality were used for interpretation in the study area, see example on Figure 4.1.3.A.

The 2D seismic survey PRKL79 was acquired in 1979 by Prakla-Seismo GmbH on behalf of ELSAM and consists of 5 profiles with poor data quality in the study area, see example on Figure 4.1.3.B.

The 2D seismic survey DNJ8183D was acquired in 1981–83 by Western Geophysical Co. with long widespread profiles across Denmark. Two profiles with good quality data were used for our interpretation in the study area, see example on Figure 4.1.3.C.

The 2D seismic survey PH84D was acquired in 1984–85 by Prakla-Seismo GmbH on behalf of Phillips Petroleum Co. Europe-Africa in the license 15/84. Sixteen profiles with good quality data were used for our interpretation in the study area, see example on Figure 4.1.3.D.

Table 4.1.1. *The seismic surveys and lines used for this study in and around the mapped Thorning area, with annotated age and data quality. The color coding refers to Fig. 4.1.1. Examples of the new data, surveys GEUS2023_THORNING and GEUS2023_THORNING-RE2024 will be shown in the next section.*

Seismic survey	Seismic lines	Year	Color	Data quality
SSL6267 (H-lines) skan	H1-H26	1962-1967	Purple	Poor
SSL6267 (S, V-lines) skan	S1-S5 V1-V35	1962-1967	Magenta	Poor
PRKL7374A skan	73218-73260, 73302-73307	1973-1974	Bright yellow	Moderate
PRKL75A	75258EXT, 75261-75262, 75265-75275	1975	Dark Blue	Moderate
PRKL79 (navigation problems)	E7901, E7904, 7906; and E79_E7902- E79_E7903	1979	Light green	Poor
DNJ8183D_DNJ30-Shifted20ms	DNJ_30, DNJ_100	1981-1983	Orange	Good
PH84D	PH84D001-PH84D006, PH85D007-PH85D016,	1984	Bright blue	Moderate
AM85D	ADK85_123 to ADK85_149	1985	Raspberry red	Good
PHD86D_skan	PH86D017-PH86D027	1986	Dijon brown	Moderate
HJARBAEK_2010	Line-1 to -3	2010	Dark red	Good
NWJ-NWDR-confidential	NWJ-12-51_dmo_mig90, NWJ-12-52_dmo_mig90,	2012	Burgundy	Excellent
GEUS2023-THORNING (processed by Uppsala University)	GEUS2023-THORNING_P1, GEUS2023-THORNING_P2, GEUS2023-THORNING_P3, GEUS2023-THORNING_P4, GEUS2023-THORNING_P5, GEUS2023-THORNING_P6, GEUS2023-THORNING_P7, GEUS2023-THORNING_P8,	2023	Not shown on map in Fig, 4.1.1	Excellent
GEUS2023-THORNING - RE2024 (re-processed by RTS)	2024_05_23_GEUS_THORNING2D_P1_Final_PSTM_Full-Stack_AGC	2024	Fat black lines	Excellent

The 2D seismic survey AM85D (ADK85-lines) was acquired in 1985 by Prakla-Seismo Gmbh on behalf of Amoco Denmark Exploration Co. in the license 3/84. Twenty profiles with good data quality were used for interpretation in the study area, see example on Figure 4.1.4.A.

The 2D seismic survey PHD86D_skan was acquired in 1986 by Prakla-Seismo Gmbh on behalf of Phillips Petroleum Co. Europe-Africa in the license 15/84 and exists as scanned paper sections in our seismic database, which means that it's not possible to use these lines for seismic well ties. Eleven profiles with good quality data were used for tying our seismic interpretation in the study area, see example on Figure 4.1.4.B.

The 2D seismic survey HJARBAEK-2010 was acquired in 2010 by DMT (Deutch Montan Technologie) Gmbh & Co. Kg on behalf of Viborg Fjernvarme as a §3-screening in the license G2012-01. The survey consists of three profiles with a seismic tie to the Kvols-1 well. All three profiles were used for tying our seismic interpretation in the study area, see example on Figure 4.1.4.C.

The 2D seismic survey NWJ-2012 was acquired in 2012 by Tesla Exploration International Ltd. On behalf of New World Resources Operations ApS in licences 1/09 and 2/09. Two profiles were used for tying our seismic interpretation in the study area, see example on Figure 4.1.4.D.

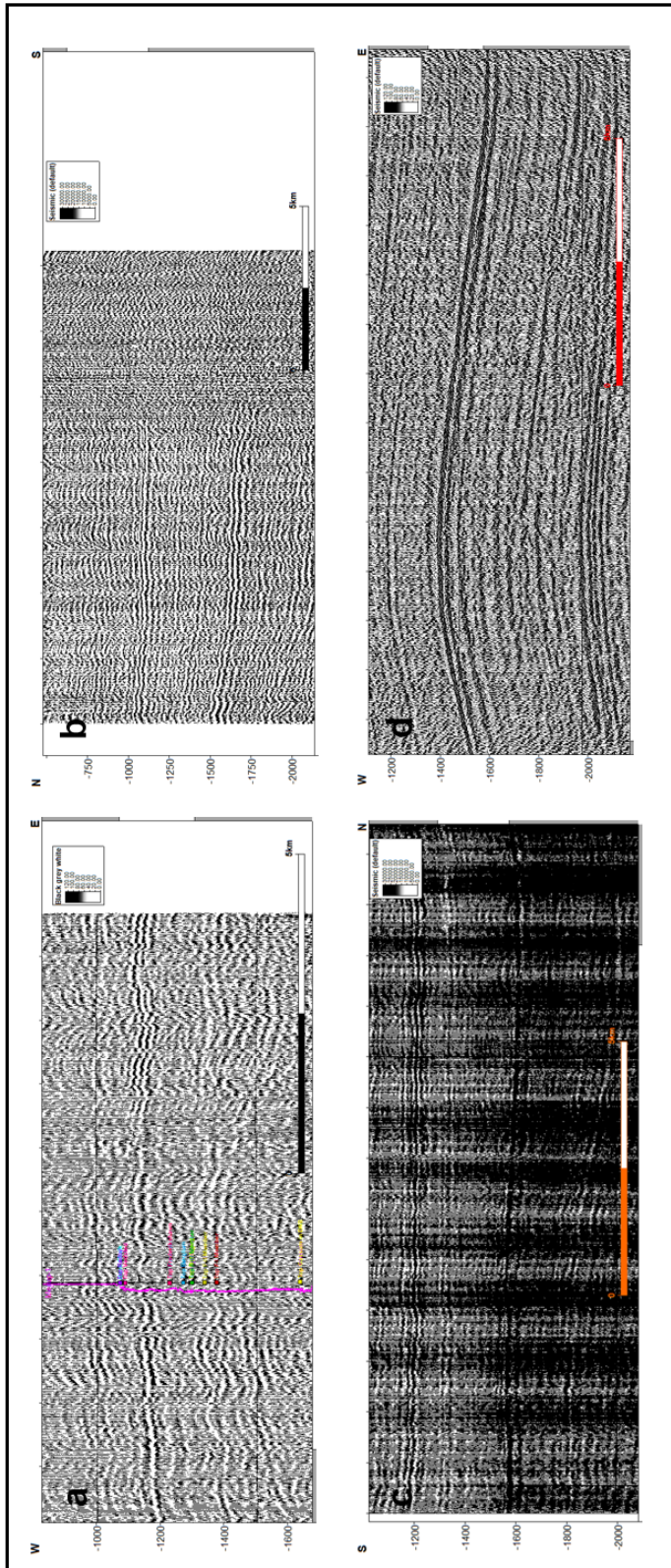


Figure 4.1.2. Examples of seismic data quality for the 2D legacy surveys (two-way time sections). All sections have the same 5 km horizontal scale. A. Very poor data quality of 1960s data (SSL6267 (H-lines) scan H25) crossing the Vinding-1 well; B. Another example of the better 1960's data along SSL6267_S1_digitized-by-geus_disp26710; C: Poor data quality of the scanned paper sections of 1960's data (SSL6267_V17_digitized-by-geus_disp26776); D. Acceptable quality of the 1973 dataset (PRKL73-73240).

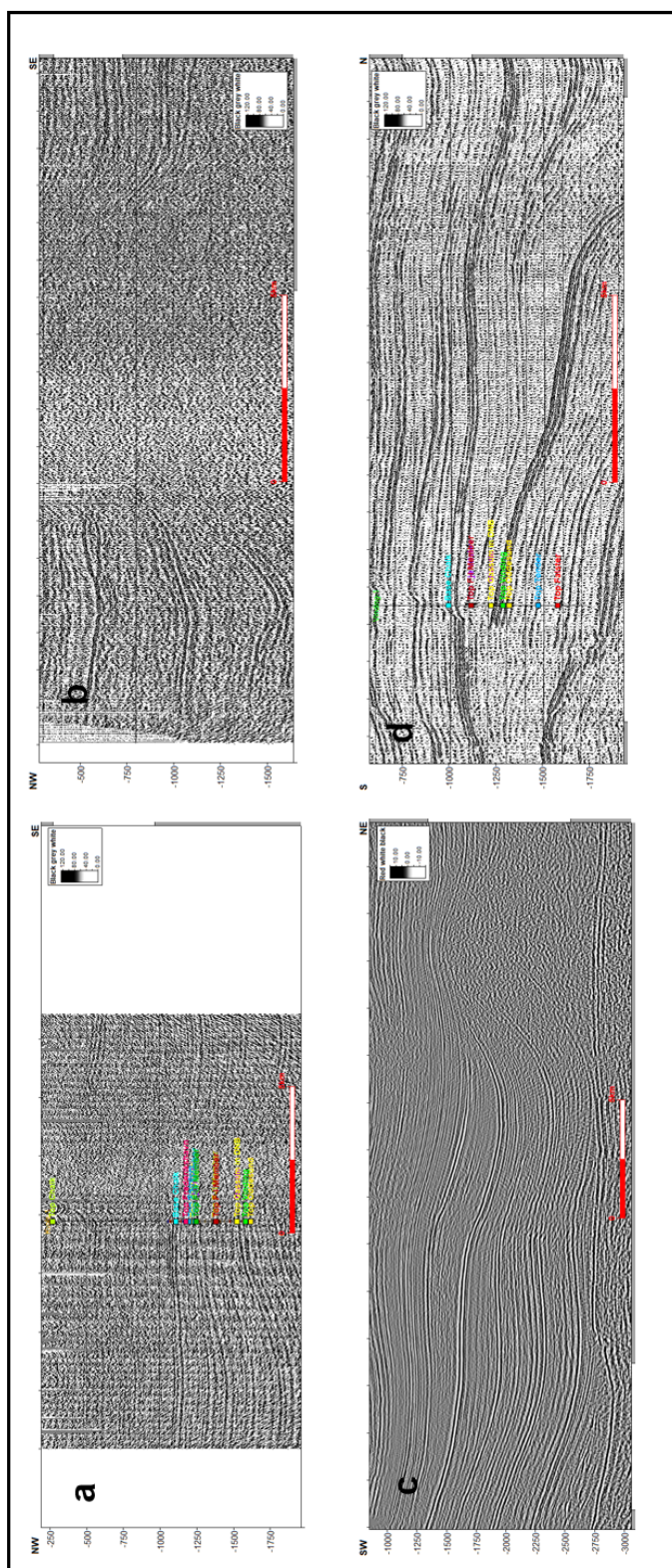


Figure 4.1.3. Examples of seismic data quality for the 2D legacy surveys (two-way time sections). All sections have the same 5 km horizontal scale. A: Poor to moderate data quality of 1970s data (line PRKL75A-75273) crossing the Skive-1 well; B: Another example of the 1970's data along line PRKL79-E7906; C: Good data quality of the 1980's data from survey DNJ8183D (line DNJ_100); D: Acceptable quality of the scanned PH84D to PH86D datasets shown by line PH84D-006 tying to the Vinding-1 well.

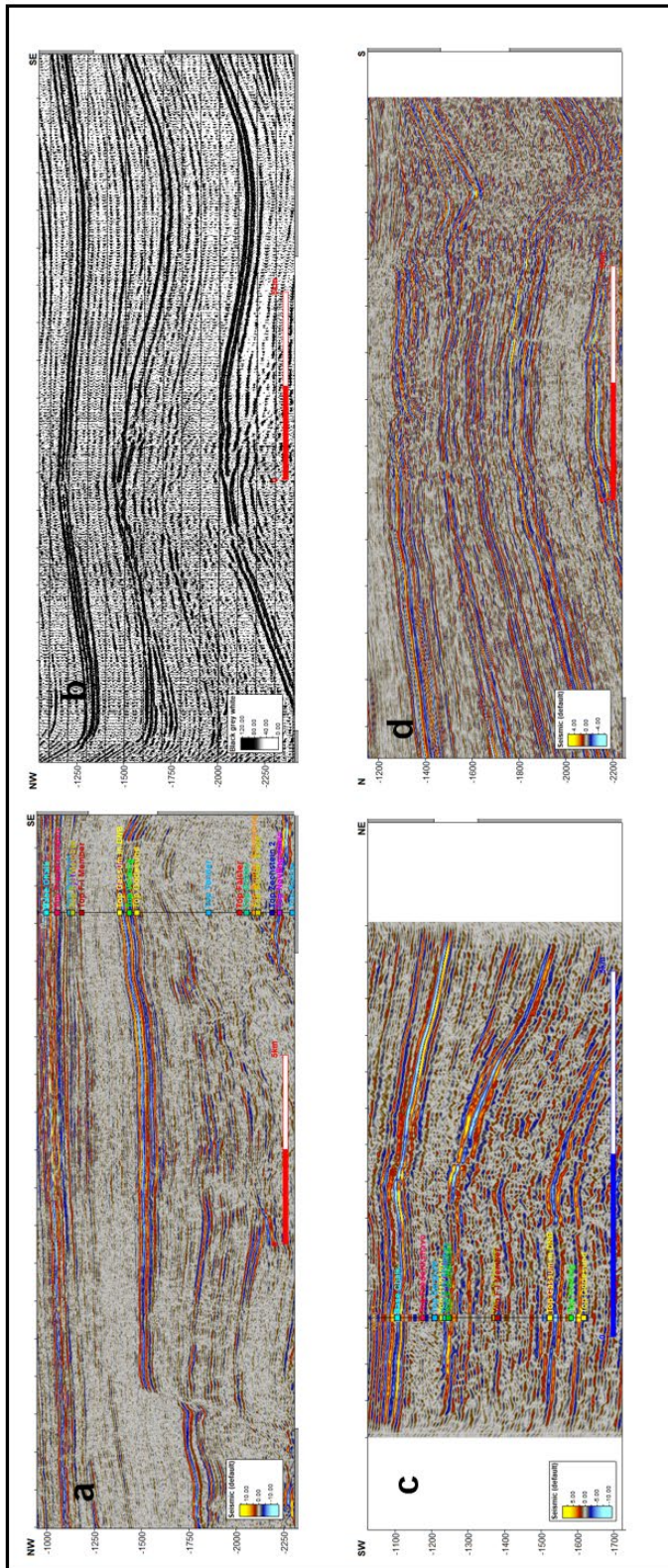


Figure 4.1.4. Examples of seismic data quality for the 2D legacy surveys (two-way time sections). All sections have the same 5 km horizontal scale. A: Very good data quality of 1980's data along ADK85_144 crossing the Nøvling-1 well; B: Another example of the scanned 1980's data along line PHD86D017; C: Good data quality from the 2010 data from the Hjarbæk Fjord area, where Line 3 provides a direct seismic tie to the Kvals-1 well); D: Excellent data quality from the 2012 data from the NWJ-2012-01 survey.

GEUS new 2D seismic survey in Central Jutland

The new 2D seismic survey GEUS2023-THORNING was acquired by Uppsala University for GEUS from August to October 2023, in the Thorning area in the central of Jutland, Denmark and was organized by GEUS as part of the ongoing initial maturation efforts regarding the application of CCS in Denmark, as described in this report. Uppsala University carried out the acquisition and first processing of the data (Putnaite & Malehmir 2024). The survey was designed to add quality data and coverage to the poorly known Thorning structure, where only a few old seismic lines existed, for a better definition of the structure geometry and closure, reservoir–seal successions, and identification of potential faults.

The initial processing is carried out by Uppsala University. For each profile, the data were delivered in several versions of the final migrated stacks in time, meaning a migrated stack for the streamer data, a migrated stack for the wireless/nodal data and a merged stack of these two datasets, see Figure 4.1.5.

However, to secure comparability between all the recent studied onshore structures, it was decided to have the data reprocessed in parallel by *Realtimeseismic* (RTS) utilizing the experience from reprocessing all the previous data from Gassum, Havnsø, Rødby and Stenlille structures. The processing objectives were to deliver an updated Pre-Stack Time Migration (PSTM) with a good quality of imaging for facilitating a reliable geological interpretation (horizons and faults picking), prospect delineation, planning and control of future development wells and to improve vintage processing.

Data and the reports for both the initial processing by Uppsala University ([Processing summary sheet \(geus.dk\)](#)) and the re-processing by RTS ([Processing summary sheet \(geus.dk\)](#)) are available via the GEUS website.

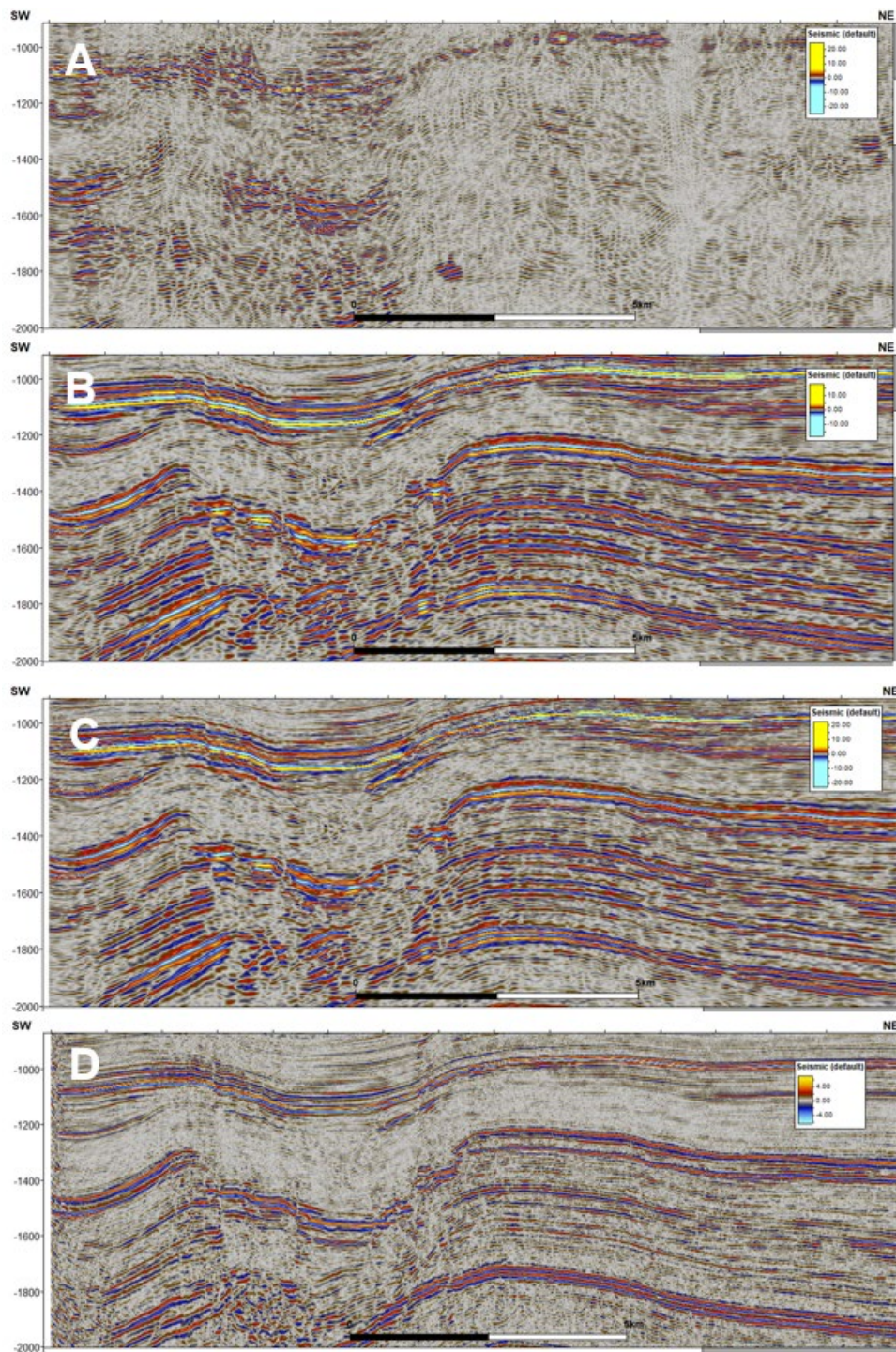


Figure 4.1.5. Comparison of the different time-migrated stacked sections of Thorning profile 5 from Uppsala University (A-C) with the reprocessed depth-migrated stack from RTS (D). A: An example showing the migrated stack for the streamer data (GEUS23_THR_P5_streamer_mig); B: An example showing the migrated stack for the wireless/nodal data (GEUS23_THR_P5_wireless_mig); C: An example showing the migrated stack for the merged streamer and wireless data (GEUS23_THR_P5_merged_mig); and D: An example showing the same section, reprocessed by RTS, GEUS_THORNING2D_P5_Final_PSTM_FullStack_AGC. All sections have the same 5 km horizontal scale.

Seismic data mis-ties

The 2D seismic profiles of different vintages in the study area have different datum elevations, mostly related to different static corrections, topography, etc. (Fig. 4.1.1). In this context and in relation to the new data acquired, also the level of the water-saturated zone (groundwater) can play a role and will be slightly different depending on the season of the year and wet or dry periods. The topography in the Thorning area is relatively variable with elevations ranging from -3 to 158 m above msl (see Fig. 4.2.1). Furthermore, the Thorning area is dominated by glacial valleys, both exposed and buried valleys (Sandersen and Jørgensen, 2022), due to the proximity to the Main Stationary Line. This line marks the limit of the ice sheet occurrence during the Weichsel glaciation separating the landscape formed below the ice sheet to the east from the glaciofluvial sandy deposits to the west, as well as pre-historic sites well due to neolithic settlements.

To compensate for many differences in the datum elevation between seismic profiles, it was decided to use processing to mean sea level (msl) as the seismic reference datum. For the purpose of mapping in this project, static vertical time shifts (a constant and non-data stretched shift) of each 2D seismic profile were conducted (Table 4.1.2). In this process, the Kvols-1 well located at the edge of Hjarbæk Fjord is excellent for calibrating to mean sea level. In chapters 5 and 6, seismic well ties from Kvols-1 to the Thorning structure, and the tying from Kvols-1 to Nøvling-1 are documented in greater details.

Table 4.1.2. *Seismic surveys & lines used in the mapped Thorning area with time-shifts.*

Seismic profile	Timeshift
PH86D023	30
73231 (PRKL7374A skan)	80
SSL6267_H11_digitized-by-geus_disp26509	60
73222	-15
73221i	-38
73221ii	-38
PH84D004	15
DNJ-15	10
NWJ-12-51_dmo_mig90	-10
PRKL7374A skan -73224	30
73207 (East))	30
DNJ_34	20
DNJ_16	20
73240	25
2024_05_23_GEUS_THORNING2D_P1_Final_PSTM_FullStack_AGC	-14
2024_05_23_GEUS_THORNING2D_P2_Final_PSTM_FullStack_AGC	-35
2024_05_23_GEUS_THORNING2D_P3_Final_PSTM_FullStack_AGC	-32
2024_05_23_GEUS_THORNING2D_P4_Final_PSTM_FullStack_AGC	-8
2024_05_23_GEUS_THORNING2D_P5_Final_PSTM_FullStack_AGC	-8
2024_05_23_GEUS_THORNING2D_P6_Final_PSTM_FullStack_AGC	-35
2024_05_23_GEUS_THORNING2D_P7_Final_PSTM_FullStack_AGC	-28
2024_05_23_GEUS_THORNING2D_P8_Final_PSTM_FullStack_AGC	-17

The visual mis-tie screening shows some considerable time shifts (data mis-ties) between different seismic surveys, and between lines of the same surveys in the order of mostly approx. 5–30 ms TWT, with ranges up to 15 and 80 ms TWT in the worst cases.

To keep it feasible, the 2D sections crossing the position of the wells were assumed to be at the same datum corresponding to mean sea level (msl) as the seismic reference datum. Each line was analyzed and in case of a mis-tie, a manual constant time-shift for each seismic line was used for adjustment was applied. The adjusted and used time-shifts are shown in Table 4.1.2.

Mis-tie corrections for the surveys were only applied in this Petrel project for mapping purposes. It was not possible within the frame of this study to sort out all mis-ties, but mis-ties are described here for the present mapping and future consideration. It is important to be aware of the mis-ties and to adjust data, to avoid errors in interpretation and mapping.

4.2 New seismic data acquired in this project

The new seismic survey: GEUS2023-THORNING

The new 2D seismic survey, GEUS2023-THORNING, acquired over the Thorning structure, was organized by GEUS for the initial maturation described in this report, and with Uppsala University in charge of acquisition and first processing of the data. Each of the survey profiles are named: GEUS2023_THORNING_P1, -P2, -P3, -P4, -P5, -P6, -P7 and -P8 with a combined total length of c. 133 km.

The positions of the profiles are shown in Fig. 4.2.1, where they are abbreviated P1 – P8. Line extensions include a reference to the type of the geophone recording: streamer, wireless and merged (streamer & wireless together), and if the version is stacked (stk), or stacked and migrated (mig) - e.g., GEUS2023_THORNING_P1_WIRELESS_FDMIG.

Link to survey: ([Processing summary sheet \(geus.dk\)](#))

In addition, as mentioned above GEUS issued a reprocessing of the GEUS2023-THORNING survey: GEUS2023-THORNING-RE2024 with a name convention indicating if the data is a post-stack time-migrated section e.g., GEUS2023_THORNING-RE2024_P4_Final_PSTM_FullStack, also available from GEUS.

Link to survey: ([Processing summary sheet \(geus.dk\)](#)). Contact GEUS on data by email: info-data@geus.dk.

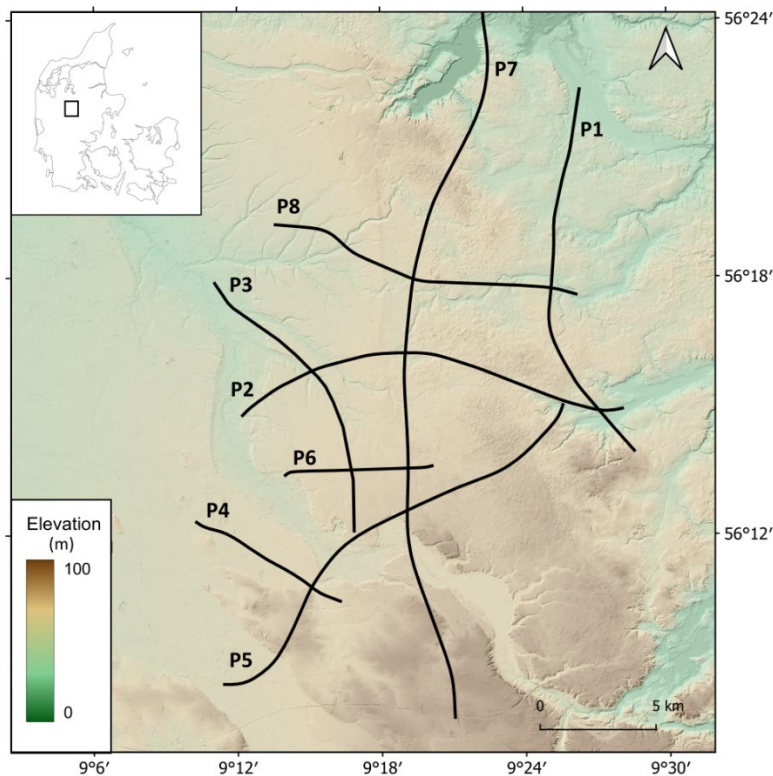


Figure 4.2.1. Topographic map of the Thorning study area with location of the seismic profiles P1 – P8 as reprocessed by Realtimeseismics. For information on data, contact GEUS (access from the website or email to info-data@geus.dk). Note the significant topographic features with a relatively flat sandur surface to the west in contrast to hilly landscape with valleys to the east.

Acquisition of the survey by Uppsala University

Background and purpose

Based on the experience from the previous onshore sites, GEUS and Uppsala University planned and designed the seismic survey for the Thorning structure, where eight profiles were acquired to establish the tie between various legacy data and extend the current seismic coverage in the study area.

The purposes of this cooperation acquisition project are mainly:

- 1) to acquire new seismic lines to improve the data coverage with modern data in the study area,
- 2) to collect new data for maturing the Thorning structure towards potential storage of CO₂,
- 3) to acquire modern high fold data for imaging and interpretation of the shallow and deeper subsurface, particularly the key reservoir-seal pair (Gassum and Fjerritslev formations), identification of faults and to obtain a better outline of the geometry of the Thorning structure,
- 4) to investigate and describe the geological development of the structure,
- 5) to expand knowledge of CCS operations through research and education, here in cooperation with universities.

The primary objectives of the survey are:

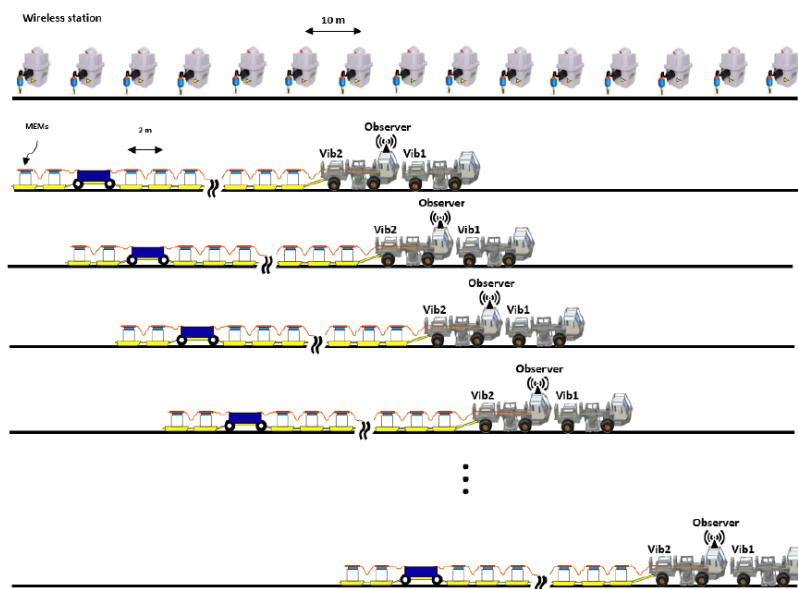
- Detailed and high-resolution reflection seismic imaging of geological features including several potential reservoirs and potential faults from near surface down to 3–4 km depth,
- Test the capability of using MEMs-based 3C seismic landstreamer and the planned setup (combined landstreamer and wireless recording as well as the sources used) for similar type studies on land in Denmark,
- Generating open access to science data for future research purposes.

The field campaign

The survey was conducted from August 9th to October 9th 2023, the seismic data were recorded along 8 lines with a total length of 133 km (Figs 4.2.1–4.2.3). Data and discussions were delivered and reported in the acquisition and processing report of April 2024 by Putnaite & Malehmir (2024) (Fig. 4.2.4).



Figure 4.2.2 A series of field photos showing different parts of the dual element acquisition setup including 4–5 segments (each 20 units and 2 m spacing) MEMs based and nodal recorders (spaced at every 10 m) where shots were generated using two 12t mini vibrators.



4.2.3 Survey layout and equipment. Sketch showing the data acquisition procedure of the dual-element recording system exemplified for a fixed geometry setup and how the field acquisition is carried out with the two mini-trucks equipped with vibration pistons, trailing behind a landstreamer system on the road and separate wireless geophones with a 10 m distance along the road.

As seismic sources, two small trucks (INOVA UNIVIB-326; operating at peak-force: 95 kN) were used with synchronized vibrating hydraulic pistons lowered in firm contact with the road (Fig. 4.2.3). Each truck has a weight of 12 tons, but this setup was changed to a single 18-ton source for profiles 6–8 due to mechanical challenges. Before the acquisition, the field personnel followed a road-safety course and were equipped with safety clothing during field-work.

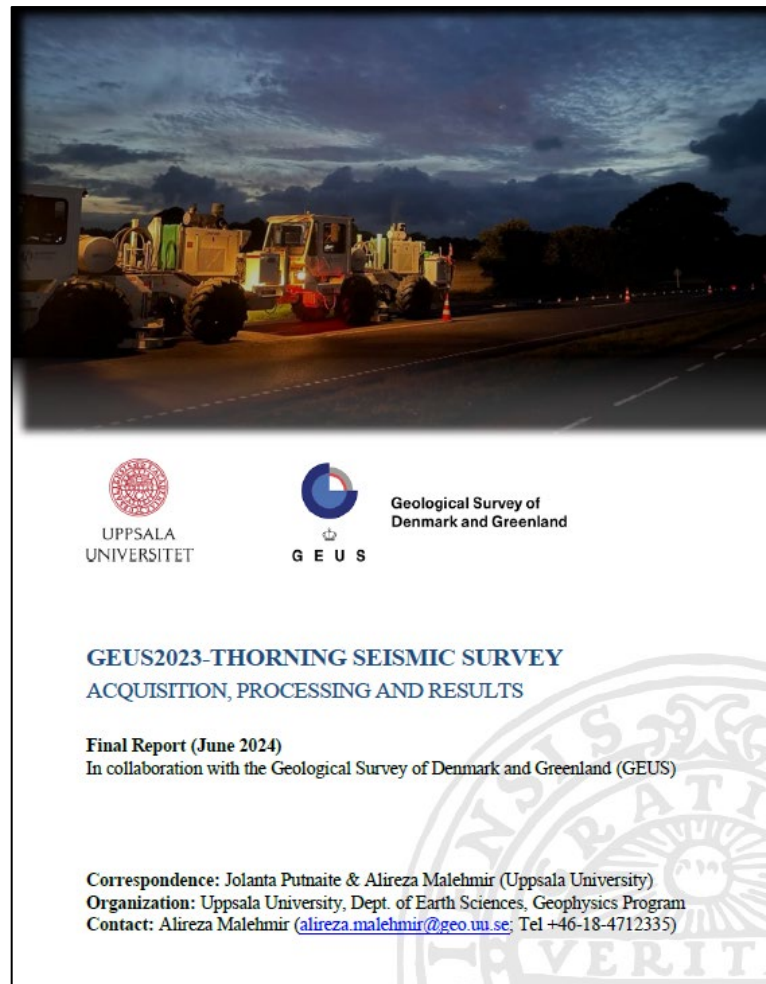


Figure 4.2.4. The front page and contents of the *GEUS2023-THORNING seismic survey: Acquisition, processing and results* (Putnaite & Malehmir, 2024), which can be purchased through GEUS (access via webpage, or email: info-data@geus.dk).

The trucks generated a simultaneous sweep lasting 18 seconds, increasing in frequency from 10 Hz to 140 Hz (Fig. 4.2.2; Table 4.2.1). At every shot-point location this sweep was repeated three times. The three sweeps were later stacked to one shot-point during the processing to improve signal-to-noise ratio. After each shot-point with three sweeps, the trucks move 10 meters (shot-point distance) to the next shot-point. The last truck drags the attached landstreamer, adjusted along the road by field assistants (Fig. 4.2.2). The selection of the frequency range, sweep frequency, and other acquisition parameters are based on the pilot and upscaling work conducted in Denmark prior to the Thorning survey (Malehmir et al., 2022; Zappalá et al., 2022; Papadopoulou, Myrto et al., 2023).

When passing close to private properties, control measurements with a sensitive ‘Micromate’ device were carried out at the properties to ensure, that vibrations stayed below a threshold,

as defined by the German norm DIN 4150-3. If the vibrations approached the threshold, the vibrations were stopped or continued with a smaller vibration level, and in some cases with sensitive properties the shot-point was skipped.

The landstreamer recording system was assembled within the second seismic vibrator, which was dragging the landstreamer. The inbuilt GPS antenna within the landstreamer allowed accurate GPS time tagging and sampling of the streamer data, which were later used for harvesting the data recorded on the nodal units. The operator was responsible for triggering the data acquisition, live quality control of the data, and to note in the observer's log any relevant information during the survey. Given that the landstreamer was dragged along the road (including gravel roads), few of the field crew members oversaw the steering of the landstreamer to make segments straight or to follow the shape of the road. DGPS measurements were taken at every nodal unit, and vibration monitoring of infrastructure was done for safety and damage reporting purposes.

Depending on the length of the profiles, a fixed or an asymmetric split-spread roll-along geometry for the nodal arrays was used (e.g., if a profile was longer than 8 km). Approximately 700–750 nodal recorders were used on average line for any shot record, providing a nominal CMP fold of approximately 350, which is judged excellent for such a purpose. As for the landstreamer, depending on the complexity of the road and logistics, up to 100 units (200 m long) were used providing a nominal CMP fold of 50 for the streamer data. The sampling rate of the nodal recorders was set to 2 ms, while for the MEMS units sampling was 1 ms. This sampling was justified given the sweep range of 10–140 Hz used for the seismic survey. A total listening time of 25 s was used to ensure that at least 5 s of data can be used for data processing and for imaging purposes. Considering that landstreamer units were dragged along with the seismic vibrators, the coordinates of the units were interpolated based on the surveyed coordinates from the fixed nodal recorders. The procedural operation of the data generation is sketched in Fig. 4.2.3.

Table 4.2.1: Key elements of the acquisition parameters of the Thorning seismic survey (Putnaite & Malehmir, 2024).

Survey Parameters		
Recording system	Sercel Lite	
Source	INOVA UNIVIB-326 (2 x 12t, 95 kN per truck; profiles 1-5) BIRDWAGEN MARK IV (1 x 18t, 128 kN; profiles 6-8)	
Source sweep	10 Hz to 140 Hz linear sweep over 18 s 3 sweeps per shot point	
Shot point spacing	10 m	
Geodetic surveying	Reach RX RTK DGPS	
Recording Parameters	Landstreamer	Nodal recorders
Receiver spacing	2 m	10 m
Spread type	End-on spread	Fixed to split spread
Offset (near, far) (average)	(120 m, 220 m)	(0 m, 7500 m)
Receiver	MEMS 3C	10 Hz spike
Sampling interval	1 ms	2 ms
Record length	25 s	25 s
(before; after cross-correlation)	5 s	5 s

Collaboration partners

Uppsala University contracted the Polish company Geopartner Sp. zo.o with two small trucks with vibration hydraulic pistons as a source for the vibro-seismic data. Students in Geophysics and Geoscience from the University of Copenhagen, Århus University and Uppsala University were hired as field assistants to conduct field support, including handling, and moving the wireless geophones with Differential GPS surveying, adjusting the landstreamer, handling the road traffic signs, distributing information folders and flyers to citizens.

COWI was contracted for acquiring permits, logistical planning, assessments in relation to landowners and supported on external contacts with authorities and citizens.

Communication & meetings

Communication with the local community was provided through two public information meetings on May 3, 2022, and November 14, 2022. A public visit day took place on June 17th, 2023, and information flyers and folders were distributed and provided to landowners in the vicinity of the acquisition prior to that date, as well as additional information on the website of the project.

In addition, local medias made interviews and articles regarding the acquisition, and the local TV stations made minor recordings from the field, e.g. <https://businesslf.dk/co%E2%82%82-lager-ved-THORNING-skal-loese-klimaproblem/>.

Processing of the seismic survey by Uppsala University

Immediately after seismic data acquisition seismic processing from raw SEG-D field data to final post stack migration was performed at Uppsala University. Almost identical processing sequences have been applied to the wireless data recordings and the short offset landstreamer recordings. In the first processing step shot and receiver geometry are included in the seismic trace header and output data are in SEG-Y data format. Secondly, cross correlation of the raw recorded vibrator signal with the theoretical source sweep has been applied to get the seismic response. Subsequently the three (3) sweeps for each source location are then summed together to increase the signal-to-noise ratio.

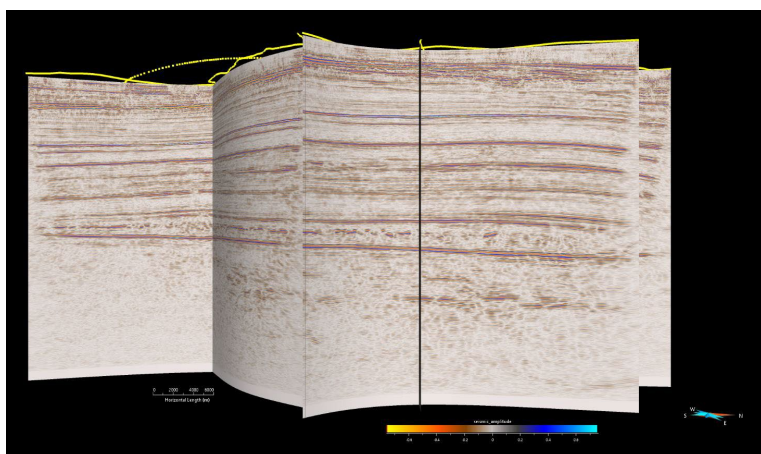


Figure 4.2.4 *Example of 3D view showing key horizons successfully imaged using nodal data after using a post-stack migration workflow by Uppsala University.*

The first run of the Uppsala University processing of the GEUS2023-THORNING seismic survey was a relatively fast-track seismic processing of the dataset and the results have immediately been included in an updated seismic mapping of the Thorning structure (Chapter 6). For getting this fast-track processing, a conventional post-stack migration has been applied to the dataset, see Tables 4.2.2 and 4.2.3.

The processing workflow for the landstreamer data are almost identical to the workflow for the wireless data. Details are found in the Final Acquisition and Processing Report of the GEUS2023-THORNING survey (Putnaite & Malehmir, 2024).

Table 4.2.2: Key elements of the processing workflow for merging the landstreamer and nodal data for the Thorning seismic survey (Putnaite & Malehmir, 2024).

Processing step	Details	
	<i>Landstreamer</i>	<i>Nodal recorders</i>
1. Import SEG-D data	✓	✓
2. Cross-correlation with theoretical sweep	✓	✓
3. Vertical stack of repeat shots (diversity)	✓	✓
4. Trace editing	✓	✓
5. Geometry setup and CMP binning	5 m CMP spacing	5 m CMP spacing
6. Conversion to minimum phase	✓	✓
7. First arrival picking		✓
8. Elevation statics	Topographic statics using replacement velocity of 1700 m/s and reference elevation of 130 m	
9. Refraction statics	✓	✓
10. FK filter		✓
11. Surface wave denoising		✓
12. Gapped deconvolution	18 ms	24 ms
13. Bandpass filter	(20–30–135–140) Hz	(10–20–120–140) Hz
14. Spherical divergence		✓
15. Amplitude balance	AGC (300)	Rolling Balance
16. Airwave attenuation (337 m/s)		✓
17. Notch	48–52 Hz 80–84 Hz	48–52 Hz 80–84 Hz
18. Velocity analysis		✓
19. Reflection-based residual statics	Nodal residual statics + one round	Two rounds
20. NMO corrections	Picked stretch mute	Picked stretch mute
21. Stack	✓	✓
22. FX-deconvolution coherency filter	✓	✓
23. Amplitude balance	Rolling Balance	Rolling Balance
24. Bandpass filter	(20–40–130–135 Hz at 0–720 ms & 20–30–130–135 Hz at 770–5000 ms)	(15–25–120–140 Hz at 0–720 ms & 10–20–120–140 Hz at 770–5000 ms)
25. Seismic reference datum correction	✓	✓
26. Mean sea-level correction	✓	✓
27. Finite-difference migration	✓	✓

Table 4.2.3: Key elements for merging the landstreamer and nodal data for the Thorning seismic survey (Putnaite & Malehmir, 2024).

	Processing step	Details
1.	Merge datasets	Both pre-stack processed datasets were merged (sampling rate 2 ms).
2.	Geometry setup and CMP binning	Re-binning using the same crooked line with 5 m bin spacing.
3.	Alignment of datasets	Bulk shift of streamer traces by 10 ms.
4.	Elevation statics	Topographic statics using replacement velocity of 1700 m/s and reference elevation of 130 m (pre-merged datasets had respective elevation statics reversed prior to merging).
5.	Reflection-based residual statics	One round
6.	Spectral equalization	(10–20–135–140 Hz, length: 30)
7.	Amplitude balance	Rolling Balance
8.	NMO corrections	Picked stretch mute
9.	Stack	✓
10.	FX-deconvolution coherency filter	✓
11.	Amplitude balance	Rolling Balance
12.	Bandpass filter	(10–20–135–140) Hz
13.	Seismic reference datum correction	Fixed datum at 130 mm
14.	Mean sea-level correction	✓
15.	Finite-difference migration	✓

Deliverables from Uppsala University

Attached to this report are the following deliverables delivered at various stages of the processing work:

- Raw SEG-D data
- Theoretical sweeps as SEG-Y (2ms and 1 ms)
- Observer logs (scanned copies, .pdf), differential gps (dgps), pft and monitoring data files
- Correlated and reduced time shot gathers with textural headers for both landstreamer and nodal arrays (SEG-Y format, SHOT_PEG: 17, CDP: 21, CDP_X: 181 and CDP_Y: 185, each four byte, SEG standard reverse polarity)
- Brute unmigrated stacks with textural headers for both landstreamer and nodal arrays (SEG-Y format, CDP: 21, CDP_X: 181 and CDP_Y: 185, each four byte, SEG standard reverse polarity)
- Final unmigrated stacks with textural headers for landstreamer, nodal and merged data (SEG-Y format, CDP: 21, CDP_X: 181 and CDP_Y: 185, each four byte, SEG standard reverse polarity)
- Final migrated stacks with textural headers for landstreamer, nodal and merged data (SEG-Y format, CDP: 21, CDP_X: 181 and CDP_Y: 185, each four byte, SEG standard reverse polarity)
- Final NMO velocity models in .txt and .seg-y format (SEG-Y format, CDP: 21, CDP_X: 181 and CDP_Y: 185, each four byte)
- Final statics in .txt formats (.shf) for elevation, refraction and residual static corrections and refraction models as SEG-Y.

Navigation files in .txt formats: CMP locations, receiver locations, active spread information and source locations.

4.3 Reprocessed seismic data applied in this project

Realtimeseismic (RTS) reprocessed the seismic data sets from the GEUS2023-THORNING 2D survey with the following objectives:

1. Obtaining optimal resolution for identifying key geologic formations and features in the study area.
2. Suppressing the crooked line artefacts.
3. Ensuring the optimal tie between the seismic lines.

The reprocessing project, GEUS2023-THORNING-RE2024, lasted around eight weeks, from 3 April to 6 June 2024. It aimed to improve the migrated stack profiles from the original processing and significantly contribute to the current geological interpretation of the Thorning structure. The reprocessed seismic data and the comprehensive reprocessing report are available on the GEUS' website: [GEUS2023-THORNING-RE2024 \(geus.dk\)](https://geus.dk/GEUS2023-THORNING-RE2024). The general processing sequence implemented in the reprocessing is shown in Table 4.3.1.

Table 4.3.1 *Reprocessing sequence for the wireless seismic data from the GEUS2023-THORNING survey*

No.	Processing component
1	Input analysis
2	Geometry QC
3	Firstbreak picking
4	3D diving wave tomography
5	Refraction statics
6	Residual refraction statics
7	Stacking velocity picking
8	Reflection statics
9	Surface wave attenuation
10	High amplitude noise attenuation
11	Surface-consistent amplitude correction
12	Surface-consistent deconvolution
13	Time-variant filtering
14	3D regularization
15	Prestack time migration
16	Migration velocity updating
17	Residual moveout correction
18	Spectral shaping
19	Time-variant filtering
20	Trim statics
21	Outside mute
22	Dip estimate
23	Structure-oriented denoising
24	PSTM common image gather stacking
25	Post-stack enhancement

Static effects

Processing onshore seismic data is usually challenged by static effects due to factors such as dynamic topography and near-surface velocity heterogeneities. The most common practice of static correction involves first arrival modelling using refracted ray theory (Palmer, 1980). This theory assumes that the modelled interval velocities always increase with depth and that there are no vertical velocity changes within subsurface intervals. However, those assumptions are often violated, leading to failure in removing persistent static effects. To anticipate such issues, the reprocessing utilized tomostatics – an advanced static correction technique based on a velocity model generated using turning ray tomography (Zhu et al., 1992; Zhang and Toksöz, 1998). Using a turning ray forward model, tomostatics can accommodate a vertical velocity gradient within defined velocity intervals by implementing first arrival inversion. Tomostatics can also tolerate velocity decrease with depth, given that the overall velocity gradients still enable the rays to return to the surface within the recording offset. Using tomostatics, the reprocessing anticipated potential static-related artefacts due to complex near-surface geology and missing near-surface refractors (Zhu et al., 1992; Zhang and Toksöz, 1998).

Besides the static correction, the implemented migration technique also plays a crucial role in the reprocessing. The reprocessing utilized a prestack time migration (PSTM) technique to anticipate conflicting dips with different stacking velocities and complex non-hyperbolic moveouts (Yilmaz, 2001).

Crooked line artefacts

Due to the logistic setup of the seismic field campaign, it was only possible to acquire the seismic data along public roads. This causes significant challenges with particular seismic signal characters in the new GEUS2023-THORNING 2D seismic data due to crookedness, i.e., bending of the roads and irregular acquisition geometry.

Crooked lines cause irregular source-receiver offsets along the lines and shift reflection points away from the lines, producing midpoint dispersion and uneven subsurface wavefield illumination, as illustrated in Fig. 4.3.1.

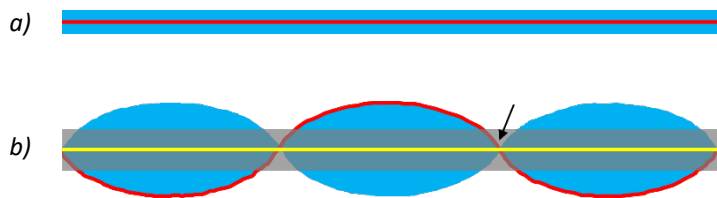


Figure 4.3.1. Illustration of the effects of seismic line shapes on midpoint locations. Red: seismic lines; blue: midpoint locations (midpoint dispersion in the case of the crooked line);

yellow: a smoothed binning line from the crooked line; grey: a binning area for the smoothed line; the arrow highlights an example of binned areas with potentially missing traces in the offset classes. (a) A straight seismic line produces midpoints exactly below the line; the crossline binning is unnecessary because all the reflections are in-plane. (b) A crooked line produces midpoint dispersion away from exactly below the line.

Crooked lines can also cause uneven fold coverage due to irregular trace distribution and missing traces in the offset classes. The low fold coverage at the crooked areas produces

migration artefacts, known as migration smiles, as the migration smears the amplitudes along the wavefield isochron. This phenomenon is similar to the migration effect at the ends of a seismic profile. Therefore, the crooked line artefacts found on a stack profile are arguably made up, at least part of it, by migration smiles.

To suppress the crooked line artefacts, the reprocessing implemented binning line smoothing followed by 3D regularization (Schonewille et al. 2009). The binning line smoothing aimed to achieve even fold coverage. On the other hand, the 3D regularization ensured even fold coverage by filling the missing traces in the bins and offset classes.

Reprocessing test to suppress crooked line artefacts

GEUS and RTS did a test to understand the crooked line artefacts and to assess the binning line smoothing approach. The test had been carried out prior to the current reprocessing project (GEUS2023-THORNING-RE2024) and implemented on line P4 (i.e. the test line) from GEUS2023-RØDBY 2D survey (Abramovitz et al., 2024), which also produced a couple of crooked lines.

Figure 4.3.2a shows the final PSTM stack profile from the test line obtained without the binning line smoothing and 3D regularization, and the profile shows prominent crooked line artefacts. In any case, the reprocessing required subtle binning line smoothing for all lines without altering the main crookedness trends. "Without line smoothing" in this context is synonymous to the subtle binning line smoothing. The intermediate processing output before the final PSTM stack is the raw PSTM stack, shown in Fig. 4.3.2b, and the same crooked line artefacts as in the final PSTM stack are also remarkable in the raw PSTM stack. Since the final PSTM stack is made up of the raw PSTM profile after residual moveout correction, demultiple, spectral shaping, time-variant filtering, trim statics, structure-oriented denoising, and poststack enhancement (Table 4.3.1), it is confirmed that the artefacts are not caused by any or the combination of those processes.

The effects of binning line smoothing and 3D regularization on the stack profile were then tested. Figure 4.3.3 shows a stack profile from the test line before the migration, with the binning line smoothing and with (Fig. 4.3.3a) and without (Fig. 4.3.3b) the 3D regularization. Both profiles in Fig. 4.3.3 show that the crooked line artefacts are barely noticeable before the migration, indicating that the artefacts are likely and mainly caused by the migration as migration smiles.

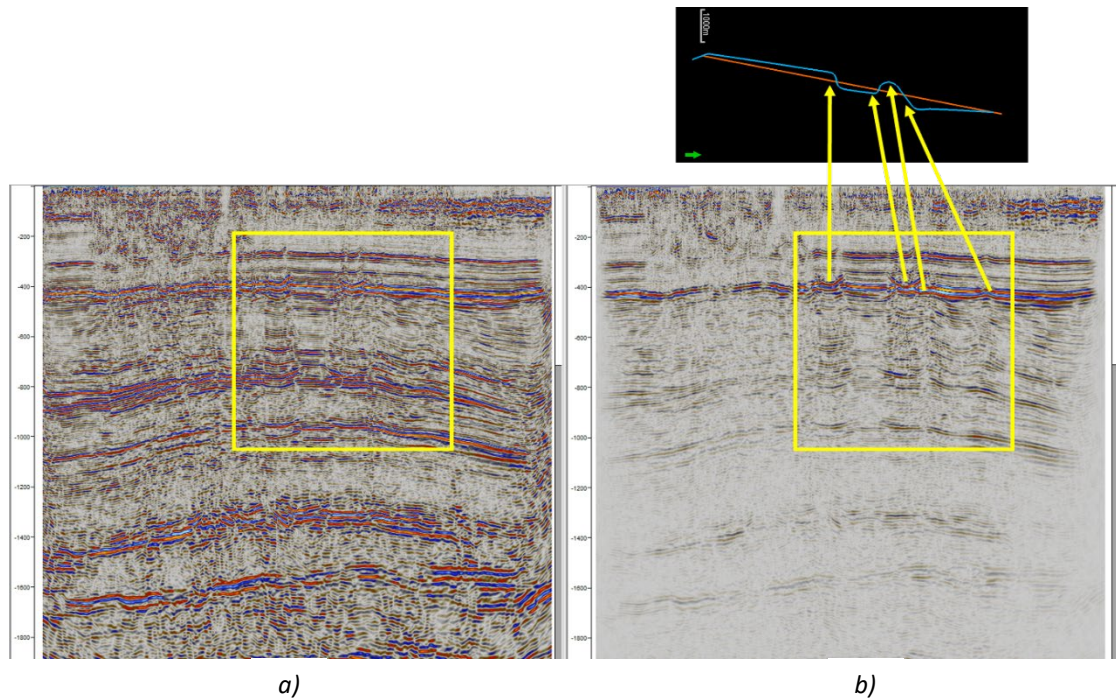


Figure 4.3.2 Prestack time migration (PSTM) stack profiles from the test line, i.e., line P4 of the GEUS2023-RØDBY survey (Abramovitz et al. 2024) without binning line smoothing. (a) Final. (b) Raw. The yellow boxes highlight the crooked line artefacts (migration smiles). The map shows the seismic line before (blue) and after (orange) smoothing. The yellow arrows show that the artefacts on the profile coincide with the crooked areas on the map.

The effects of 3D regularization on the test line independently from the binning line smoothing were also tested. Figure 4.3.4 shows the raw PSTM stack profiles (after migration) from the test line with binning line smoothing and with and without the 3D regularization. The figure shows that the migration smiles are not completely suppressed on the profile without the 3D regularization but mostly removed on the profile with the 3D regularization.

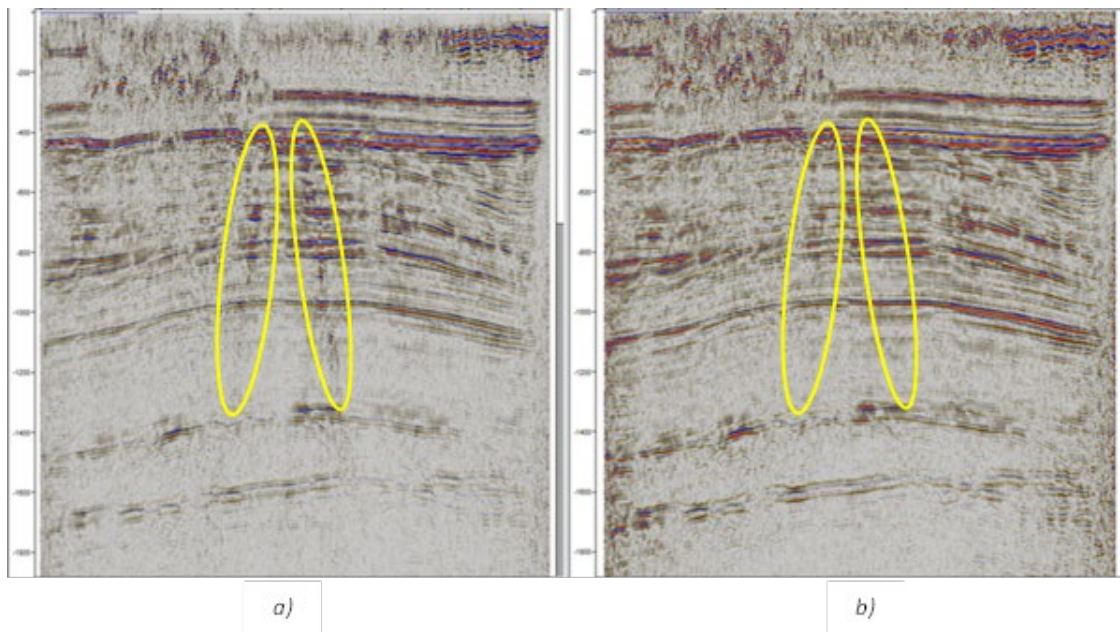


Figure 4.3.3 Stack profiles from line P4 of the GEUS2023-RØDBY survey (Abramovitz et al. 2024) before the migration and with the binning line smoothing. (a) Without the 3D regularization. (b) With the 3D regularization. Note the differences highlighted with the yellow boxes in the figure.

Overall, the test results confirm that the migration smiles make up the crooked line artefacts and that they can be suppressed by the binning line smoothing followed by the 3D regularization.

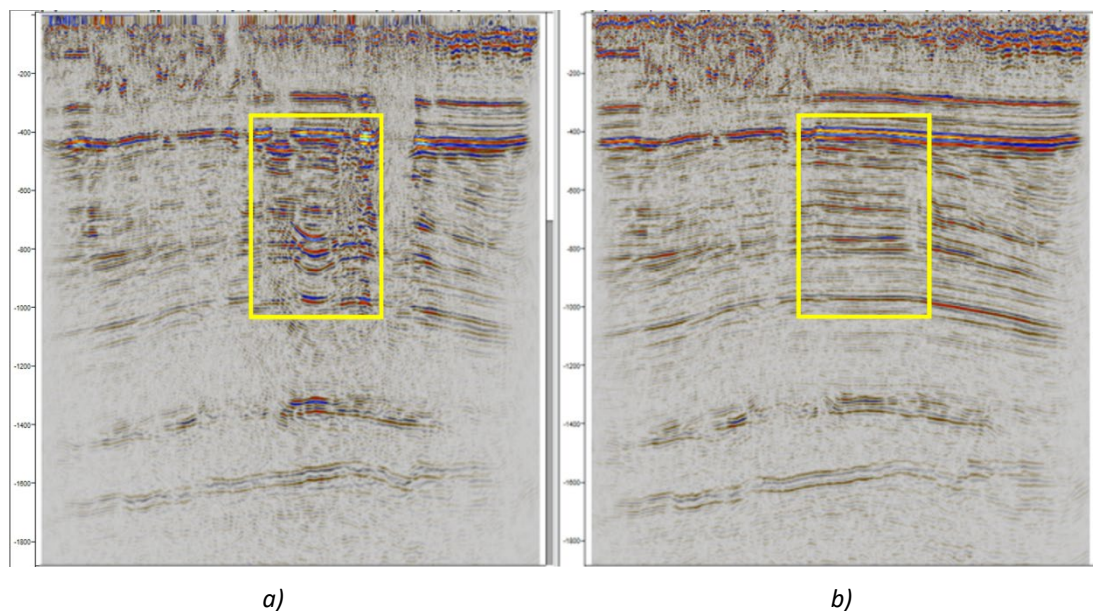


Figure 4.3.4 Raw PSTM stack profiles from the test line, i.e., line P4 of the GEUS2023-RØDBY survey (Abramovitz et al. 2024), with the binning line smoothing. (a) Without the 3D regularization. (b) With the 3D regularization. The yellow boxes highlight the migration smiles that are not entirely suppressed on the profile without the 3D regularization but mostly removed on the profile with the 3D regularization.

Reprocessing results

The reprocessing final results in terms of PSTM stack profiles show improvement from the poststack time migration (POSTM) stack profiles produced by the original processing.

As an example, Fig. 4.3.5 shows the comparison of the original and reprocessed migrated stack profiles from profile P6 of the GEUS2023-THORNING survey (see map in Fig. 4.2.1). The comparison indicates that the reprocessing has revealed more coherent reflectors than the original profile, and such improvement has allowed us to interpret geologic features and key reflectors associated with more confidence.

Discussion

The binning line smoothing followed by the 3D regularization is probably the quickest solution to suppress the crooked line artefacts – yet there are likely better approaches that can lead to more accurate seismic interpretation. Binning line smoothing of a crooked line means projecting the complex midpoint dispersion due to the line crookedness into a smooth binning line traverse. This approach basically shifts the seismic interpretation from the original line geometry onto another binning line traverse and likely includes unintended out-of-plane reflections from the dispersed midpoints. Nevertheless, although the approach of the binning line smoothing followed by the 3D regularization might not be the best to suppress the crooked line artefacts, it is considered the most reasonable approach that could still assist the seismic interpretation within a relatively short time.

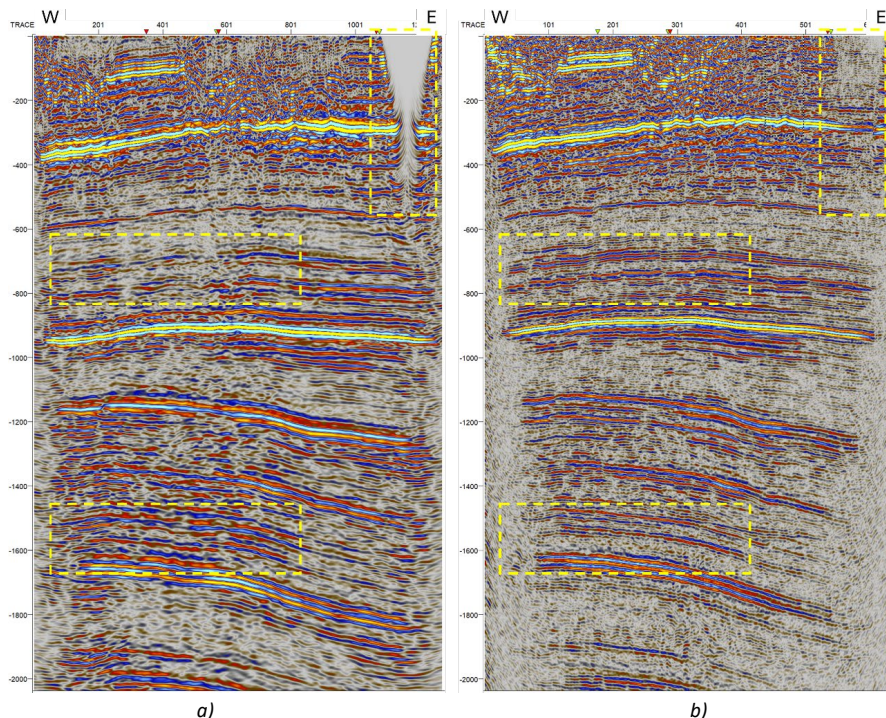


Figure 4.3.5 The comparison of (a) the original processing and (b) the reprocessing of line P6 from the GEUS2023-THORNING survey. The yellow boxes highlight examples where the

reflectors have been revealed more coherently in the reprocessed profile than in the original processing profile.

In principle, crooked seismic lines violate a fundamental assumption in 2D seismic imaging, that is, a straight-line geometry with a regular offset pattern and an even fold coverage. Therefore, problems related to the midpoint dispersion and the uneven fold coverage caused by crooked lines can hardly be resolved only by conventional 2D seismic imaging (Wu 1996). Conventional 2D seismic processing includes normal moveout (NMO) and dip moveout (DMO) corrections, which affect only the inline reflections. In addition to the NMO and DMO corrections, 2D crooked line seismic processing requires a correction also for the out-of-plane reflections in the presence of dip through so-called cross-dip moveout (CDMO) correction (Nedimović & West 2003).

Instead of simply projecting the midpoint dispersion onto a smooth binning line traverse, studies show that more appropriate ways to deal with a crooked line can generally be grouped into two categories: 1) correcting for the cross-dip reflections and 2) processing the crooked line in 3D.

Including in the cross-dip analysis techniques are the constant shift (Larner et al. 1979), the cross-dip moveout (CDMO) correction (Nedimović & West 2003), the iterative cross-dip moveout correction (Beckel & Juhlin 2019), the generalized cross-dip moveout (GCDMO) correction (Mancuso & Naghizadeh 2021), and the 2.5D multifocusing imaging (Fam et al. 2023). Nevertheless, all these techniques have considerable limitations, including laborious computation and limited accuracy for far-offset data acquired from a severely crooked line.

On the other hand, processing a crooked line in 3D is relatively more straightforward than a cross-dip correction-based approach. Processing a crooked line as 3D takes the advantage of having the midpoint dispersion by using it as pseudo-3D or 2.5D reflection points (Schmelzbach et al. 2007; Wu 1996). The pseudo-3D nature of midpoint dispersion from crooked lines allows us to image complex 3D structures around the crooked areas by binning and processing the data from the crooked lines in 3D. The main limitation of this approach is that it can produce low-resolution images due to a low fold coverage in areas not well illuminated by the recorded wavefield.

Looking to the future, we propose further studies to implement seismic processing techniques for overcoming crooked line artefacts, particularly the 2.5D multifocusing imaging (Fam et al. 2023) and the crooked line processing as 3D. These innovative approaches hold great promise, as they have the potential to bring more accurate subsurface seismic images, thereby enhancing the reliability of subsurface geologic interpretation.

4.4 Well data

The Thorning structure is an undrilled structure with the nearest well, Nøvling-1, located c. 33 km to the west. The Nøvling-1 and Kvols-1 wells are suitable for performing seismic well tie (see Chapter 5). However, numerous wells exist in central Jutland around the greater Thorning area and 14 wells are thus used for tying the seismic marker horizons (Fig. 1.2, Table 4.4.1). The wells Vemb-1, Linde-1, Vinding-1 (no logs), Mejrup-1 and Oddesund-1 are situated to the west; the Rødding-1, Skive-1 and Skive-2 to the north; the Hobro-1, and Gassum-1 (no sonic log) to the northeast, as well as the Horsens-1 located further to the southeast, Grindsted-1 to the southwest, Jelling-1 and Løve-1 to the south.

Well logs are used for interpretation of lithology, formation picks and selected logs are used for well log-based sequence stratigraphy, seismic to well ties and for seismic reservoir characterization and interpretation. See Chapters 5–7 for the specific used well logs.

Original logs: Caliper (CAL), Gamma-Ray (GR), Spontaneous Potential (SP), Compressional Sonic (DT), Deep Resistivity (R_DEEP), Neutron Porosity (NPHI), and Density (RHOB) logs.

Derived (interpreted) logs: Volume of shale (V_{shale}), Effective porosity (PHIE), and Permeability (PERM_GEUS) estimates. The latter were derived from porosity-permeability relationships, established based on an analysis of core analysis data.

Table 4.4.1. List of the wells utilized in this study, with information on the year of drilling completed, operator, Kelly Bushing (KB, meter above mean seal level), Total Depth (TD, meter below Kelly Bushing, measured drilled depth), deviation and chronostratigraphy of the TD units.

Well	Year	Operator	KB a. msl (m)	TD b. KB (m)	Deviated	TD
Nøvling-1	1966	Gulf	69,2	3762	No	Permian
Kvols-1	1976	MÆRSK OLIE OG GAS AS	19,2	2641	No	Triassic
Mejrup-1	1987	Phillips	50,0	2532	No	Triassic
Vinding-1	1947	(DAPCO) GULF	61,6	2434	No	Triassic
Oddesund-1	1976	MÆRSK OLIE OG GAS AS	11,0	2551	No	Triassic
Skive-1	1976	MÆRSK OLIE OG GAS AS	28,0	2318	No	Triassic
Skive-2	1985	BP	35,1	1456	No	Triassic
Hobro-1	1974	Gulf	32,3	2619	No	Triassic
Gassum-1	1951	(DAPCO) GULF	557,9	3462	No	Permian
Rønde-1	1966	Gulf	42,1	5300	No	Permian
Horsens-1	1958	(STANDARD) DAPCO	56,8	1729	No	Triassic
Grindsted-1	1958	(STANDARD) GULF	34,9	1650	No	Trias/Pre-Cambrian
Jelling-1	1992	DANOP	97,6	1992	No	Permian
Løve-1	2011	GMT Exploration Co.	95,0	2461	No	Permian

5. Methods

5.1 Seismic interpretation and well-ties (Chapter 6)

The undrilled Thorning structure, its formation and stratigraphy with reservoir-seal pairs, is investigated and evaluated from a structural and stratigraphic perspective, based on the available 2D seismic data and seismic well-ties to nearest wells (Nøvling-1 and Kvols-1).

Seismic horizons and successions are identified and interpreted using reflector terminations such as onlap, downlap and truncation and have been correlated to numerous wells in central Jutland around the greater Thorning area, such as the wells Nøvling-1, Vemb-1, Linde-1, Vinding-1 (no logs), Mejrup-1 and Oddesund-1 to the west; the Rødding-1, Kvols-1, Skive-1 and Skive-2 to the north; the Hobro-1, and Gassum-1 (no sonic log) to the northeast; the Horsens-1 located further to the southeast, as well as the Grindsted-1 to the southwest, and Jelling-1 and Løve-1 to the south. Seismic well tie is the process in seismic interpretation where surface measurements obtained at a wellbore measured in depth is calibrated to the seismic data measured in time by establishing a time-depth relation that ensures a reasonable match between synthetic and seismic data at the target level.

The seismic stratigraphic horizons are viewed as representing chronostratigraphic surfaces and in this limited study area they are regarded as near base or top formation boundaries. Horizon names are for simplicity identical to the formation names tied from the nearest wells, particularly the deep Nøvling-1 and Kvols-1 wells. The seismic stratigraphic boundaries and units should on a regional scale have more neutral naming (as e.g., in Nielsen 2003; Boldreel et al. in review). At the same time, faults, salt structures, and folds were identified and mapped together with internal configuration and thickness patterns. A structural and tectonostratigraphic interpretation was carried out using the chronostratigraphic framework from the well ties.

The Petrel (2024) software was used for establishing the database, seismic interpretation with manual and auto-tracking of the horizons and seismic well-ties including generation of synthetic seismograms. In total, twelve regional seismic stratigraphic horizons were interpreted in the Thorning area to determine the stratigraphy, geological evolution, and most important to define reservoir-seal pairs and structural closures (see Chapter 6). The regional horizons are from the oldest to youngest: (1) Top pre-Zechstein Group, (2) Top Zechstein Group, (3) Top Skagerrak Formation / Bunter Sandstone Formation, (4) Top Ørslev Formation, (5) Top Falster Formation, (6) Top Tønder Formation, (7) Top Vinding Formation, (8) Top Gassum Formation, (9) Top Fjerritslev Formation, (10) Top Frederikshavn Formation, (11) Base Chalk Group, and (12) Top Chalk Group (Figs 5.1, 5.2; and Table 5.1).

In addition, the deepest mappable horizon (Top pre-Zechstein) was interpreted on most lines and correlated from the Nøvling-1 to the Rønde-1 well further east outside the study area, to explain the earliest part of the tectonostratigraphic evolution of the region. These two deep wells contain the Silurian Nøvling and Rønde Formations that are the oldest drilled sedimentary rocks in central Jutland. The Nøvling-1 well terminates in the Silurian siltstones of the Rønde Formation at 3692 m below msl of Lower Ludlovian age.

Nevertheless, the most comprehensive and detailed mapping of horizons and faults has been performed of the successions from the Top Zechstein Group to the Top Fjerritslev Formation,

comprising the primary reservoir (Gassum Formation), primary seal (Fjerritslev Formation). Lithostratigraphic and sequence stratigraphic well-log boundaries (well-tops) are adjusted by time-depth relations to the seismic data and synthetic seismograms of the wells are used to constrain the seismic interpretation (see below; Fig. 5.1).

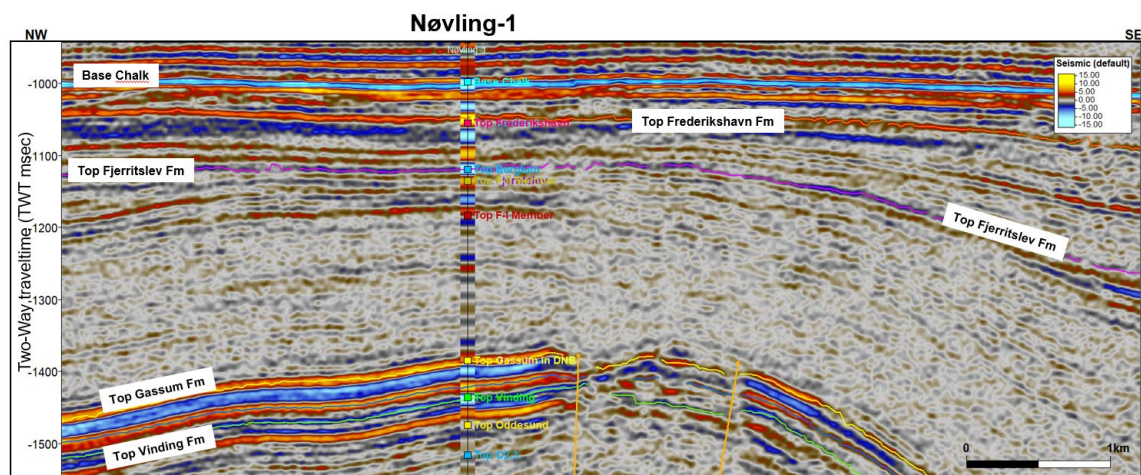
5.2 Well-to-seismic tie and synthetic seismogram

To utilize well log data and well tops (depth domain) with seismic data (time domain), a seismic-well tie procedure was performed on the Nøvling-1 and Kvols-1 wells, which both contains sonic and density logs as well as check shots, which were used as an initial time-depth relationship (Figs 5.1, 5.2). The time-depth relationship was adjusted manually by matching defined seismic reflections and corresponding TWT depths, and well tops in the wells.

Synthetic seismograms were produced to study and connect wells to seismic reflections for interpretation of the horizons (see also Chapter 6). The legacy 2D seismic lines in the greater study area vary between European SEG reverse or normal polarity, where a peak in the European SEG reverse polarity corresponds to a soft kick with downward decreasing acoustic impedance (AI). We use here mostly colored seismic profiles displayed in red-white-blue (red peaks and blue troughs) or black-grey-white (black peaks and white troughs) (this is valid for all figures in Chapter 6). The seismic follows normal polarity, with a positive reflection (boundary to higher acoustic impedance) placed in a peak (red or black) and a negative reflection (boundary to lower acoustic impedance) in a trough (blue or white) on the seismic displays of the new seismic data.

The Nøvling-1 well is located c. 33 km to the west of the Thorning study area and was drilled in 1966 by *Dansk Undergrunds Consortium*. The wireline logging program included sonic logs, density logs, electrical log, micro-resistivity, calliper, gamma-ray log, and check shots.

For the seismic well-tie, a synthetic seismogram was produced for the Nøvling-1 (Fig. 5.1) and Kvols-1 wells (Fig. 5.2) using the available density and sonic logs and compared to seismic data. Figure 5.3 is showing a composite seismic profile from Nøvling-1 to Kvols-1 with the marker horizons. For both wells, an analytical Ricker wavelet gave a good match, resembling a zero-phased wavelet with reverse polarity, and having several sidelobes due to the noisy seismic data (Figs 5.1, 5.2). The well-tie was made by a combination of bulk shifts and slight stretching to get the main marker horizons shifted to their correct positions with main emphasis on matching the Top Gassum to Top Vinding Formation intervals. The tie was quality controlled by observing reasonable interval velocities for the given lithologies. This resulted in a good correlation between the synthetic seismogram and the seismic data, thereby ensuring correct depths of well log information and well tops.



The Kvols-1 well is located at the coastline of the Hjarbæk Fjord c. 30 km to the north of the Thorning structure and was drilled in 1976 by *Dansk Undergrunds Consortium*. The wireline logging program included sonic logs, density logs, electrical log, micro-resistivity, calliper,

gamma-ray log, and check shots. The coastline location is suitable for calibrating the interpreted horizons to sea-level.

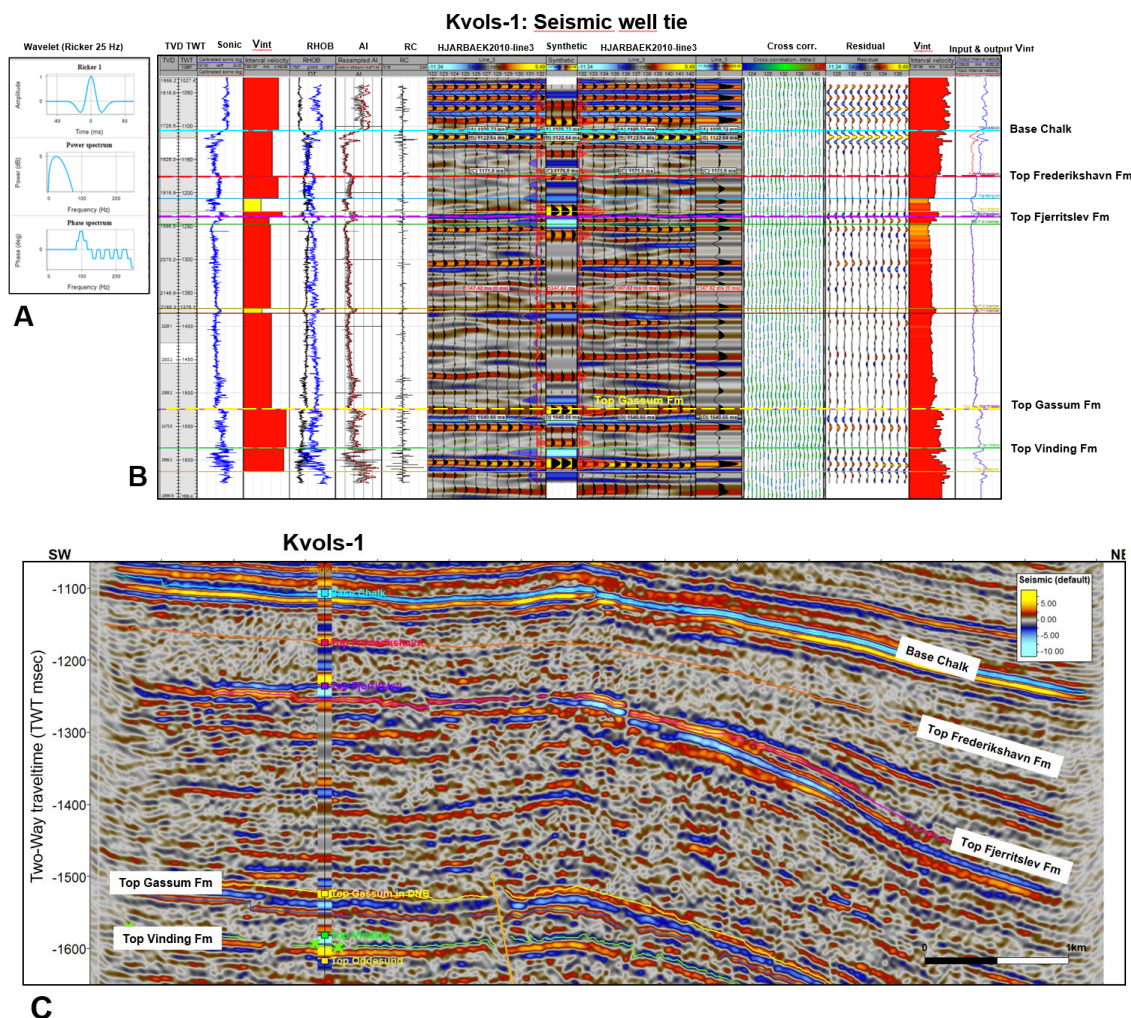


Figure 5.2 Seismic well tie of the Kvals-1 well A: The analytical Ricker wavelet used for the seismic well tie. B: Well to seismic tie of the Kvals-1 well using density and sonic logs, which cover the entire section from Base Chalk to Top Vinding Formation. Synthetic seismic trace is shown down along the well in red-black-blue display and on the 2D seismic line-3 from the Hjarbæk-2010 survey through the well. Well-tops and formations are also marked. C: A close up on the seismic section along Line-3 from the Hjarbæk-2010 survey showing the overall match between the real seismic data and the synthetic trace generated by the seismic well tie analysis inserted at the well position.

Based on the well ties to Nøvling-1 and Kvals-1, and with a similar approach as in the Stenlille and Havnsø areas, the Base Chalk follows a peak due to a significant drop in velocity from the Chalk Group into lower velocity marl and chalk of the underlying Rødby Formation (Gregersen et al., 2022; Gregersen et al., 2023). In the Thorning study area, we similarly define each interpreted horizon in either a peak or a trough seismic reflection (Table 5.1), where e.g., the Base Chalk follows a peak, the Near Top Fjerritslev follows a trough, and the Top Gassum follows a peak reflection etc.

Table 5.1 The interpreted thirteen regional seismic horizons, and the polarity picked.

#	Seismic horizon	Correlation on SEG normal polarity	Amplitudes
12	Top Chalk Group	Peak	Positive
11	Base Chalk Group	Trough	Negative
10	Top Frederikshavn Fm	Peak	Positive
9	Top Fjerritslev Fm	Trough	Negative
8	Top Gassum Fm	Peak	Positive
7	Top Vinding Fm	Trough	Negative
6	Top Tønder Fm	Peak	Positive
5	Top Falster Fm	Peak	Positive
4	Top Ørslev Fm	Trough	Negative
3	Top Skagerrak Fm / Bunter Sandstone) Fm	Peak	Positive
2	Top Zechstein	Peak	Positive
1	Top pre-Zechstein	Peak	Positive

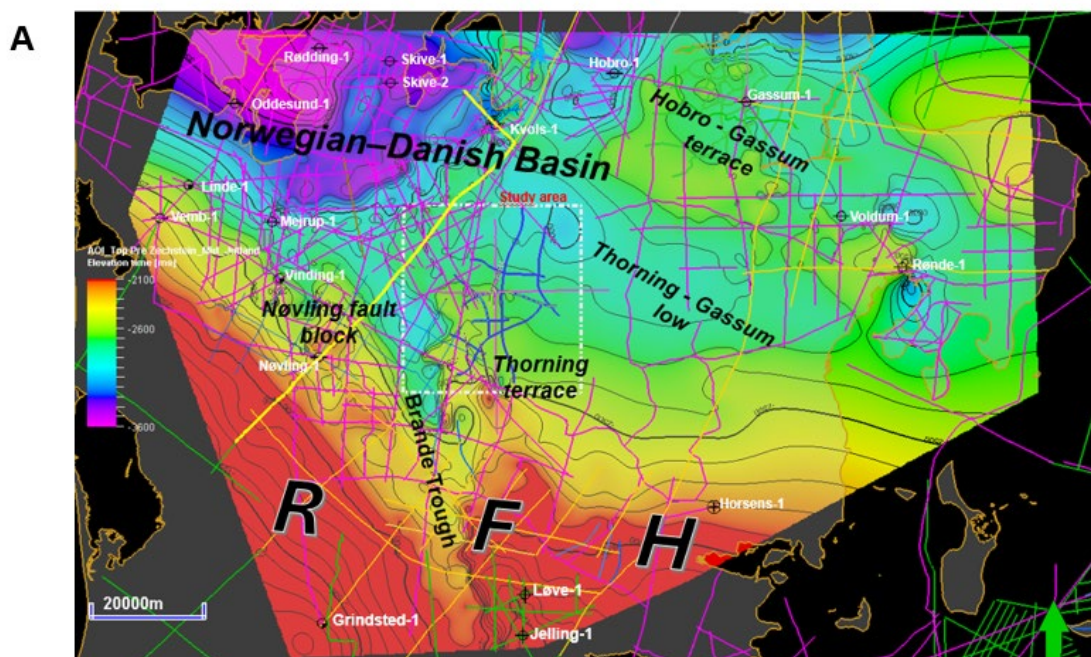
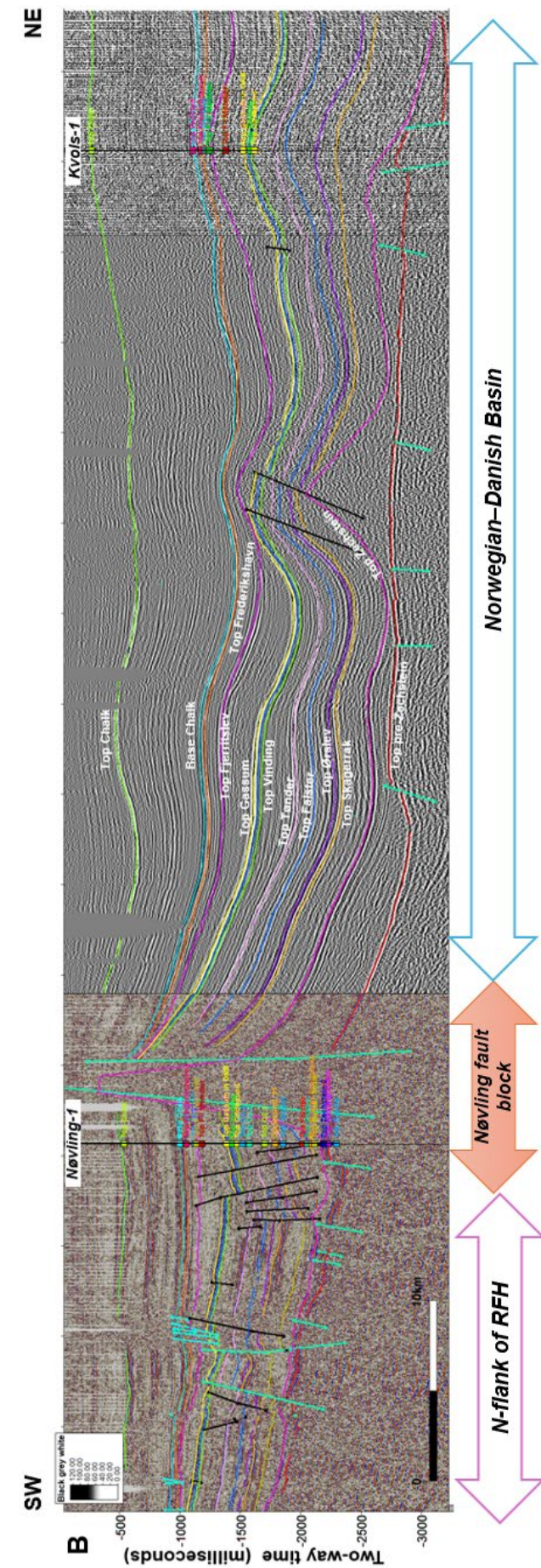


Figure 5.3 A: Location map showing the position of a composite seismic profile (yellow) from Nøvling-1 to Kvols-1 well imaged on top of the contoured structural depth map in milliseconds (ms) two-way time (tw) below mean sea level of the Top Pre-Zechstein surface. The structural depth map outlines the deepest parts of the sedimentary basin mapped over a large part of Central Jutland as is discussed in further details in Chapter 6. The main structural elements are the NE–SW-striking deeper part of the Norwegian–Danish Basin to the north, the Nøvling fault block (a continuation of the Ringkøbing–Fyn High), the NNW–SSE striking deep Brønde Trough, and the roughly N–S striking structural high or terrace underlying the Thorning area. B (next page): Seismic stratigraphic correlation of marker horizons along composite key profile with well-ties at the Nøvling-1 and Kvols-1 wells. The horizontal scale is 10 km, and the depth axis is shown in msec Two-Way travel-time. Major structural elements are indicated as corresponding to the map in (A).



5.3 Seismic time to depth conversion

A regional velocity model was constructed to convert the interpreted horizons from time domain to depth domain. The general idea of velocity modelling and depth-conversion is to have in 3D space a model of the average velocities in the subsurface. With these data, the corresponding depth of a Two-Way-Time horizon can be obtained since:

$$\text{Depth} = \text{One-Way-Time} * \text{Average Velocity}; \text{ or}$$

$$\text{Depth} = (\text{Time-Way-Time})/2 * \text{Average Velocity}.$$

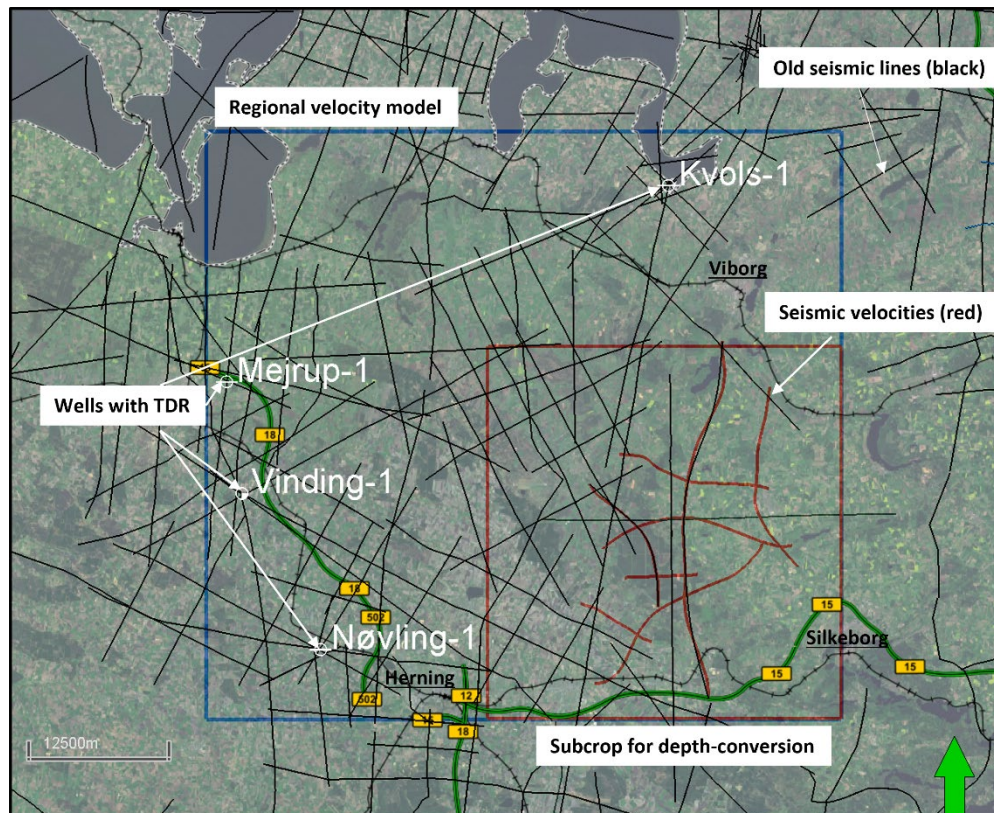


Figure 5.4 Area (55 by 50 km) of the regional velocity model (blue outline), showing the used four wells, vintage seismic data (black), and the RMS migration velocities from the new GEUS2023-THORNING-RE2023 2D seismic lines (red lines). The final depth-migration was performed within a subcrop area (31 x 32 km, red outline) defined by the Thorning structure.

Since data availability and quality deviates between the different structures (e.g. Gassum, Havnsø, Stenlille, and Jammerbugt), slight adjustments to the velocity model workflow are made to overcome technical challenges and uncertainties. Due to the absence of well data on the Thorning structure, from which normally the Time-Depth Relationship (TDR) is used for velocity corrections, and a complex regional geological structure, it was decided to use a simplified regional rectangular grid (55 x 50 km, 2750 km², blue outline in Fig. 5.4) to propagate seismic migration velocities. These velocities were corrected by using the TDRs from the four boreholes by using kriging (average velocities from TDRs) with 3D trend (propagated 3D seismic migration velocities). A subcrop that covered the entire Thorning structure with the new seismic data and the surrounding spill points defined the subcrop area (31 x 32 km, 992 km², red outline in Fig. 5.4).

The data available include:

- 1) Three wells (Mejrup-1, Nøvling-1, and Kvols-1) with checkshot data, where a seismic-well-tie procedure was made, and correlation of seismic markers were made based on regional tie-lines to the Thorning structure.
- 2) Estimated TDR in Vinding-1 from Nielsen and Japsen (1991) due to absence of density and sonic logs.
- 3) 12 Two-Way-Time (TWT) seismic horizons of the main stratigraphic units within the subcrop area, utilizing the legacy 2D lines (listed in Table 4.1.1) and including the new GEUS2023-THORNING-RE2023 lines):
 - a. Gridded to 100x100m,
 - b. Taking into fault polygons for the top of the Gassum Formation,
 - c. Smoothing of 1 iteration and a filter width of 5.
- 4) One additional TWT seismic horizon mapping a mounded structure on top of the Gassum Formation (Top Mounded Structure).
- 5) Seismic migration (RMS) velocities from the 2D lines (GEUS2023-THORNING-RE2023) (red lines in Fig. 5.4).

The general workflow was to establish a rectangular corner point grid first in TWT between 0 and 4500 ms and model the available average velocity sources within this 3D grid using geostatistical methods (kriging with 3D trend). This 3D average velocity function is then used to find the depth of each mapped horizon (Fig. 5.5).

The following steps were taken to account for vertical and lateral variations in average velocities found within the stratigraphic units as seen in the well TDRs and the seismic migration velocities.

2. *First*, a seismic-well-ties to Mejrup-1, Nøvling-1, and Kvols-1 was performed to tie borehole information and well tops to the seismic data. This time-depth relationship provided average velocities and formed input as primary data for kriging.
3. *Second*, a 3D average velocity cube was constructed using kriging with 3D trend (slightly adjusted methodology compared to the Stenlille study (Gregersen et al., 2022)):
 - a. A rectangular structural model in time was constructed spanning 0 and 4500 ms TWT, horizontal cell size of 250 m x 250 m, and vertical resolution of 50 ms (Fig. 5.5A).
 - b. The average velocities from the well time-depth relationship in the four wells were sampled (upscaled) into the structural grid (Fig. 5.6).
 - c. Seismic RMS velocities within the *GEUS2023-THORNING-RE2023* seismic survey were extracted as a point cloud with 30 ms sampling rate and sampled (upscaled) into the structural grid (Fig. 5.5A). The data was subsequently extrapolated within the grid using full tension option in Petrel (Spline in Tension algorithm).
 - d. A co-kriging operation was performed using the average velocities as primary data and 3D extrapolated seismic velocities as trend data (Fig. 5.5B). The co-kriging operation reduced the seismic velocities with ca. 200 m/s (~5 – 10%), like what has been encountered using velocity corrections with boreholes in the other 4 structures (Stenlille, Havnsø, Rødby, Gassum, Jammerbugt) (Fig. 5.6).
 - e. The velocity model was cropped to the subcrop area where seismic TWT horizons have been mostly constrained by the new 2D seismic data.

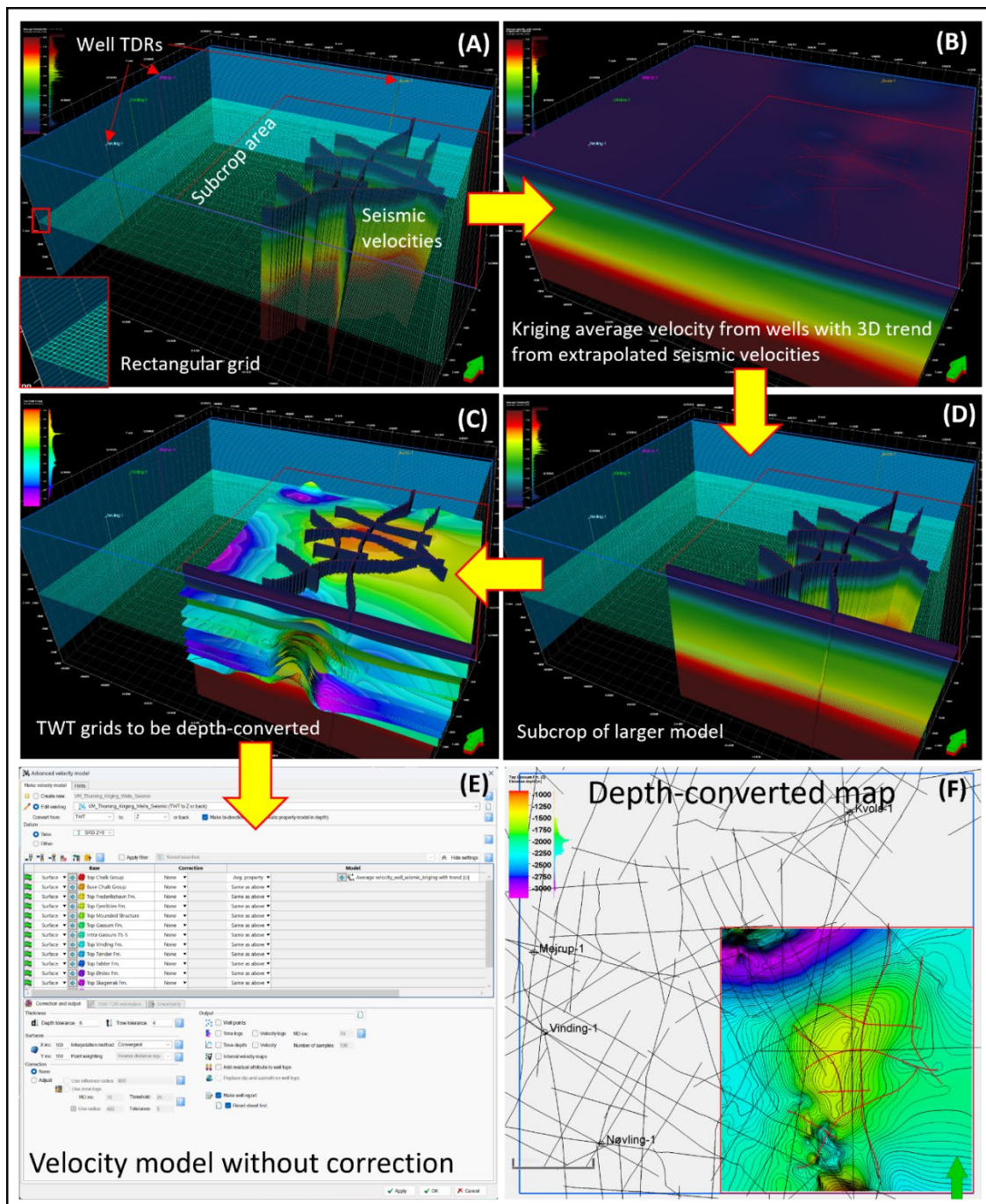


Figure 5.5. Velocity model workflow. A: Rectangular grid (250 m x 250 m x 50 ms) in the regional area to include average velocities from the time-depth relationships in the four wells. Also indicated are the seismic velocities from the new seismic survey GEUS2023-THORNING-RE2023. These data were sampled into the grid. Seismic velocities were extrapolated using Spline in Tension algorithm. B: The upscaled average velocity values were used as primary data for co-kriging, and the extrapolated 3D seismic velocities as 3D trend. C: 13 TWT horizons were carefully QC-ed and defined the subcrop area around the Thorning structure. D: Velocity model was cropped according to these outlines. E: The velocity model was created using the TWT horizons and 3D average velocity property. F: The surfaces were depth-converted with this velocity model.

4. *Third*, a multi-layer velocity model was created using the modelled 3D average velocities as velocity input, and 3D horizons were subsequently depth-converted using the co-kriged 3D average velocity property.
5. The velocity model is named VM_Thorning_Kriging_Wells_Seismic

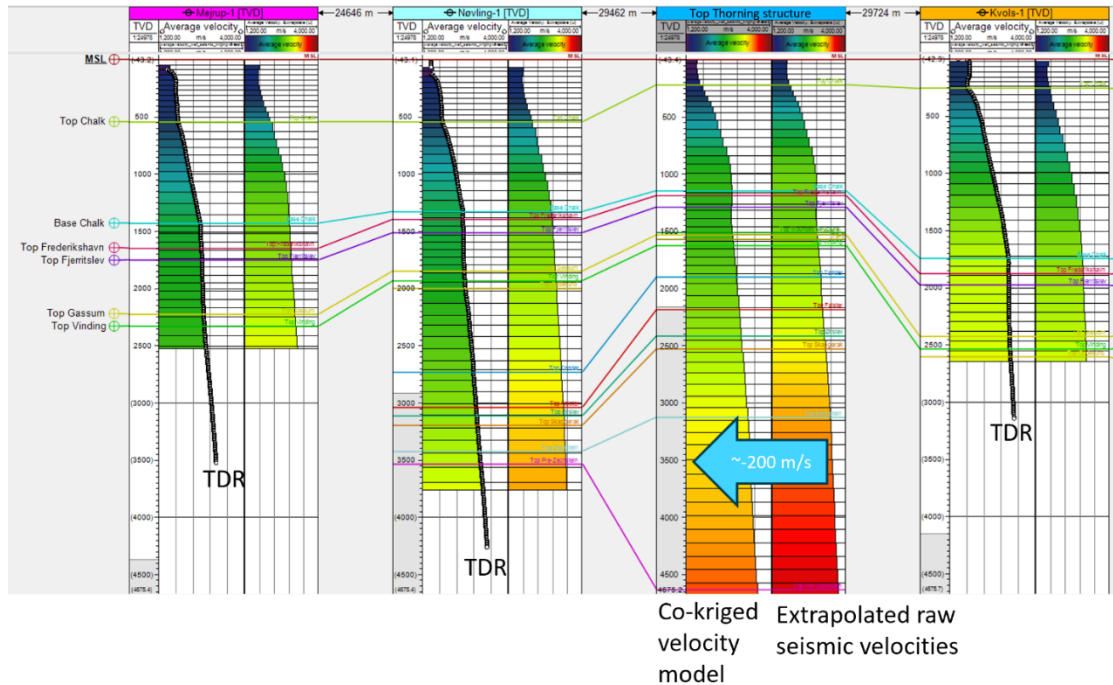


Figure 5.6. Average velocities (scale 1200–4000 m/s) from TDRs (dots) and upscaled and co-kriged values (left column). Right column raw seismic average velocities (same color scale) extrapolated within grid before being co-kriged with well derived velocities. Comparison shows approximately 200 m/s decrease in seismic velocities, or between 5–10 % decrease, similar to what has been observed in other structures.

Without a deep well within the Thorning structure, it is difficult to estimate the accuracy of the velocity model and therewith the depth uncertainty of the obtained surfaces. Since the surrounding wells provide the primary data for the kriging operation, the depth residuals are low here (1 – 10 m). Due to the correlation of the well-tied wells through regional seismic lines to the new 2D seismic data at the Thorning structure, the seismic TWT picks at Thorning are considered to be accurate (maximum few ms off the actual formation tops due to seismic resolution). The velocity trends at the Thorning structure (in a projected well-section at the crest of the top Gassum Formation surface) are consistent compared to the well location, thereby adding confidence in the general depth-conversion. The real values may only be known once a well is drilled, or more accurate values may be obtained when a 3D seismic survey is acquired.

5.4 Investigation of reservoir and seal (Chapter 7)

The geology of the reservoir and seal successions are described using well completion reports, publications, and in-house studies of well-logs and geological well samples mainly from cores. In addition, a limited number of studies focusing on lithology and biostratigraphy

are available. The data used are from the wells closest to the Thorning structure. The aim of these studies is to provide a more detailed understanding of reservoir and seal characteristics (see Chapter 7).

The reservoir characteristics presented and discussed in Chapter 7 are derived mainly from the acquired wireline logs from wells in vicinity of the Thorning structure, that are calibrated against conventional core analysis, descriptions of cuttings and sidewall cores. Potential reservoir units were identified from wireline logs by low formation resistivity, characteristic neutron-density log responses, pattern of the spontaneous potential log, and low natural radioactivity as recorded by the GR log and documented by cuttings containing sand-sized quartz grains.

In petrophysical terms, a sandstone reservoir is herein defined as a rock having < 50% volume of shale, and an effective porosity (PHIE) of > 10%. The permeability is estimated using published relationships between porosity and permeability, which is based on conventional core measurements.

Seal lithology, thickness and grain-sizes were similarly evaluated based on petrophysical logs, ditch cuttings samples and cores.

5.5 Methods – Storage Capacity Assessment (Chapter 8)

To compare the potential CO₂ storage of structures GEUS here uses a simple and accepted equation for saline aquifers, where static theoretical storage capacity of reservoir units with buoyant trapping is estimated from (e.g. Goodman et.al., 2011):

$$SC = GRV * N/G * \phi * \rho_{CO2R} * S_{Eff} \quad (1)$$

where:

- SC** Storage Capacity in mass of CO₂ (Mt).
- GRV** Gross rock volume (GRV) is confined by the upper and lower boundaries of the gross reservoir, where outline area of the structure is defined by the top point depth and deepest closing contour constrained by the spill point depth.
- N/G** Average net to gross reservoir ratio of the aquifer across the entire trap (GRV).
- ϕ** Average effective reservoir porosity of the aquifer within GRV.
- ρ_{CO2R}** Average CO₂ density at reservoir pressure and temperature.
- S_{Eff}** Storage efficiency factor relates to the fraction of the available pore volume that will store CO₂ within the GRV. This fraction depends on many subsurface aspects including the size of storage domain, heterogeneity of formation, compartmentalization, permeability, porosity, and compressibility, but can also describe different well configurations, injection schemes and displacement efficiency (e.g. Wang et al. 2013).

Evaluation and estimation of the CO₂ storage capacity in deep saline aquifers is complex and accurate estimations of storage capacity are only practical at local site-specific scales. For

open aquifers, as evaluated here, the reservoir pressure is assumed to stay constant during CO₂ injection, as the water will be pushed beyond the boundaries. The calculated storage volume of CO₂ is the maximum amount that theoretical may be injected until the CO₂ reaches the boundaries (e.g. 'lowermost closed contour').

Static CO₂ storage capacity (Eq. 1) estimations are uncertain due to lack of knowledge on the storage efficiency factor that reduce the storage capacity to a more realistic estimation. The CO₂ storage efficiency factor was first introduced in 2007 in regional-scale assessments of storage capacity in the United States and Europe. The efficiency of CO₂ storage is regarded as a combination of various factors combined into one efficiency factor, and many published papers show factors values from <1% to more than 20%, emphasizing that no single factor value or set of values can universally be used. Regional storage efficiency factors are estimated to be 1–4 % (e.g. CO₂ Storage Atlas of the US and Canada 2008), while trap specific storage efficiency have values around ~4–18% for clastic sediments (*Gorecki et.al., 2009*); ~3–10% (*US-DOE; Goodman et.al., 2011*) and ~5–20% for traps in German North Sea area (*BGR, 2023 on-going project*).

The Stenlille is the best-known case in the Danish onshore area. A maximum storage efficiency factor of 0.4 (or 40%) for a 4-way dip-closure has previously been estimated and was used for the geologically excellent and well described Gassum Fm sandstone reservoir in the Stenlille structure. Furthermore, the Stenlille structure has been used for natural gas storage for many years and consists of high-permeable sandstone layers with no faults offsetting the reservoir and overlying seal. For comparison reasons GEUS uses a storage efficiencies factor of 40% in the Stenlille structure and a value of 10% in all other potential structures, and structures where the primary reservoir is not the Gassum Fm but e.g. the deeper situated Bunter Sandstone Fm. These lower storage efficiency values reaching more realistic values from 5 to 10% are used in structures with no or older well data and where only minor faults offsetting the reservoirs/seals.

The storage efficiency represents the fraction of the total available pore volume of the saline aquifer that will be occupied by the injected CO₂ in the trap volume (e.g. the Gross Rock Volume (GRV)) and is regarded as the fraction of stored CO₂ relative to the pore volume. It depends primarily on the relationship between the vertical and horizontal permeability, where a low vertical to horizontal permeability ratio will lateral distribute the CO₂ better over the reservoir than a high ratio, why an internally layered reservoir with alternating sandstones and impermeable or poorly permeable claystones acting as seals may have an advance. The storage efficiency to also depends on the size of the storage domain, heterogeneity of the formation, compartmentalization, porosity, permeability, pressure increase, temperature, salinity, and compressibility, all parameters that are influenced by number of injection wells, configuration, injection strategy and displacement efficiency.

Furthermore, injection and storage of CO₂ in deep saline formations requires estimates of fluid pressures that will not induce fracturing or create fault permeability that can lead the CO₂ to escape from the reservoir. To ensure this, identification of faults and analyses of fault stability are necessary and requires precise evaluation of e.g. fault orientations, pore fluid pressure distribution and in-situ stresses in and around the storage site. Changes in injection rates induce stress can changes formation pressures and CO₂ storage volumes, why determination of in situ stresses and modelling of fault stability are essential for the safe CO₂ injection and detailed modelling of storage capacity.

In this study estimation of static storage capacity assume a static approach where the pores in the trap is expected to be 100% connected and does not include dynamic pressure build-up and movement of CO₂ and in-place brine (water) in the saline aquifer, neither in-side nor out-side the trap. Furthermore, it does not consider the solubility of CO₂ in brine, CO₂ mineralisation reactions, where more than 10% can normally be dissolved in the water, and the presence of salt with possible movement of CO₂ and causing scales inside the storage reservoir reducing the efficiency of CO₂ injection. A dynamic reservoir simulation will take these factors into account and will obviously produce different storage capacity results, depending on the selected parameters. A more realistic dynamic reservoir simulation of the potential storage capacity is normally carried out by the awarded license holders and operators and should be used for local-scale CO₂ storage reserves estimates.

Estimation of static storage capacity is biased by imperfect seismic and reservoir data, depth conversion, reservoir thickness estimates and CO₂ density. To address this uncertainty ranges have been chosen to reflect the uncertainty of each parameter, and the distribution has been modelled utilizing a simple Monte Carlo simulation in-house tool. To achieve stable and adequate statistical representation of both input distribution and result output, 10.000 trials are calculated for each simulation. This methodology is simplistic and does not incorporate e.g., correlations of input parameters. However, for the purpose of initial estimation of volumes, CO₂ storage capacities and for comparison of potential structures for CO₂ storage, the methodology is considered relevant and adequate. The method is used for the estimations in Chapter 8.

6. Results of seismic and well-tie interpretation

Previous mapping of the Thorning structure (e.g. Hjelm et al. 2022) relied on two old legacy seismic lines from 1973 of poor quality available at the time. The interpretation presented here is based on a denser line coverage with the old lines integrated with the new and better seismic data collected in 2023.

6.1 Stratigraphy of the structure

The interpreted seismic stratigraphic horizons with well-ties document the local stratigraphy in the vicinity of the Thorning structure. The key tie between seismic stratigraphy and the Nøvling-1 well is shown in Figure 6.1.1 with correlation to the regional lithostratigraphy. In total, twelve regional seismic stratigraphic horizons have been interpreted for the study area and are from the deepest to the shallowest: (1) Top pre-Zechstein, (2) Top Zechstein Group, (3) Top Skagerrak Formation / Bunter Sandstone Formation, (4) Top Ørslev Formation, (5) Top Falster Formation, (6) Top Tønder Formation, (7) Top Vinding Formation, (8) Top Gassum Formation, (9) Top Fjerritslev Formation, (10) Top Frederikshavn Formation, (11) Base Chalk Group, and (12) Top Chalk Group (Figs 6.1.1–6.2.19). The horizons are essentially interpreted as sequence stratigraphic boundaries (and essentially chronostratigraphic), which are picked in a certain reflection (a trough or a peak, Table 5.1). The seismic horizons were picked near to the base or top of a formation or a group and are named after the nearest base or to (e.g. 'Top Gassum' horizon is near to the top of the Gassum Formation). In most cases, on a local scale, the seismic horizons occur close to formation boundaries as defined in the wells. Thus, the seismic horizons are here named after the approximate formation boundaries. More regionally, it may be considered to use naming independent of lithostratigraphy such as letters or ages, as on a regional scale, some of the lithostratigraphic units are diachronous. However, the naming serves to directly relate mapped horizons and formations defined by well data and thus to describe key reservoir-seal pairs.

The deepest mappable horizon interpreted in the Thorning area is the Top pre-Zechstein horizon tied to the Nøvling-1 well, which is located on a fault-bounded block and records the Top pre-Zechstein boundary represented by Zechstein halite overlying 227 m drilled Paleozoic sedimentary rocks of the Nøvling and Rønde formations below (Fig. 6.1.2). Crystalline basement of Proterozoic age has been drilled in the Grindsted-1 well located on the uplifted Ringkøbing–Fyn High c. 85 km south of the Thorning area. The Proterozoic basement in the well represents the southerly extension of the Fennoscandian Shield (Olivarius et al., 2015), and indirectly suggest a comparable Fennoscandian basement underlying the Thorning area to the north. The Nøvling and Rønde formations drilled in Nøvling-1 and Rønde-1 are of Late Silurian age and consist of interbedded basalts, grey and red brown claystones and sandstones with some carbonates.

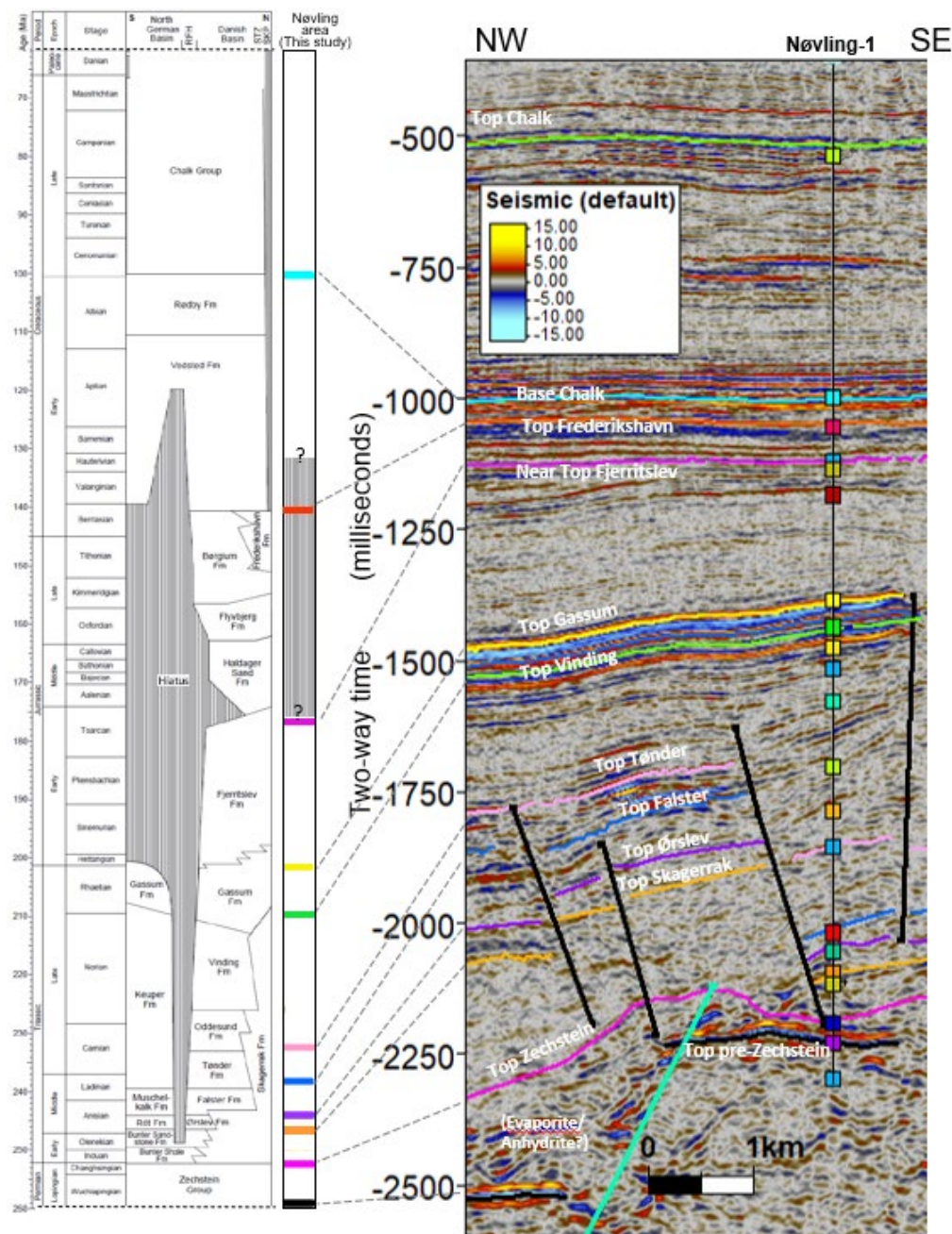


Figure 6.1.1 Lithostratigraphy and seismic horizons with well-ties at the Nøvling-1 well located 33 km to the SW of the Thorning structure and close to the northern flank of the elevated basement high in the Ringkøbing–Fyn High (RFH). The lithostratigraphic scheme, based on Bertelsen (1980) and Nielsen (2003), summarizes the general stratigraphy from the North German Basin in the south to the Danish Basin in the north. Most of the formations in the Danish Basin are interpreted to be present in the Thorning region apart from M. and U. Jurassic formations. Colored seismic stratigraphic horizons are shown at the stratigraphic position in the separate stratigraphic column (this study). The profile shows correlation to the Nøvling-1 well with well-tops (colored squares). The structural setting at Nøvling-1 is highly complex impacting the picking of Triassic surfaces. Triassic stratigraphy and structures should be studied further for a potential revision. Dashed horizontal lines at the top and base of the scheme (left) indicate omitted younger Cenozoic/Quaternary successions, and pre-Zechstein successions, respectively due to space limitation.

The deep subsurface underneath the Thorning-Nøvling area is characterized by several large fault blocks, (see Fig. 6.1.2 and 6.1.3) outlining the Thorning terrace and Nøvling fault block, and the Brande Trough. The Top pre-Zechstein surface at the Thorning and Nøvling terraces delineates two structural highs that are attached to and creates a north-ward continuation of the Ringkøbing-Fyn High.

In this study, the deepest horizons: Top Pre-Zechstein and Top Zechstein are included to constrain the structural evolution. The Top Chalk horizon mainly constrain the late structural evolution, the thickness of the Chalk Group, and the depth conversion.

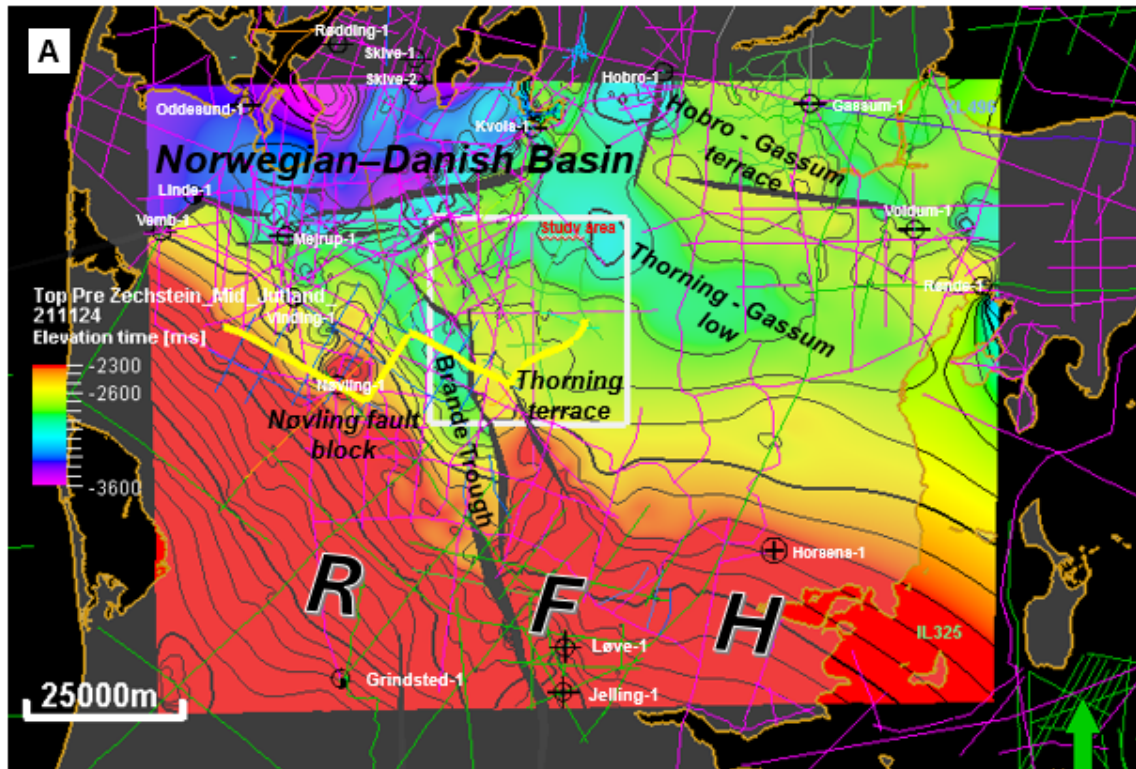
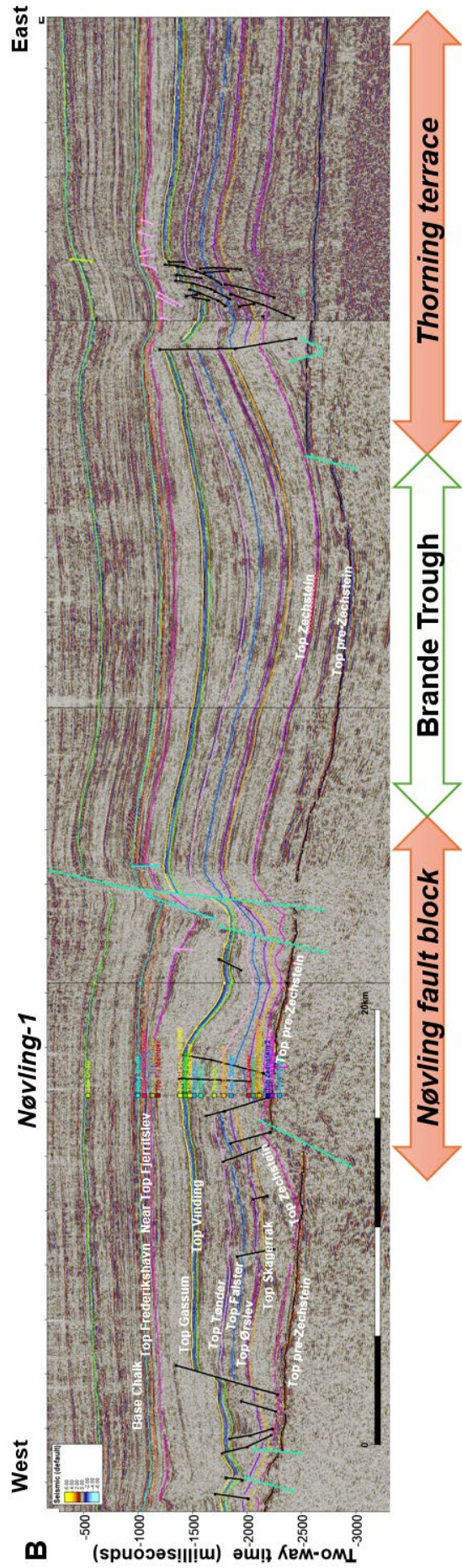


Figure 6.1.2 A: Location map of key seismic profile (yellow) from Nøvling-1 to the Thorning terrace shown on top of the contoured structural depth map in milliseconds (ms) two-way time (TWT) of the Top Pre-Zechstein surface below mean sea level. The structural depth map outlines the deepest parts of the sedimentary basins mapped over a large part of central Jutland. A few of the most prominent faults offsetting the Top Pre-Zechstein surface have been mapped to illustrate the main structural elements of the area with respect to the location of the NW–SE-striking deeper part of the Norwegian–Danish Basin to the north, the Nøvling fault block (attached to the Ringkøbing–Fyn High), the NNW–SSE striking deep Brande Trough, and the roughly N–S striking structural high or terrace underlying the Thorning area.

B (next page): Seismic stratigraphic correlation of marker horizons along composite key profile with well-ties at the Nøvling-1 well to the southern part of the Thorning structure. The horizontal scale is 20 km, and the depth axis is shown in ms TWT. Major structural elements are indicated as corresponding to the map in (A).



The seismic data over the Thorning structure documents a salt pillow structure cored by Zechstein Group evaporites overlain by Lower Triassic strata presumably consisting of mudstones and sandstones of the Bunter / Skagerrak Formations. The study has emphasized that the Triassic stratigraphy in the Danish Basin would benefit from a revision, although this is beyond the scope of this study.

In this report, we use a dual Skagerrak Formation / Bunter Sandstone Formation nomenclature referring to the sand prone Lower Triassic (see also Chapter 7). The top of each of the Ørslev, Falster, and Tønder formations are also mapped. The Oddesund Formation and Vinding Formation are grouped together and mapped as the Top Vinding / Base Gassum horizon, as the Top of Oddesund Formation is not mapped in this study. Also, there is a major gap in the stratigraphy in the study area interpreted from well data near the Top Fjerritslev horizon and corroborated by reflector truncation along the surface (Fig. 6.1.1). The succeeding Middle to Upper Jurassic succession of the Haldager Sand, Flyvbjerg and Børglum formations are not mapped here although it cannot be ruled out that a thin Middle–Upper succession may be present (see Chapter 7). The overlying mapped horizon Top Frederikshavn Formation outlines the top of a potential secondary reservoir within the Thorning structure overlain by mudstones (seal) of the Vedsted Formation and the Chalk Group (see Chapter 7).

Faults in the Thorning structure

Due to the time limits for preparing this Thorning study, only main faults affecting the primary reservoir interval has been mapped to identify potential zones of leakage and compartmentalisation within the Gassum Formation. In addition, some of the most pronounced faults offsetting the Top pre-Zechstein TWT-surface has been mapped to include the main structural topographic units that affects the general structural evolution of the Thorning area, Fig. 6.1.3, 6.2.1N and 6.2.2N). The structural depth map outlines the deepest parts of the sedimentary basins mapped over a large part of central Jutland with respect to the location of the NW–SE-striking deeper part of the Danish Basin to the north, the Nøvling fault block (attached to the Ringkøbing–Fyn High), the NNW–SSE striking deep Brande Trough, and the roughly N–S striking structural high or terrace underlying the Thorning area.

Inside the main Thorning study area which covers 985 km², two different types of fault sets offset the Top Gassum Formation, Figure 6.1.3. The first type of minor faults is extensional in nature and are observed at both the eastern and western rim of the domal structure to the north (labelled as A in Fig. 6.1.3; and shown in detail in Fig. 6.1.4). Interestingly, the W-dipping faults are only observed on E–W striking profiles in the new GEUS lines (P2 and P8), not on any of the legacy data. This may suggest that the orientations of the remaining new (P1, P3–P7) and legacy seismic data are not ideal for imaging and resolving these structures due to the structural configuration of the fault planes (as they are only observed on the new E–W striking seismic lines), and/or the size of these faults are below seismic resolution on vintage seismic lines. The faults offset the Top Gassum Formation horizon with throws up-to c. 20–25 ms TWT, corresponding to c. 30–37 m offset assuming an average seismic velocity of 3000 m/s for the Gassum Formation interval at 1160–1170 ms TWT. This estimated assumes a seismic average velocity of 3115 m/s corresponding to the velocity measured in the Gassum Formation in the Kvols-1 well at a slightly deeper TWT-level.

Higher up in the section at a more near-surface level, similar matching sets of younger, W-dipping fault planes (shown in bright green lines in Fig. 6.1.3B) are observed to offset the Base Chalk and the Fjerritslev Formation horizons with throws up to 20 ms TWT. Interestingly, these two fault systems appear to be isolated (i.e. not directly linked) as the deeper faults seem to terminate upward within the (more than 250 ms) thick Fjerritslev Formation, suggesting no upward continuation or clear link of these fault planes (see Figs. 6.1.3B and 6.1.3C), which could otherwise affect potential storage capacity negatively inducing a risk of leakage along the fault planes. This is significant, if the Thorning structure should be chosen as a potential CO₂ storage site. More accurate mapping of these faults will require acquisition of a denser seismic grid, which would also allow further investigation of interconnectivity of the two fault tiers.

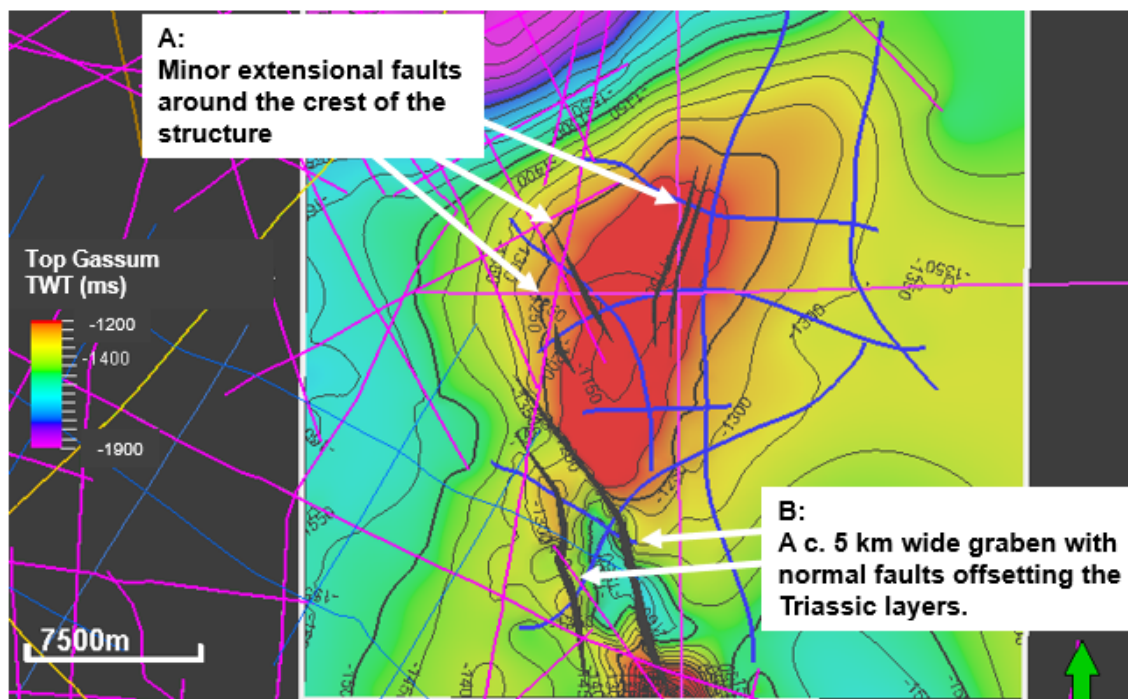


Figure 6.1.3 Two-way travel-time (TWT) structural map at the Top Gassum level showing the different types of fault sets (labelled A and B) observed at the top of the TWT-map of the Gassum Fm, contour interval 50 ms. The faults labelled B corresponds to the Thorning Fault Zone as mentioned in the text. Note that not all the faults are shown on the map, only the main outer bounding fault planes. The size of the Thorning study area is 985 km².

Based on the new seismic data, it appears that the fault type labelled A juxtaposes rocks of different composition and competences, i.e. the mudstones of the lowermost Fjerritslev Formation against the interbedded sandstones and mudstones of the uppermost Gassum Formation. The origin of these extensional faults (type A) is most likely associated to stretching caused by up-doming of overlying layers during Triassic and Jurassic salt movements. The fault movements were thus probably triggered by salt pillow growth in the Thorning structure resulting in decoupled faulting of the overlying units.

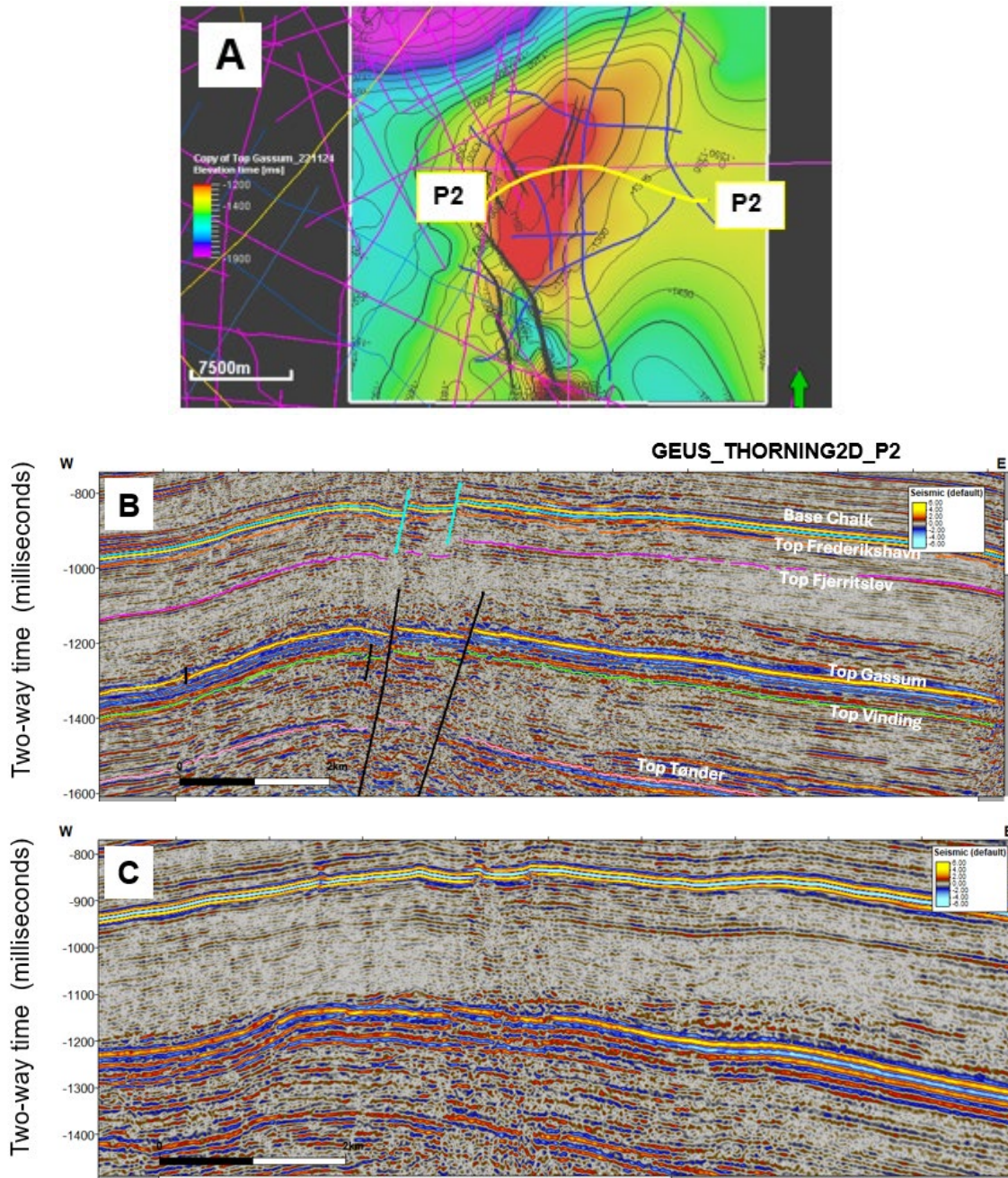


Figure 6.1.4 Example of the normal faults that are offsetting the top Gassum Fm with up to c. 20–25 ms TWT at the northeastern crest of the structure, corresponding to 30–37 m offset. The location of these faults is also shown on Fig. 6.1.2 and marked as fault types A. A: Location of the W–E striking GEUS_THORNING2D_P2 profile (shown in yellow) across the northern end of the Thorning structure on top of the TWT-map of the Gassum Fm, contour interval 50 ms. B: A close-up on the profile GEUS_THORNING2D_P2 including the interpreted horizons. The black faults are offset the top Gassum Fm with up to 21–23 ms TWT at the northeastern crest of the structure. The faults offsetting the Upper Jurassic and Base Cretaceous are shown by bright green lines. C: Same seismic profile (GEUS_THORNING2D_P2) without any interpreted horizons. Note that the horizontal scale bar is 2 km (black, white).

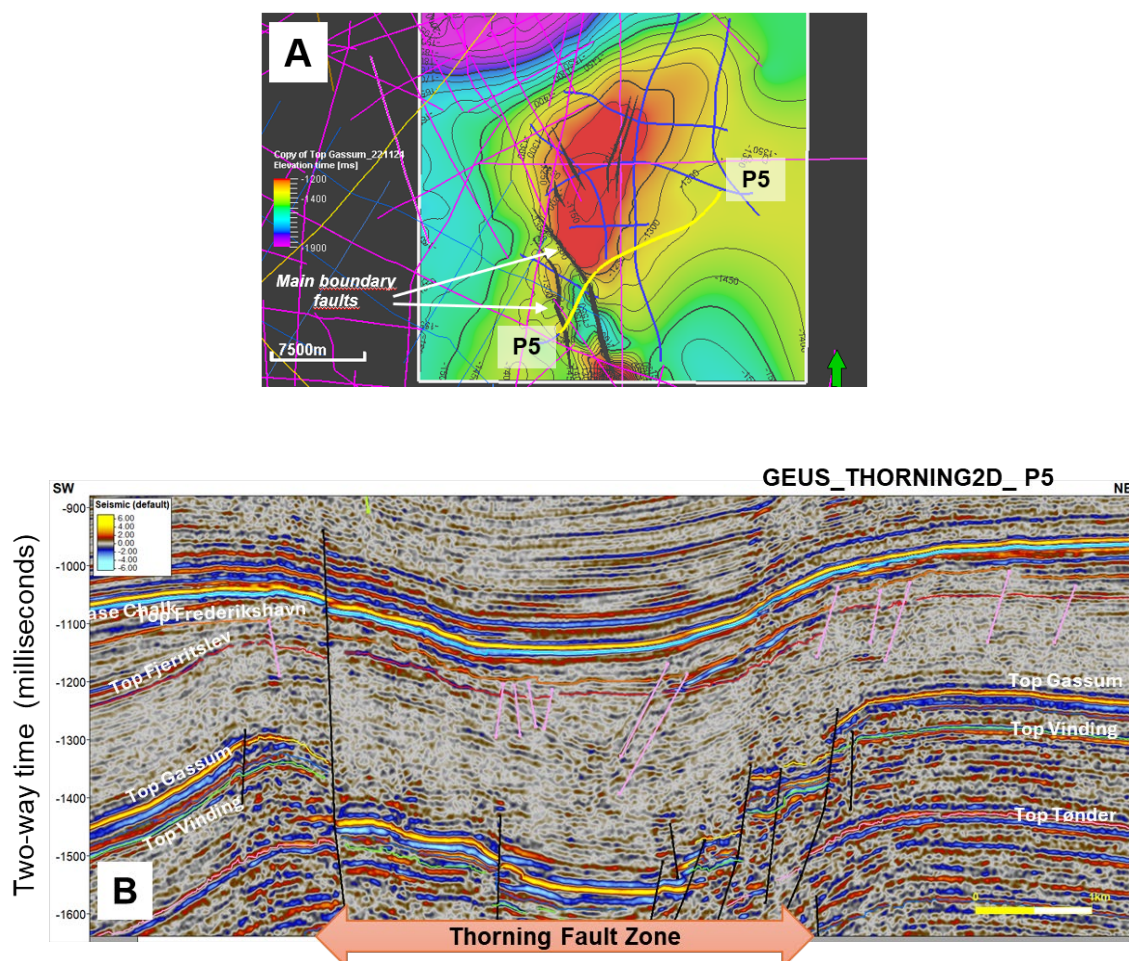
The second type of faults labelled B in Fig. 6.1.3 on the south-western slope of the Thorning structure is observed on two of the new seismic profiles, (P4 and P5) and a few of the legacy

lines, and represents a c. 5 km wide NW–SE striking fault zone forming a graben structure bounded by listric normal (synthetic and antithetic) faults offsetting the entire Triassic section from the Gassum Formation horizon to the Skagerrak Formation / Bunter Sandstone Formation horizon, Fig. 6.1.5 and terminating within the Zechstein Group.

The graben structure, which we name the Thorning Fault Zone, probably formed as a collapse mini-basin due to salt withdrawal resulting in a marked thickening of the Fjerritslev Formation in the fault zone. The large throws at the Top Gassum to Top Falster horizons indicate faulting during and immediately after deposition of the Fjerritslev Formation. The salt likely migrated northeastwards to the Thorning salt pillow and/or southwards to the Bording salt diapir (see Figs 6.1.3 and 6.2.7).

The southern main listric boundary fault plane is dipping to the NE and downfaults the Top Gassum horizon with a throw of >100 ms TWT, corresponding to c. 150–170 m offset. The main listric boundary fault is the only visible fault that extends upwards and offsets the Top Fjerritslev to Base Chalk horizons, with a throw of c. 10 ms at Base Chalk, corresponding to c. 15–20 m offset. The opposite boundary fault, the northern-most Triassic fault of the graben structure, is SW-dipping and located along the boundary of the deepest closing contour for the Top Gassum Formation horizon at the 1360 ms TWT-contour curve (Fig. 6.1.5D).

Another set of younger normal faults is observed overlying the graben structure with minor faulting of the Top Fjerritslev to Top Frederikshavn Formation horizons shown by pink lines on Fig. 6.1.5B. The existing seismic database has a rather open grid, and hence closer spaced seismic data is required to map the faults more accurately to evaluate their potential significance for seal integrity in the structure.



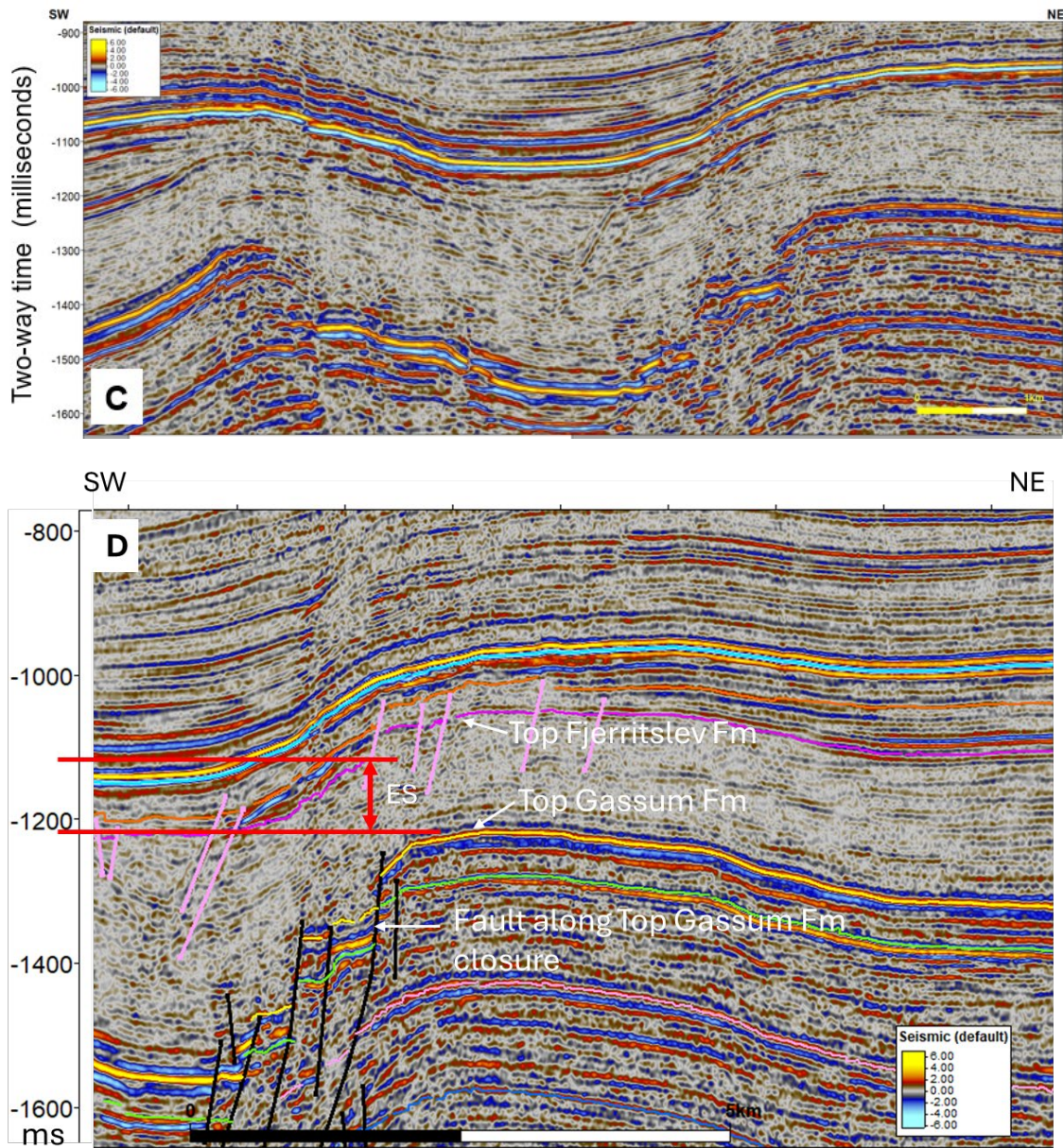


Figure 6.1.5 Example of the Thorning Fault Zone, a graben structure offsetting the top Gassum Fm with more than 100 ms TWT towards the southwest. The location of these faults is also shown on Fig. 6.1.3 and marked as fault types B. The location of the deepest closing contour, 1360 ms TWT, is interpreted as the spill point assuming that the main fault is sealing. A: Location of the NE–SW striking GEUS_THORNING2D_P5 profile (shown in yellow) across the southern part of the Thorning domal structure shown on the TWT-map of the top Gassum Fm, contour interval 10 ms. B: A close-up on the profile GEUS_THORNING2D_P5 including the interpreted horizons. The black faults are Jurassic normal faults that are offsetting the Top Gassum Fm with >100 ms TWT at the southwestern flank of the structure. The Jurassic faults are shown by pink lines. C: Same seismic profile (GEUS_THORNING2D_P5) without any interpreted horizons. Note that the horizontal scale bar is 1 km (yellow). D: Part of P5 showing example of effective seal (ES, marked by red arrow) interval of the Fjerritslev Fm along boundary fault that defines top Gassum Fm closure: Depth top Fjerritslev Fm on hangingwall – Depth Top Gassum Fm in footwall: c. 1220 ms – 1120 ms = c. 100 ms.

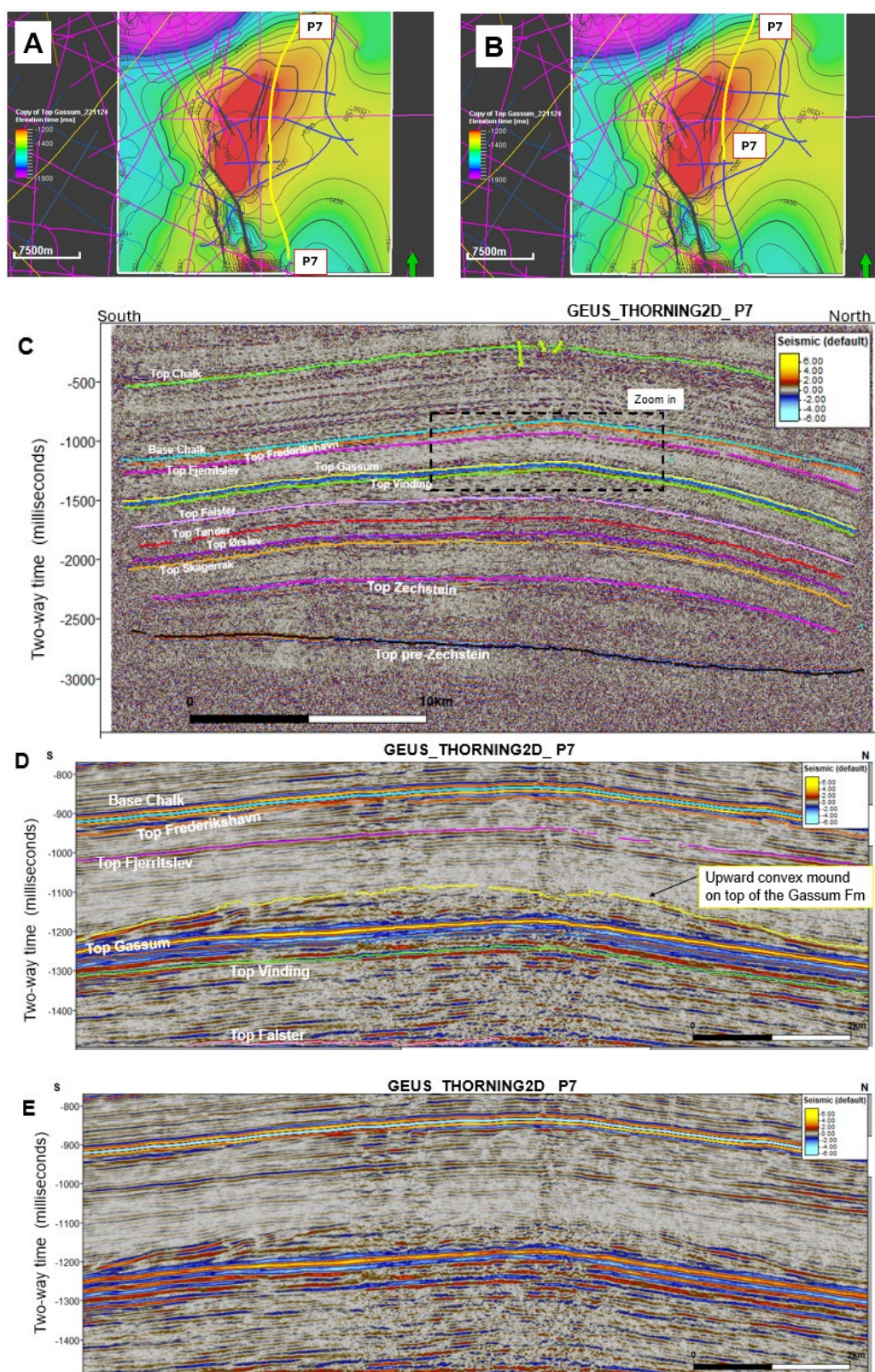


Figure 6.1.6. A: Location of GEUS_THORNING2D_P7 profile (P7, yellow) along the central part of the Thorning domal structure shown on top of the TWT-map of the Gassum Fm, contour interval 50 ms. B: Same as A but showing the location of the central part of GEUS_THORNING2D_P7 profile shown in D and E. C: The seismic interpretation of P7. Horizontal scale bar is 10 km. D: A close-up on the profile P7 including the interpreted horizons. The horizontal scale bar is 2 km. E: A close-up on the profile P7 without the interpreted horizons. Note the strong coherency of the Top Gassum reflection along P7. Horizontal scale bar is 2 km.

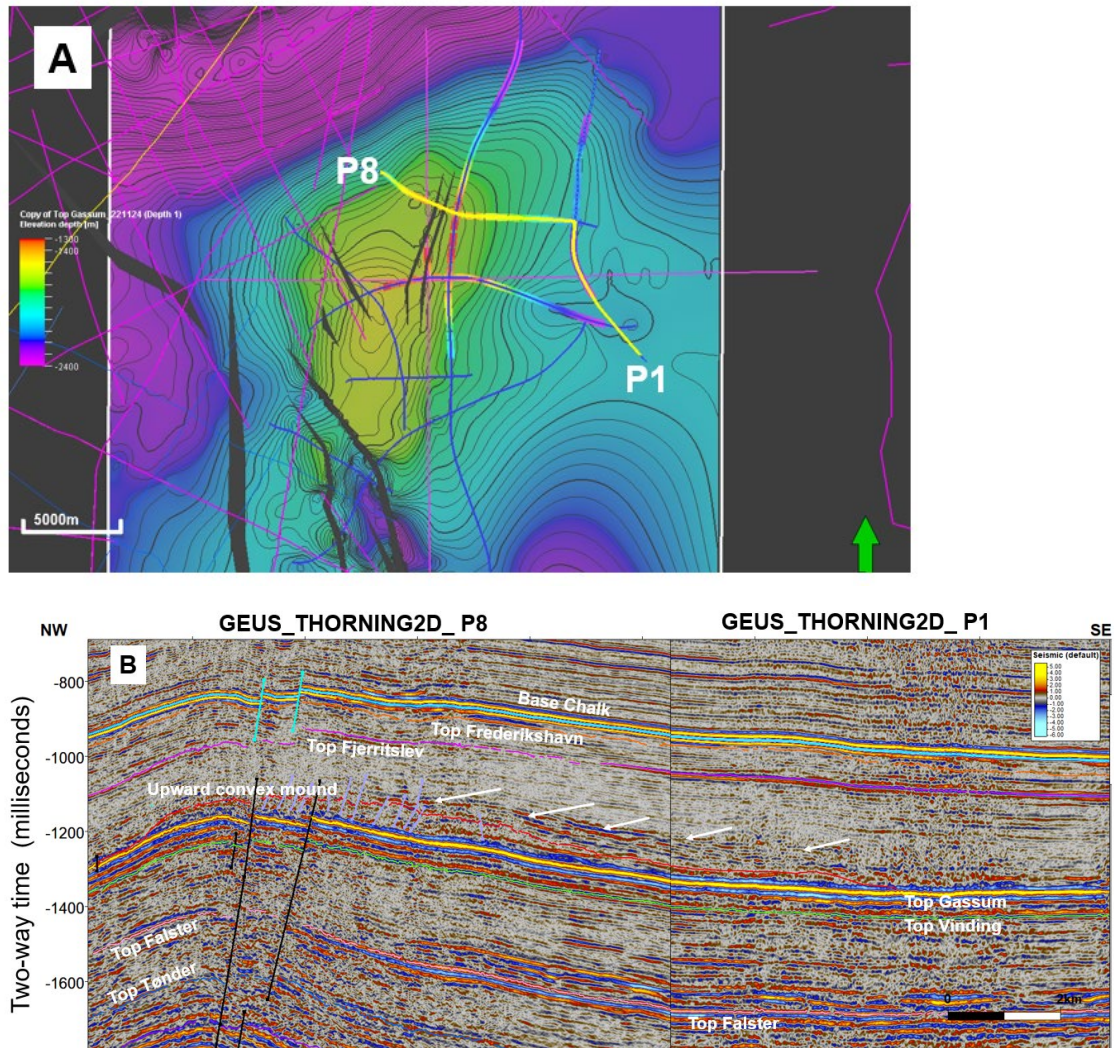


Figure 6.1.7. High reflective layers from the lower Fjerritslev Formation onlap the upward-convex structure. A: Location of composite profile between GEUS_THORNING2D_P8 profile (P8, yellow) and GEUS_THORNING2D_P1 profile (P1, yellow) on the NE flank of the Thorning domal structure shown on top of the TWT-map of the Gassum Fm, contour interval 50 ms. B: White arrows indicate the position of the high reflective layers from the lower Fjerritslev Formation which onlap the upward-convex structure. Horizontal scale bar is 2 km.

6.2 Structure description and tectonostratigraphic evolution

The seismic stratigraphic interpretation is tied to well-tops in the Nøvling-1, Kvols-1, Mejrup-1 and Gassum-1 wells and extended further into the 2D seismic lines as described in Section 6.1.

Structural maps of the Thorning structure

Structural maps in two-way time have been generated from horizons by gridding and smoothing (see chapter 5). The depth-structure maps are shown in milliseconds (ms) two-way time (TWT) below mean sea level for all horizons in Figure 6.2.1; A: Top Chalk; B: Base Chalk; C: Top Frederikshavn; D: Top Fjerritslev; E: Top Gassum; F: Top Vinding; G: Top Falster; H: Top Tønder; I: Top Ørslev; J: Top Skagerrak / Bunter Sandstone; K: Top Zechstein. The depth converted maps in meters below mean sea level of all horizons from shallow to deep are shown in Figure 6.2.2. Figure 6.2.3 shows key thickness maps of the primary reservoir (Gassum Formation) and its primary seal (Fjerritslev Formation). The maps in Figs. 6.2.2–6.2.3 are used in the following descriptions of the geological evolution, stratigraphy and for calculation of storage capacity.

Structure description from mapped surfaces and units

Top pre-Zechstein

The Top pre-Zechstein surface is outlined by a strong “hard kick” (peak) reflector denoting the top of a well-reflected, parallel reflector set (shown as a black horizon on Fig. 6.1.2, 6.1.5, and 6.2.4). The surface represents a distinct upwards change in seismic facies and forms the base of the Zechstein evaporites and defines the deepest regional mappable reflector in the area (see Figs 6.2.1N; 6.2.2N and 6.2.10A). The Top pre-Zechstein horizon represents a major unconformity separating the base of the Upper Permian – Cenozoic sedimentary cover from the older and largely unknown pre-Zechstein successions that can be seen as dipping reflections on a large part of the legacy seismic data from Central Jutland.

In the Thorning study area, the Top pre-Zechstein TWT-surface forms an overall NE–SW striking, NE-dipping elongated “ridge” or terrace, the Thorning terrace. The western margin of the Thorning terrace is outlined by an NNE–SSE striking deep seated fault, separating the 12–15 km narrow structural low in the Brande Trough to the SSW from the wider (c. 20 km) depression located between Thorning and Gassum (see Fig, 6.2.1N and 6.2.2N). The Top pre-Zechstein surface is slightly undulating and un-faulted below the Thorning terrace (see Fig. 6.1.2, 6.1.5C, 6.2.4 and 6.2.5). The transition from the Thorning terrace and the deeper parts of the Norwegian Danish Basin to the north is faulted like a staircase (Fig. 6.2.4), and similarly for the transition to the Brande Trough to the west (Fig. 6.2.5).

Top Zechstein

The Top Zechstein surface is outlined by a strong “hard kick” reflector (Fig. 6.1.2, 6.1.5, and 6.2.10). In the study area, the Top Zechstein surface forms an NNW–SSE elongated domal structure with a four-way fault dip closure (Figs 6.2.1M and 6.2.2M). The closure has a relief of c. 600 m with an apex located at c. 3100 m depth (b.msl) (Figs 6.2.1M, 6.2.2M). Above

the Thorning terrace, the thickness map of the Zechstein Group shows that the Zechstein Group forms a well-defined salt pillow structure - the Thorning salt pillow - with a thickness of up to c. 1700 meters at the apex of the structure (Fig. 6.2.3N and Fig. 6.2.6A).

The westernmost domal structure is c. 12 km long, c. 6 km wide and elongated in an NNW–SSE direction, while the eastern minor dome is more circular (c. 7 km long, c. 6 km wide) with an NE–SW orientation. The maximum thickness of the main salt pillow along the elongated western structure is >1700 m, and the maximum thickness of the minor salt pillow in the northeastern structure is > 1500 m, see Fig. 6.2.3N and Fig. 6.2.6A.

Across the central part of the Thorning study area, the 2023 seismic data show that the surface marks the upper boundary of a c. 100 ms (millisecond) thick, strongly reflected, parallel-bedded interval which may consist of cyclic evaporites (Fig. 6.2.6). The Zechstein interval is not homogenous but display a mixture of varied reflectivity changing from parallel-bedded reflections to transparent zones (probably representing zones with more pure halite) to areas with broken or incoherent bands of parallel-bedded reflections forming rafts of deformed evaporites. Similarly, towards the base of the Zechstein interval, the Top pre-Zechstein surface is overlain by a weakly reflective to transparent interval and thus denoting a general upwards decrease in reflection amplitude. In the larger Thorning area of central Jutland several salt diapirs exist formed by post-depositional salt movements due to loading and compaction of the sedimentary overburden. The evolution of the Thorning salt pillow will be discussed in the next section. Just south of the Thorning salt pillow, there's a large diapir in the Bording salt structure (Figure. 6.2.7).

Top Skagerrak (former Bunter Sandstone and Bunter Shale Formation)

In the Thorning study area, the Top Skagerrak surface is characterized by a strong “hard kick” reflector (Fig. 6.1.1 and 6.2.6B). The Top Skagerrak reflector separates sub-parallel reflectivity of the overlying Ørslev Formation from semi-parallel to chaotic reflectivity in the Skagerrak Formation below the surface. The Top Skagerrak surface forms a N–S striking elongated dome overlying the Thorning salt pillow having a closure relief of c. 600 m towards NW (Figs 6.2.1L, 6.2.2L). The apex is situated at c. 2600 m depth (b.msl).

Top Ørslev

The Top Ørslev surface is characterized by a strong “*soft kick*” (trough) reflector (Fig. 6.2.14) and separates cyclic to parallel reflectivity of the Ørslev Formation from the overlying Falster Formation, which is more characterized by sub-parallel, transparent to chaotic reflectivity above the surface. Similarly, the Top Ørslev surface forms a N–S striking dome overlying the Thorning salt pillow having a closure relief of c. 700 m towards NW (Figs 6.2.1K, 6.2.2K). The apex is situated at c. 2400 m depth (b.msl).

Top Falster to Top Tønder

Both the Top Falster and the Top Tønder surfaces are characterized by strong, continuous “hard kick” reflectors separating to two intervals characterized by sub-parallel, transparent to chaotic reflectivity and both intervals of fairly constant thickness (Falster Formation with an average thickness of c. 130 ms TWT (250 m) and Tønder Formation c. 155 ms TWT (300–350 m)) across the study area. Both the Top Falster and the Top Tønder surfaces form a N–S striking dome (three-way dip closure) overlying the Thorning salt pillow.

Top Tønder to Top Vinding

The interval between the Top Tønder and Top Vinding surfaces covers both the Vinding and the Oddesund formations, as we have not mapped the top of the underlying Oddesund Formation in this study.

The Top Vinding surface is characterized by a strong, continuous “soft kick” reflector between few parallel to semi-parallel, strong reflections (Figs 6.1.5C, 6.2.10, 6.2.11) as supported by the seismic well ties in both Nøvling-1 and Kvols-1 wells (see Section 5.1). The Top Vinding surface outlines a dome (three-way dip closure) with a slight NE–SW orientation in the central part of the mapped area (Figs 6.2.1H, 6.2.2H). The crest of the closure is located at c. 1700 m depth (b.msl). The thickness map of the combined Oddesund and Vinding formations (Fig. 6.2.3I) shows thicknesses from c. 250–400 m across the Thorning structure.

The Top Vinding surface marks the transition from the base of the Gassum Formation to Top of the Vinding Formation.

Top Gassum and TS 5

The Top Gassum surface is characterized by distinct “hard kick” (peak) reflector forming the top of a strongly reflected, parallel to semi-bedded unit with typically high reflection amplitudes that correlates with the Gassum Formation in the Nøvling-1 and Kvols-1 wells. In general, the seismic reflectivity of the Gassum Formation is very distinct and easy to identify, also on legacy data, due to the amplitude peak and troughs especially in the upper part of the formation, see Fig. 6.2.8.

The Top Gassum surface outlines an NNE–SSW elongated dome (three-way dip fault closure) with a series of roughly N–S striking extensional faults along the northern flank and a remarkable graben structure on the southern flank in the mapped Thorning area, as discussed in section 6.1.1 (Figs 6.2.1F, 6.2.2F). The crest of the domal closure is located at c. 1520 m depth (b.msl), and the deepest structural closure is located at 1950 m depth (b.msl) resulting in a relief of c. 430 m. The interpreted spill point at 1950 m depth (b.msl) is dependent on the main boundary faults separating the hanging and footwall wall blocks of the graben structure on the southern flank, being sealing. The fault plane may be sealing due to the increased clay content of the overlying Fjerritslev Formation (see discussions in Chapter 7).

The Gassum Formation is divided by an internal reflector, interpreted to reflect the transgressive surface TS 5 (see in Chapter 7), that separates the more reflective upper part dominated by high amplitude peak and troughs, coherent sub-parallel reflectors from the lower part which has a highly variable reflectivity alternating between low amplitude, chaotic to transparent to more sub-parallel to semi-bedded units. The upper part of the formation above TS 5 has been interpreted as being a more shale-rich and the lower unit to be more sand prone (discussed in further details in Chapter 7).

The Gassum Formation thickness map (Fig. 6.2.3G) defined between the Top Vinding and Top Gassum surfaces suggest a relatively uniform thickness of c. 100 m across the Thorning structure, but the thicknesses vary locally and are larger to the south, where it is affected by faults in the graben structure. The thickness map of the lower Gassum Formation below the TS 5 surface (Fig. 6.2.3H) suggests a uniform thickness between c. 60–70 meters in the central and eastern part of the structure separated by a belt of much thinner unit with thickness between c. 20–50 meters to the W and SW.

The upward convex structure

The Top Gassum surface is overlain by the Fjerritslev Formation, another parallel bedded unit characterized by generally lower reflection amplitudes and higher reflection frequencies (the Fjerritslev Formation), that denotes a distinct upwards change in seismic facies.

However, remarkably the new 2023 GEUS_THORNING2D seismic data have revealed a, yet so far unknown succession deposited on top of mapped Top Gassum surface in the NE part of the Thorning study area (Fig. 6.1.5 and 6.1.7). This layer has been mapped as upward convex structure and is only observed on P7, P2, P8, P1 and possibly on one legacy profile, all located at the NE part of the domal structure over an area of around 153 km² (Fig. 6.2.2E and 6.2.3E). The NW–SE elongated structure is up to c.150 m thick and forms a large convex upward structure onto which strong amplitude reflections of the lower Fjerritslev Formation onlaps (Figs 6.1.5, 6.1.7, 6.2.10 and 7.1.10).

The internal seismic reflectivity of the mound is dominated by discontinuous to sub-horizontal or slightly dipping reflections, which in places resembles downlap onto the Top Gassum surface near the edges of the structure before it merges with the Top Gassum surface. The overlying deposits from the lower Fjerritslev Formation, presumably the F-1a member, onlaps onto the surface of the upward convex structure (Fig. 6.1.7) and may represent laminated sand-rich layers and alternating mudstone layers similar to the findings in the Gassum-1 well, as discussed in Chapter 7.

The formation and deposition of the upward convex structure most likely took place in a local deposition center at the NE-flank of the Thorning structure and is most likely associated with ongoing syn-depositional salt tectonics. See further discussion about the mounded structure in Chapter 7.

Top Fjerritslev

The Top Fjerritslev surface is characterized by a strong, continuous “*soft kick*” (trough) reflector between few parallel to semi-parallel, strong reflections and is outlined by a subtle angular unconformity (Figs 6.2.9). The surface outlines a NE–SW oriented dome (four-way dip closure) in the central part of the mapped area ((Figs 6.2.1D, 6.2.2D). The crest of the closure is located at c. 1250 m depth (b.msl) and the deepest structural closure is located at 1600 m depth (b.msl) resulting in a relief of c. 350 m.

The Fjerritslev Formation thickness (Fig. 6.2.3F) defined by the difference in depth between the Top Gassum and Top Fjerritslev surfaces is affected by truncation along the Top Fjerritslev surface. The thicknesses vary between 100–350 m across the Thorning structure except for the graben structure on the southern flank of the dome where it attains a thickness of c. 560 m. The largest thicknesses with >400 meters of the Fjerritslev Formation are found around the central part of the structure.

In the mapped area with the upward convex mounded structure; the mapped intra Fjerritslev surface onlaps onto the structure (see Fig. 7.1.12A) which may represent submarine fan deposits that have been eroded from a higher-lying structural area and re-deposited to its present position where a local accommodation space was created because of halokinesis. See Chapter 7 for further discussions.

Top Frederikshavn

The Top Frederikshavn surface is characterized by a “hard kick” (peak) reflector and the surface delineates an NNE–SSW striking dome (three-way dip closure; Figs 6.2.1C, 6.2.2C). The top point is in c. 1165 m depth (b.msl) and the deepest closing contour at c. 1450 m (b.msl) a resulting in a structural relief of c. 285 m.

The thickness of the Frederikshavn Formation is about 100 m thick across the structure (Fig. 6.2.3G), it shows minor thickness increase to the W and NE and a prominent thickness increase to the NE in the deeper parts of the Danish Basin where it exceeds 250 m. A local thickness increase is recorded in the graben to the SW. The thickness variations may indicate salt pillow growth. It should be noted that the succession between Top Frederikshavn and Top Fjerritslev most likely include a thin unit of the Børglum Fm.

Base Chalk

The Base Chalk surface is characterized by a strong, continuous “soft kick” (trough) reflector between few parallel to semi-parallel, strong reflections (Figs 6.1.1 and 6.2.10). The surface forms a NE–SW striking dome (four-way dip closure; Figs 6.2.1B, 6.2.2B). Top elevation is at c. 1150 m (b.msl) and spill point at the shallowest saddle structure is at c. 1400 m (b.msl) (Fig. 6.2.2B).

The interval between the Top Frederikshavn and the Base Chalk surfaces correlates with the Vedsted Formation in the Kvols-1 and Gassum-1 wells. The thickness of the Vedsted Formation (Fig. 6.2.3B) varies from c. 40–80 meters over the top of the structure to more than c. 134 meters towards the Kvols-1 well. This formation also shows slightly increase in thickness towards the southwest. The Lower Cretaceous Vedsted Formation is overlain by the regional mapped Base Chalk surface, which marks the base of the Upper Cretaceous Chalk Group (light blue reflector on Fig. 6.1.1).

Top Chalk

The Top Chalk surface is characterized by a “hard kick” (peak) reflector and the surface delineates an E–W striking nearly circular dome (three-way dip closure; Figs 6.2.1A, 6.2.2A). The top point is in c. 200 m depth (b.msl) and the deepest closing contour at c. 300 m (b.msl) with a saddle point to the west, resulting in a structural relief of c. 100 m.

Across the Thorning study area, the thickness map of the Chalk Group (Fig. 6.2.3A) images a NE–SW striking depression with thicknesses varying from c. 950–1150 meters separating two areas with very thick Chalk Group occurrences to the SE and NW with thicknesses more than 1200 m. A complete Chalk Group succession including the Danian part is interpreted present in the Thorning Structure based on nearby wells, see Chapter 7.

The Chalk Group is in general >950 m thick in the Thorning area and is overlain by Paleocene mudstones covering and draping over the Thorning structure. However, erosional thinning of the overlying Paleocene unit at the intersection between profiles P7 and P8, suggests additional salt growth of the northern smaller salt pillow during the Late Cretaceous to post-Paleocene, see Fig. 6.1.4C.

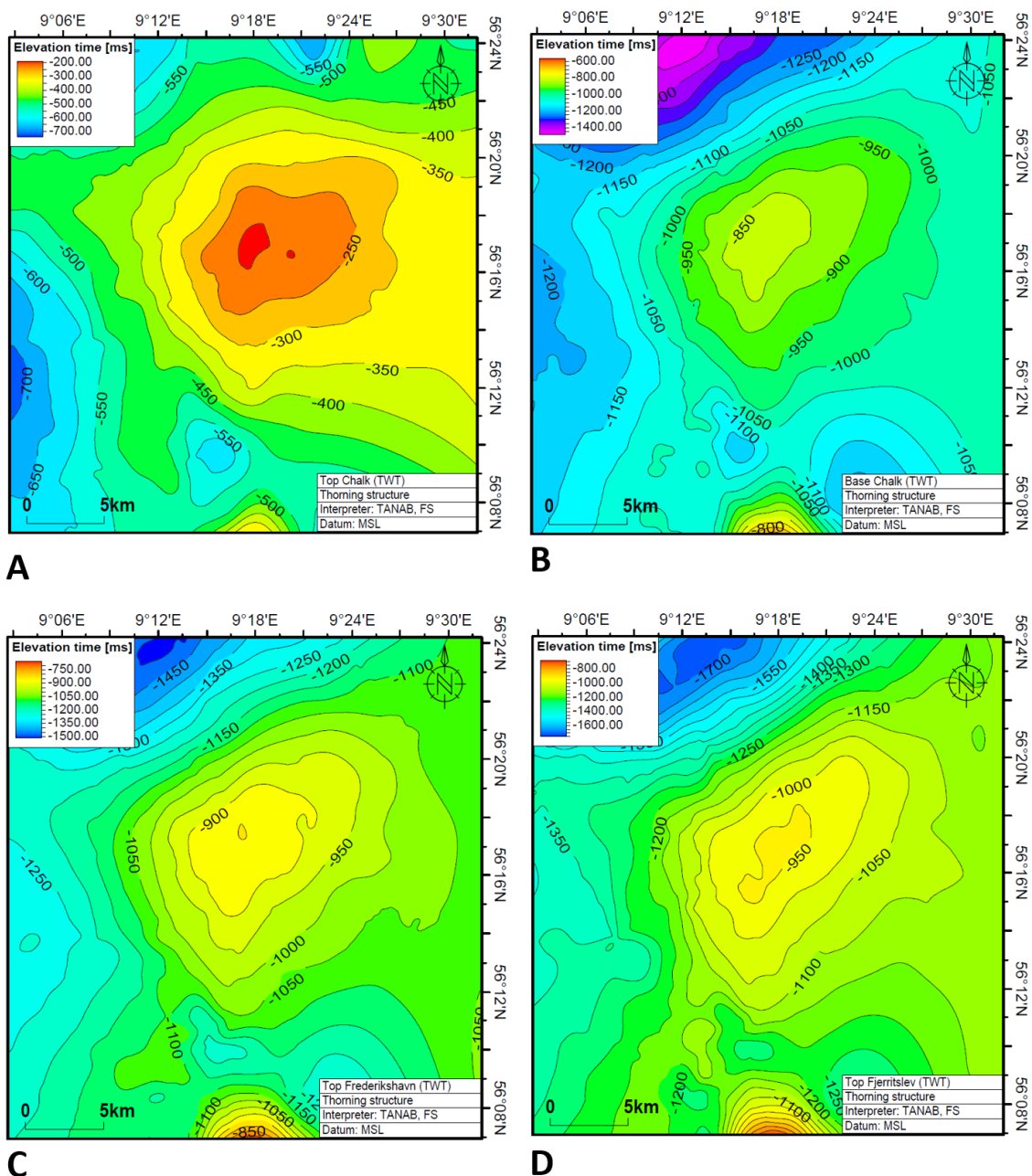


Figure 6.2.1 Time-structure maps (TWT) in milliseconds (ms) of the Thorning structure. Faults are not shown. A: Top Chalk; B: Base Chalk; C: Top Frederikshavn; D: Top Fjerritslev. The maps are produced with a 100x100 m grid and mildly smoothed (iteration x1; filter width 3). The contour interval of the maps is 50 ms.

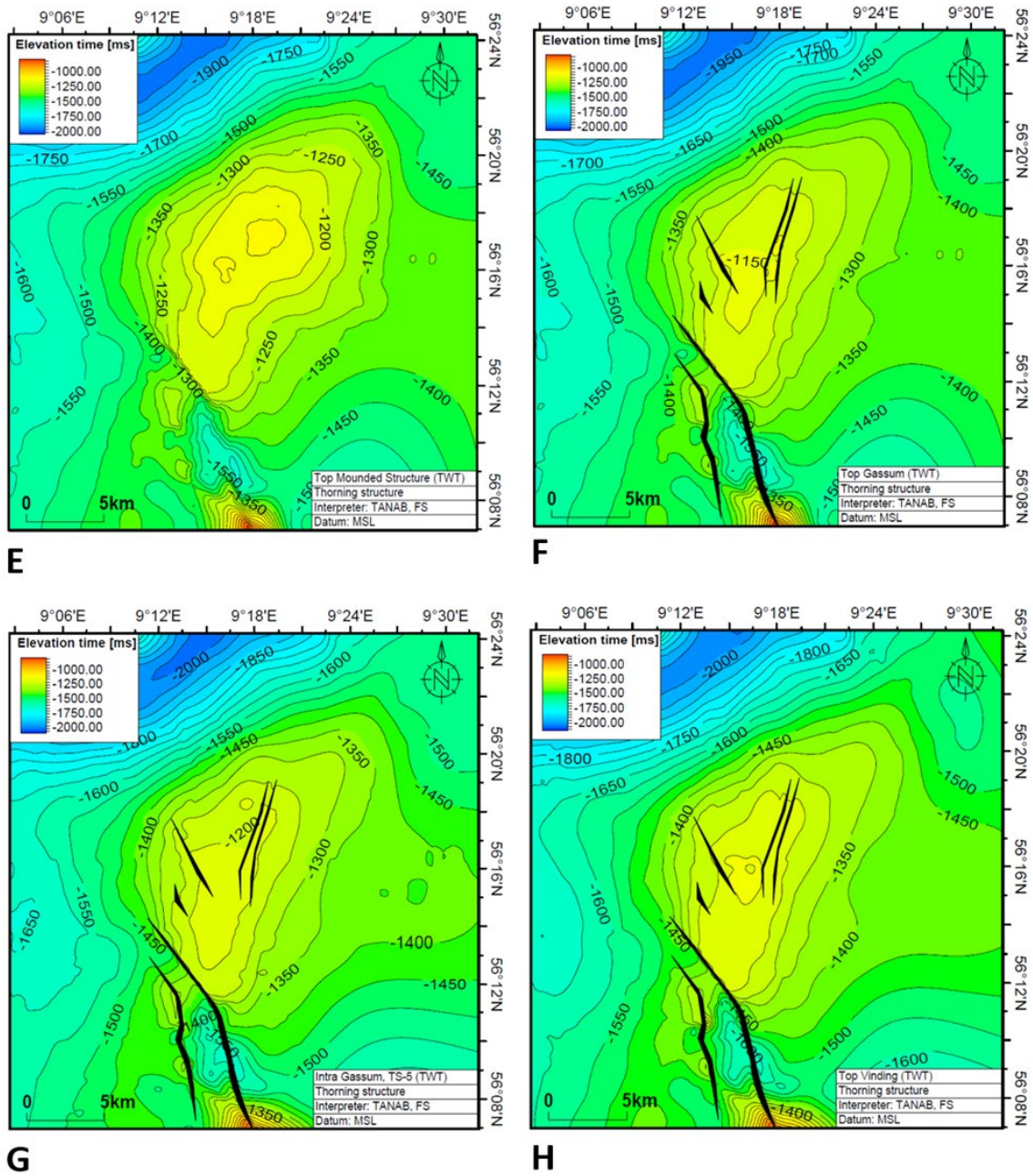


Fig. 6.2.1 continued. Time-structure maps (TWT) in milliseconds (ms) of the Thorning structure. Faults are only shown on the Top Gassum and Intra Gassum TS 5 horizons. E: Mounded Structure; F: Top Gassum; G: Intra Gassum, TS 5; H: Top Vinding (Base Gassum). The maps are produced with a 100x100 m grid and mildly smoothed (iteration x1; filter width 3). The contour interval of maps is 50 ms.

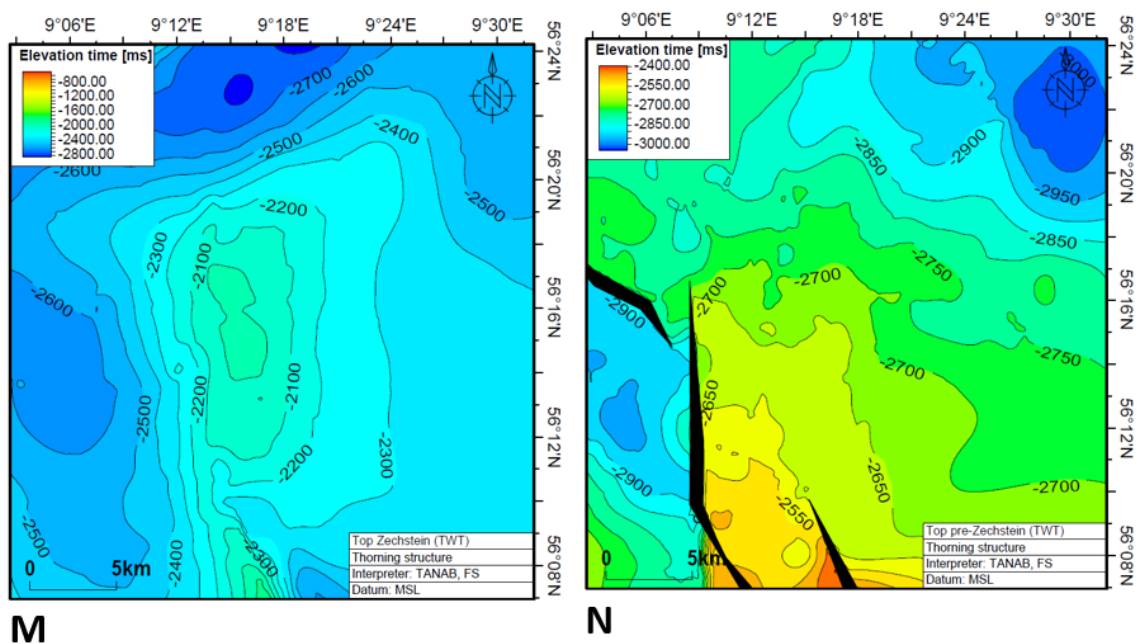


Fig. 6.2.1 continued. Time-structure maps (TWT) in milliseconds (ms) of the Thorning structure. Faults are not shown. M: Top Zechstein; N: Top pre-Zechstein. The maps are produced with a 100x100 m grid and mildly smoothed (iteration x1; filter width 3). The contour interval of the maps is 100 ms for Top Zechstein and 50 ms for Top pre-Zechstein.

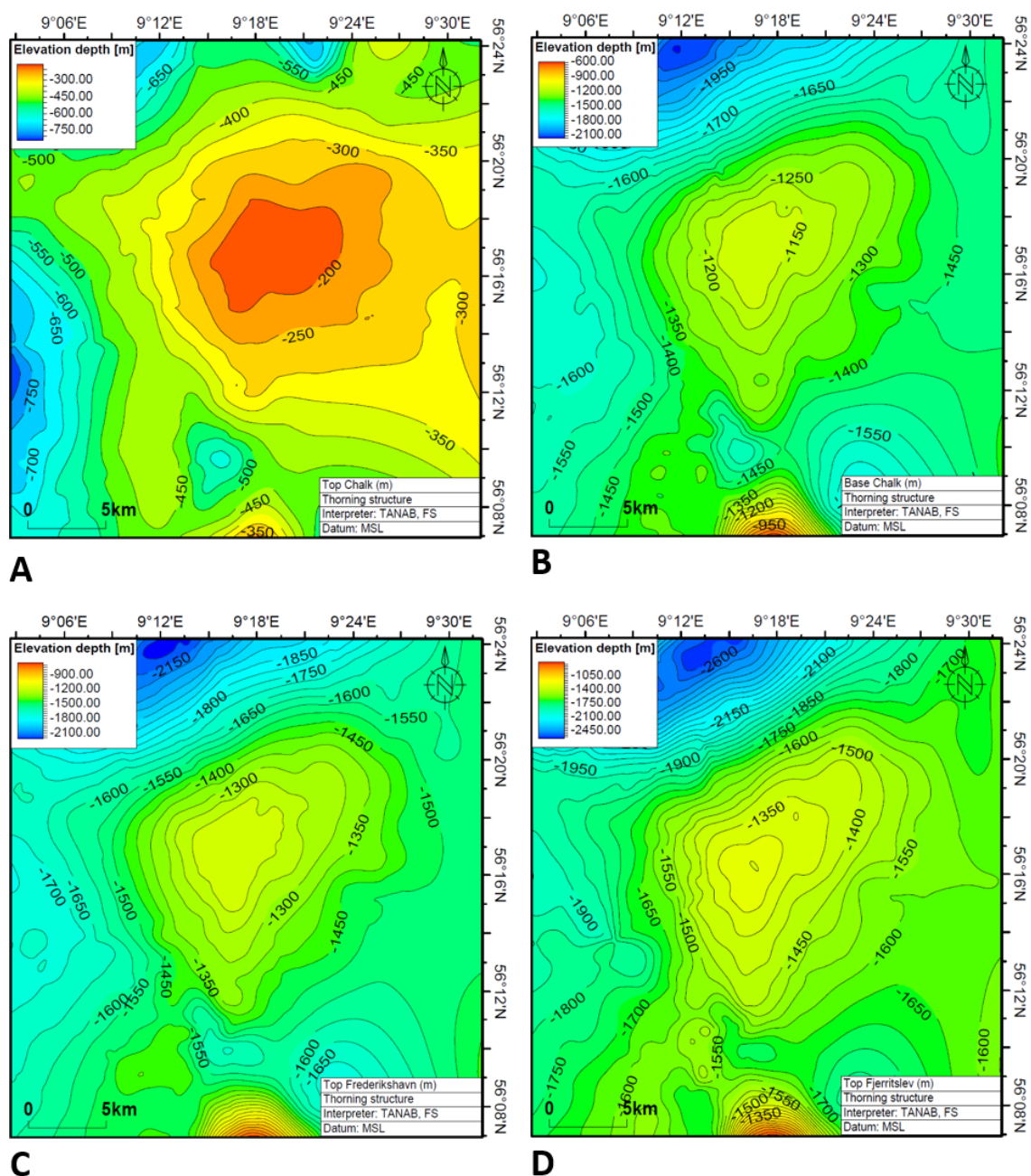


Fig. 6.2.2 Depth-structure maps (meter) of the Thorning structure. Faults are not shown. A: Top Chalk; B: Base Chalk; C: Top Frederikshavn; D: Top Fjerritslev. The maps are produced with a 100x100 m grid and mildly smoothed (iteration x1; filter width 3). The contour interval of the maps is 50 m.

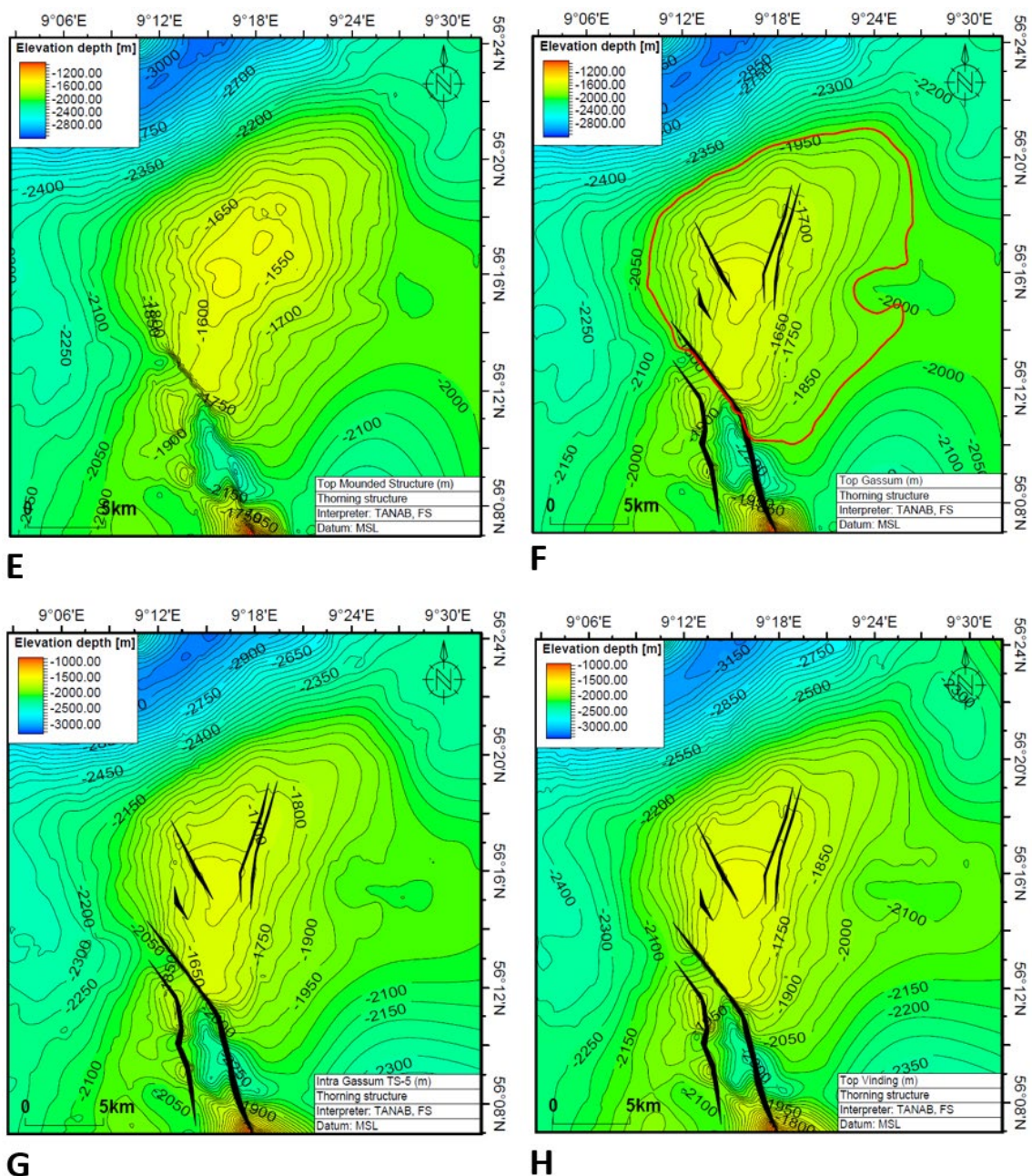


Fig. 6.2.2 continued. Depth-structure maps (meter) of the Thorning structure. Faults are shown on Top Gassum, Intra Gassum-TS 5 and Top Vinding. E: Top Mounded Structure (within the Fjerritslev Fm); F: Top Gassum – the deepest structural closure (red polygon) at 1950 m is cut by a fault to the south (3-way closure); G: Intra Gassum, TS 5; H: Top Vinding (Base Gassum). Note the thickness variations in F and G affected by faults. The maps are produced with a 100x100 m grid and mildly smoothed (iteration x1; filter width 3). The contour interval of the maps is 50 m.

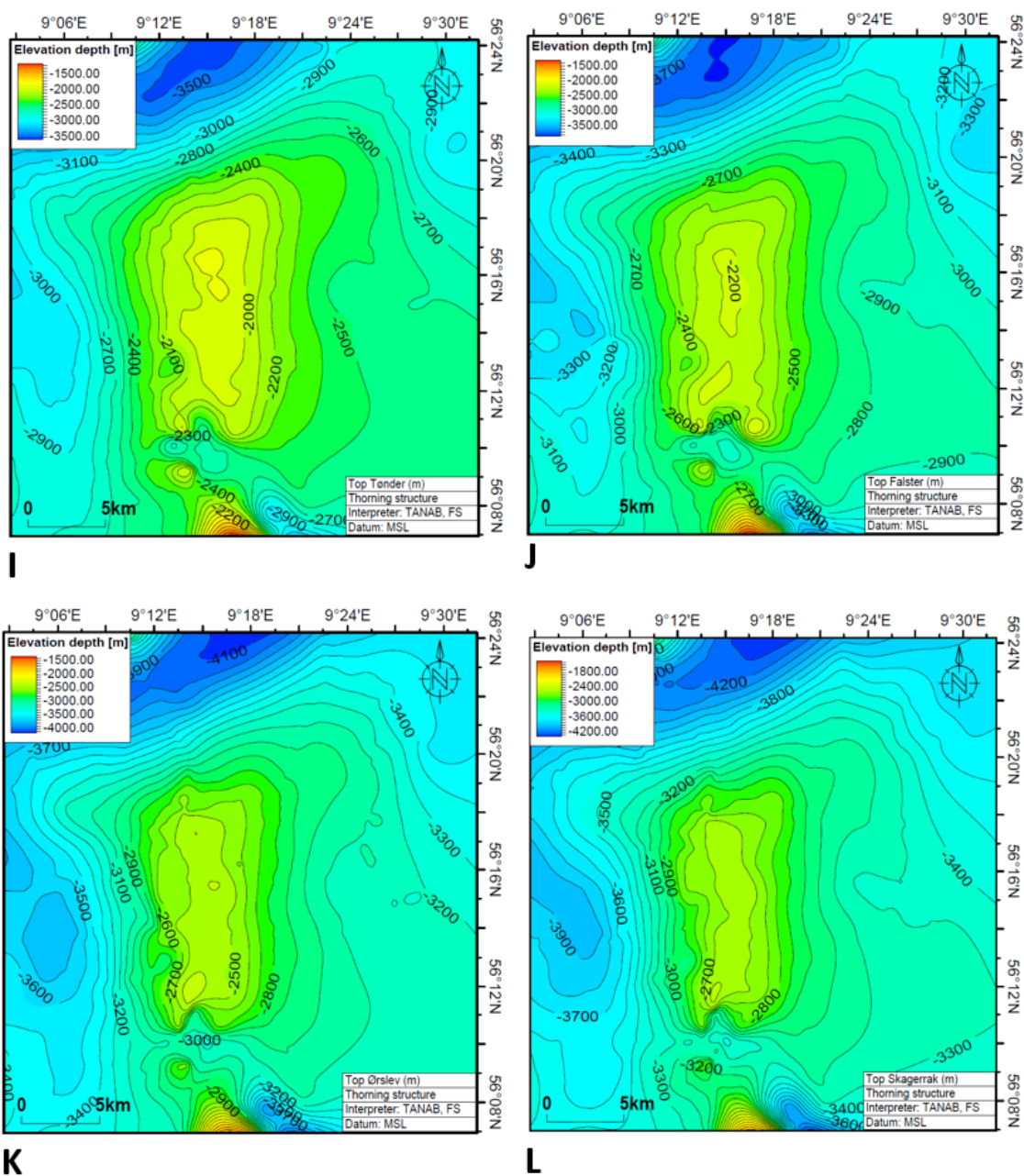


Figure 6.2.2 continued. Depth-structure maps (meter) of the Thorning structure. Faults are not shown. I: Top Falster; J: Top Tønder; K: Top Ørslev; L: Top Skagerrak. The maps are produced with a 100x100 m grid and mildly smoothed (iteration x1; filter width 3). The contour interval of the maps is 100 m.

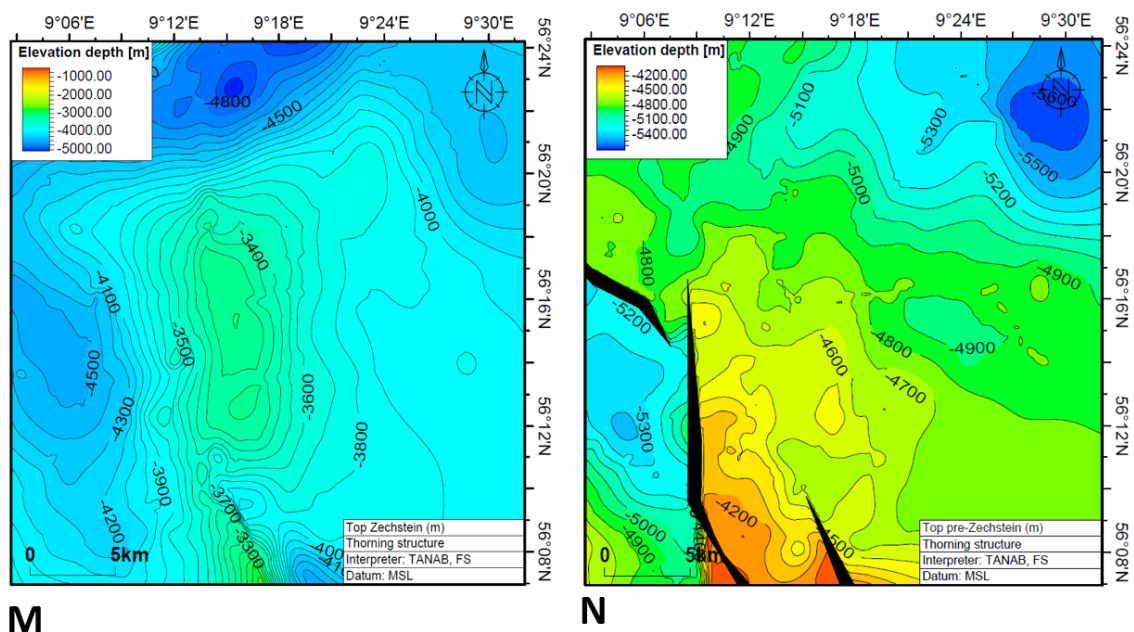


Fig. 6.2.2 continued. Depth-structure maps (meter) of the Thorning structure. Faults are not shown. M: Top Zechstein; N: Top pre-Zechstein. The maps are produced with a 100x100 m grid and mildly smoothed (iteration x1; filter width 3). The contour interval of the maps is 100 m.

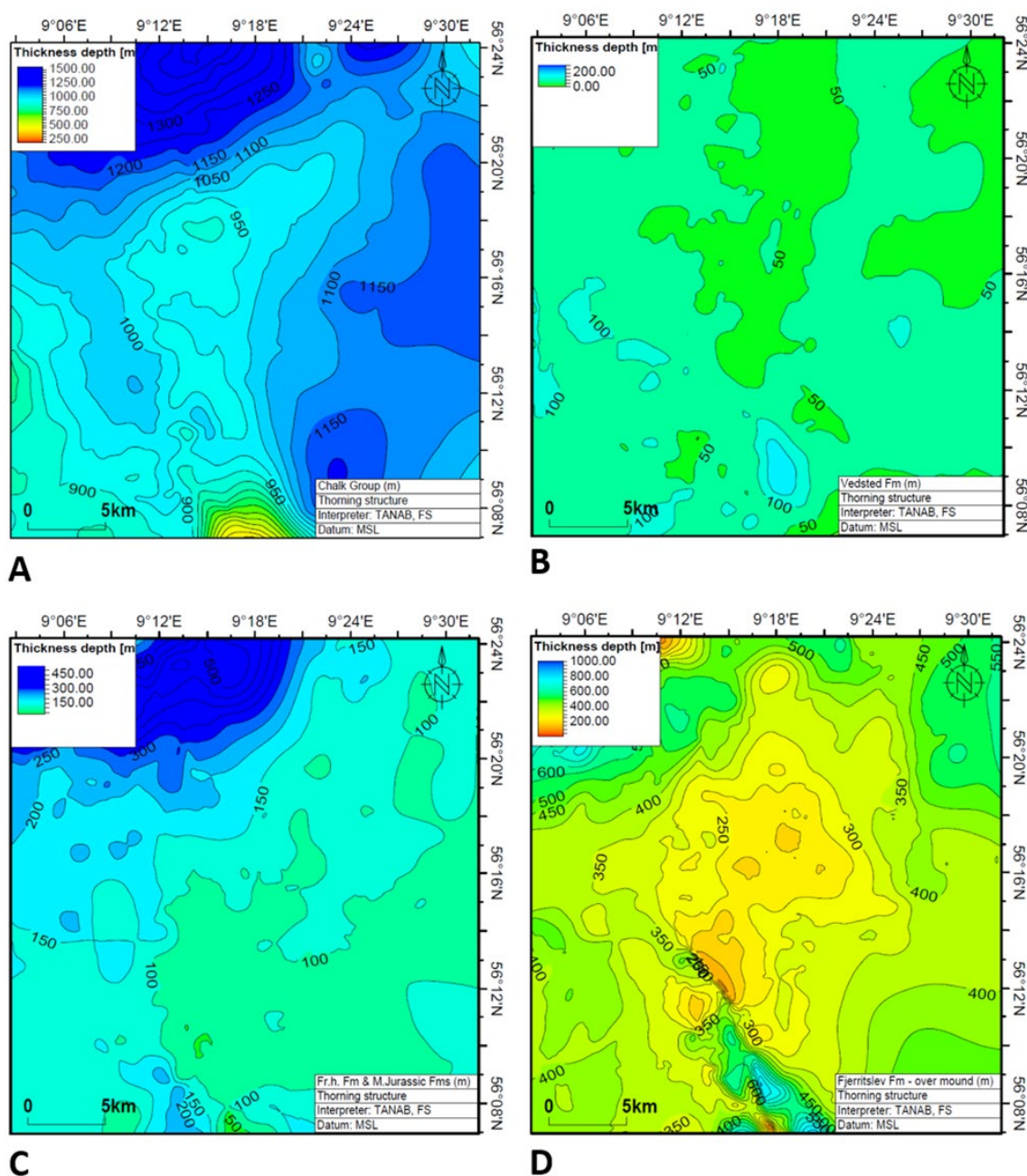


Fig. 6.2.3. Thickness maps (meter) of group and formations in the Thorning structure. Faults are not shown. Approximate thicknesses are indicated within the structure. A: Chalk Group (c. 900–1100 m thick); B: Vedsted Fm (c. 40–80 m thick); C: Frederikshavn Fm and other Middle Jurassic formations (c. 100–200 m thick); D: Fjerritslev Fm over mound (shown in E) (c. 100–300 m thick). The maps are generated from the previously shown depth-structure maps. The contour interval of the maps is 50 m.

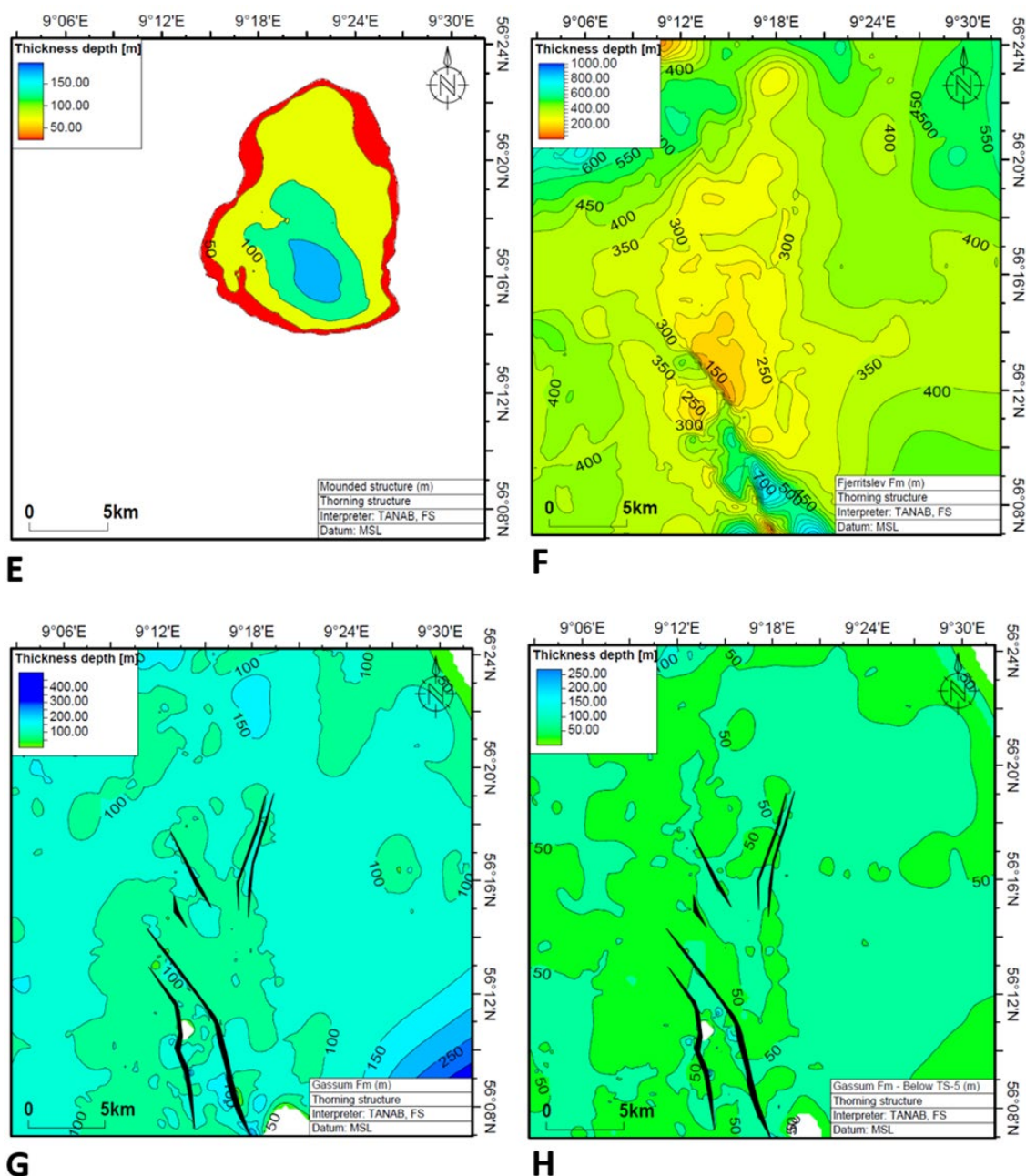


Fig. 6.2.3 continued. Thickness maps (meter) of formations and sub-units in the Thorning structure. Faults are only shown on G. Approximate thicknesses are indicated within the structure. E: Mounded structure (up to c. 150 m thick); F: Fjerritslev Fm (c. 100–350 m thick) – including mounded structure. Large thickness variations to the south at large faults that were active during deposition of the Fjerritslev Fm. G: Gassum Fm (c. 100 m thick in the structure), but thickness locally larger to the south, where it is affected by faults; H: Gassum Fm below TS 5. The maps are generated from the previously shown depth-structure maps. The contour interval of the maps is 50 m.

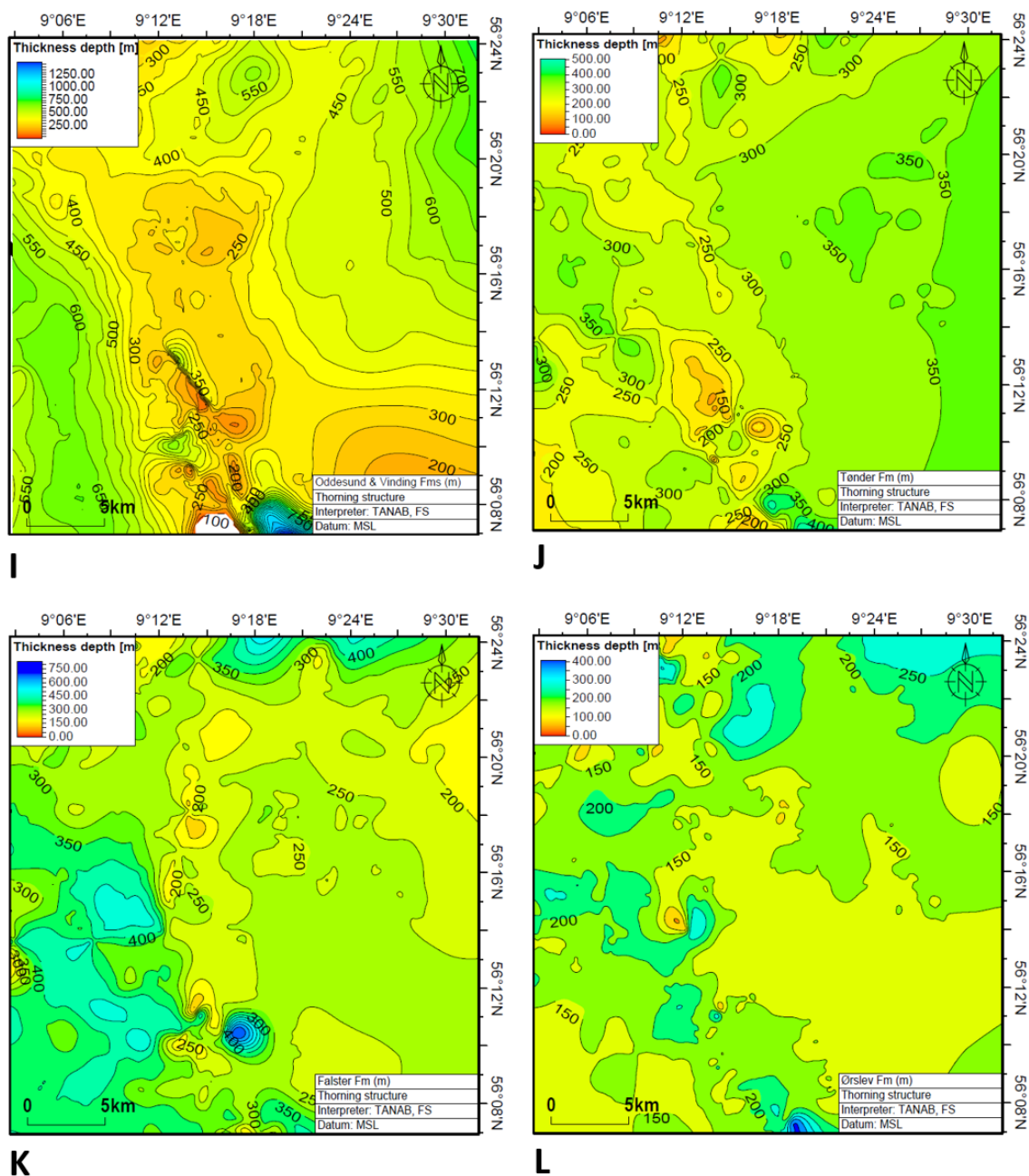


Fig. 6.2.3 continued. Thickness maps (meter) of formations in the Thorning structure. Faults are not shown. Approximate thicknesses are indicated within the structure. I: Oddeund & Vinding Fms (c. 250–400 m thick). J: Tønder Fm (c. 250–325 m thick); K: Falster Fm (c. 200–400 m thick); L: Ørslev Fm (c. 100–200 m thick). The maps are generated from the previously shown depth-structure maps. The contour interval of the maps is 50 m.

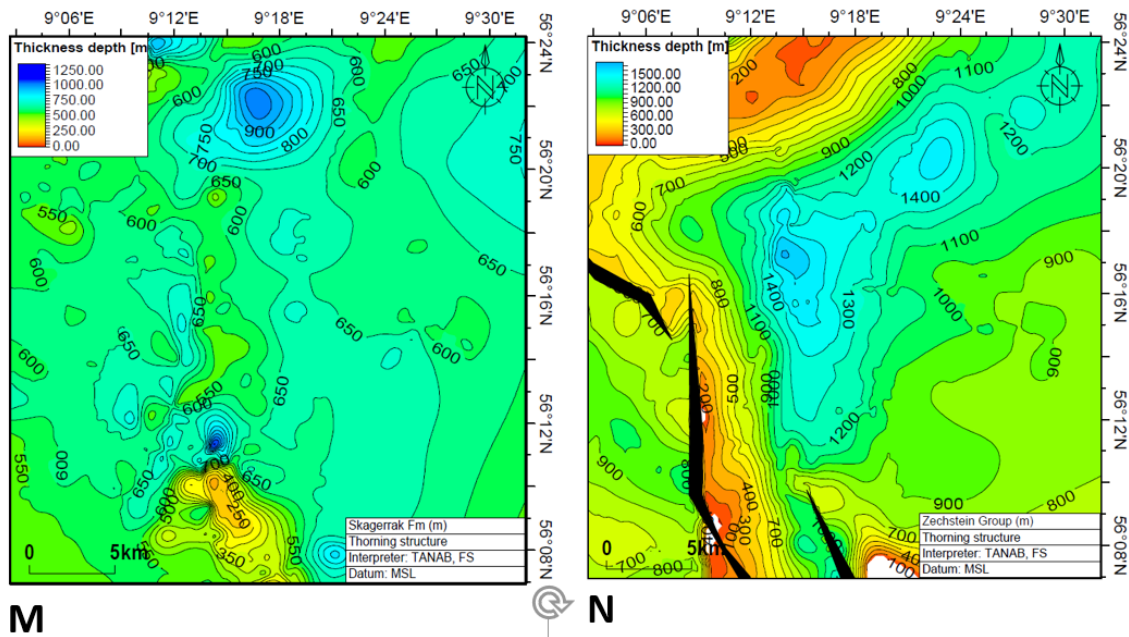


Figure 6.2.3 continued. Thickness maps (meter) of formations and group in the Thorning structure. Faults are shown for the Zechstein Group, mainly for its basal parts, near Top pre-Zechstein. Approximate thicknesses are indicated within the structure. M: Skagerrak Fm (c. 550–650 m thick). N: Zechstein Group (c. 1000–1500 m thick). Note the significant thicknesses of the Zechstein Group with the Thorning Salt Pillow, centrally and NE. The maps are generated from the previously shown depth-structure maps. The contour interval of the maps is 50 m for M and 100 m for N.

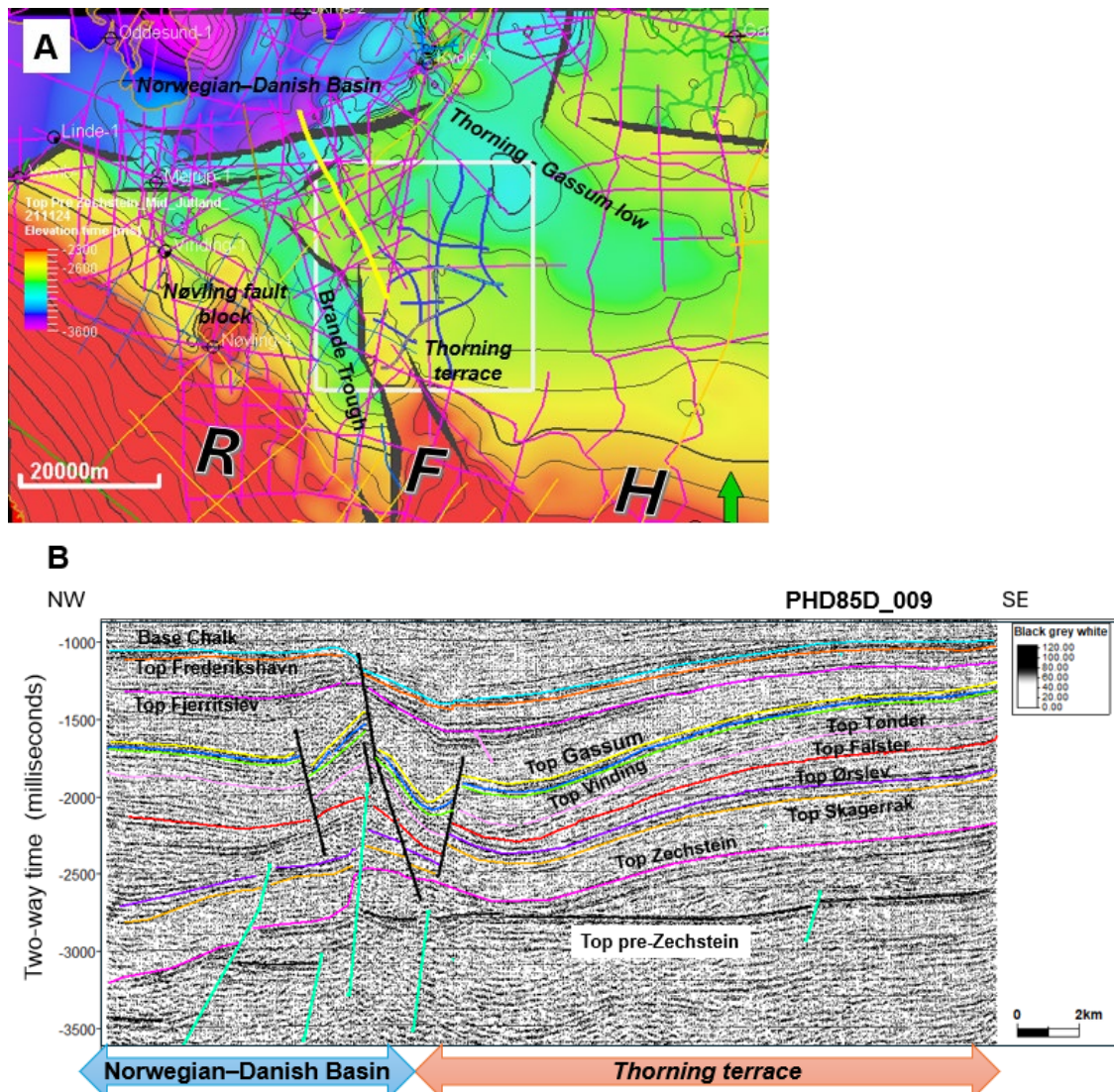


Figure 6.2.4 The shape of the NE-dipping ridge outlining the Thorning terrace. A: Location of the old seismic profile PH85D_009 shown on top of the TWT-map for the Top pre-Zechstein horizon. B: The old seismic profile PH85D_009 illustrates the N-ward faulted transition from the deeper parts of the Norwegian-Danish Basin to the Thorning terrace. The deep-seated faults affecting the Top pre-Zechstein horizon are shown by a clear green color. Horizontal scale is 2 km.

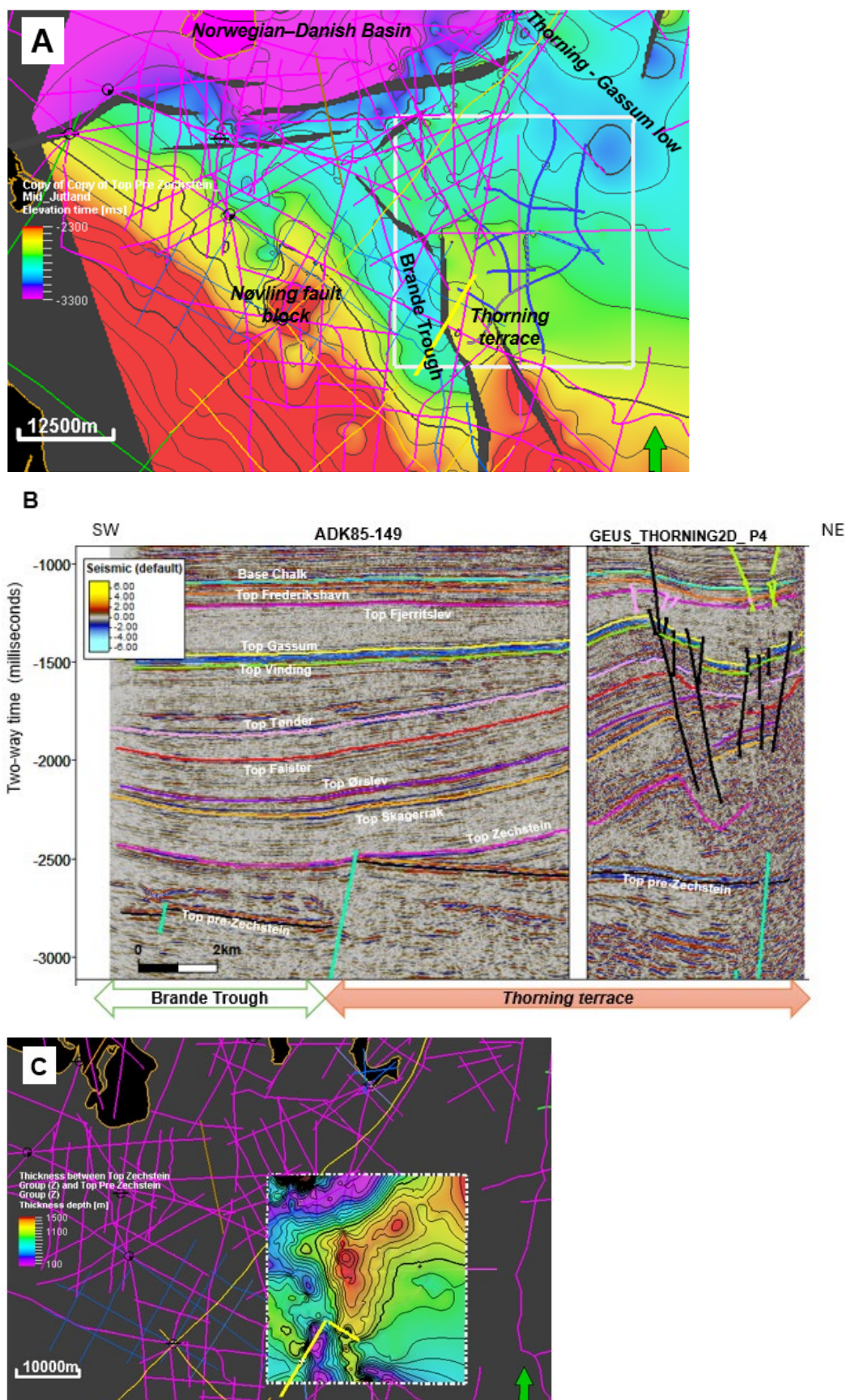


Figure 6.2.5 The faulted transition from Brande Trough to the Thorning terrace. A: Location of the old seismic profile ADK85-149 and the new GEUS_THORNING2D_P4 shown on top of the TWT-map for the Top pre-Zechstein Group. B: The composite seismic ADK85-149 and

GEUS_THORNING2D_P4 profile illustrates the W-ward faulted transition from the Brande Trough to the Thorning terrace. The deep-seated faults affecting the Top pre-Zechstein horizon are shown by a clear green color. Horizontal scale is 2 km. C: Thickness of the Zechstein interval is ranging between 0–1700 m as seen on the depth map obtained from the depth conversion.

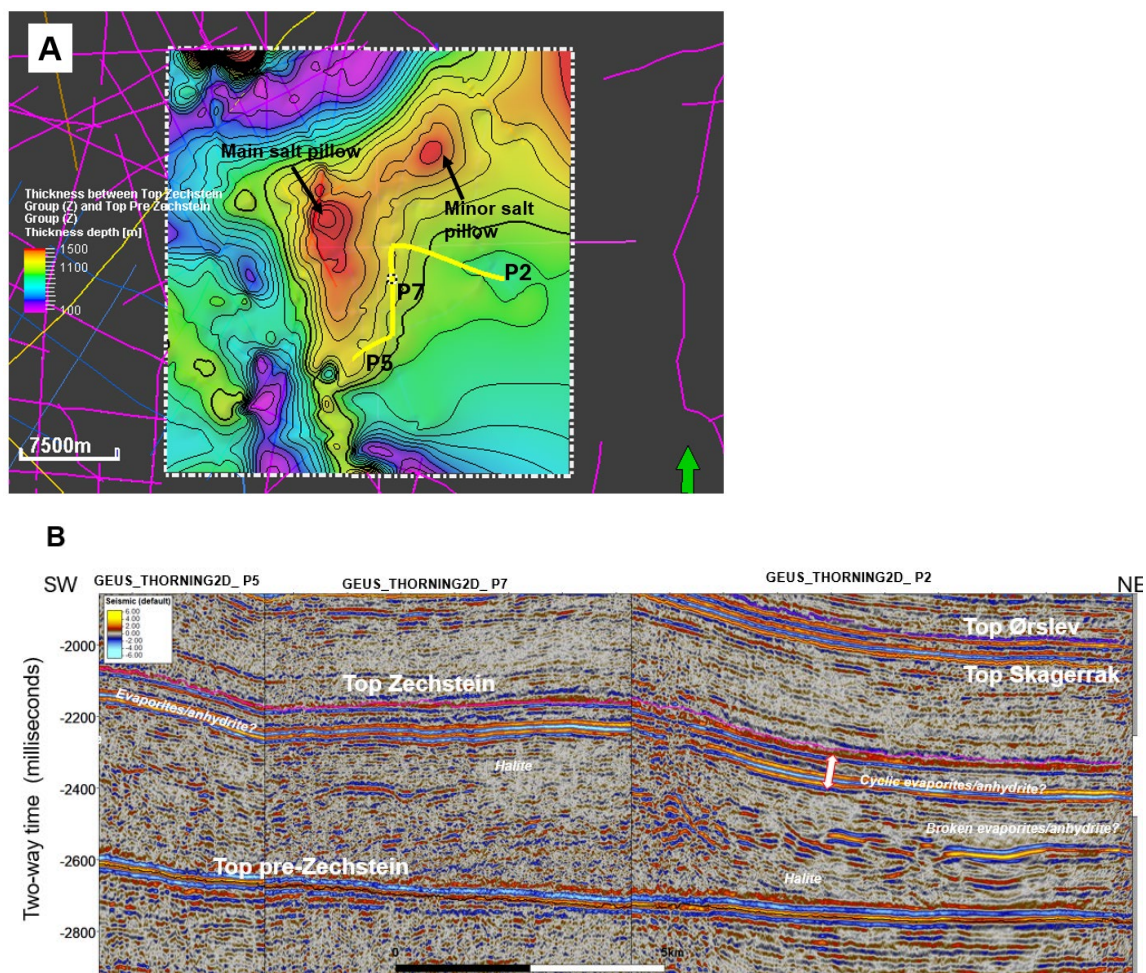


Figure 6.2.6 Illustration of the varied reflectivity observed on GEUS' new seismic data representing a mixed lithological variation from cyclic evaporites (parallel-bedded reflections), deformed evaporites (incoherent bands of parallel-bedded reflections) to more pure halite (transparent zones). A: Location map of composite section along GEUS_THORNING2D_P5, P7 and P2 overlain on a thickness map (m) of the Zechstein interval. B: The composite section along GEUS_THORNING2D_P5, P7 and P2 showing the varied reflectivity of the Zechstein Group. Horizontal scale is 5 km.

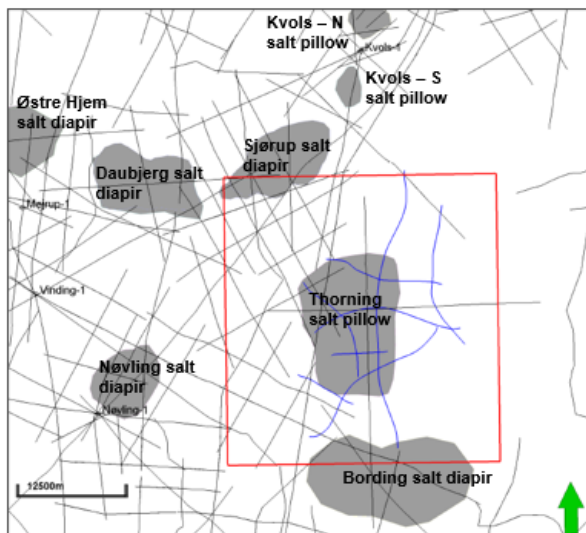
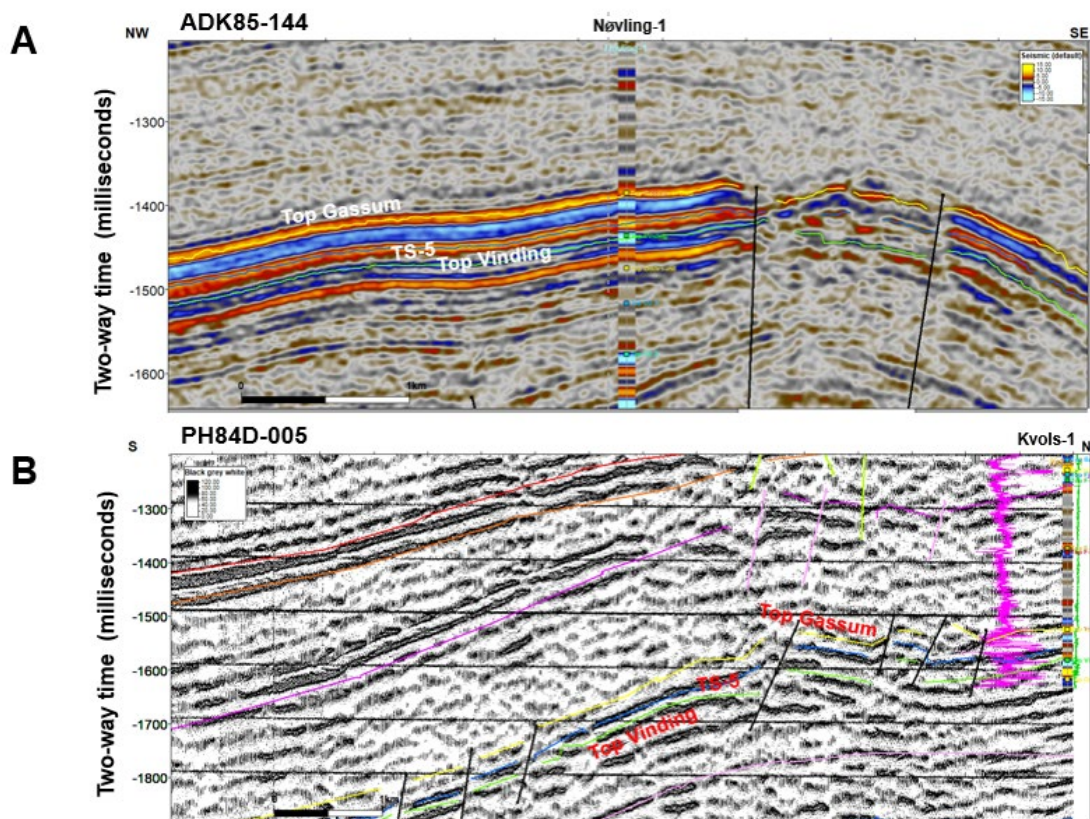


Figure 6.2.7 Mapped salt structures in the vicinity of the Thorning study area (red box).



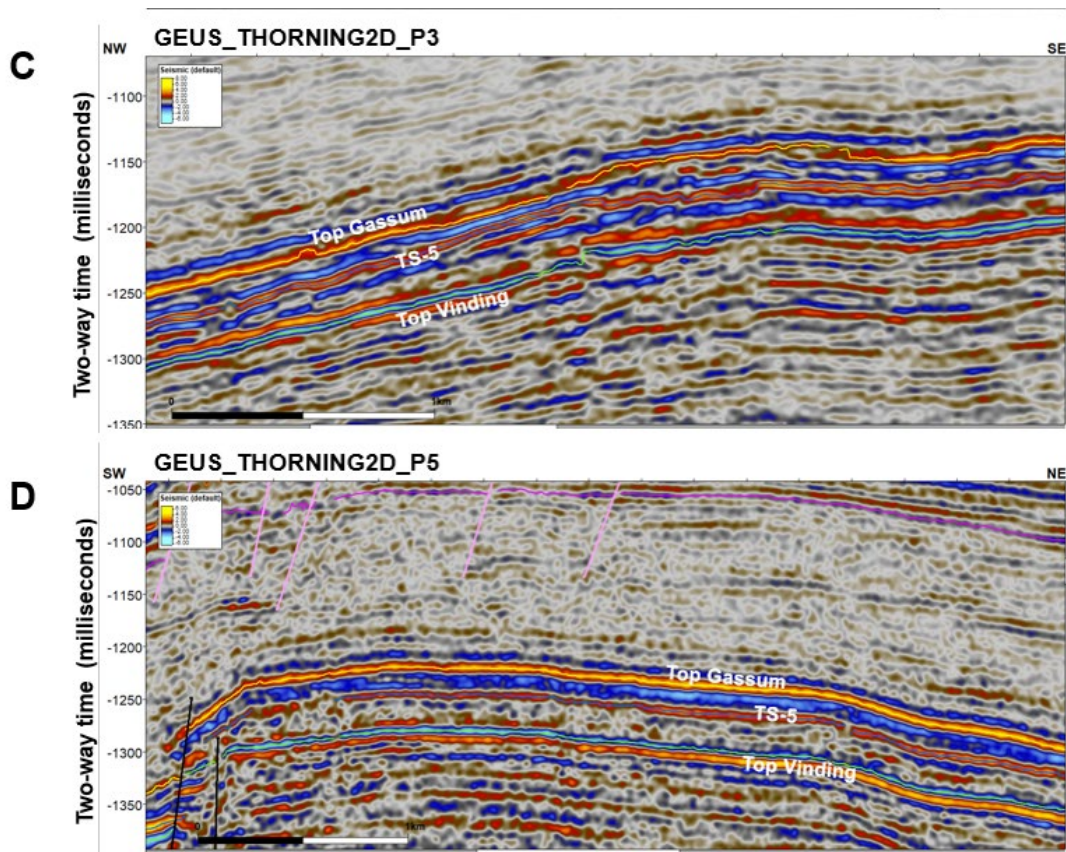


Figure 6.2.8 Variation of seismic signature of the Top Gassum to Top Vinding seismic marker reflections on different seismic vintage. A: Vintage line ADK85-144 through the Nøvling-1 well showing the high amplitude, characteristic seismic signature of the Top Gassum to Top Oddesund Fm interval. B: Vintage line PH84D-005 through the Kvols-1 well showing the characteristic seismic signature of the Top Gassum to Top Oddesund Fm interval easy recognizable by three peaks and two wide troughs. C: New 2023 GEUS_THORNING2D profile 3 showing a reflective upper and lower Gassum Fm separated by the TS 5 surface. D: New 2023 GEUS_THORNING2D profile 5 showing the reflective upper Gassum Fm separated from the more transparent lower Gassum Fm below the TS 5 surface. Horizontal scale is 1 km.

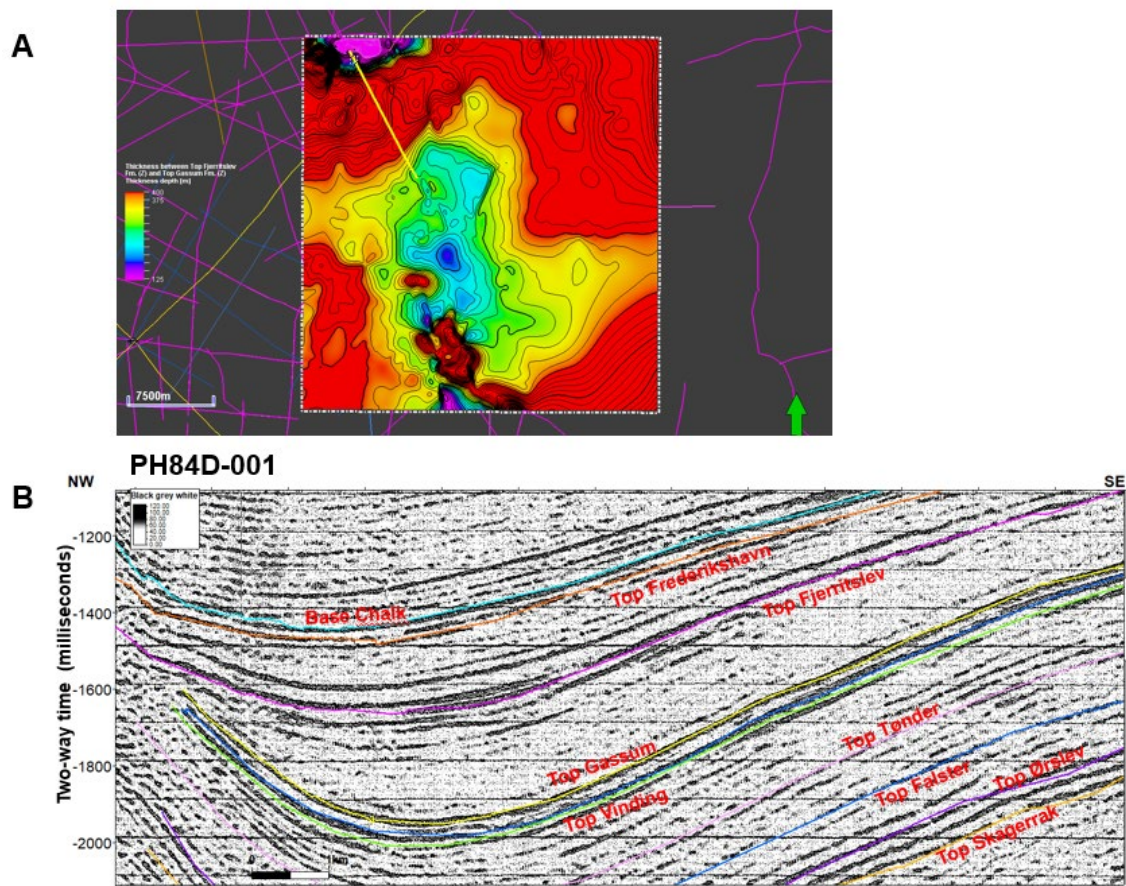


Figure 6.2.9 Example of the angular unconformity constituting the Top Fjerritslev surface where it truncates the Top Gassum to Top Vindinge Fm succession in the northern part of the Thorning study area. A: Thickness map of the Fjerritslev Fm is defined by the difference in depth between the Top Gassum and Top Fjerritslev surfaces and illustrates the general thinning of the Fjerritslev Fm across the Thorning structure. B: Legacy seismic profile (PH84D-001) illustrating the truncation of the older sequences. Horizontal scale is 1 km.

Tectonostratigraphic evolution of the Thorning structure

Resolving the tectonostratigraphic evolution of the Thorning structure is based on the seismic interpretation including stratigraphic control from the few wells that occur in vicinity of the Thorning structure as well as the regional development of the basin (Fig. 6.2.10A). The interpreted tectonostratigraphic development is constrained by seismic stratigraphic horizons correlated to key wells, where lithostratigraphy and ages are defined. The stratigraphy described here includes information from completion reports and in-house GEUS work on the wells mentioned in Table 4.4.1.

A c. 15 km long, composite seismic profile covering parts of GEUS_THORNING2D_P5_Final_PSTM, GEUS_THORNING2D_P7_Final_PSTM and GEUS_THORNING2D_P2_Final_PSTM (now referred to as P5, P7 and P2) was selected for tectonostratigraphic reconstruction across the NW–SE axis of the Thorning structure on the southern flank and includes important insights to both deep and shallow structures (Figs 6.2.10, 6.2.11).

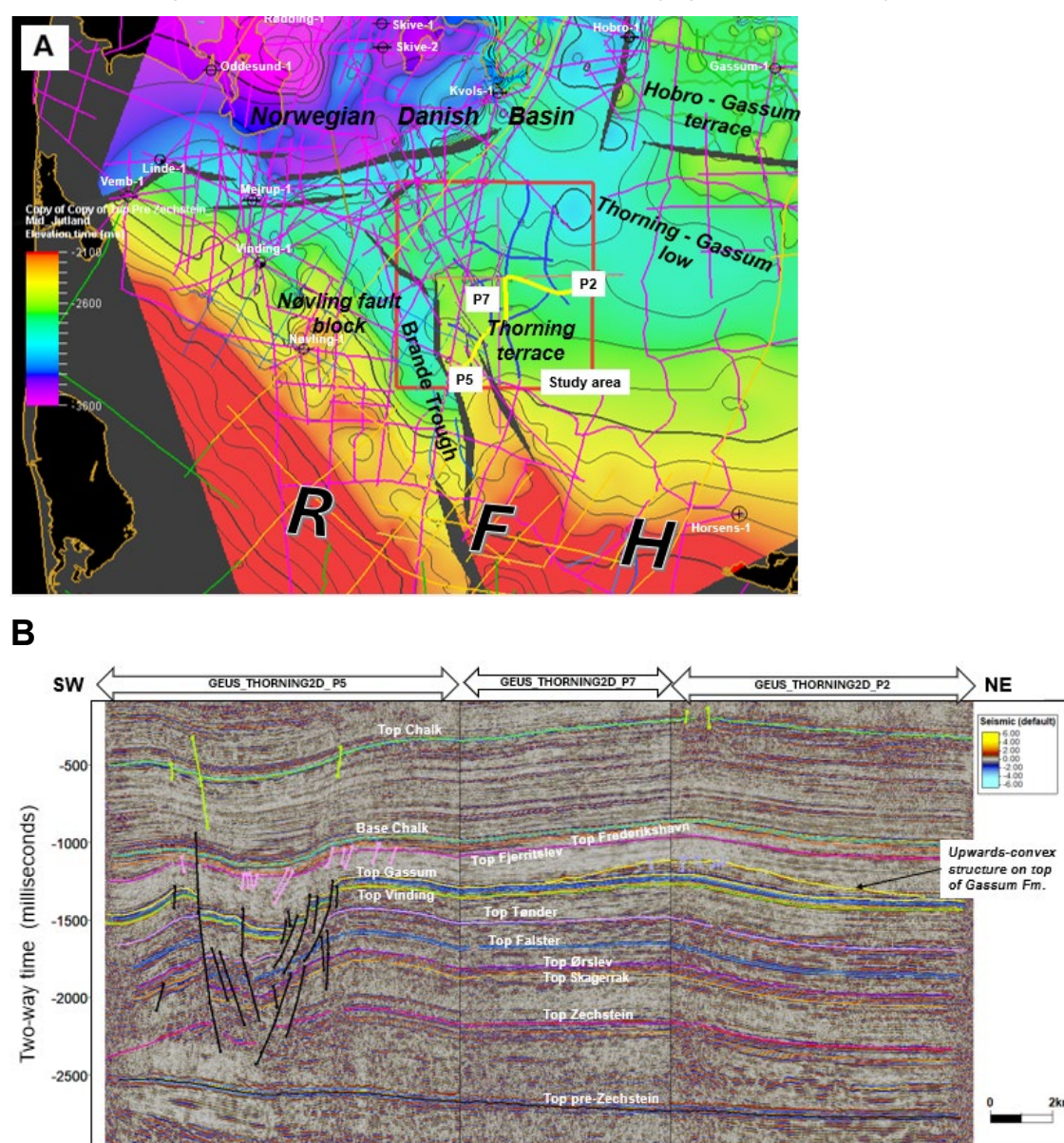
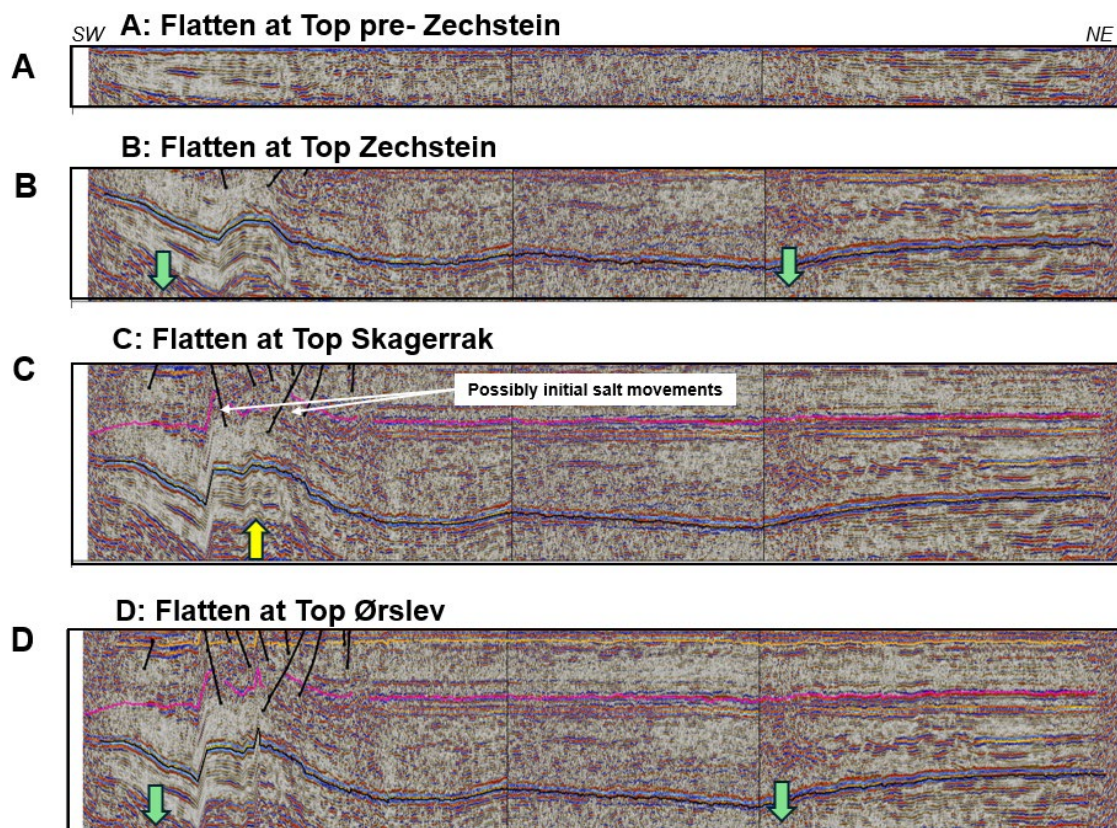
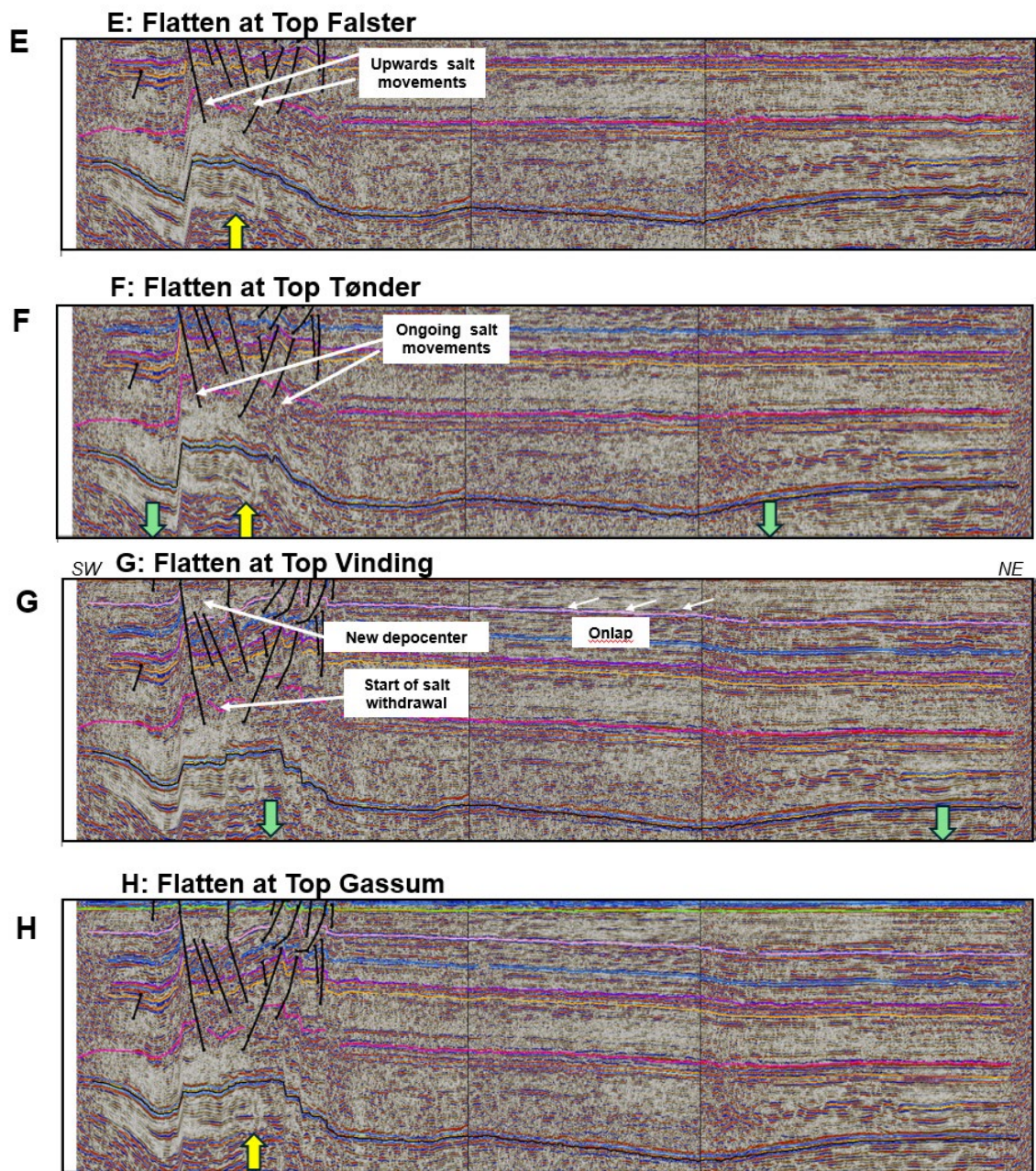


Fig. 6.2.10 A: Location of the composite key reference profile across the NW–SE axis of the Thorning structure shown as a yellow line on top of a tentative structural Top pre-Zechstein map

in ms TWT below mean sea level. B: Composite seismic profile covering parts of GEUS_THORNING2D_P5, GEUS_THORNING2D_P7 and GEUS_THORNING2D_P2 (now referred to as P5, P7 and P2) across the southern flank of the Thorning structure used for the tectonostratigraphic reconstruction discussed in the text.

The tectonostratigraphic reconstruction and evolution of the area is summarized, based on three key profiles, interpretation and mapping of seismic horizons delineating interpreted stratigraphic units and faults, using horizon flattening and back-stripping for a palinspastic or structural restoration (Figs 6.2.10, 6.2.11). The tectonostratigraphic evolution of the area is described below, mainly from sections with flattened horizons, from the Top pre-Zechstein to the top of the Chalk Group (Top Chalk), suggesting that the initial formation of the Thorning structure started in the Triassic.





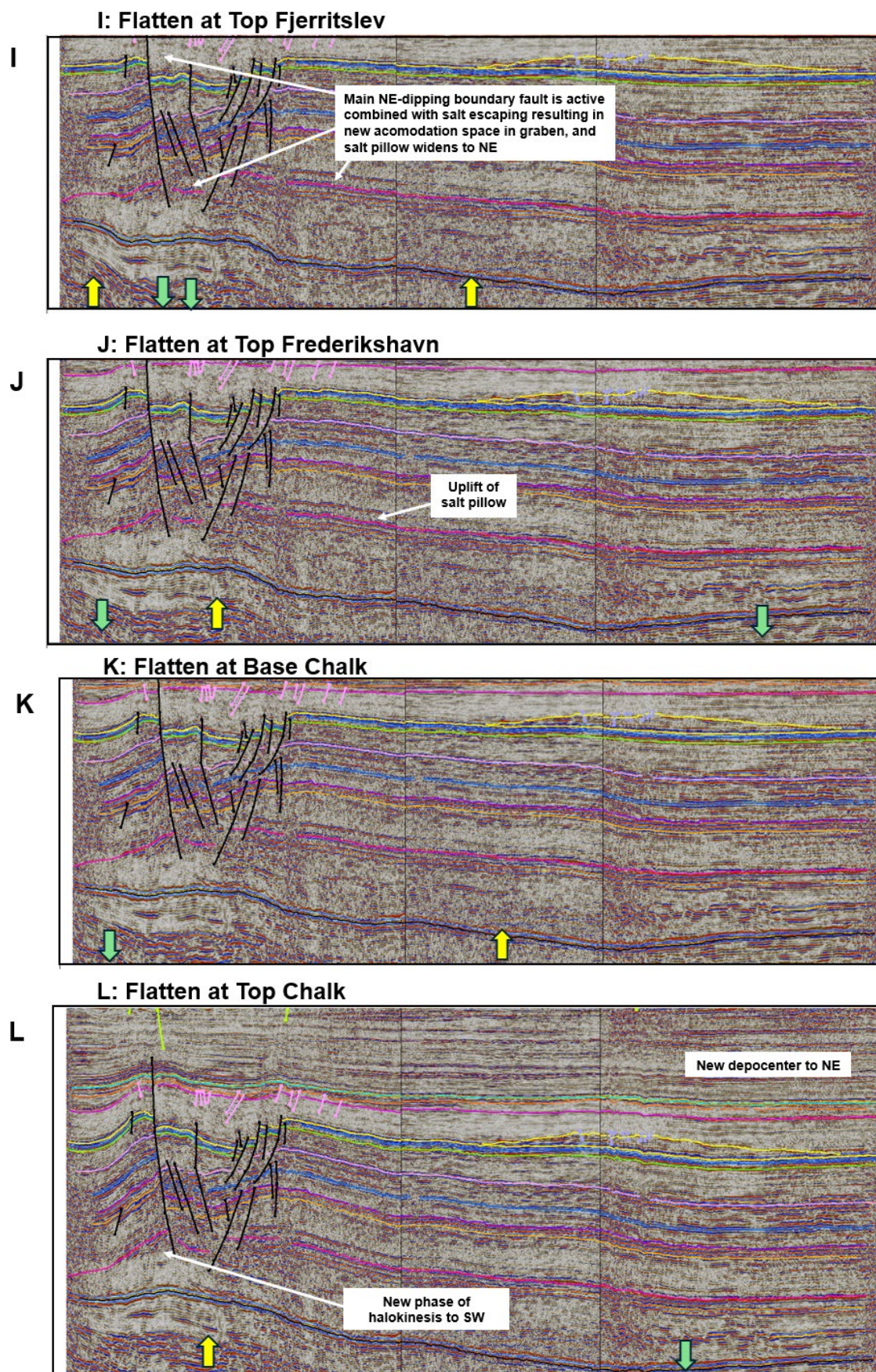


Fig. 6.2.11 A tectonostratigraphic reconstruction along the profile shown in Fig. 6.2.10, with horizon flattening of key-horizons illustrating the Palaeozoic (A) to Cretaceous (L) structural evolution of the Thorning structure described in the text.

The tectonic framework of the Thorning area

The Thorning area is situated at the transition from the Ringkøbing–Fyn High in the south to the Norwegian–Danish Basin in the north, the two fundamental geological features in Central Jutland. The Ringkøbing–Fyn High is a major structural element defining an approximately 450 km long, WNW–ESE-striking set of basement highs (*sensu* Peacock & Banks, 2020) consisting of the Grindsted High, Glamsbjerg High, Møn High and Arkona High to the east of Denmark (according to the nomenclature used by Vejrbæk, 1997).

Our study area is located north of the Grindsted High where the transition from the major elevated basement high into the deeper parts of the Norwegian–Danish Basin further north is not defined by a clear straight line, but rather dominated by N-ward extending outliers of elevated fault-bounded basement blocks, such as the Nøvling fault block, and the Thorning terrace or intra-basinal structural high, see Fig. 6.2.10A.

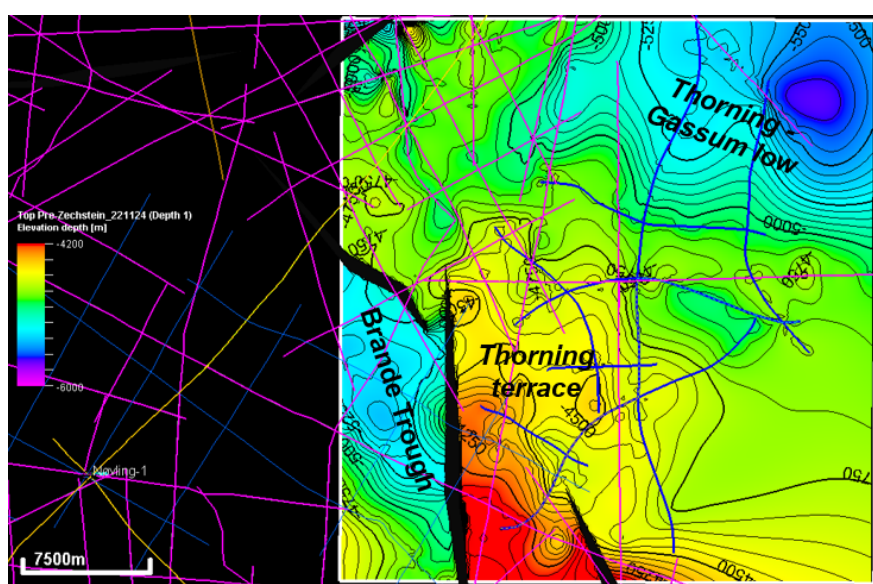


Figure 6.2.12 Structural depth-structure map of the depth to the Top pre-Zechstein horizon in the Thorning study area in meter (b.msl). The depth-structure map is a result of the depth conversion described in Chapter 5. The elevated N–S to NNW–SSE striking Top pre-Zechstein surface underlying the Thorning area is clearly imaged with a gentle dip from south to north across the study area. The depth to the Top pre-Zechstein horizon varies between 4000–5600 m below mean sea level as determined by the new depth conversion within the study area.

During the Late Permian, Denmark was in palaeogeographical low latitudes and experienced a generally hot and dry climate. Several marine incursions into the Norwegian Danish Basin led to evaporation and the deposition of the Zechstein evaporites, which formed numerous salt structures in the Norwegian Danish Basin during the Mesozoic–Cenozoic (e.g. Maystrenko *et al.* 2008). During the Triassic, the Ringkøbing–Fyn High subsided faster compared to during in the Late Permian but still at a slower pace compared with the North German and Norwegian–Danish basins. This led to the thinning of the Triassic successions across the Ringkøbing–Fyn High (Clausen & Pedersen, 1999).

The Thorning study area is located north of the Ringkøbing–Fyn High which was formed during the pre-Zechstein extension, driven by Late Carboniferous–Early Permian dextral strike-slip movements within the Trans-European Suture Zone, during which the

Ringkøbing–Fyn High experienced less stretching than the adjacent subsiding North German and Norwegian–Danish basins (Thybo, 1997, 2001; Vejbæk, 1997; Clausen & Pedersen, 1999). Accordingly, in most parts of the highs, the crystalline Baltica-type basement is relatively shallow and directly underlies the top pre-Zechstein horizon as dated by Olivarius et al., 2015 in the Grindsted-1 well.

Pre-Zechstein and Zechstein evolution

In the Thorning study area, the Top pre-Zechstein horizon is the deepest regional mappable surface, and its overall topography may to a certain extent reflect or mirror the topography of the buried deeper-lying crystalline basement (see Figs 6.2.1N; .6.2.2N and 6.2.10A). The thickness of the pre-Zechstein successions in the Thorning study area is unknown due to the lack of regionally coherent seismic reflections from the seismic acoustic basement in the greater study area. However, dipping reflections from the older unknown pre-Zechstein deposits can be observed on a large part of the legacy seismic data from Central Jutland. The depth to the Top pre-Zechstein horizon varies from c. 3–6 km, see Fig. 6.2.12.

The Top pre-Zechstein unconformity was transgressed by the Zechstein Sea in the Late Permian and a restricted Zechstein Sea formed where evaporites were deposited (Vejbæk 1997). This was followed by lithospheric thermal contraction creating subsidence and accommodation space for Zechstein evaporites and the overlying thick Triassic successions. The evaporites formed in an arid climate during the Late Permian time in large parts of the Danish Basin, where later mobilization of the halite led to formation of numerous diapirs and pillows in the area.

Triassic to Early Jurassic evolution

Skagerrak Formation (former Bunter Sandstone Formation and Bunter Shale Formation)

The relatively uniform thickness of the Skagerrak Formation (Figs 6.2.3M) suggests sparse, if any signs of syn-depositional faulting and salt tectonism. However, local uplift occurs at the southern end of the Thorning terrace during the deposition of the deeper Top Skagerrak (former Bunter Sandstone and Bunter Shale) Formation resulting in initial extensional faulting and evolution of a graben structure in the Thorning Fault Zone labelled B in Fig. 6.1.2. This localized faulting is probably associated with the first onset of salt movements (halokinesis), Fig. 6.2.11C.

Ørslev Formation

During deposition of the Ørslev Formation, the study area undergoes gentle and uniform subsidence, and syn-depositional faulting in the graben structure at the southern end of the Thorning terrace which is in good agreement with the uniform thickness of the Ørslev Formation.

Falster to Tønder formations

The tectonostratigraphic reconstruction for the Top Falster surface (Fig. 6.2.11E-F) suggests local uplift and ongoing salt movements inside the graben structure to the SW, followed by a slight NE-ward widening of the salt pillow and a gentle subsidence to the NE during the deposition of the Top Tønder surface.

Oddesund to Vinding formations

The first significant sign of a salt withdrawal phase is recognized by the abrupt change in thickness of the Top Vinding and Oddenund successions inside the graben of the Thorning Fault Zone to the SW. Here, formation of a local depocenter place during this period as evidenced by the thick accommodation space occurring near the NE-dipping main boundary fault (Fig 6.2.13).

The structural reconstruction at Top Vinding level (Fig. 6.2.11, 6.2.13) show the increased thickness of the Vinding and the Oddenund formations to the NE corresponding to a general tilt of the main deposition centre to the NE due to salt withdrawal within the graben. The salt that migrated away from below the graben structure may either have moved into the Thorning salt pillow to the NW or moved in an up-dip direction to the Bording salt diapir located c. 5–7 km to the south at the edge of the Thorning study area, see Fig. 6.2.7.

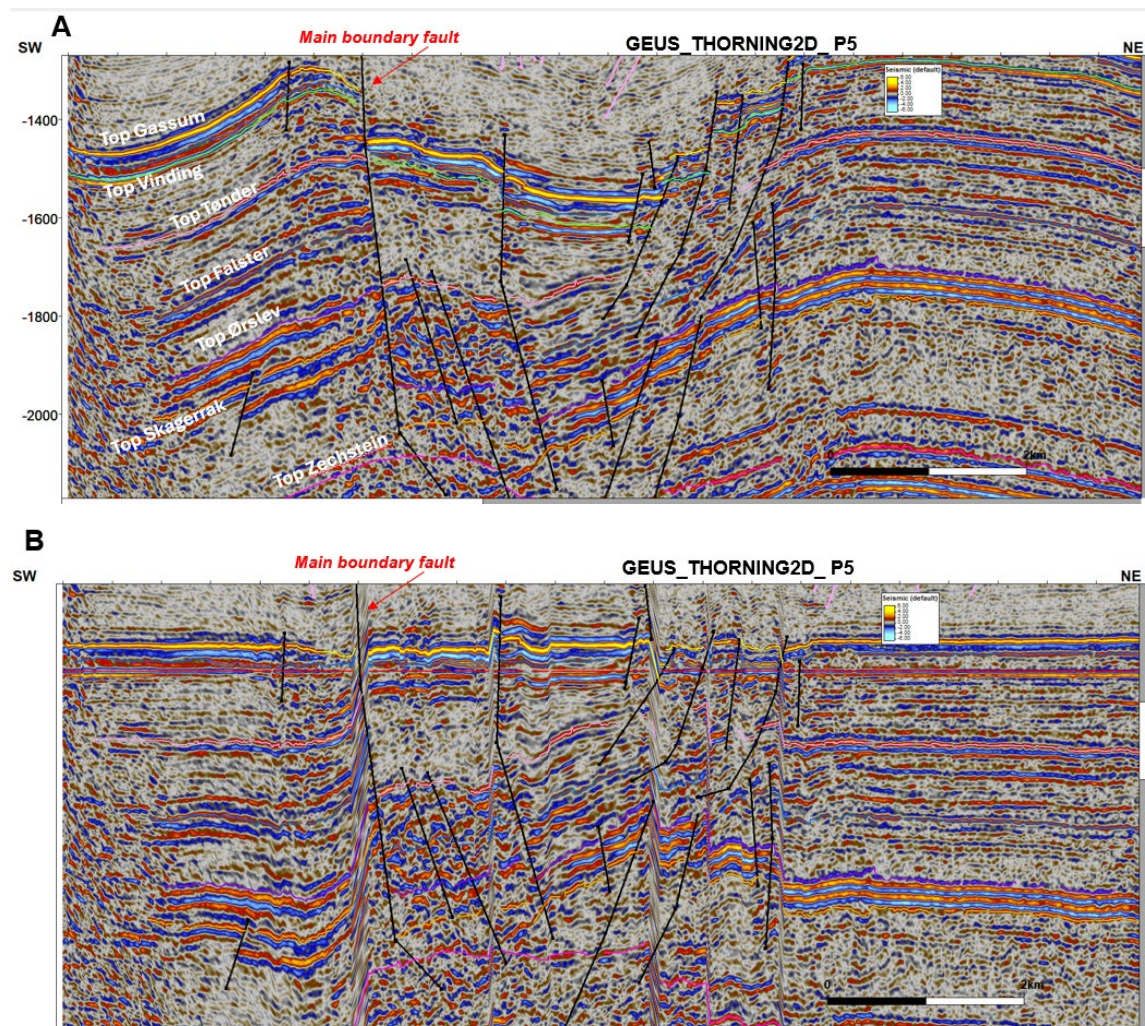


Figure 6.2.13 Illustration of a graben structure with extensional faulting of the Top Gassum and Top Vinding formations on GEUS_THORNING2D_P5 due to salt withdrawal. A: Seismic interpretation of GEUS_THORNING2D_P5. B: Structural flattening along the Top Vinding surface to illustrate the thick accommodation space occurring near the NE-dipping main boundary fault. Horizontal scale is 2 km.

Gassum Formation and TS5

During deposition of the Gassum Formation, the graben structure in the SW area was uplifted due to ongoing salt tectonics causing pushing from below and up doming, and possibly re-activation of the boundary faults as reverse faults. The thinning of the lower part of the Gassum Formation (below TS5) in the graben structure may suggest less accommodation space for deposition, possibly due to uplift caused by syn-depositional salt tectonics.

Early Jurassic to late Early Cretaceous

The seismic stratigraphic unit above the Top Gassum Formation has been drilled by nearby wells and consists of mudstones from the Lower Jurassic Fjerritslev Formation. The Top Fjerritslev horizon is interpreted as a significant seismic stratigraphic unconformity corresponding to the 'Base Middle Jurassic unconformity' or 'Mid-Cimmerian Unconformity' (Nielsen 2003) associated with uplift and erosion (creating a major hiatus) over structures and margins of the Danish Basin (Fig 3.3).

Fjerritslev Formation

The tectonic reconstruction and flattening at the top Fjerritslev Formation horizon (Fig. 6.2.11I) suggest that the Thorning area underwent a structural re-organization due to reactivation of the main NE-dipping boundary fault creating additional accommodation space and a local depocenter in the graben structure. This coincided with increased salt movements and a widening growth of the salt pillow to the north combined with subsidence to the northern flank, resulting in an overall tilt of the Thorning structure with a main depocenter away from the top of the structure and widespread erosion along truncation patterns at the flanks of the structure.

Frederikshavn Formation

During deposition of the Frederikshavn Formation (Fig. 6.2.11J), the northern part of the area underwent gentle subsidence while the graben area on the southern flank indicates a lateral thinning of the Frederikshavn Formation due to ongoing salt movements. The block located south of the graben area also subsided resulting a local accommodations space for Frederikshavn Formation deposits which explains the observed thickness variations in the area.

During the Early Cretaceous, the sand-rich Frederikshavn Formation was deposited over the area forming a secondary reservoir, which is overlain by the Vedsted Formation mudstones (seal) (see more in Chapter 7).

The Cretaceous to Pleistocene evolution

Chalk Group

The Lower Cretaceous Vedsted Formation is overlain by the regional mapped Base Chalk surface, which marks the base of Upper Cretaceous Chalk Group. The tectonic reconstruction and flattening of the Base Chalk surface along the key reference profile (Fig. 6.2.11K), reveals a general episode of subsidence during Late Cretaceous.

Tectonic reconstruction at the Top Chalk surface (Fig. 6.2.11K), suggests that a new episode of salt movements took place leading to local uplift and reactivation of the extensional

boundary faults of the graben structure as reverse faults, and thereby inverting the layers of the graben to pop-up as an antiform structure. General subsidence along the NE part of the key profile corresponding to a thickening of the Chalk Group to the N and NE (see Fig. 6.2.14). The reactivated faulting is interpreted to have been associated with salt motion, and consequently, the youngest salt movements must be Late Cretaceous and/or Cenozoic in age. This is confirmed by the decreasing chalk thickness over the crest of the Thorning structure, possibly controlled by erosion after Cenozoic salt pillow growth (Fig. 6.2.3A).

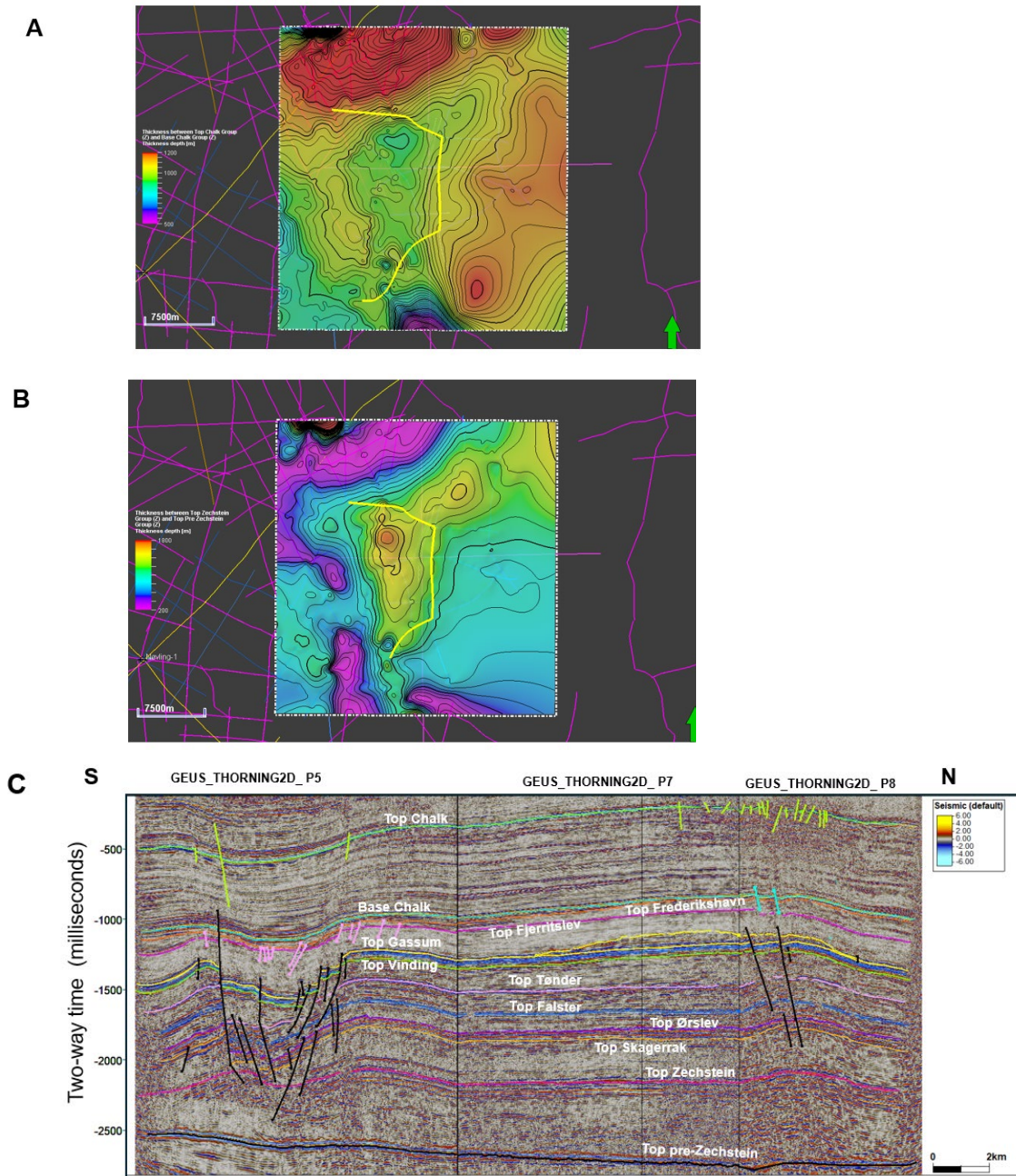


Figure 6.2.14 Example of the varying thickness of the Chalk Group across the Thorning study area. A: Thickness map of the Chalk Group is defined by the difference in depth between the Top Chalk and base Chalk surfaces and illustrates the general thinning across the Thorning structure. B: Thickness map of the Zechstein Group The thickness variation on the Chalk Group is associated with halokinesis and the growth of the Thorning salt pillow. C: Composite seismic profile (GEUS_THORNING2D_P5, P7 and P8) illustrating the structural variations of the Chalk Group.

The Chalk Group is in general >950 m thick in the Thorning area (Fig. 6.2.3A) and is overlain by Paleocene mudstones covering and draping over the Thorning structure. However, erosional thinning of the overlying Paleocene unit at the intersection between profiles P7 and P8, suggests additional salt growth of the northern smaller salt pillow during the Late Cretaceous to post-Paleocene, see Fig. 6.2.14C.

Post-Chalk successions

Sandersen and Jørgensen (2016) have mapped glacial buried valleys in the Thorning study area using SkyTEM electromagnetic data (Fig. 6.2.15). Screening and mapping of buried valleys on the different available processed versions of the 2023 GEUS_THORNING2D survey datasets (Fig. 6.2.16) show a very close correlation to the results by Sandersen and Jørgensen (2016). Here, a composite seismic TWT-section along GEUS_THORNING2D_P8 and P7 demonstrates how the incised valley extends deep and almost intersect the Top Chalk surface. Such near-surface structures and in general the nature of the shallow section, should be closely mapped and investigated for the successions above the top seals and other risks.

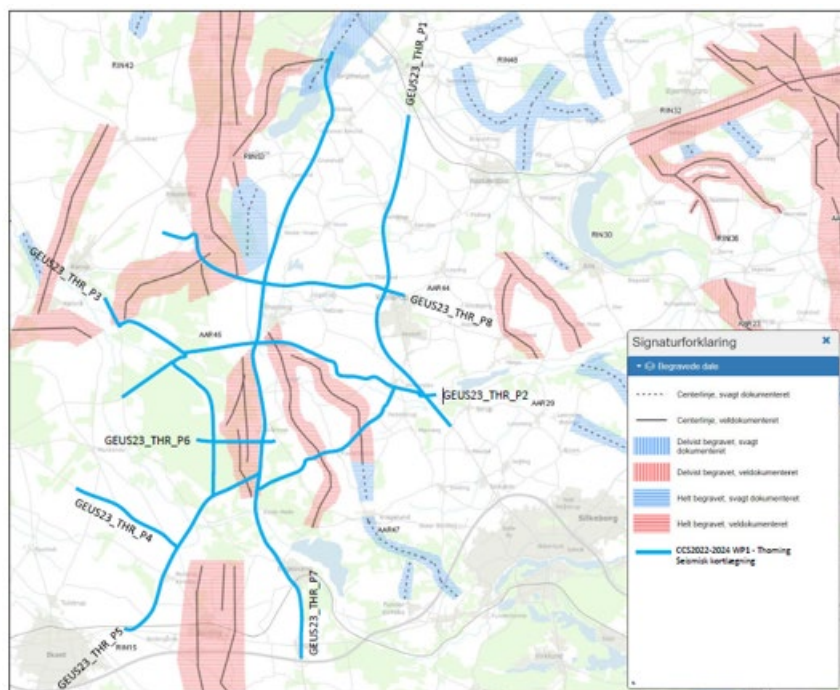


Figure 6.2.15 Glacial buried valleys have been mapped in the Thorning study area using SkyTEM data imaging the incisions in the pre-Quaternary surface which is made of mainly Oligocene clay with high conductivity values. On SkyTEM data the valleys can be identified as elongated structures with low conductivity (more sand-rich deposits). The N–S striking buried valleys can be correlated for more than 10 km with widths between 700–1200 m and depths up to 150 m b.sl. (Sandersen & Jørgensen, 2016). The thick blue lines indicate the position of the Thorning 2D lines.

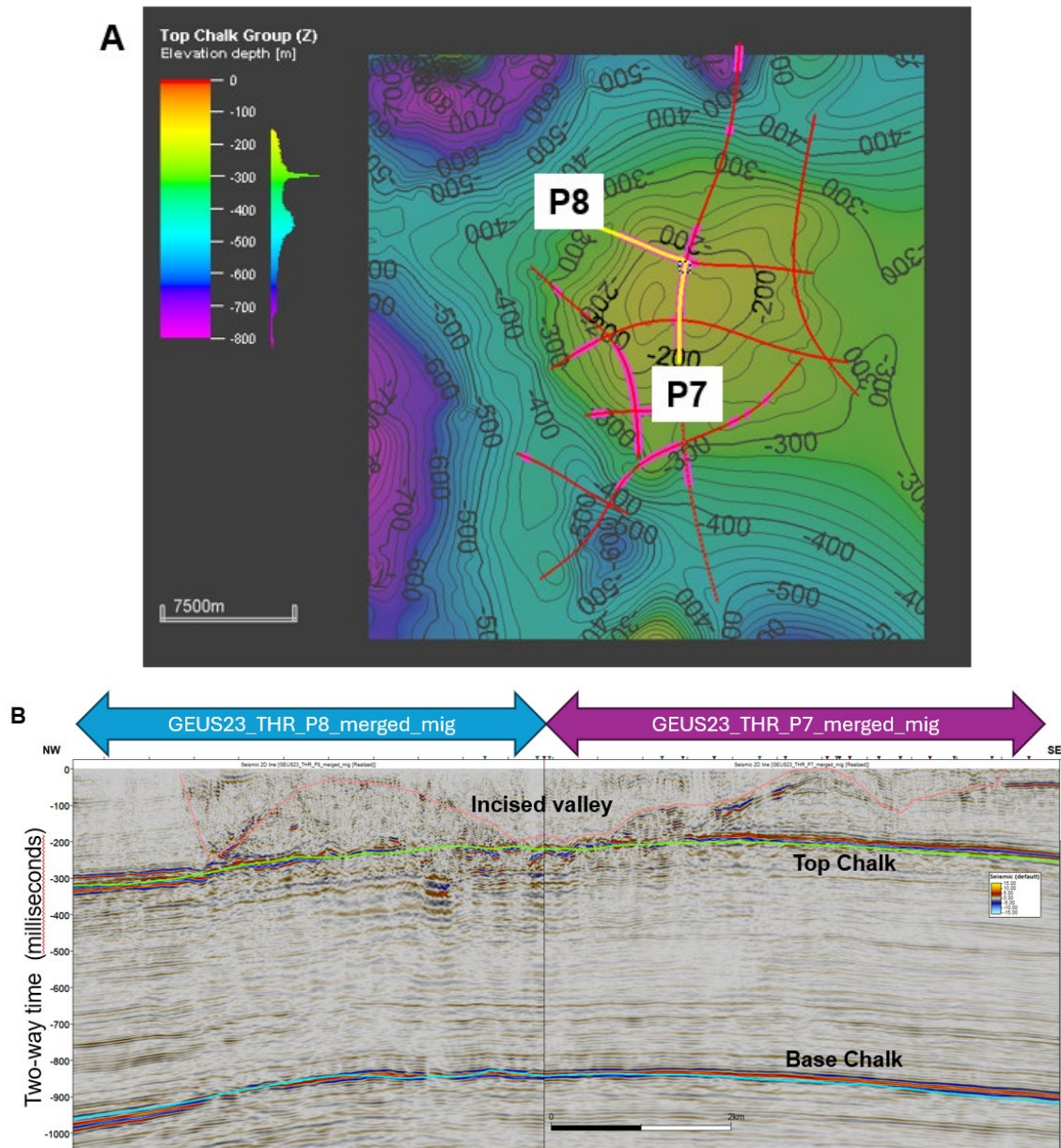


Figure 6.2.16 Glacial buried valleys observed in the 2023 GEUS_THORNING2D survey. A: Location map of the composite seismic section (shown in B) on top of depth-structure map to the Top Chalk surface. Thick pink lines indicate presence of incised glacial valleys. B: Composite seismic TWT-section along GEUS_THORNING2D_P8 and P7 showing how the incised valley (red line) extends deep and almost intersect the Top Chalk surface.

Japsen et al., (2007) interpreted around 500 m of Cenozoic uplift and erosion in the greater Thorning area, which is in line with the observed sub-crop pattern towards the base of the Pleistocene. However, this study has only been able to confirm the result of the Cenozoic uplift by the presence of incised glacial valleys (probably Pleistocene) that carved into the pre-Quaternary surface.

6.3 Summary of the structural evolution – The Thorning structure

The structural reconstruction of the development of the Thorning area spanning the time from the Late Paleozoic to the Cenozoic has been facilitated by horizon flattening at key horizons. The salt migration observed in the study of the Thorning structure involves both up doming due to gravitational instability and salt withdrawal.

In summary, the Thorning structure mainly evolved by separate/discrete episodes of salt pillow growth forming the overlying structural doming anticline seen today. At least five main episodes of salt migration are identified:

1. Initial growth of the Thorning salt pillow started in Triassic time during deposition of the Skagerrak Formation as indicated by gentle up doming salt at the location of the present-day the graben structure in the SW part of the study area.
2. Main episode of salt withdrawal and collapse under the small graben at the southwestern resulting in a local depocenter during deposition of the mid-late Triassic Oddeund Formation and Vinding Formation.
3. Secondary episode of salt withdrawal resulting in remarkable thickness variations at the time of Top Fjerritslev Formation combined with lateral growth of the salt pillow and uplift during Middle Jurassic–Early Cretaceous.
4. New episode with growth of the larger salt pillow took place during deposition of the Frederikshavn Formation–Chalk Group combined with tectonic inversion of the graben structure at the southern flank of the large pillow.
5. Final growth of the Thorning salt pillow took place during deposition of the Pleistocene as part of the Cenozoic uplift.

The structural evolution of the Thorning structure suggests that the tectonic framework and outline of the present-day Thorning structure may have been controlled by the paleo-topography of the Top pre-Zechstein surface, which may be seen as a proxy for the deep-seated basement structures. The salt pillow evolution occurred above a N-ward dipping Top pre-Zechstein terrace and the onset of halokinesis was most-likely triggered by faulting in the deep-seated basement structures.

7. Geology and parameters of the reservoirs and seals

In this study the Upper Triassic – Lower Jurassic Gassum Formation is considered the primary reservoir for CO₂ storage in the Thorning structure. This is because it generally has good reservoir properties and not least because the seismic data from the Thorning structure area shows that it is overlain by 100–350 m thick mudstone-dominated succession of the Lower Jurassic Fjerritslev Formation which is known to have good seal properties. Hence, the Gassum–Fjerritslev formations are considered as the primary reservoir–seal pair in the structure (Fig. 7.1.1). The Upper Jurassic – Lower Cretaceous Frederikshavn Formation may form a secondary reservoir in the structure with its seal consisting of the Lower Cretaceous Vedsted and Rødby formations (Fig. 7.1.1). The deeper situated Triassic Tønder, Bunter Sandstone and Skagerrak formations possibly form additional reservoirs but as discussed below their composition is uncertain. Consequently, the report only contains a very brief review of these reservoirs and their associated seals. The Middle Jurassic Haldager Sand Formation and the overlying Upper Jurassic Flyvbjerg Formation are not included in the review of potential reservoirs for CO₂ storage as these are considered not to be present or only very thinly developed in the Thorning structure based on the seismic mapping and interpretation together with data from the nearest wells to the structure.

No wells penetrate the Thorning structure and therefore well data information concerning reservoirs and seals must be obtained from the offset wells that surrounds the structure in a distance of c. 30–70 km. It is not possible to point out one of these wells as being representative for the Thorning structure since the wells represent either more proximal or distal depositional settings compared to the site of the structure. Thus, estimates of reservoir and seal properties for the formations in focus in the Thorning structure are largely based on mean value considerations of data from the wells representing more proximal and distal depositional settings. Through the Triassic–Jurassic period the Danish Basin is in general considered as mainly sourced with sediments from Fennoscandia in the northeast. Wells northeast and southwest of the Thorning structure can therefore be considered to represent more proximal and distal depositional settings, respectively, compared to the site of the structure. However, as the content of sandstone in the reservoir units of “the distal wells” is markedly lower than in “the proximal wells” it is associated with large uncertainty to evaluate the most likely sandstone content in the Thorning structure. In some cases, internal seismic features on the seismic sections through the Thorning structure can give hints about the presence of sand-prone depositional systems (reflectors resemble progradation, channel features etc.). In this study, Gassum-1 has been chosen as a representative key well for the proximal depositional setting and the Nøvling-1 well as a representative key well for the distal setting. Considerations of reservoirs being present in the Thorning structure, and their possible reservoir properties, will thus largely rely on data from these wells. Interpreted well logs of the two wells are shown in Figs 7.1.2–5 and furthermore in Appendix B together with the other deep wells that are located closest to the Thorning structure and considered valuable for the evaluation.

The Gassum Formation, consisting of interbedded sandstones and mudstones, is subdivided into depositional sequences that are correlated between the wells to outline possible reservoir subunits in the formation. Likewise, is the Fjerritslev Formation subdivided into its informal members which have variable seal properties. The subdivision of the formations is based on integration of sedimentological interpretations of cores, petrophysical log patterns and palynological data (Nielsen 2003 and present study). The biostratigraphic zonations used

include the ostracod zonation of Michelsen (1975a, b), the dinocyst zonation of Poulsen 1996 and Poulsen & Riding (2003) and a combination of the spore-pollen zonations of Dybkjær (1991) and Lindström et al. (2023). The biostratigraphic database varies from well to well. Thus, from some wells a solid biostratigraphic framework exists while the database is more sporadic from others. In Appendix B, the available biostratigraphy is summarized for each well based on data from reports and publications combined with new data from some of the wells. In addition, links are given to stratigraphic summary charts for each well. The charts combine the chronostratigraphy, lithostratigraphy, biostratigraphy and sequence stratigraphy and further include the bio-events and biozonations.

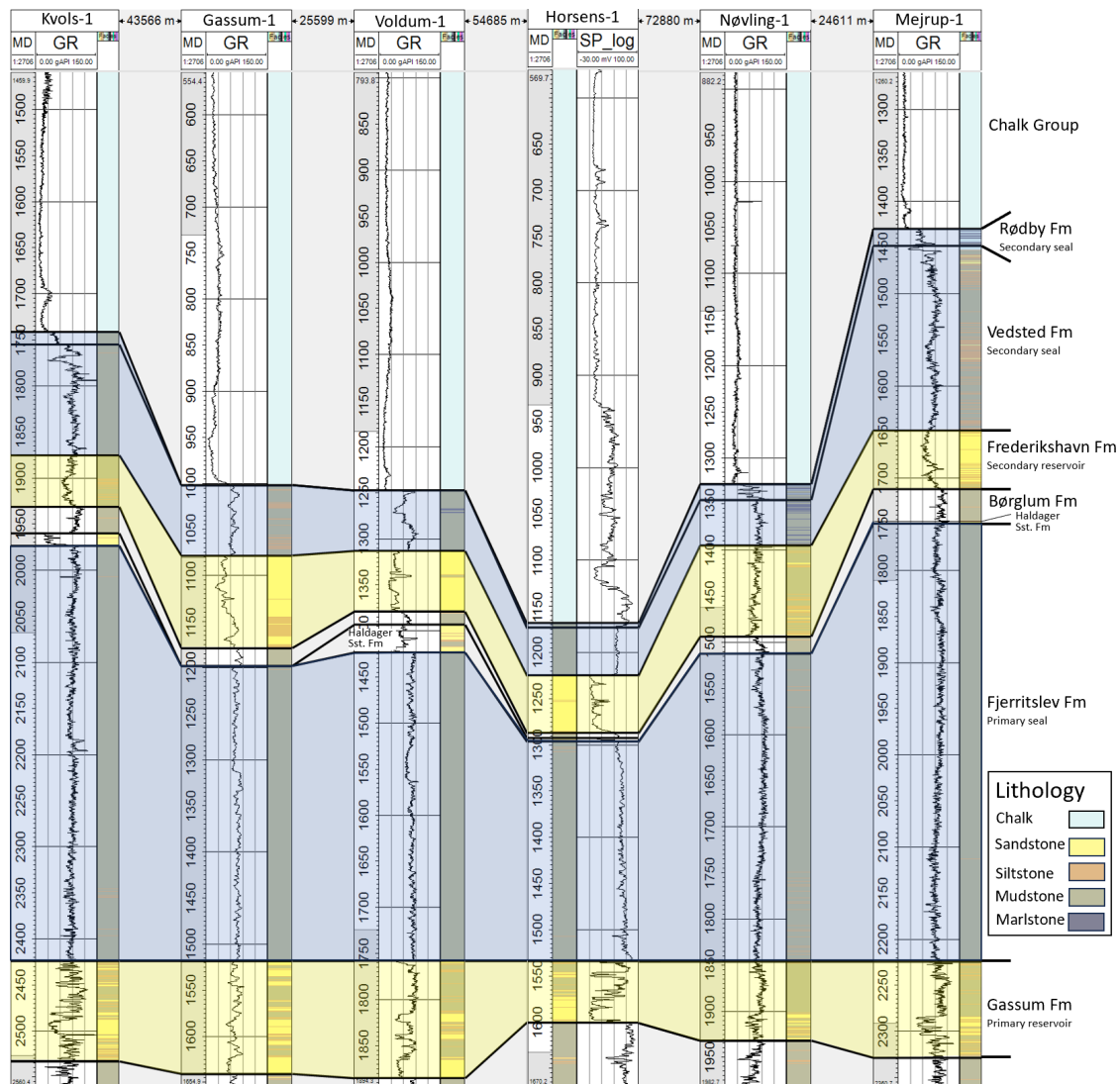
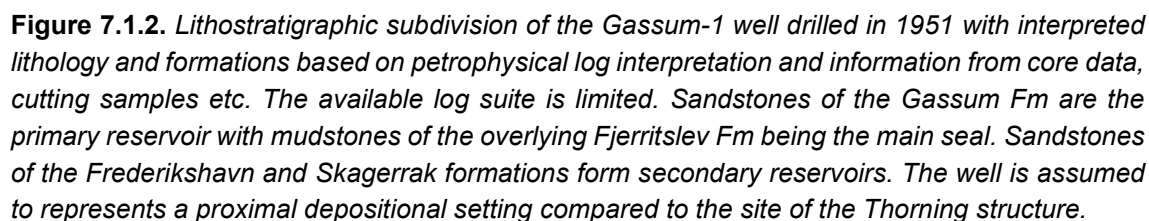


Figure 7.1.1. Correlation panel of the nearest wells around the Thorning structure, showing the primary reservoir formation (Gassum Fm) with alternating sandstone and clay/mudstone intervals, as well as the overlying, thick, primary seal (Fjerritslev Fm), which consists almost entirely of claystones/mudstones. A possible secondary reservoir (Frederikshavn Fm) with an overlying composite seal (Vedsted–Rødby fms) is also shown. The top of the Gassum Fm is used as datum line and corresponds approximately to the transgressive surface TS 9. Location of wells relative to the Thorning structure is seen in Fig. 3.1.



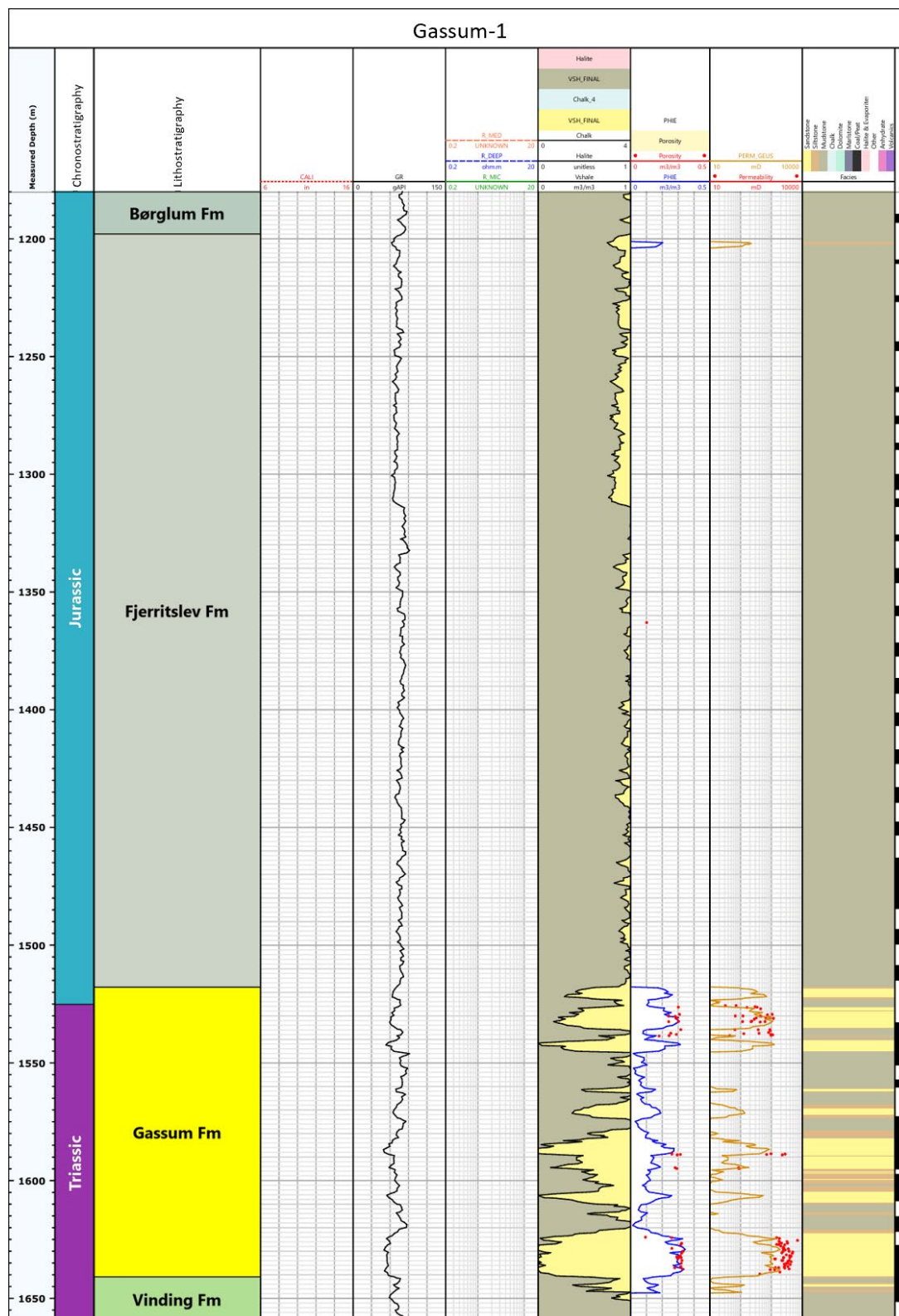
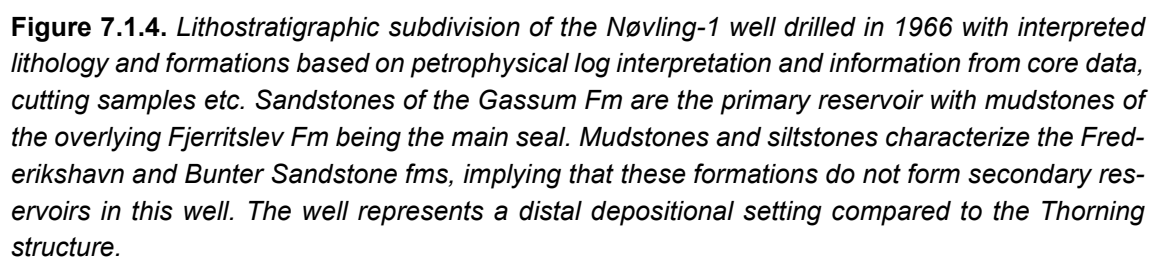


Figure 7.1.3. The Gassum-1 well with interpreted lithology based on petrophysical log interpretation and information from core data, cutting samples etc. Zoom section of the Gassum Fm and its primary seal (Fjerritslev Fm) in Figure 7.1.2. Cored parts of the Gassum and Fjerritslev formations (black columns to the right) are here marked at the depth positions that are indicated on the core boxes. However, core depths need to be reduced approximately 20–25 ft. (Nielsen 2003).



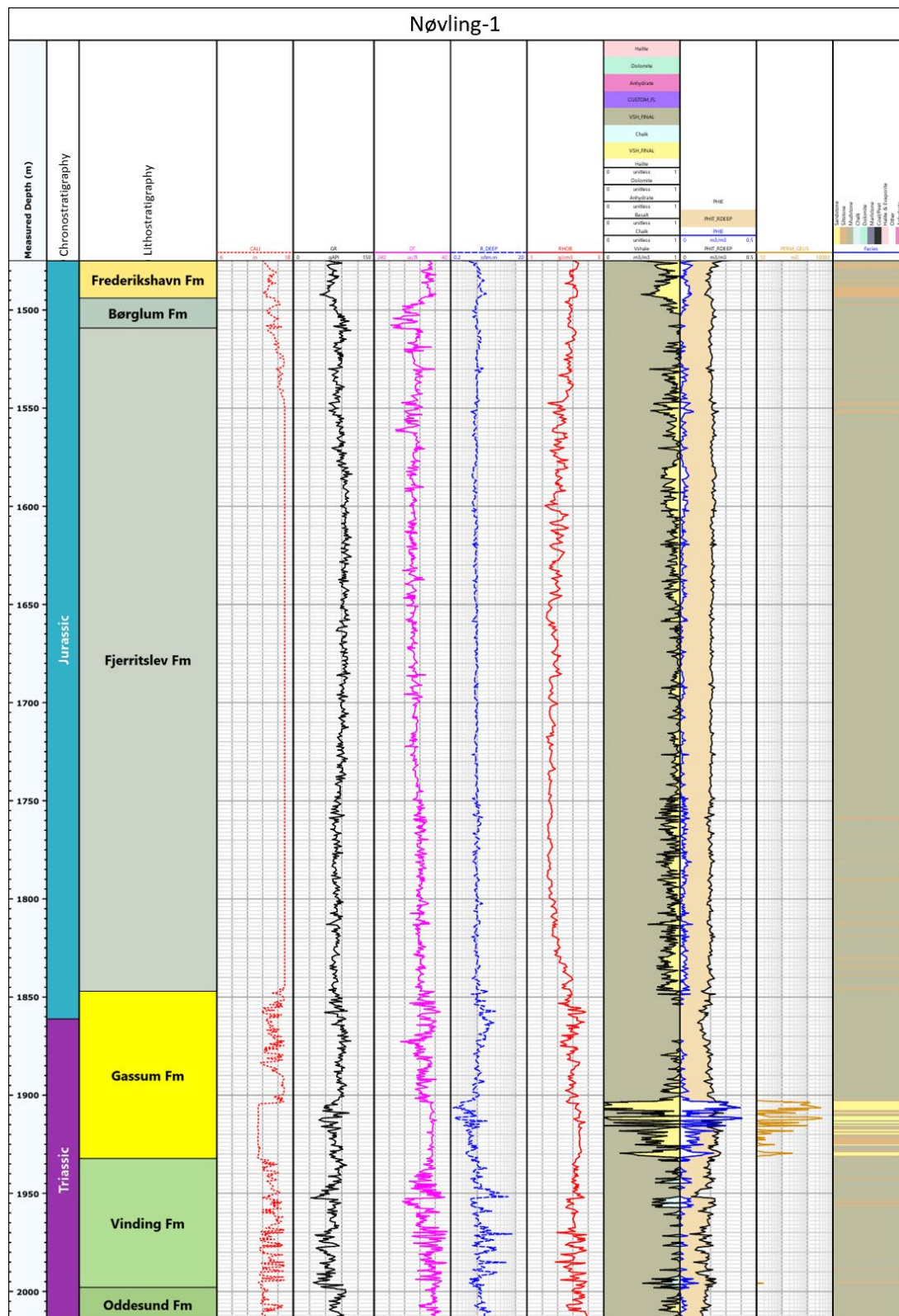


Figure 7.1.5. The Nøvling-1 well with interpreted lithology based on petrophysical log interpretation and information from cutting samples etc. Zoom section of the Gassum Fm and its primary seal (Fjerritslev Fm) in Figure 7.1.4. The sandstone rich lower part of the Gassum Fm can be correlated to the proximal Gassum-1 well and is considered to be present also in the Thorning.

7.1 Reservoirs – Summary of geology and parameters

In the following description of reservoirs, emphasis is on the Gassum Formation whereas the possibly secondary reservoirs, Frederikshavn, Tønder, Bunter Sandstone and Skagerrak formations, are described more briefly.

The primary reservoir: The Gassum Formation

The Gassum Formation is the best-known sandstone reservoir in the Danish onshore subsurface. It is used for geothermal energy in Thisted and Sønderborg and has also been used for seasonal storage of natural gas for more than 30 years in the Stenlille structure. The good reservoir properties of the formation have thus been proven at several places in Denmark. The formation is widespread in the Danish Basin and locally in the Danish part of the North German Basin (Fig. 7.1.6). It has a general thickness of 30–160 meters (Nielsen & Japsen 1991, Nielsen 2003). Locally it is missing due to uplift and erosion related to regional uplift in the Middle Jurassic, at the 'Base Middle Jurassic unconformity' or the 'Mid-Cimmerian Unconformity' *sensu* Nielsen (2003), and above structures formed by vertical salt movements. The Gassum Formation is of Late Triassic–Early Jurassic age with the upper boundary showing a significant younging towards the northern, north-eastern, and eastern basin margins (Fig. 7.1.6B) (Bertelsen 1978, 1980, Michelsen et al. 2003, Nielsen 2003). The upper formation boundary is thus of latest Rhaetian age in the central parts of the basin whereas it is of Early Sinemurian age along the basin rims (Nielsen 2003 and references therein). This diachronic development of the boundary reflects an overall backstepping of the general coastline toward the basin margins during latest Triassic – Early Jurassic time owing to an overall rise in relative sea-level, interpreted as caused by a combination of regional basin subsidence and a eustatic sea-level rise (Nielsen 2003).

In general, the Gassum Formation is dominated by fine to medium-grained, in places coarse-grained, light grey sandstones, alternating with darker colored clay- and siltstones and locally thin coal layers (Bertelsen 1978, Michelsen et al. 2003, Nielsen 2003). The sandstones are classified as subarkoses and arkoses following the classification of McBride (1963) (Weibel et al. 2020). The sediments were deposited during repeated sea-level fluctuations in Late Triassic – Early Jurassic times when the Danish Basin was mainly a shallow marine to coastal area. Large quantities of sand were transported into the basin by rivers which were sourced by erosion of the Fennoscandian Shield and, to a lesser degree, locally from the Ringkøbing–Fyn High in periods when this was exposed (Nielsen 2003 and references herein).

Recent provenance studies suggest that the basin was sourced also with sand from southerly Variscan source areas (Olivarius et al. 2020, 2022) (Fig. 7.1.7), perhaps transported into the basin through grabens intersecting the Ringkøbing–Fyn High such as the Øresund Basin, Storebælt Gate and Brande trough.

The high influxes of sediment almost balanced subsidence implying that the intracratonic basin largely remained shallow and almost flat-based, but with its deepest part located near its center (Hamberg & Nielsen 2000). Due to the flat, low-gradient basin floor and overall shallow water conditions, sediment accumulation was very sensitive to Late Triassic and Early Jurassic fluctuations in relative sea level which resulted in repeated long-distance progradation or retrogradation of the coastline. A large part of the sandstones in the formation therefore represents shoreface deposits, but significant amounts are also fluvial or estuarine in origin. This is especially the case for the lower part of the formation where pronounced

high-order relative sea level falls led to the progradation of rivers into the central part of the basin and the establishment of estuaries during succeeding rise in relative sea level.

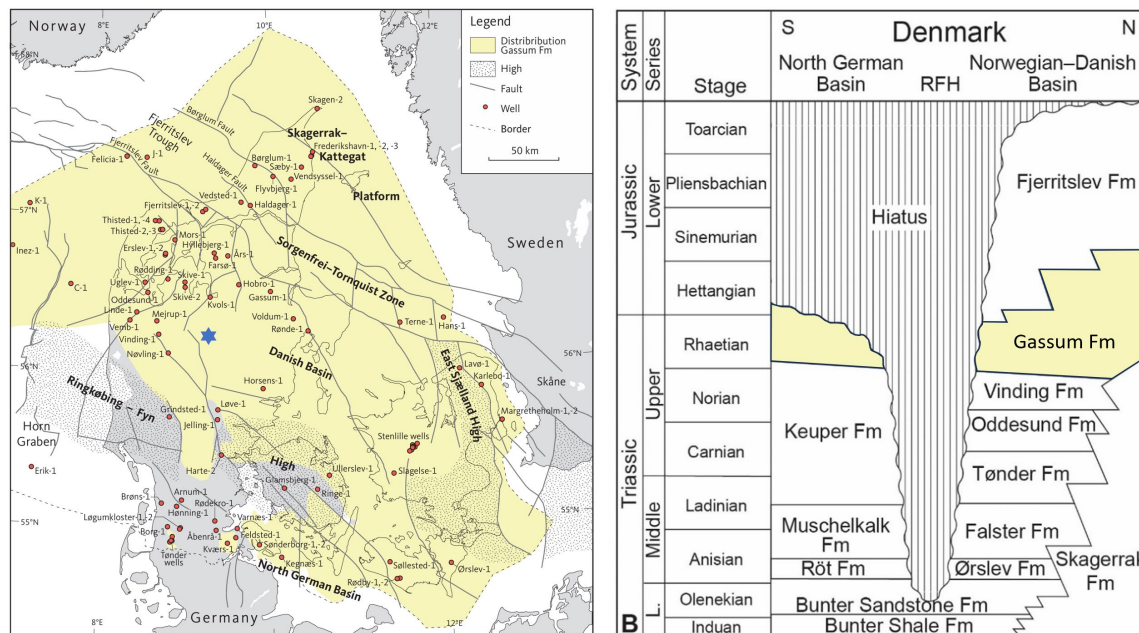


Figure 7.1.6. A) Estimated distribution of the Gassum Formation in the Danish onshore and nearshore area shown in yellow. Also shown is selected wells and main structural elements including the Norwegian–Danish Basin and the North German Basin which are separated by the Ringkøbing–Fyn High (RFH). Blue star marks the approximately location of the Thorning structure. B) Stratigraphic scheme of the Lower Triassic–Lower Jurassic succession onshore Denmark revealing among others the time-transgressive nature of the top of the Gassum Formation. The hiatus relates to uplift and erosion in Middle Jurassic time. For the RFH, maximum age of the hiatus is shown but in some areas younger strata may be preserved on the high as also suggested for the Gassum Fm on the map to the left. However, over the central parts of Fyn the distribution of the Gassum Fm is difficult to map due to limited seismic data coverage. The formation is present in the Ullerslev-1 well but missing in the Ringe-1 and Glamsbjerg-1 wells located in this area. Modified from Olivarius et al. (2022).

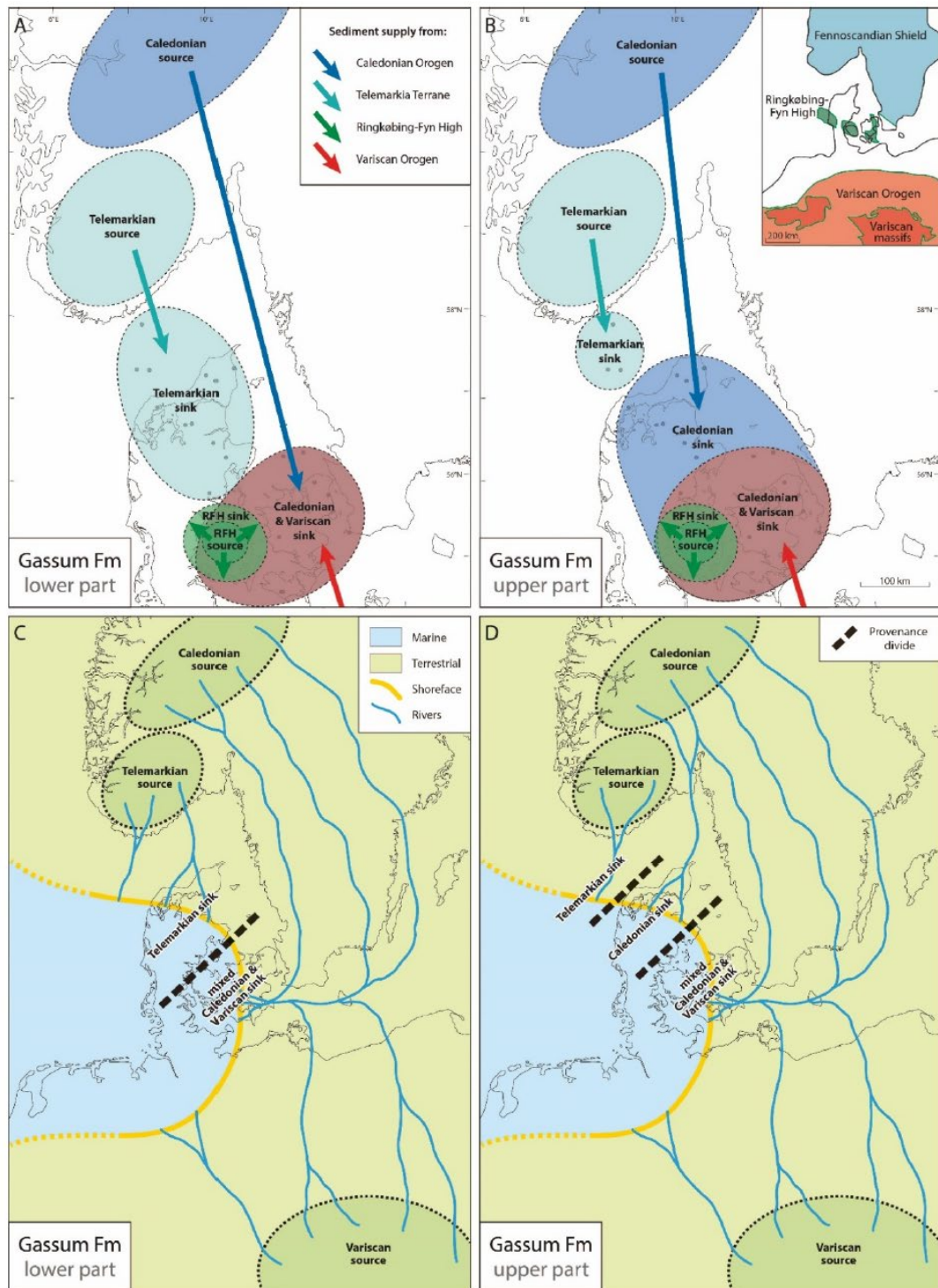


Figure 7.1.7. Provenance of the lower (A) and upper (B) parts of the Gassum Formation showing the location of the primary source areas (Caledonian, Sveconorwegian, and Variscan) and the minimum extend of their sinks as evident from zircon U-Pb data from wells in the Danish Basin and the northern North German Basin. Sediments were locally supplied from exposed parts of the Ringkøbing–Fyn High. Tentative and generalized paleogeographic reconstructions for the lower (C) and upper (D) parts of the formation, where the primary difference is which of the Fennoscandian source areas that supplied most sediments to the basin. The maps represent snapshots since the coastline moved back and forth due to repeated transgressions and regressions in time. From Olivarius et al. (2022).

The Gassum Formation in the Thorning structure:

Depth, thickness and extent: The seismic mapping and interpretation show that the formation is present in the entire structure. The depth to the top of the formation at its shallowest level is c. 1520 m below mean sea level (Fig. 6.2.2F) corresponding to c. 1580 m below terrain. At this location the formation has an estimated thickness of around 95 m. The present depth of c. 1520 m below sea level corresponds roughly to a maximum burial depth of around 2030 m prior to later exhumation events (based on the maximum burial map in Japsen et al. 2007). For comparison, thicknesses and depths of the formation in the nearest wells to the Thorning structure are shown in Table 7.1.1.

Table 7.1.1. *Approximately depths to the Top and Base of the Gassum Fm and its thickness in the nearest wells surrounding the Thorning structure (order of wells are given clockwise according to their location relatively to the Thorning structure and starting with the Kvols-1 well). Data are given in Nielsen & Japsen (1991). See Fig. 3.1 for location of wells.*

Well	Rotary Table – m above terrain	Measured/True vertical depth (meter below Rotary Table)		Thickness (m)
		Top Gassum Fm	Base Gassum Fm	
Kvols-1	6.8	2424	2533	109
Hobro-1	5.0	2376	2521	145
Gassum-1	4.6	1518	1648	130
Voldum-1	4.8	1757	1885	128
Rønde-1	6.5	2613	2753	140
Horsens-1	3.3	1506	1600	94
Løve-1	<i>Gassum Fm not present</i>			
Grindsted-1	<i>Gassum Fm not present</i>			
Nøvling-1	7.1	1847	1932	85
Mejrup-1	5.5	2224	2329	105

Subdivision: The Gassum–Fjerritslev interval has been sequence stratigraphic subdivided in some of the nearest wells to the Thorning structure (Fig. 7.1.8). In most of the wells, the Gassum Formation is subdivided into eight depositional sequences, SQ 2–SQ 9, based on integration of sedimentological interpretations of cores, petrophysical log patterns and biostratigraphic data (Nielsen 2003 and present study). However, for SQ 2 and SQ 9 it is only the highstand and lowstand system tracts, respectively, that form part of the formation. The numbering of sequences and their associated surfaces follows the sequence stratigraphic nomenclature in Nielsen (2003). This was developed for the Upper Triassic – Jurassic

sedimentary succession in the Danish Basin and showed that individual sequences in most cases can be correlated basin-wide from well to well.

Each sequence is based by a sequence boundary (SB) formed at the time of maximum fall in relative sea level. Lowstand systems tracts (LST) formed between sequence boundaries (SB) and the first transgressive surface (TS). Transgressive systems tracts (TST) formed between the TS and the maximum flooding surface (MFS). Highstand systems tracts (HST) formed between the MFS and the SB of the next sequence. This simple sequence stratigraphic approach (e.g., Payton 1977) is following the divisions of Nielsen (2003). There are also other concepts (see e.g., Catuneanu 2019), but these are not discussed further here.

In general, the LST and HST deposits of the sequences are dominated by shoreface sandstones whereas the MFS occurs in intervals of offshore mudstones. The sequences reflect an overall aggradational to progradational stacking pattern from the base of the Gassum Formation and up to SB 5. This sequence boundary is interpreted to have formed by fluvial erosion and bypass followed by the deposition of fluvial or estuarine sand during relative sea-level rise. From SB 5 and upwards to MFS 7 the overall stacking pattern is retrogradational with the shoreface sandstone intervals of the sequences becoming thinner on behalf of thicker offshore mudstone intervals. After a shorter progradational event (from MFS 7 to SB 9), when sand deposition resumed in parts of the basin, the overall transgression culminated in Early Jurassic times with deposition of the overlying Fjerritslev Formation which in most of the wells closest to the Thorning structure is more than 300 m thick and consists almost entirely of offshore mudstones.

High order sea-level variations formed the individual sequences and generated the complex internal reservoir architecture of the Gassum Formation with mainly lowstand and highstand intervals forming internal sandstone reservoirs that are separated by transgressive intervals of mudstone and heteroliths (Fig. 7.1.8).

The logpanel indicates that internal sandstone and mudstone units have regional extent (Fig. 7.1.8). However, some of the sandstone units appear to thin out towards the central part of the Danish Basin as seen by sandstone units being less and thinner in Nøvling-1 (representing a distal depositional setting) compared to the remaining wells. Especially it is striking that no sandstone intervals are interpreted to be present in the upper part of the Gassum Formation in the Nøvling-1 well (from a little bit above TS 5 and upwards in the formation) whereas sandstone units are present in this interval in the wells representing a more proximal depositional setting. This is also made clear by a direct comparison of the key wells Nøvling-1 and Gassum-1 (Fig. 7.1.9). Thus, the Gassum-1 well as well as other wells contains several thick sandstone intervals in the upper part of the Gassum Formation which likely wedges out distally before reaching the Nøvling-1 well. In Nøvling-1, sandstone units are only present in the lower part of the Gassum Formation (from base Gassum Fm to a little bit above TS 5). As this part of the formation can be correlated also to the Gassum-1 well, and the Thorning structure is located in between the two wells, it seems reasonable to assume that the interval is also present within the structure. Sandstones being overall more abundant in the lower part of the Gassum Formation, especially in SQ's 4 and 5, is in line with the general geological model saying that sequences reflect increasing depositional progradation upwards towards SB 5 which represents the maximum progradation in "Gassum time" (Nielsen 2003).

Also worth noticing on the seismic sections from the Thorning structure, is the dipping reflectors and hummocky clinoform facies pattern that in places characterize the Gassum

Formation below the reflector tentatively interpreted to represent the transgressive surface TS 5 (Fig. 7.1.12). This may be interpreted as reflecting a sandy, high-energy depositional system, although it is difficult to deduce the specific depositional environments the seismic facies reflect. In contrast, a parallel to subparallel, high amplitude reflection pattern characterize the formation above the likely (near) TS 5 reflector, possibly reflecting a lateral more homogenous distribution of offshore mudstones and subordinate shoreface sandstones (Fig. 7.1.12). This seismic reflectivity pattern is very comparable to what have been observed on seismic sections through the Gassum structure (Fig. 7.1.16 in Keiding et al. 2024).

The lower part of the Gassum Formation in the Thorning structure contains most likely at least as much sandstone as in the Nøvling-1 well. The distance between the Gassum-1 well and the Thorning structure is around double the distance between Nøvling-1 well and the structure. A simplistic approach for estimating the sandstone content and reservoir properties of the lower Gassum Formation in the Thorning structure could then be to make a weighted average where the data from Nøvling-1 counts two thirds and Gassum-1 one third. This could then be considered as a representative reservoir case for the Gassum Formation in the Thorning structure with possible sandstone units in the upper part of the formation, known from the Gassum-1 well, forming an upside of the reservoir if some of these are also present in the Thorning structure. This simplistic approach is followed below in the reservoir characterization of the Gassum Formation in the Thorning structure. Another and more optimistic approach in the reservoir characterization is to consider the Gassum-1 well as representative for the Gassum Formation in the Thorning structure due to the similarities in the seismic reflectivity pattern. This approach is also included in reservoir characterization below.

Comparison of the key wells also shows that the lower Gassum Formation cannot be considered as one coherent sandstone reservoir as the presence of mudstone intervals may form internal seal. These are up to c. 13 m and 3.5 m thick in the lower part of the formation in the Gassum-1 and Nøvling-1 wells, respectively (Fig. 7.1.9). The resolution of the seismic data is not high enough to deduce if some of the internal seals are truncated, e.g. due to erosion related to fall in relative sea level and the associated formation of sequence boundaries.

An ambiguous mound structure: A very striking seismic feature immediately above the Gassum Formation in the Thorning structure is a large convex upwards structure onto which deposits of the Fjerritslev Formation onlaps (Fig. 7.1.10). The structure is up to around 150 m thick (Fig. 7.1.11). It covers an area of around 153 km² and its thickest part has an overall NW–SE elongated shape (Fig. 7.1.11). Internally, the seismic reflectors are discontinuous or show parallel reflectors that are subhorizontal or slightly dipping, in places separated by what resemble surfaces of truncation (Fig. 7.1.12). Also, internal downlap reflectors in places are seen near the edges of the structure. At its edges, the top surface of the structure nearly merges with the Top Gassum seismic horizon (Fig. 7.1.10). This horizon has been correlated to the nearest wells as representing the TS 9 surface which in these wells is overlain by a continuous Fjerritslev Formation succession. Since the Fjerritslev Formation appears to onlap the convex upwards structure (Fig. 7.1.12A), this suggests that the whole structure was formed “shortly” after the formation of TS 9.

As such the structure may resemble a submarine fan deposit. However, such an interpretation seems unlikely as the amount of sediment supply into the central part of the Danish Basin was low in post TS 9 time where overall rise in relative sea level most of the time forced the coastline and the hinterland towards the basin margins. However, submarine fan

deposition may still be a possible explanation for the formation of the mound structure if tectonism or salt diapirism in the region caused local uplift and erosion of former deposits which then were redeposited in nearby deeper parts of the basin. Perhaps more likely the convex upwards structure represents large submarine landslide blocks of former deposits. The slides may have been triggered by initial salt diapirism in the region which caused elevation and inclination of overlying deposits resulting in a gravity driven downwards slide of blocks of these deposits along a décollement plane. The deposits may have remained relatively intact during block movement, but the apparently internal truncation surfaces may in this context represent surfaces of overthrust and downdip repetitions of the gliding blocks at the place where the gliding ceased, and compressional forces took over (in the translational to toe domain sensu Bull et al. 2009). The identified mound will then most likely contain deposits of the Gassum Formation, and perhaps the lowermost parts of the Fjerritslev Formation, as these were the uppermost sediments exposed for sliding at the time. A clayey interval within the Gassum Formation or around the Vinding–Gassum boundary perhaps acted as the basal shear surface, but during downslope movement, mudstones of the basal Fjerritslev Formation may have become the main décollement plane. The large thickness of the mound and the onlapping nature of the Fjerritslev Formation indicate that the structure formed a positive morphological feature, possibly an island, during the period the mud of the lower part of the Fjerritslev Formation was deposited. Intervals of reflectors dipping away from the structure are in places seen within the Fjerritslev Formation (Fig. 7.1.12A). These gradually flattens out in a distance of around 4 km from the structure. The dipping reflectors may reflect that the structure in periods sourced sediments into the “Fjerritslev sea.” In the slide block interpretation, the convex-upwards structure may add additional reservoir sandstones to the Gassum Formation and still leave a seal thickness of the Fjerritslev Formation of around 180 m or more above the top of the mound (Fig. 6.2.3D).

A very different interpretation may be that the area formed a local submarine depression which was filled up with sediments and then subsequently turned into a dome structure. This may be explained by lateral and vertical salt movements which may vary during the formation of a salt pillow and thereby also cause local variations in subsidence and uplift of overlying sediments through time. A more detailed regional seismic mapping focusing on the identification of e.g. headwall scarps and extensional ridges and blocks in the headwall domain (sensu Bull et al. 2009) may help to clarify the likelihood of the submarine landslide hypothesis or alternative interpretations. At present, the origin of the mound/convex upwards structure remains highly speculative.

Lithology, provenance and depositional environment: Data on the Gassum Formation is much more comprehensive from the Gassum-1 well than the Nøvling-1 well. This is because abundant core material is available from Gassum-1 (Figs. 7.1.3 and 7.1.13) whereas the formation was not cored in Nøvling-1. In the Gassum-1 well, the sandstones of the Gassum Formation are mainly fine or fine to medium grained (Danish American Prospecting 1951, Nielsen 2003, Fig. 7.1.14). The mineralogical maturity is relatively low revealed by a high feldspar content (Fig. 7.1.15). This is assigned to a direct sediment supply from Fennoscandia and limit distance of transport from the source areas (Fig. 7.1.7). Fennoscandia being the source area is supported by zircon dating of samples from SQ’s 2 and 7 in the well. These suggest sediment supply from northern source areas (Telemarkian and Caledonian in Fig. 7.1.7) as is also the picture for zircon dating of the Gassum Formation from other wells in Northern Jylland (Olivarius et al. 2022). Nielsen (2003) interpreted the depositional

environments of the Gassum Formation in the Gassum-1 well based on an interpretation of its cores (Fig. 7.1.13) supplemented with palynological data and interpretation of the vertical gamma-ray motif (Fig. 7.1.14). The results of these core interpretations are transferred to the well in the Gassum-1 – Nøvling-1 log panel where also the sequence stratigraphic subdivision of the well is shown (Fig. 7.1.9). As mentioned, the formation is interpreted as mainly reflecting alternating shoreface and offshore deposition under the influence of relative sea-level variations. The exception is the presence of estuarine and lacustrine deposits above SB 5 and SB 7, respectively (Fig. 7.1.9).

In Nøvling-1, descriptions of sandstones in the Gassum Formation are very sparse. The sandstones are overall described as being quartzitic and varying in grain size from fine to very coarse, in places being conglomeratic (Gulf Oil Company Denmark 1967). Sub-angular grain forms and in places a mica content indicate that the sandstones in some levels are immature. This together with the very coarse grain size in places, which is unusually for the formation, may indicate sediment supply from a local source area and not only from the NE. This could have been the Ringkøbing–Fyn High considering the relatively close location of the Nøvling-1 well to the high. This may have an impact on whether the lower Gassum Formation in Nøvling-1 can be considered as a representative reservoir case for the Thorning structure (as suggested above) as some of the sandstone units sourced from the south then may wedge out into mudstone towards the structure. However, this is speculative. According to the completion log the conglomeratic sandstones seem to appear close to SB 5 which represents a time with low sea-level and fluvial progradation from the N and NE far into the basin including its southern parts. It is also possible that the low sea-level caused exposure of the nearby Ringkøbing-Fyn High and thus northern supply of erosion material at this time. In addition, the seismic reflectivity pattern on seismic sections through the Thorning structure likely reflects a sandy, high-energy depositional system in the lower part of the Gassum Formation as mentioned above.

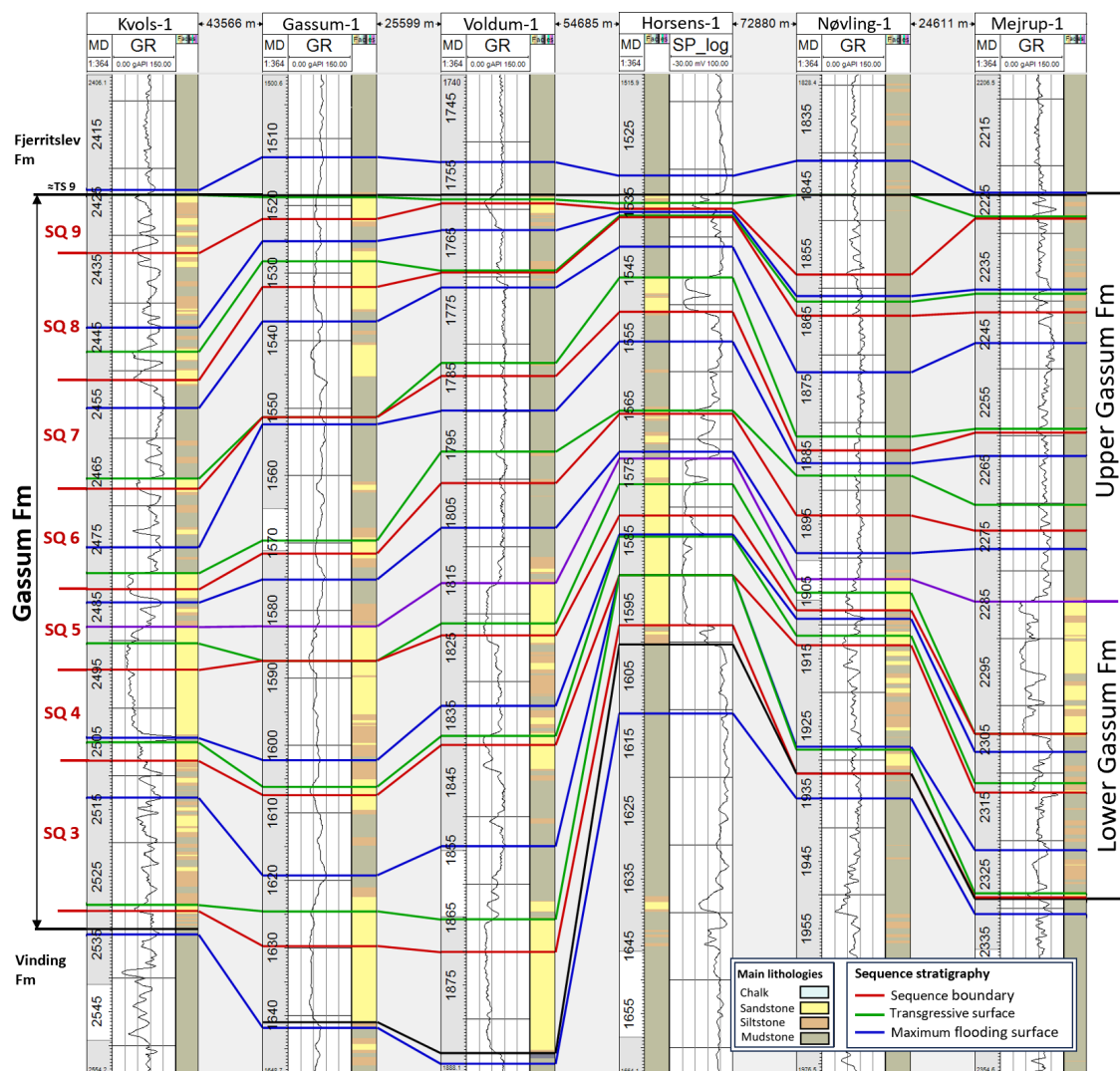


Figure 7.1.8. Correlation panel focusing on the Gassum Fm in the nearest wells to the Thorning structure. Placement of sequence stratigraphic surfaces is based on Nielsen (2003) and the present study. The top of the Gassum Fm is used as datum line and corresponds approximately to the transgressive surface TS 9. The outlined lower half of the Gassum Fm is most sandstone rich and considered to form the main reservoir in the Thorning structure as discussed in the text. Location of wells relative to the Thorning structure is seen in Fig. 3.1.

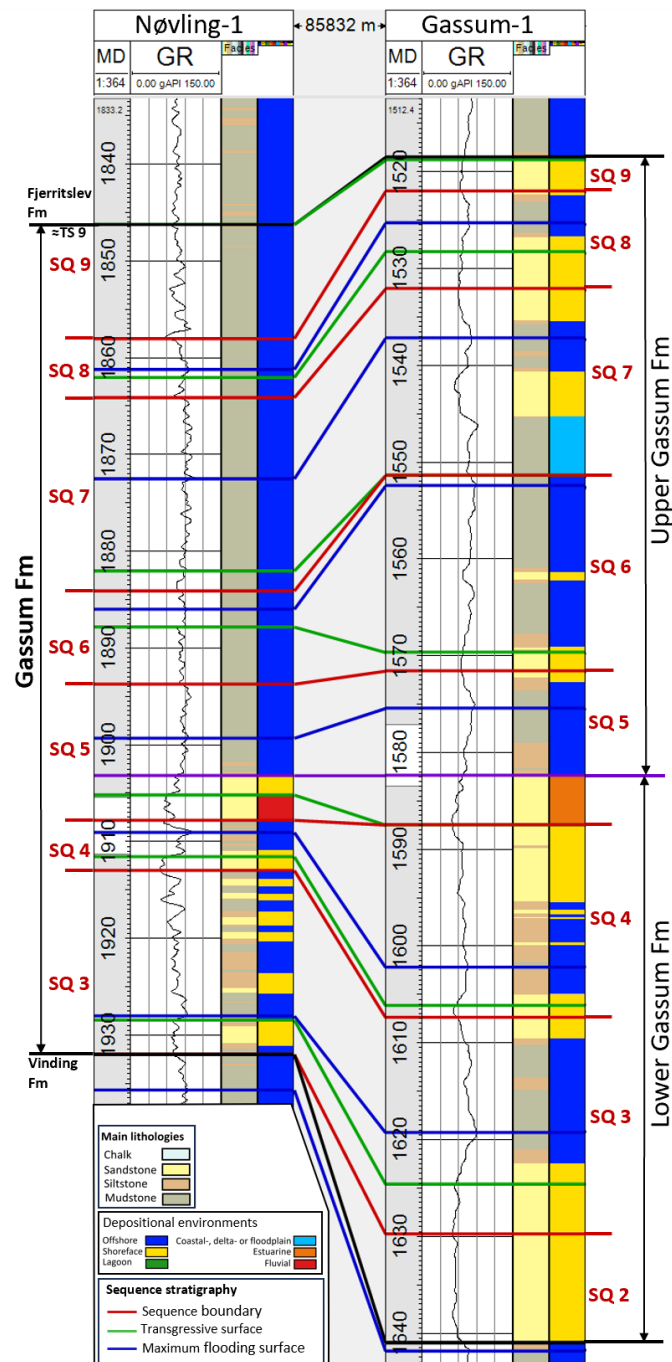


Figure 7.1.9. Interpretation of depositional environments of the Gassum Fm in the Gassum-1 and Nøvling-1 wells and their sequence stratigraphic correlation. For the Gassum-1 well the interpretation of depositional environments relies on extensive core interpretations given in Nielsen (2003) (Fig. 7.1.13). Compared to the site of the Thorning structure, Nøvling-1 and Gassum-1 are considered to represent a more distal and proximal depositional setting, respectively. Purple line in SQ 5 is not a sequence stratigraphic surface but is used to subdivide the Gassum Fm in a lower and upper part with the former being overall more sandstone rich than the latter, especially in the Nøvling-1 well. The outlined lower half of the Gassum Fm is most sandstone rich and considered to form the main reservoir in the Thorning structure as discussed in the text. The sandstone units in the upper part of the formation in Gassum-1 may upside the reservoir conditions if some of these are also present in the Thorning structure. Location of wells relative to the Thorning structure is seen in Fig. 3.1.

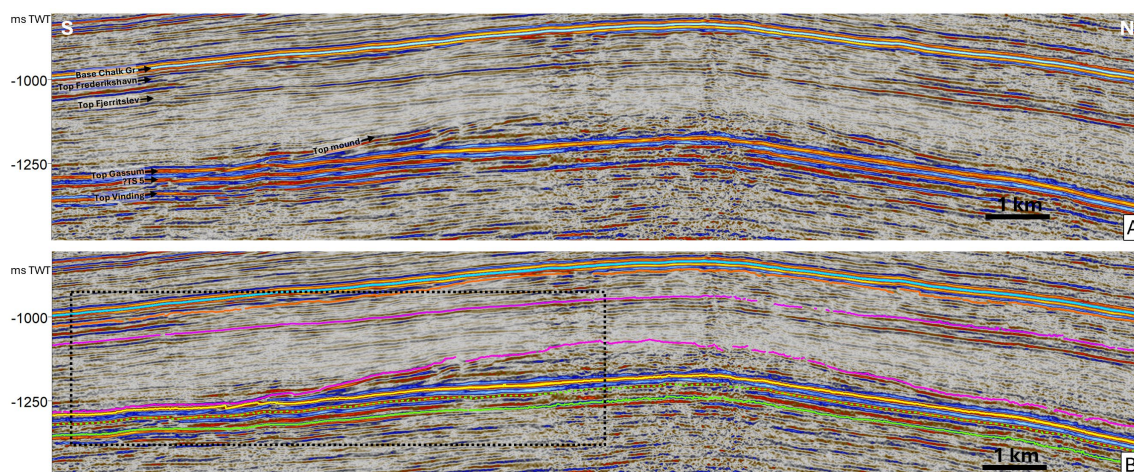


Figure 7.1.10. Seismic section P7 revealing a convex-upwards structure on top of the Gassum Fm, and onto which deposits of the Fjerritslev Formation onlaps. The structure is up to around 150 m thick (Fig. 7.1.11). The structure is recognized on several of the new Thorning-lines (P7, P8, P1 and the eastern part of P2) and is mapped out to cover an area of around 153 km² with a cut off at 25 m thickness (Fig. 7.1.11). A: without mapped top surfaces of lithostratigraphic units, B: with mapped top surfaces of lithostratigraphic units. Dotted rectangle in B is seen as a zoom-in in Fig. 7.1.12A.

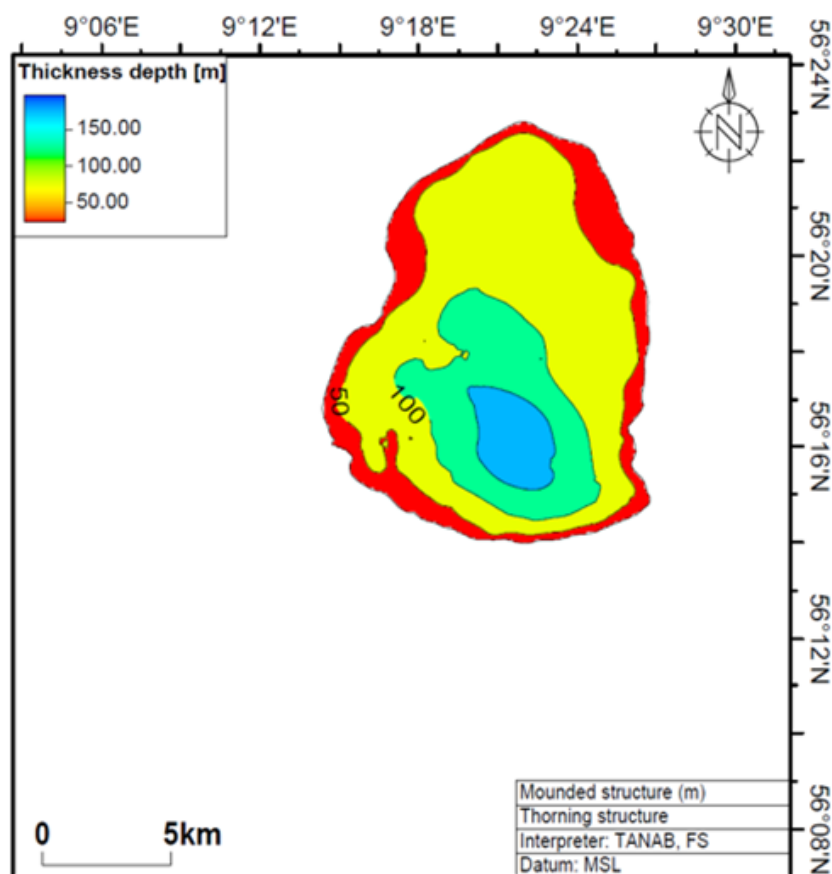


Figure 7.1.11. Thickness map of the convex-upwards structure on top of the Gassum Fm in the Thorning structure. The convex-upward structure is up to around 150 m thick. It covers an area of around 153 km² and its thickest part has an overall NW–SE elongated shape. Figure is from Chapter 6 (Fig. 6.2.3E).

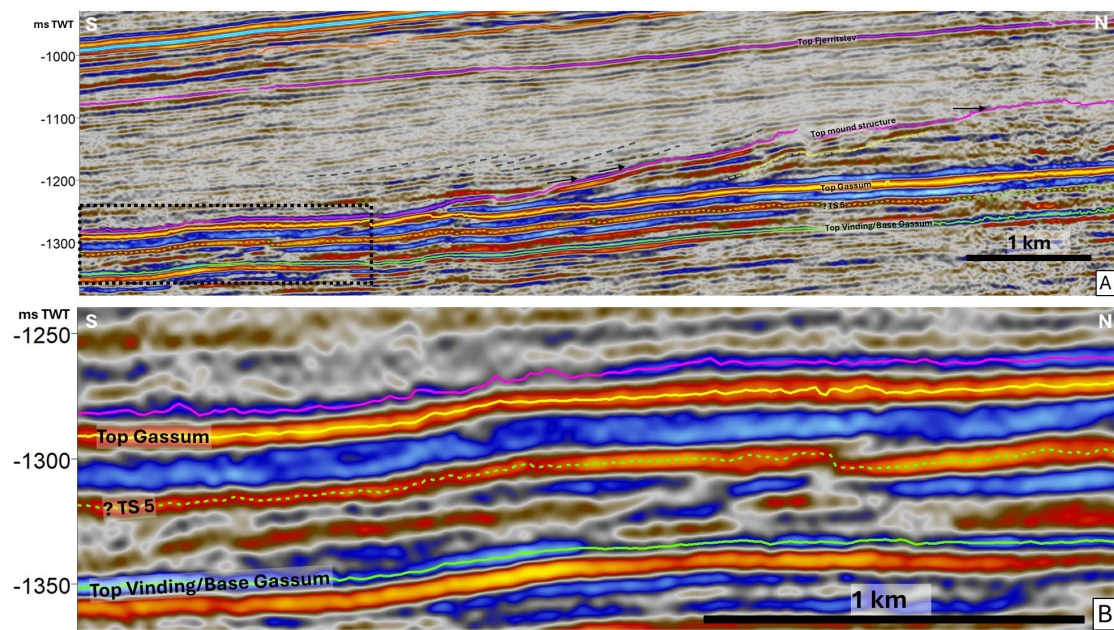


Figure 7.1.12. A: Zoom-in of dotted rectangle shown on seismic section P7 in Fig. 7.10.B. Notice reflectors of the Fjerritslev Fm onlapping the mound structure (marked with arrows) and within the Fjerritslev Fm an interval of reflectors dipping away from the structure (some of them emphasized with grey dashed lines). A possible erosional or overthrust surface within the mound structure is indicated with a yellow dashed line. B: Zoom-in of dotted rectangle seen in lower left corner of A. Dipping reflectors and a hummocky clinoform facies pattern in places characterize the Gassum Fm below a reflector which is a candidate for the transgressive surface TS 5. In contrast, a parallel to subparallel, high amplitude reflection pattern characterize the formation above the near TS 5 reflector.



Figure 7.1.13. Cores of the Gassum Fm in the Gassum-1 well showing mainly fine- and medium-grained shoreface sandstones. Core diameter is c. 8.5 cm. Cored intervals are marked on the petrophysical log of the well in Fig. 7.1.2. Photos by Emil Fønss Jensen (Jensen 2023).

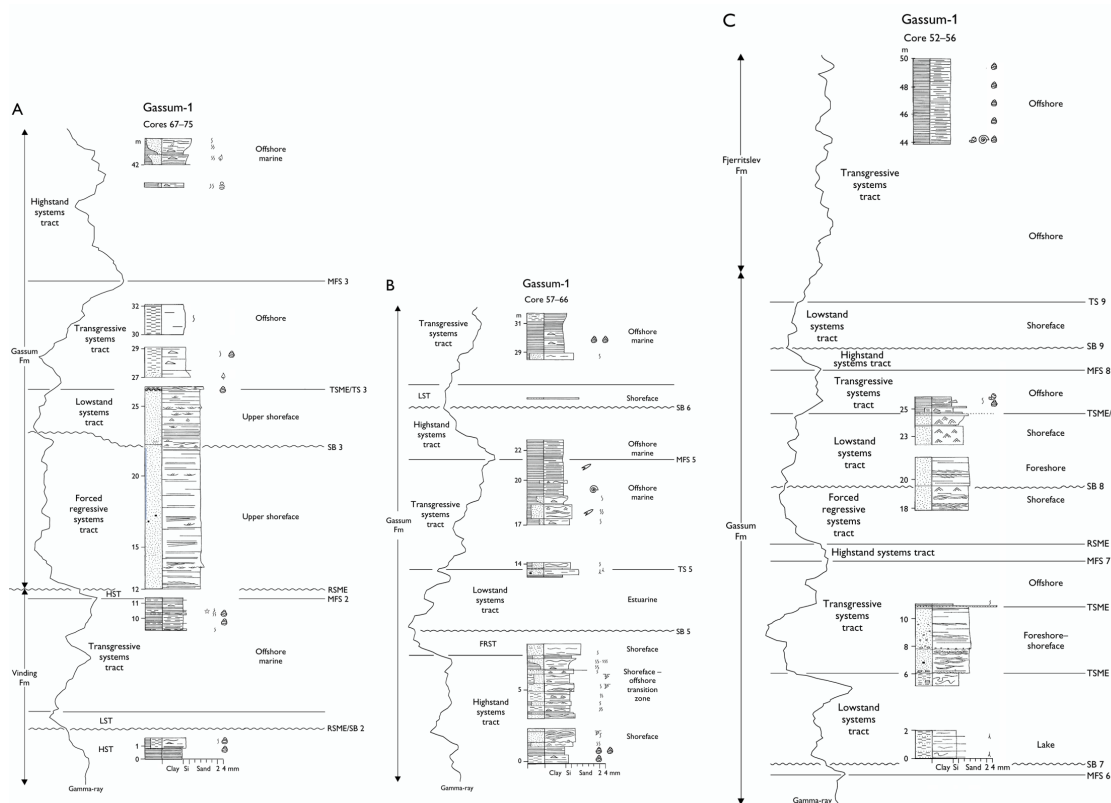


Figure 7.1.14. Core interpretation of the Gassum Formation in the Gassum-1 well shown together with the gamma-ray motif and sequence stratigraphic surfaces (moving stratigraphic upwards from A to C). The location of the boundary to the underlying Vinding Fm and the overlying Fjerritslev Fm is indicated next to the gamma-ray log. From Nielsen (2003). Note that core depths are corrected to log depths by subtracting 20–25 ft (Nielsen 2003).

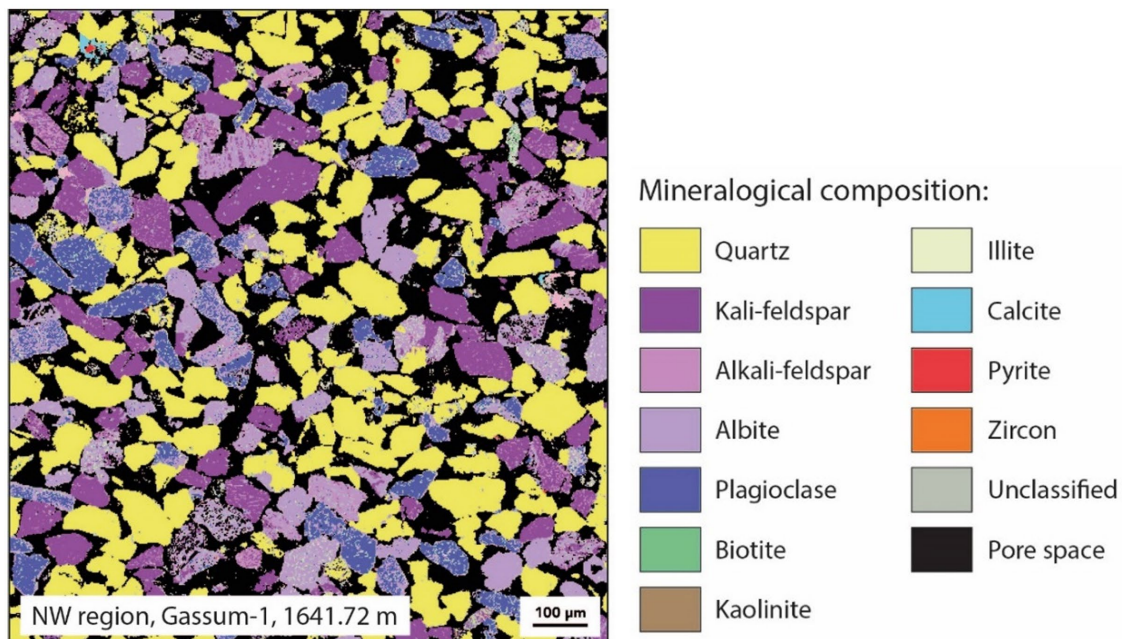


Figure 7.1.15. Mineral map of a sample from SQ 2 in the Gassum-1 well constructed by the automated quantitative mineralogy method (AQM). A low mineralogical maturity is revealed by the high feldspar content. Also notice the abundant pore space. From Olivarius et al. (2022).

Reservoir quality (porosity and permeability):

Characterization of the reservoir quality of the Gassum Formation in the Thorning structure is primarily based on lithological interpretation of the Gassum-1 and Nøvling-1 wells, representing a more proximal and distal depositional setting, respectively, compared to the site of the structure. For the purpose of characterizing the potential reservoir of the lower and the whole Gassum Formation within the Thorning structure three scenarios are considered as introduced above: Scenario 1 is a weighted average of data from the proximal Gassum-1 and the distal Nøvling-1 wells, awarding 2/3 weight to data of the geographical nearer Nøvling-1 well and correspondingly 1/3 weight of data from the Gassum-1 well. Scenario 2 is based heavily on data from the Gassum-1 well. This approach puts more emphasis on the seismic interpretations, reflection pattern and facies that show large similarities in seismic characteristics for the Gassum Formation in the Thorning and Gassum structures. Scenario 3 mirrors Scenario 1 but includes also the upper Gassum Formation.

In the Gassum-1 well only gamma ray (GR) log was recorded within the Gassum Formation, hence the volume of shale (V_{shale}), as indicated in Figures 7.1.2 and 7.1.3, is based on this log. The quality of the GR log itself seems to be reasonably fair, as there seems to be good agreement between the log derived lithologies and the descriptions of the corresponding cores when the core depths are shifted. The baseline of the GR representing clean sand is relatively high, which is expected in a sandstone containing a high content of feldspar. The V_{shale} curve forms the basis for the classification of the rocks into mudstones, siltstones and sandstones.

In the Nøvling-1 well, the logs used for the petrophysical interpretations are of higher quality, and in addition to the GR log there are caliper (CALI), sonic (DT), resistivity (R_DEEP), and density (RHOB) logs available. The CALI shows that severe caving has occurred during drilling and this effect the logs in various amounts. All these logs are used in the interpretation of the lithology of the Gassum Formation in this well, and there is a good correspondence between the individual V_{shale} curves that can be derived from the various petrophysical methods. The confidence in the petrophysical interpretation is thus high, also at stratigraphic levels where it varies from the descriptions in the Final Well Report (Gulf Oil Company Denmark 1967), which is mainly based on cuttings. This is especially true for the interval near the top of the Gassum Formation, where the Final Well Report suggests the presence of more sandy intervals. However, the GR, DT, R_DEEP and RHOB logs all support the interpretation that this interval consists of mudstones and subordinate siltstones.

Sandstones are assigned in intervals where V_{shale} is < 50% and siltstones have V_{shale} in the range of 50–75% and mudstones > 75%. 'Net sand' is defined as sandstone intervals characterized by fairly high porosities (> 10%) and low shale content (< 50%).

In Figures 7.1.2–7.1.5 the log derived effective porosity, PHIE, is shown for the Gassum-1 and Nøvling-1 wells. This curve is estimated very differently in the two wells. In Gassum-1 this curve is a linear fitting of the V_{shale} and porosity values obtained from core measurements, hence it is not derived by proper/standard petrophysical interpretation. It is included in the figures mainly for illustrative purposes and does not contribute to the evaluation of the reservoir quality of the Gassum Formation in this well, as these parameters are derived from the abundant core measurements. There are no cores from the Nøvling-1 well and the effective porosity, PHIE, has been derived separately from the R_DEEP, DT, and RHOB logs, where the most reliable was the R_DEEP which forms the basis for the reservoir characterization.

Scenario 1

As described above, sandstone intervals are considered to be present in the lower half of the Gassum Formation whereas they are most likely considerably less significant in numbers and thickness in the upper part of the formation. Hence the estimation of the sandstone content and the sandstones reservoir properties in the Thorning structure focus on the sandstones from the lower part of the Gassum Formation in the Nøvling-1 and Gassum-1 wells (the division of the Gassum Formation in the two wells is shown in Fig. 7.1.9).

In the Gassum-1 well, the interval corresponding to the lower Gassum Formation is 59.6 m thick and contains 38.9 m of sandstone, resulting in a net-to-gross ratio of 0.65. The lowermost sandstone unit in the Gassum-1 well (from 1622.5–1641.0 m MD) has unusually high permeabilities compared to others wells in Denmark. The only exception is the lowermost sandstone unit in the Stenlille-19 well that displays similarly high values. Thus, the reservoir properties of the lowermost sandstone unit in Gassum-1 are probably not representative for the sandstones in the Thorning structure. In addition, there are many more core measurements within this lower sandstone unit (from 1622.5–1641.0 m MD) in the Gassum-1 well compared to the upper sandstones (from 1582–1609 m MD, i.e. in the lower Gassum Formation), thereby introducing a bias when calculating an average. Therefore, the representative value of the porosity transduced from the Gassum-1 well is the average of the lower (1622.5–1641.0 m MD) and the upper sandstones (1582–1609 m MD) both contained within the lower Gassum Formation, resulting in an average porosity of 28.8% in the Net Sands for the lower Gassum Formation in the Gassum-1 well. This same approach has been followed for the estimation of the permeability leading to an average permeability of 1531 mD of the relevant sandstone.

In the Nøvling-1 well, the lower Gassum Formation is 28.1 m thick and contains 11.3 m of sandstone, resulting in a net-to-gross ratio of 0.40. The average porosities in the Net Sand in the relevant interval is calculated to be 24.1% and the average permeability to be 756 mD. The relation of the porosity and the permeability is based on a GEUS in-house correlation containing all core measurements from the Gassum Formation in the Danish area. This result is displayed in the Figs. 7.1.4 and 7.1.5.

Scenario 2

The seismic data indicate that sandstones are present in the lower part of the mapped Gassum Formation, and the similarity between the reflection pattern in the Thorning structure and the Gassum structure suggests corresponding depositional environment and thus similar sandstone properties and reservoir characteristics. Therefore, the reservoir characteristics are based on the Gassum-1 well, where the interval corresponding to the lower Gassum Formation is 59.6 m thick and contains 38.9 m of sandstone, resulting in a net-to-gross ratio of 0.65, with average porosities in the Net Sand of 28.8 % and average permeability of 1531 mD (as also outlined in scenario 1).

Scenario 3

Scenario 3 assumes that also the sandstone intervals contained within the upper Gassum Formation from the Gassum-1 well are present within the Thorning structure. Therefore, the

entire thickness of the formation forms the basis for the reservoir characterization of this particular Scenario 3.

In the Gassum-1 well the thickness of Gassum Formation is 123 m, of which Net Sand is 56.7 m resulting in a net-to-gross ratio of 0.46. In the Nøvling-1 well the thickness of the Gassum Formation is 85.3 m and here 11.3 m Net Sand leading to a net-to-gross ratio of 0.13. The average porosities and permeabilities within the Gassum-1 well are based on the core measurements. The average porosity within the Gassum Formation in the Gassum-1 well are estimated to 28.5 % and average permeabilities to be 1531 mD. In the Nøvling-1 well the average porosities and permeabilities are derived from the petrophysical log interpretations, where the average porosity is estimated to 24.1 % and the permeability to be 756 mD.

Table 7.1.2. Summarizing the reservoir characteristics of the lower Gassum Fm (for Scenarios 1 and 2) and entire Gassum Formation (for Scenario 3) within the Thorning structure. Regardless the Scenario the Gassum Formation shows excellent reservoir qualities, including a transmissivity that ranges between 21–54 Dm. The thickness values in the Thorning structure are based on seismic data.

	Thickness	Net Sand	Net to Gross	PHIE	PERM	Transmissivity
	<i>m</i>	<i>m</i>	<i>v/v</i>	%	<i>mD</i>	<i>Dm</i>
Gassum-1	59.6	38.9	0.65	28.8	1531	60
Nøvling-1	28.1	11.3	0.40	24.1	756	9
Scenario 1	55	21	0.37	25.7	1014	21
Scenario 2	55	36	0.65	28.8	1531	55
Scenario 3	95	26	0.28	25.6	1004	27

Conclusion on Reservoir Characterization

The reservoir characteristics within the Thorning structure are interpreted on the basis of data from the Gassum-1 and Nøvling-1 wells which represent a more proximal and distal depositional setting, respectively, compared to the site of the Thorning structure. Focus is on the lower Gassum Formation (Figs 7.1.2–5) which is most sandstone prone, and which in the Thorning structure is estimated to be 54 m thick based on the seismic data. In Scenario 1, the estimation also takes into account that the Nøvling-1 well is located closer to the Thorning structure than the Gassum-1 well. In scenario 2, the estimation relies entirely on data from the Gassum-1 well. In Scenario 3 the includes the sandstones in the upper Gassum Formation observed in the Gassum-1 well are assumed to be present also in the Thorning structure and their thicknesses and reservoir characteristics are estimated in the same way is in Scenario 1.

Table 7.1.2 shows the estimated reservoir values of the sandstones within the lower Gassum Formation in the two Scenarios 1 and 2. Regarding Scenario 1, the thickness of the lower Gassum Formation at the apex of the Thorning structure (at top Gassum Formation level) is estimated to be 54 m. This results in a Net Sand interval of 21 m, with a net-to-gross ratio of 0.38. Further, the average porosity of the reservoir is calculated to 25.7 %, leading to an average permeability of 1014 mD. Defining the transmissivity as the product of the permeability and the Net Sand gives 21 Dm. Regarding Scenario 2 the Net sand is 35 m, the average porosity is 28.8 % and the average permeability is 1531 mD, hence a Transmissivity of 54

Dm. Scenario 3 utilizes the full thickness of the Gassum Formation (estimated to c. 95 m at the apex of the structure at top Gassum Formation level), and results in a Net sand of 26 m, an average porosity of 25.6% and an average permeability of 1004 mD, and hence a transmissivity of 27 Dm.

The secondary reservoirs

The Frederikshavn Formation

The Upper Jurassic–Lower Cretaceous Frederikshavn Formation is known from wells drilled in the Danish Basin in northern and central Jylland. The formation is generally 50–150 meters thick but can be more than 230 m thick in the Sorgenfrei–Tornquist Zone (Nielsen & Japsen 1991). The formation is dominated by layers of siltstones and fine-grained sandstones alternating with silty claystones (Michelsen 1978, Michelsen & Bertelsen 1979, Michelsen et al. 1981, 2003). The sediments may contain glauconite and marine fossils. Thin layers of limestone occur in the lower and upper part of the formation, and in Northern Jylland there are a few cm-thick coal layers in the upper part of the formation; In Gassum-1, coal fragments are also present. The sediments were supplied to the Danish Basin from the Scandinavian bed-rock area. Thus, the grain size and the thickness and proportion of sandstone layers in general increase towards NE. Sand was mainly deposited in deltaic and coastal environments that prograded into the basin during periods of stable or falling sea level and were subsequently flooded during periods of rising sea level, whereby the deposition of sand was replaced by the deposition of silt and clay. The formation typically comprises two to three coarsening-upwards successions from offshore mudstones to shoreface sandstone, best developed in the central and northern part of the Skagerrak–Kattegat Platform (Michelsen 1978, Michelsen & Nielsen 1991). Distally, the formation thins out and becomes finer-grained until it is replaced by the claystone-dominated Børglum Formation. The presence of sandy layers in the southwestern part of the basin indicates that the Ringkøbing–Fyn High may also have been a sediment source during periods of low sea level. In some wells, the formation appears to consist entirely of mudstones and subordinate siltstones, and it is debatable why the interval is then not assigned to the Børglum Formation. This is the case with the Nøvling-1 well where the present petrophysical log interpretation reveals on very limited sandstones in the interval assigned to the Frederikshavn Formation (Fig. 7.1.16).

The Frederikshavn Formation in the study area

The seismic mapping and interpretation indicate that the formation is present in the entire structure, with a thickness of around 100 m (Fig. 6.2.3C), however which possibly also include some minor deposits of the Børglum Formation. The vertical depth to the top of the formation is estimated to c. 1187 m below mean sea level (Fig. 6.2.2C) corresponding c. 1247 m below terrain. This is estimated from a reference point at sea level located above where the structure has its apex at top Gassum Formation level (Fig. 6.2.2F). At this location, the thickness of the formation is estimated to c. 101 m. The present depth of c. 1187 m below mean sea level corresponds roughly to a maximum burial depth of around 1687 m prior to exhumation events (based on maximum burial map in Japsen et al. 2007).

The Frederikshavn Formation show large lateral variations in lithology between wells. This is especially evident by a comparison of the Gassum-1 and Nøvling-1 wells which are considered representative for a proximal and distal depositional setting, respectively, relative to the site of the Thorning structure (Fig. 7.1.16). Thus, the formation is largely dominated by sandstones in Gassum-1 whereas it consists almost entirely of mudstones and subordinate siltstones and only a few thin sandstone layers in Nøvling-1. Three to four overall coarsening-upwards successions, reflected by the GR motif, are recognized in the Gassum-1 well and are tentatively correlated to the Nøvling-1 well (Fig. 7.1.16). In Gassum-1, these probably reflect shoreface shallowing-upwards successions, possibly related to delta progradation. Distally, towards Nøvling-1, nearly all the shoreface sandstones pinches out into mudstones and siltstones. Based on the seismic data, it is not possible to deduce if this occurs before or after reaching the Thorning structure. Predicting the lithological composition of the Frederikshavn Formation in the Thorning structure is therefore not straightforward. A similar simplistic weighted average approach, as described for the Gassum Formation, is followed below for estimating the sandstone content and reservoir properties of the Frederikshavn Formation in the Thorning structure.

Cores of varying quality largely covers the formation in the Gassum-1 well (Figs. 7.1.2 and 7.1.17). The cores may form a good basis for studies of depositional environments, reservoir properties, mineralogy, diagenesis etc. as an input for their possible more distal editions in the Thorning structure.

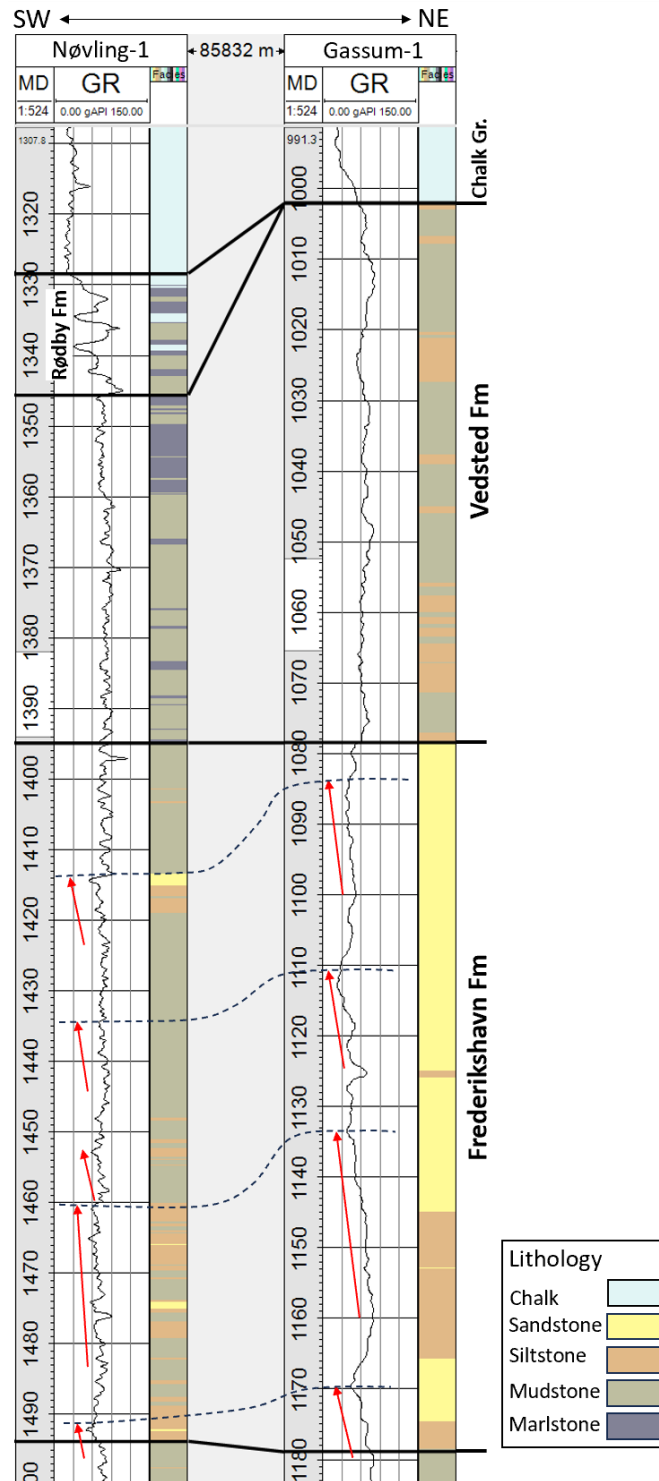


Figure 7.1.16. Comparison of the Frederikshavn Fm in the Nøvling-1 and Gassum-1 wells which compared to the Thorning site represent a more distal and proximal depositional setting, respectively. In the Gassum-1, the formation consists almost entirely of sandstones, locally with coal fragments, whereas mudstones and siltstones dominate the formation in the Nøvling-1 well. Four to five overall coarsening-upwards successions are reflected by the GR motif of the wells (in both wells emphasized with red arrows) and tentatively correlated. In the Gassum-1 well these probably reflect shoreface shallowing-upwards successions, possibly related to delta progradation, whereas they reflect slightly increasing sediment supply in a prodelta/offshore environment in the Nøvling-1 well.



Figure 7.1.17. Core examples of the Frederikshavn Fm from the Gassum-1 well dominated by very fine-grained sandstones that are greenish grey in colour, probably due to a content of glauconite. In general, the cores are fragmented or even disintegrated, but more coherent (cemented) sections still exist. Given the state of preservation the cores may form a basis for studies of depositional environments, reservoir and seal properties including porosity, permeability, grain size, mineralogy, diagenesis. Core diameter is c. 8.5 cm.

Reservoir quality (porosity and permeability)

Characterization of the reservoir quality of the Frederikshavn Formation in the Thorning structure is likewise based on lithological interpretation of the Gassum-1 and Nøvling-1 wells, representing a more proximal and distal depositional setting, respectively, compared to the site of the Thorning structure. For the purpose of characterizing the potential reservoir within the Thorning structure a weighted average between the proximal Gassum-1 and the distal Nøvling-1 wells has been applied, awarding 2/3 weight to the geographical nearer Nøvling-1 well and correspondingly 1/3 of the weight to the Gassum-1 well (similar approach as done for the Gassum Formation).

The data availability and types mirror the case for the evaluation of the Gassum Formation, where only a GR log is available for the Gassum-1 well supplementing a substantial number of cores and core measurements. While in the Nøvling-1 well there are no cores, but more logs of higher quality.

Figures 7.1.2 and 7.1.4 shows the lithological interpretation of the two wells revealing that the Net Sand interval in the Gassum-1 and the Nøvling-1 wells are markedly different. Thus, there are almost no sandstones present in the Nøvling-1 well whereas there are 74.4 m of sandstones in the Gassum-1 well. In Nøvling-1, the sandstones in the Frederikshavn Formation are so thin, that the reservoir values in terms of average porosity and permeability are not considered to be representative for the potential reservoir sandstones in the Thorning structure. Therefore, only the Net Sand is estimated on the basis of the geographical

distances from the Gassum-1 and Nøvling-1 wells, while the average porosity and permeability are copied from the Gassum-1 well. Comparing the porosity and permeability values of the Gassum Formation in these wells shows that the values are close to each other. This is also considered to be the case for any sandstones of the Frederikshavn Formation in the Thorning structure if these have thicknesses of minimum a few meters.

Table 7.1.3 shows the reservoir characteristics of the Frederikshavn Formation in the two wells, and based on these, the estimated reservoir values of the formation in the Thorning structure ('Thorning' in the table). The thickness of the Frederikshavn Formation in the Thorning structure is estimated to be c. 101 m based on seismic data, resulting in a Net Sand interval of 26.3 m, with a net-to-gross ratio of 0.26. Further, the average porosity of the reservoir is estimated to 28.7% and the average permeability to 830 mD. Defining the transmissivity as the product of the permeability and the Net Sand gives 22 Dm.

Table 7.1.3. Summarizing the reservoir characteristics of the Frederikshavn Fm within the Thorning structure that is expected to have excellent reservoir qualities, and transmissivity of 22 Dm (Darcymeter). Thickness of the Frederikshavn Fm is based on seismic data.

	Thickness	Net Sand	Net to Gross	PHIE	PERM	Transmissivity
	<i>m</i>	<i>m</i>	<i>v/v</i>	%	<i>mD</i>	<i>Dm</i>
Gassum-1	100.0	74.4	0.74	28.7	830	62
Nøvling-1	99.1	1.52	0.02	11.7	17	0.03
Thorning	100	26.3	0.26	28.7	830	22

Tønder, Bunter Sandstone and Skagerrak formations

The Danish Triassic interval below the Gassum Formation is generally under-investigated and would benefit from a regional stratigraphic revision integrating both well- and seismic data.

In the Thorning area, the nearest wells reaching pre-Gassum Formation strata show that potential sandstone reservoirs may also be present in the Triassic Bunter Sandstone, Tønder and Skagerrak formations (Fig. 7.1.18). As briefly outlined in the following, their presence and lithological composition in the Thorning structure is uncertain. This is because no sandstone reservoirs are identified below the Gassum Formation in the Nøvling-1 well which is the closest well to the Thorning structure (location of wells relative to the Thorning structure is seen in Fig. 3.1). However, the well was drilled in a complex structural setting, and it cannot be ruled out that a part of the Lower–Middle Triassic succession has been faulted out in the well. This is also mentioned as a possibility in the well completion report based on dipmeter data (Gulf Oil Company Denmark 1967). Seismic data substantiate intersection of at least one normal fault in the Nøvling-1 borehole and next to the well document the existence of down-faulted Triassic strata slightly older than the intersected succession.

Sandstone intervals are present in the Bunter Sandstone and Tønder formations in the Løve-1 and Grindsted-1 wells (Fig. 7.1.18) and may potentially also be present in the Thorning structure as the formations are described as northwards lateral equivalent to the Skagerrak Formation (Berthelsen 1980, Michelsen et al. 1981). These formations have also been interpreted in the Nøvling-1 well but here primarily consist of mudstones and evaporites. Therefore, it is uncertain if these formations are sand-prone in the Thorning structure. However,

the interval attributed to the Bunter Sandstone Formation in Nøvling-1 consists entirely of mudstones and subordinate layers of dolomite and siltstone (Fig. 7.1.18) and do not resemble the classical Bunter Sandstone described briefly below. It is therefore doubtful if the interval in fact should belong to the Bunter Sandstone Formation as suggested by Bertelsen (1980).

The Skagerrak Formation contains several hundred meters of sandstone in the Gassum-1 well and is considered to form a very good secondary reservoir in the Gassum structure (Keiding et al. 2024). The sediments were deposited as alluvial deposits along the Fennoscandian Border Zone and in braided streams and ephemeral lakes in the more distal part of the basin towards the southwest (Pedersen & Andersen 1980, Olsen 1988, Weibel et al. 2017). In the literature, the stratigraphic interval has for some wells in the Danish Basin been referred to as the Lower Triassic Bunter Sandstone Formation. This was also the case for the interval in the Gassum-1 well (e.g. in Nielsen & Japsen 1991, Pedersen & Andersen 1980). However, the very thick sandstone succession which characterizes the interval in the Gassum-1 well do not resemble the classic Bunter Sandstone Formation known from the North German Basin. For instance, the interval lacks the characteristic depositional cycles of the Bunter Sandstone Formation consisting of ephemeral fluvial and aeolian sandstone that grade upwards into thick successions of lacustrine/playa mudstone. In Weibel et al. (2017) the stratigraphic interval, considered to be the Bunter Sandstone Formation in the Gassum-1 well, was instead assigned to the Skagerrak Formation due to similarities to this formation, e.g. in the large thickness of the sandstone intervals and mineralogical composition. Keiding et al. (2024) interpreted good reservoir properties of the c. 695 m thick, sand-dominated Skagerrak Formation in the Gassum-1 well (Table 7.1.4).

A sand-prone Skagerrak/Bunter Sandstone Formation is not intersected in Nøvling-1. Alternative explanations may account for this unusual absence. One potential explanation would be incomplete stratigraphy due to normal faulting cutting the well-section. Alternatively, the scarcity of sand in the well may reflect that the thick sandstone succession of the Skagerrak/Bunter Sandstone Formation wedges out or laterally becomes more fine grained before reaching the location of Nøvling-1. Nøvling-1 is located on a structural high next to the Ringkøbing–Fyn High (see Chapter 6) in line with both wedging and lateral fining. However, regional seismic correlation to the Gassum area shows that the interval stratigraphically equivalent to the Skagerrak Formation at least in part extends to the Thorning structure. Depth converted seismic thicknesses show a comparably or slightly thinner thickness of the Skagerrak Formation in the Thorning area ranging between 550 and 650 m compared to in Gassum-1 (c. 695 m) (Fig. 6.2.3M). The Thorning area is located farther from the Scandinavian Craton hinterland than the Gassum area and Skagerrak Formation may very well be less sand-prone in the Thorning area. None the less, until the lack of Lower and Middle Triassic sandstones in Nøvling-1 can be solidly explained it introduces uncertainty for the reservoir potential of the Skagerrak Formation in the Thorning structure. Therefore, the reservoir potential of the Skagerrak Formation in the Thorning structure has not been addressed any further. However, the estimated reservoir data for Gassum-1 and the presence of sandstones in the Lower Triassic successions of for example Grindsted-1 and Løve-1 elucidate the large reservoir potential the Skagerrak Formation may have in the Thorning structure although the more distal depositional setting this site represents will imply a reduction of the reservoir values shown in Table 7.1.4.

Table 7.1.4 Summarizing the reservoir characteristics of the Skagerrak Fm within the Gassum structure. The formation has excellent reservoir qualities and thicknesses quantified by the transmissivity of 85 Dm (Darcymeter). Data from Keiding et al. (2024).

	Reservoir (m)	Net to Gross (v/v)	PHIE (%)	PERM (mD)	Transmissivity (Dm)
Gassum-1	693.7	1.0	15.4	123	85

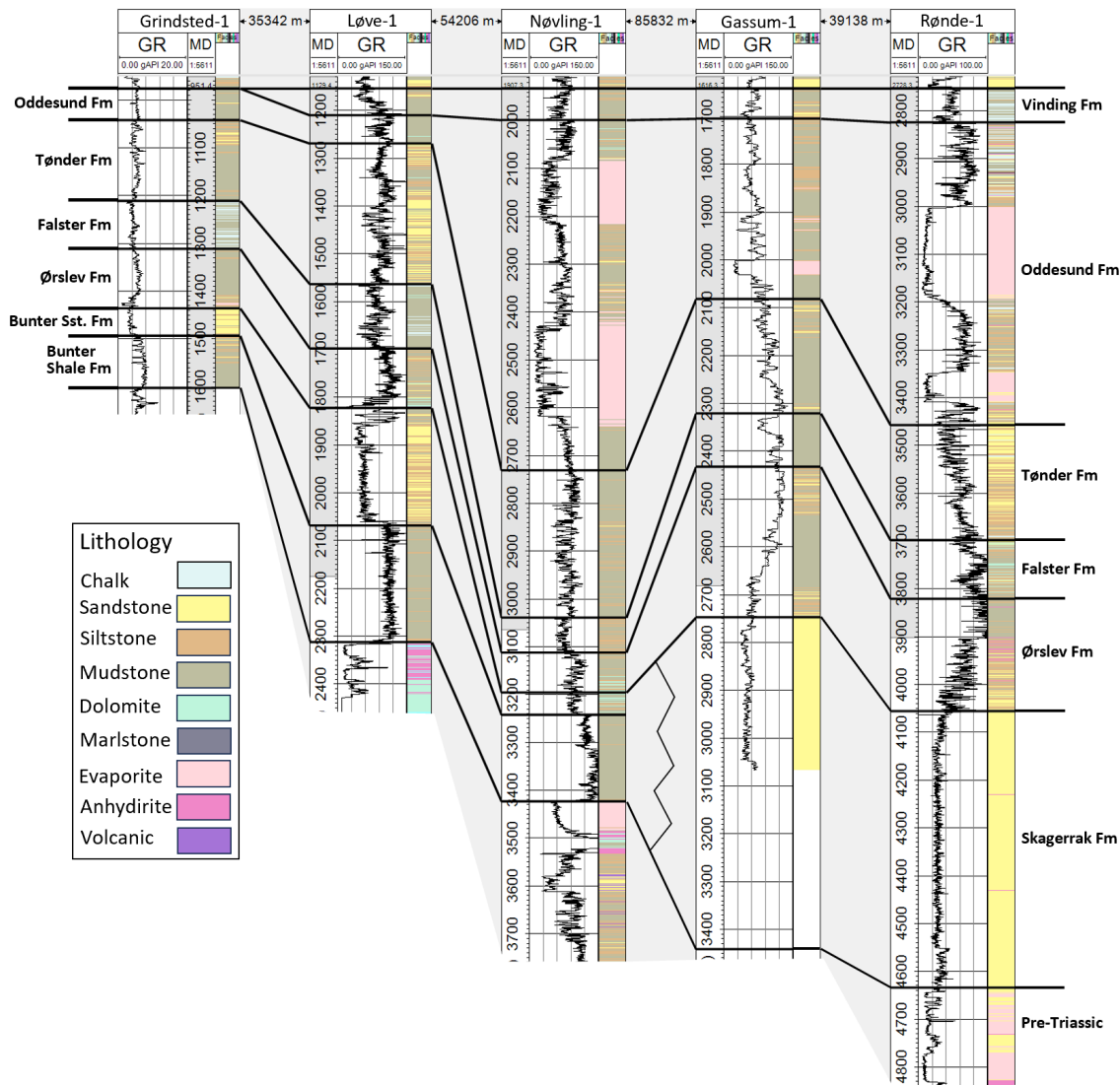


Figure 7.1.18. Correlation panel focusing on the Triassic below the Gassum Fm. Sandstone intervals are present in Bunter Sandstone, Tønder and Skagerrak fms but whether these form sandstone reservoirs in the Thorning structure is very uncertain, mainly because such intervals are not present in the Nøvling-1 well. However, as also mentioned in the text it cannot be ruled out that sandstone intervals of the Skagerrak or Bunter Sandstone formations have been faulted out of the Nøvling-1 well. In general, the Triassic interval below the Gassum Formation has not been in much focus and would benefit from a throughout regional revision. Location of wells relative to the Thorning structure is seen in Fig. 3.1.

Risks associated with formation water composition

Understanding the significance of salt content in the context of CO₂ storage is important for several reasons:

- Corrosion and material selection: High salt concentrations can accelerate corrosion in the materials used for storage wells and associated infrastructure. This can lead to increased maintenance costs and potential safety risks. An accurate assessment of salt content is crucial for selecting the right materials and designing effective corrosion protection systems.
- Scaling and operational efficiency: Salts, especially when present in high concentrations, can precipitate and form scales inside the storage reservoir and in the equipment. Scaling can reduce the efficiency of CO₂ injection and retrieval processes, potentially leading to operational challenges and increased costs.
- CO₂ solubility and storage capacity: The solubility of CO₂ in formation water is affected by the salinity of the water. Higher salt content typically reduces the solubility of CO₂, which could impact the overall storage capacity of the reservoir. Understanding the salt content helps in accurately estimating how much CO₂ can be stored.
- Geochemical reactions and long-term stability: Salt content can influence the geochemical reactions between CO₂, formation water, and reservoir rocks. These reactions are crucial for the long-term stability of stored CO₂. Predicting and monitoring these reactions require a thorough understanding of the formation water chemistry, including its salt content.

Assessing the formation water chemistry in the Thorning structure

Background and Challenges in the Thorning Area: Since the Thorning structure is un-drilled no data on brine composition exist. Near the structure, there is compositional data from the Gassum-1 well. However, the composition of formation water in onshore Denmark is relatively well documented in the Danish Basin. Here, it is recognized to vary both geographically and with burial depth, as highlighted in studies by Laier (2002, 2008) and Holmslykke et al. (2019).

Methodology for Estimating Salinity in Thorning structure: For the assessment of formation water chemistry within the Thorning structure reservoirs, we have leveraged the established relationship between geological depth and salinity derived from the Danish Basin (Fig. 7.1.19, Table 7.1.5). Utilizing this methodology, we estimate that at the median depth of the Frederikshavn Formation in Thorning, situated approximately at 1297 m below ground, the formation water exhibits a chloride concentration around 99,000 mg/l Cl⁻ (equivalent to 165,000 mg/l Total Dissolved Solids (TDS)). Within the primary reservoir of the Gassum Formation median depth, located at roughly 1640 m below terrain, the estimated salinity reaches approximately 111,000 mg/l Cl⁻ (184,000 mg/l TDS). Meanwhile, at the median depth of the possible Skagerrak/Bunter sandstone reservoir, around 2880 m below terrain, salinity is estimated to be approximately 198,000 mg/l Cl⁻ (327,000 mg/l TDS), indicating that it is nearing saturation with respect to halite (cf. Holmslykke et al. 2019 for comparative calculations in the Tønder area). Further geochemical modelling will be presented elsewhere (Schovsbo et al. submitted).

Table 7.1.5. Estimated salinities (Cl^- and TDS, Total Dissolved Solids) in the Thorning structure for median depth (below terrain) of reservoirs. Estimations based on Schovsbo et al. (submitted).

Formation	Depth (m)	Estimated Cl^- (mg/L)	Estimated TDS (mg/L)
Frederikshavn	1297	99,118	164,140
Gassum	1637	111,033	183,871
Skagerrak	2885	197,559	327,158

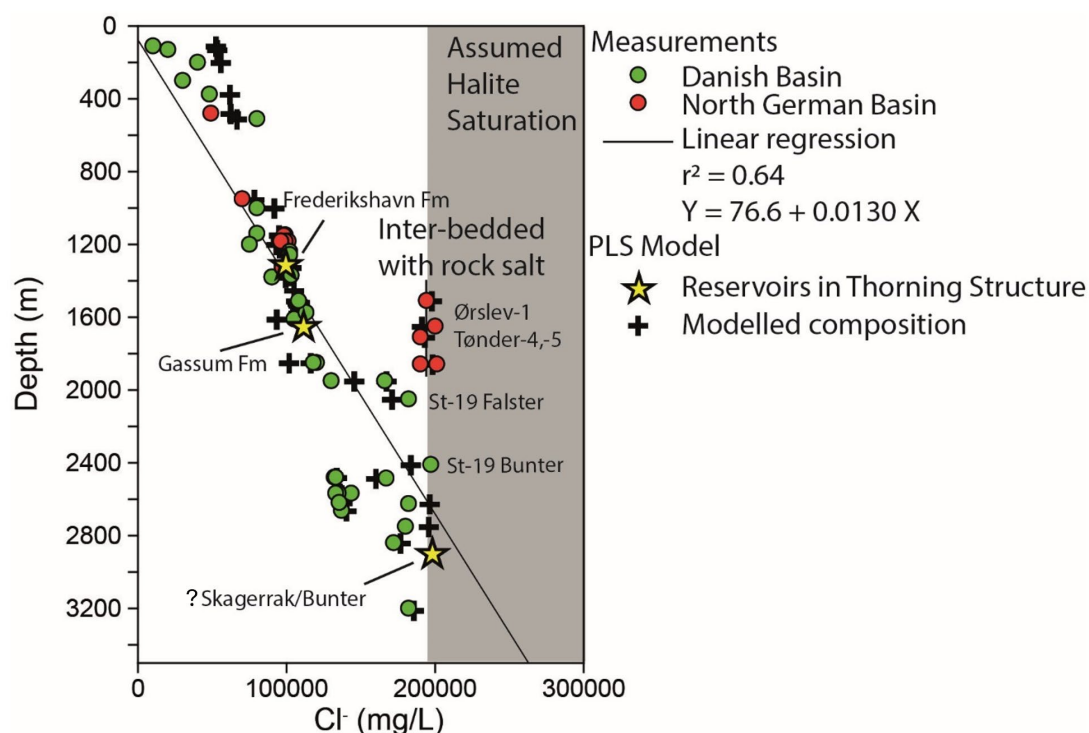


Figure 7.1.19. Salinity with depth in Denmark and Sweden. This figure is derived from the data compilation by Laier (2008), incorporating minor updates based on recent findings (full database presented in Schovsbo et al. (submitted)). Modelled salinity (PLS model) is based on a numerical analysis (Schovsbo et al. submitted). Field of halite (NaCl) saturation (grey) assumes stoichiometric concentration of Na^+ and is loosely based on Holmslykke et al. (2019). No account for temperature and pressure effect has been made but will be made in later refinements of the model.

7.2 Seals – Summary of geology and parameters

There are no wells penetrating potential primary and secondary reservoir-seal pairs in the Thorning structure. However, the seismic interpretation with ties to deep wells in the region indicate the presence of the Fjerritslev Formation, the primary seal to the Gassum Formation, as well as the Vedsted Formation, Rødby Formation and lower part of Chalk Group which are the seal units to the Frederikshavn Formation. The deeper lying Ørslev and Falster Formations are seals to sandstone reservoirs of the Skagerrak Formation/Bunter Sandstone Formation and additionally the Oddesund Formation is the seal to sandstone reservoirs of the Tønder Formation (Fig. 7.2.1). However, as mentioned above the presence of sandstone reservoirs in these deeper-lying Triassic formations (below the Gassum Formation) is less certain in the Thorning structure.

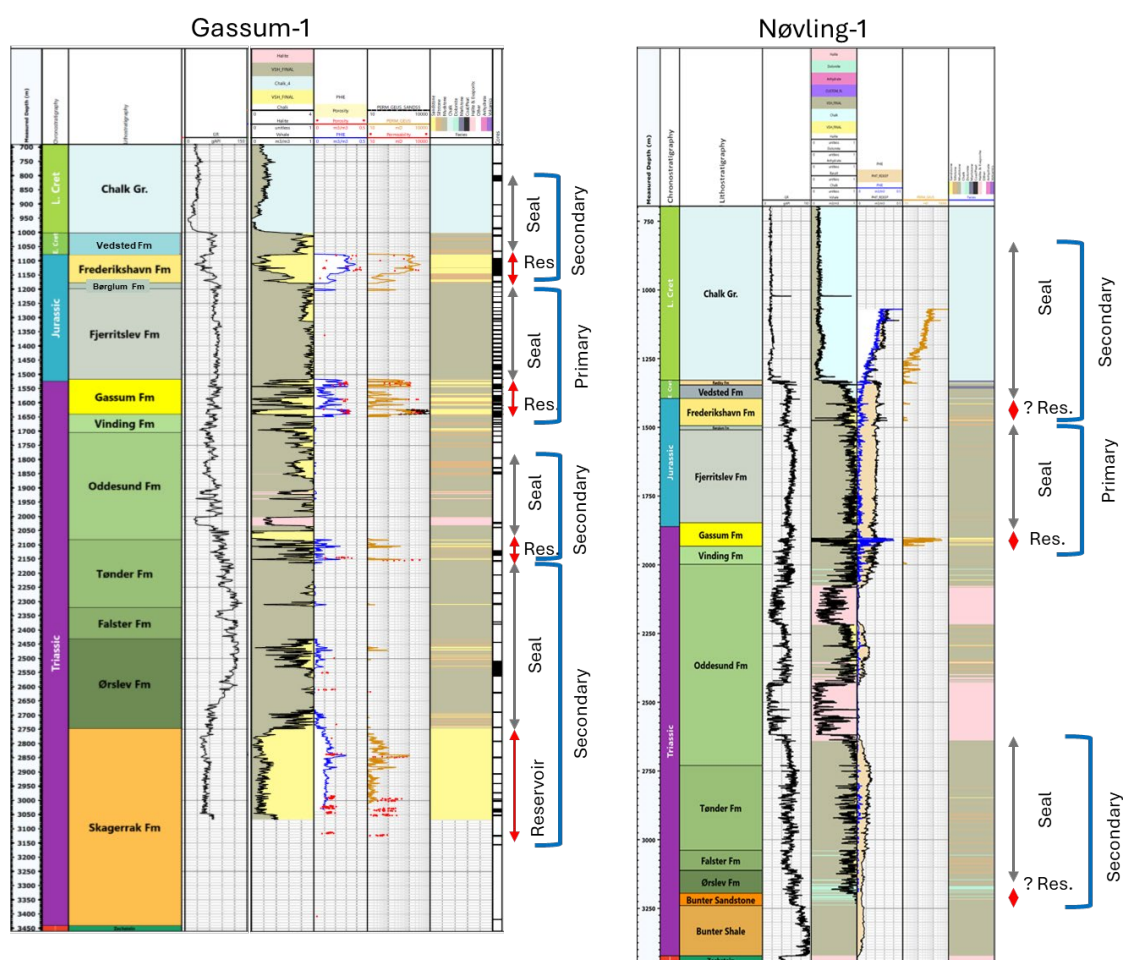


Figure 7.2.1. Two reference wells for the Thorning structure; Gassum-1 and Nøvling-1 with petrophysical logs displaying the potential primary and secondary reservoir-seal pairs. Note the pre-susmable lack of reservoir sandstones within the Frederikshavn Fm, Tønder Fm and Bunter Sandstone Fm in the Nøvling-1 well. Possible reasons for this are discussed above in section 7.1.

The primary seal of the Gassum Formation: The Fjerritslev Formation

The Lower Jurassic Fjerritslev Formation is drilled by several deep wells within 30–40 km from the Thorning structure, and the following wells are included in the evaluation of the formation: Voldum-1, Gassum-1, Hobro-1, Kvovls-1, Mejrup-1, Nøvling-1, Vinding-1 and Horsens-1 (Fig. 7.2.2). Mapping of the Fjerritslev Formation on legacy seismic data show large thickness variations on regional and local scale especially across faults and along salt structures (e.g. Michelsen et al 2003).

Depth conversion of the newly collected seismic data suggests that the Fjerritslev Formation attains a thickness of 100–350 m in the Thorning structure showing an overall thickness decrease towards the apex of the structure (Fig. 6.2.3F). A marked thickness decrease is recorded towards the SW along the boundary fault of the Thorning structure. The general thickness trend in the region shows a significant increase towards the north with prominent local modulations caused by diapiric halokinesis of e.g. the Bording, Mønsted and Nøvling diapirs and associated fault systems (see Chapter 6). A prominent thickness increase is in this context also recorded across the minor faulted graben SW of the structure (Fig. 6.1.5) that is related to halokinesis of the Thorning pillow and the Bording diapir. As mentioned above, a large convex upwards structure, onto which the Fjerritslev Formation onlaps, has been mapped out on the seismic data immediately above the Gassum Formation (Figs 7.1.10–12). The structure possibly represents a major submarine landslide complex and if so, diminish the thickness of the Fjerritslev Formation with c. 150 m in this part of the Thorning structure (Fig. 6.2.3E). The base of the Fjerritslev Formation is estimated at c. 1520 m b. msl (1580 m below terrain) at the apex of the structure at top Gassum Formation level (Fig. 6.2.2F). The top of the Fjerritslev Formation is associated with a marked truncation surface with an apparent deeper truncation in a regional southern direction (Figs. 3.3–4).

The reference legacy well data shows a thickness variation of 146–475 m and a southward wedging out towards the Ringkøbing–Fyn High, e.g. towards Løve-1 (Table 7.2.1, Appendix A, B). Core material exist from the Gassum-1 well (Cores 32–52), although these are in poor condition today due to long-term storage and intensive sampling (Fig. 7.2.3). Apart for this, core material from the Farsø-1, and Aars-1 and in the Stenlille area exist but are not included in this report. Data from the Vedsted-1 well in northern Jylland and the detailed knowledge of the seal from the Stenlille gas storage facility on Sjælland are also included regarding assessment of seal capacity.

The geology of the Fjerritslev Formation in the Thorning structure is interpreted similarly to that in the Gassum structure recently reported by Keiding et al. (2024). Regionally the formation spans the latest Rhaetian–Early Aalenian; in Gassum-1 it is of Early Jurassic Hettangian–Toarcian in age (Dybkjær 1988, 1991). The formation comprises a succession of marine claystones and mudstones, interbedded with subordinate thin sandstone beds. It is present in the Danish Basin, north of the Ringkøbing–Fyn High, and in the North German Basin south of the Ringkøbing–Fyn High but absent on the high itself. In the central and western part of the Danish Basin, including the area of the Thorning structure, the formation is expected to conformably overlie the fluvial to shallow marine Gassum Fm of Rhaetian (latest Triassic) to Hettangian (earliest Jurassic) age. The Thorning area represents a more distal depositional setting in the Danish Basin compared with the Stenlille area on Sjælland and probably also a more distal setting than the Gassum area (Nielsen 2003). The Danish Basin was sourced roughly from the northeast during the Early Jurassic (Nielsen 2003), and consequently the Fjerritslev Formation is expected to be more fine-grained and containing less

siltstone and sandstone layers in the Thorning structure compared to the two other sites. The formation is unconformably overlain by Upper Jurassic marine mudstones of the Børglum Formation that may be regarded as an additional seal unit.

The structural evolution based on the seismic interpretation show that the Thorning structure formed due to halokinesis of the Zechstein halites with initial growth of the salt pillow during the Triassic (Chapter 6). Pulses of halokinesis affected the sedimentary accumulation especially during deposition of the Fjerritslev Formation in the Thorning area with synsedimentary faulting and the formation of a minor graben in the SW part of the structure (Chapter 6).

Lithological subdivision

The Fjerritslev Formation was defined by Larsen (1966) and revised by Michelsen (1978, 1989a; Michelsen et al. 2003). The formation is subdivided into five informal members F-Ia, F-Ib, F-II, F-III, and F-IV using the Hyllebjerg-1 in northern Jylland as reference section (Michelsen 1989a). A detailed correlation between wells located centrally in the Danish Basin shows that characteristic log-patterns can be traced across long distances suggesting that the formation comprises several laterally continuous depositional units (Michelsen 1989b). A high-resolution palynostratigraphy combined with petrophysical logs patterns enables a sequence stratigraphic subdivision of the formation (Dybkjær 1991, Nielsen 2003 and GEUS in house data). The Fjerritslev Formation in the Gassum-1 well is thus represented by sequences 9 to 15 (*sensu* Nielsen 2003) and the informal lithostratigraphic members F-I to F-III (Appendix B). Semi regionally the same base of the Fjerritslev Formation (corresponding approximately to the transgressive surface TS 9) is recorded in Hyllebjerg-1, Kvols-1, Hobro-1 but the stratigraphical range is expanded in some of these wells to also include the upper member F-IV and thus well into the Toarcian (Appendix B).

A sequence stratigraphic division of the Gassum Formation and Fjerritslev Formation was presented by Nielsen (2003), and the base of Fjerritslev Formation is defined at TS 7 (late Rhaetian) in the central part of the Danish Basin and is probably defined slightly younger at TS 9 (early Hettangian) in the Thorning area, as seen in the surrounding wells (Fig. 7.2.2). In these wells, the F-Ia and F-Ib members are generally present. Due to the Mid Jurassic unconformity and associated erosion of the Fjerritslev Formation, the F-II, F-III and F-IV members are only partly present (Table 7.2.1). The boundaries between the members corresponds to sequence stratigraphic surfaces of either transgressive surfaces recognized by prominent increases in the GR log or sequence boundaries (Fig. 7.2.2). The sequence stratigraphic breakdown is based on updated GEUS inhouse data in the region that builds on the sequence stratigraphic framework in Nielsen (2003).

The core material from the Gassum-1 well represents different intervals of the Fjerritslev Formation (Figs. 7.2.1, 7.2.3, Appendix B). The cores have been described and studied with regards to the bivalve composition by Pedersen (1986). The formation is characterized by mudstones and silt-streaked mudstones with subordinate layers of mottled sandy siltstones in the lower part. All facies are bioturbated and the bivalve content suggest that the mudstones represent deposition in normal marine outer shelf environments (Pedersen 1986). The organic content is only known from cuttings samples between cored sections (Petersen et al. 2008).

The seismic sections (Chapter 6) shows that the Fjerritslev Formation is characterized by a subtle low amplitude parallel reflectivity, indicating a rather uniform lithology (mudstone). This reflectivity pattern applies to the succession above the prominent convex upward structure

overlying the Gassum Formation in the eastern central part of the Thorning structure (Figs 7.1.10–12). High reflectivity reflectors seem to onlap the convex upward structure from the east and may indicate the presence of sandstone beds in the lower part of the Fjerritslev Formation in this area (Fig. 6.1.7).

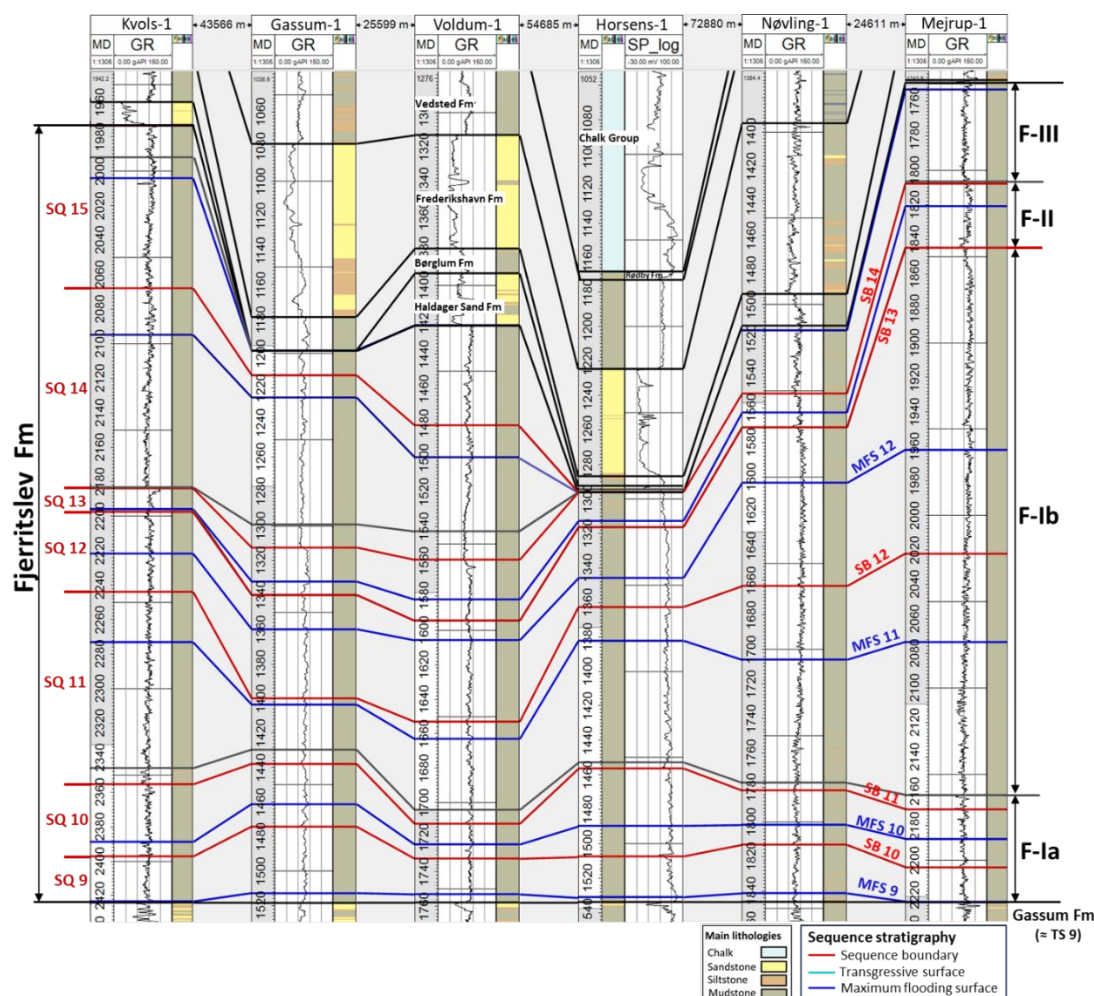


Figure 7.2.2. Correlation panel focusing on the Fjerritslev seal in the nearest wells to the Thorning structure. The placement of sequence stratigraphic surfaces and interpretation of depositional environments is tentative and would benefit from supplementary palynological data. The transgressive surface TS 9 represents the base of the Fjerritslev Fm in the wells and is used as datum line. Location of wells relative to the Thorning structure is seen in Fig. 3.1.

The F-Ia member

Based on the well correlation panel the member is 54.3–90 m thick in the area. It is bounded by the sequence stratigraphic surfaces TS 9 and TS 11 (Table 7.2.1). In Gassum-1, ca 50 km NE of the Thorning structure, the member is represented by the cores 47–52 that comprise mainly very dark grey planar laminated mudstones with few thin fine sandstone laminae and is interpreted as deposited in offshore environments (Pedersen 1986). Based on the well log correlation panel, the thickness of the member is relatively uniform towards the north and west and show a thickness decrease towards the east in Voldum-1 to about 50 m. Minor sandstone units may in some wells be associated with sequence boundaries SB 10 and SB 11.

The F-Ib member

The thickness of this member varies between 66–317 m in the wells closest to the Thorning structure, with an average of 160 m. The thinnest development (66 m) is recorded in Vinding-1 and is not included in the above average because the boundary to the overlying upper Jurassic Børglum Formation is an unconformity in this well. The unusual thick member recorded in Mejrup-1 (317 m) may represent a local Early Jurassic depocenter in the Danish Basin (Nielsen 2003).

In general, the member is bounded by the sequence stratigraphic surfaces TS 11 and SB 13 (Table 7.2.1). In Gassum-1, it is represented by the cores 41–46 of mainly very dark grey mudstones with few thin fine sandstone laminae that are interpreted as deposited in an off-shore environment (Pedersen 1986). The GR log readings in the wells are relatively uniform medium–high values. A few subtle low GR readings, e.g. associated with the sequence boundary SB 12, may indicate the presence of thin sandstones or siltstones. Based on the well log correlation panel, the thickness of the member nearly doubles towards the north and west but also show significant increase towards the east and south.

Table 7.2.1. Thicknesses of the members of the Fjerritslev Fm in the nearest wells to the Thorning structure in the Danish Basin. * The lower boundary of the F-IV member is positioned between MFS 15 and SB 16 according to Nielsen 2003. Nø-1, Nøvling-1; Vi-1, Vinding-1; Me-1, Mejrup-1; Kv-1, Kvols-1; Hb-1, Hobro-1; Ga-1, Gassum-1; Vo-1, Voldum-1; Rø-1, Rønde-1; Hr-1, Horsens-1. The biostratigraphy conducted in this study is modified from Dybkjær (1991). Sequence stratigraphy and thicknesses of members partly modified after Nielsen (2003).

Fjerritslev Fm													Regional age			
Location/wells				Nø-1	Vi-1	Me-1	Kv-1	Hb-1	Ga-1	Vo-1	Rø-1	Hr-1				
Measured Depth (m) to	Top Fjerritslev Fm			1512	1475.6	1749.2	1973.5	1923.7	1198.5	1423	2138	1294.4	Toarcian – E. Aalenian			
	Base Fjerritslev Fm			1847	1603.8	2229.2	2424	2376.7	1517	1758.4	2613	1533.8	L. Rhaetian – E. Sinemurian			
Thickness (m)				335	146.3	480	450.5	453	318.5	335.4	475	239.4				
				Sequence stratigraphy		Thickness (m)										
				Lower boundary	Upper boundary											
Lithostratigraphy	F-IV mb	SB 16*	SB 19	None	None	None	18.5	31.3	None	None	38	None	Middle Toarcian– E. Aalenian			
	F-III mb	TS 14	SB 16*	None	None	57.2	191	167.6	100.6	119.6	145		L. Pliensbachian – Mid. Toarcian			
	F-II mb	SB 13	TS 14	60	None	38.5	13	23.2	40.8	51.8	73	21.9	Pliensbachian			
	F-Ib mb	TS 11	SB 13	185.0	64.3	317.2	149.9	150.1	89.7	109.7	141	136,4	Sinemurian– E. Pliensbachian			
	F-Ia mb	TS 7 / TS 9	TS 11	90.0	82.0	67.1	78.1	80.8	87.4	54.3	64	83	Rhaetian – Hettangian			

The F-II member

The member shows thickness variations of 13–73 m (with an average thickness of 38 m), where it is present in the nearest wells, and is overlain by member F-III. The member is bounded by the sequence stratigraphic surfaces SB 13 and TS 14. The top of the member is marked by an unconformity and is overlain by the Upper Jurassic Børglum Formation in the Nøvling-1 and Horsens-1 wells. In Gassum-1, the member is represented by the cores 38–40 that comprise very dark grey mudstones commonly laminated with few thin fine sandstone laminae. It is interpreted to represent deposition in an offshore environment (Pedersen 1986). The GR log readings in the well show a relatively low amplitude peak at SB 13

indicating a minor input of fine sand and silt constituents. An interval with prominent high GR readings is represented from MFS 13 to SB 14. The interval correlates with a relatively high organic content as measured on the ditch cuttings samples in e.g. Gassum-1 (Schovsbo & Petersen 2024). The high organic content in the unit is recognized regionally, especially in the northern part of Jutland (Nielsen 2003).



Figure 7.2.3. Core photos of the Fjerritslev Fm, Gassum-1 well. A. F-Ia mb, Hettangian–Sinemurian transition. The SB 11 is present in sandy grey mudstone in the lower part of the core and is overlain by very dark grey mudstones. Core 47, 4702–4722' (c.1433–1439 m), B. F-III mb, Pliensbachian. Grey bioturbated silty mudstone, sequence 14. Core 33, 4016–4021' (c.1224–1226 m) C. F-III mb, Toarcian. Grey bioturbated silty mudstone above SB 15. Core 32, 3967–3972' (c.1209–1211 m). D. Børglum Fm, Oxfordian–Kimmeridgian. Greenish grey and reddish mudstones indicating diagenetic overprinting due to subaerial weathering. Core 31, 3903–3914', (c.1190–1193 m). Note general poor core conditions, core diameter 8.5 cm. Core depths may differ from log depths, see Nielsen (2003, fig. 13).

The F-III member

The member is partly present in the reference wells (Table 7.2.1), and where it is present it shows thickness variations between 57–191 m. In those wells where it is overlain by the F-IV member, the thickness variation is 145–191 m with an average of 168 m. The member has a lower boundary at sequence stratigraphic surface TS 14. An unconformity separates

the member from the overlying Upper Jurassic Børglum Formation in the Mejrup-1, Gassum-1 and Voldum-1 wells. The member is not present in Horsens-1, Nøvling-1 and Vinding-1 reflecting a general thickness decrease and wedging out towards the south and west, most likely related to Middle Jurassic regional uplift and erosion. The F-III member is represented by the cores 32–37 in Gassum-1 and comprises dark grey mudstone with few thin fine sandstone laminae. It is interpreted to reflect deposition in an offshore environment (Pedersen 1986).

The lower part of the member is characterized by an increase of thin siltstone and sandstone beds towards the north in Hobro-1 and towards the west in Mejrup-1. The GR log readings show a minor low amplitude peak at SB 13 indicating a moderate input of fine sand and silt, but otherwise the member has relatively uniform medium to high GR readings with a slightly upward increasing trend. Petersen et al. (2008) examined the amount and composition of the organic matter contained in the Toarcian marine mudstones of the F-III and F-IV members in the central part of the Danish Basin. These members locally include intervals with hydrogen index (HI) values of 300–400 mg HC/g TOC (HC: hydrocarbons; TOC: total organic carbon), see also Michelsen (1989b).

The F-IV member

The F-IV member is only recorded in the wells to the north and east, e.g. being 31.5 m thick in Hobro-1, and 18.2 m thick in Kvols-1. The thickness increases northward to 55 m in Hyllebjerg-1. It is not present in Voldum-1 but is 45 m thick in Rønde-1 towards the east. Palynomorphs from the F-IV member indicate that deposition of marine mud continued into the Toarcian (Dybkjær 1991).

The unconformity on top of the Fjerritslev Formation in the Thorning structure is interpreted as caused partly by uplift and erosion due to growth of the Thorning salt pillow, and partly by the regional mid Jurassic uplift as also recognized for the salt pillow structures of Stenlille, Havnsø and Gassum areas (Gregersen et al. 2023, 2024, Keiding et al. 2024). The mid Jurassic uplift and erosion with expanded hiatus along the Ringkøbing–Fyn High is well documented by Nielsen & Japsen (1991) and Nielsen (2003), (Fig. 3.3).

Bulk mineralogy

The bulk mineralogy of the Fjerritslev Formation mudstones is known from 10 cutting samples in the Kvols-1 and Kvols-2A wells situated 30 km to the north of the Thorning structure. They show that quartz is the dominant mineral in all samples with little or minor amounts of kaolinite and illite or mica and calcite (Vosgerau et al. 2016). Pyrite occurs in small or trace amounts. Feldspars, siderite and ankerite may occur in trace amounts. Calcite, siderite or pyrite are present in some samples, mainly in the mudstones. Mbia et al. (2014) presented petrophysical and mineralogical data from the Vedsted-1 and Stenlille-2 wells, showing a total clay content less than 50 wt% and a dominance of vermiculite and mixed layered minerals.

Clay minerals

The clay fraction in the mudstones of the Fjerritslev Formation in Kvols-1 and Kvols-2A generally ranges between 42 and 46 wt% and accordingly the silt–very fine sand fraction ranges between 54–58 wt% (Vosgerau et al 2016). A single outlier analysis shows a clay content of

26 wt%. The clay mineral assemblages record kaolinite with 35–39 wt%, vermiculite and mixed layer minerals with 45–49 wt% and illite, mica with 10–14 wt%.

Burial and exhumation

Vitrinite reflectance (VR) values increase with increasing temperature and are thus a proxy for maximum burial depth in undisturbed sedimentary successions. The process is irreversible, and the VR values therefore always record the maximum temperature, normally the maximum burial depth, the organic matter has experienced. Petersen et al. (2008) measured 560 vitrinite reflectance values in samples from 26 wells in the Danish Basin and showed that the Fjerritslev Formation is immature with respect to oil generation. 25 of the studied wells had, however, too high VR values compared to present-day depth due to a significant post Early Cretaceous uplift. The geographical position of the Gassum-1 well is probably roughly analogous in terms of maximal burial depth to that of the Thorning structure and it shows VR values from 0.49–0.52% in the F-Ia and F-III members of the Fjerritslev Formation in the depth interval from 1231–1480 m. Based on chalk sonic velocity data a net-exhumation magnitude of 579 m is suggested (Petersen et al. 2008, Japsen et al. 2007). The VR values indicate that the Fjerritslev Formation is thermally immature with regards to hydrocarbon formation. The 579 m of net-exhumation suggests a corrected maximum burial depth of c. 2570 m of the Fjerritslev Formation in the Gassum-1 well. This maximum burial depth should be considered when the capacity and quality of the Fjerritslev seal is evaluated. It is, however expected that the seal is still immature with respect to oil generation in the area (i.e. $V_r < 0.65\%$).

Seal capacity of the Fjerritslev Formation

The seal capacity of the Fjerritslev Formation has been investigated by Mbia et al. (2014), Springer et al. (2020) and Gregersen et al. (2023). The studies highlight the formations good seal integrity in relation to carbon capture and storage (CCS). The Fjerritslev Formation has been investigated primarily in the Stenlille area where it features a seal succession approximately 250–300 m thick. The succession is characterized mainly by mudstones but with interbedded porous sandy-silty layers especially within the F-Ia member but also in the overlying FI-b–F-IV members. Key findings for the seal include an average porosity of 11%, air-permeability of 160 μD , and liquid permeability reaching 3 nD – comparable to the best-known caprocks for petroleum accumulations. Additional overburden measurements indicated liquid permeabilities around 200 nD, underscoring the formation's excellent seal quality, which at the Stenlille structure has been validated by over 30 years of natural gas storage in the underlying Gassum Formation.

Capillary entry pressure, a critical factor for assessing seal capacity, was assessed from Mercury Injection Capillary Pressure (MICP) experiments. Despite the challenges in converting results from the mercury/air system to the CO_2 /brine system, due to differences in contact angle and interfacial tension, standard conversion values suggest capillary entry pressures ranging from 5–10 MPa, with newer samples indicating a lower range of 1–5 MPa. The buoyancy force exerted by the supercritical (sc) CO_2 on the caprock, influenced by the density difference between formation water and injected CO_2 , dictates the seal capacity for scCO_2 storage. Estimations show that the caprock capillary system can support scCO_2 column heights ranging from approximately 290 m to over 1000 meters. Although site specific data from the Fjerritslev Formation in Thorning are needed, the comparison to the Stenlille area

suggests its excellence as a primary seal for the Gassum Formation, possessing potential robust sealing capabilities here also.

Comparison between the Gassum-1 and Vedsted-1 wells

No HH-XRF data have been collected from the Stenlille wells, from which the good seal properties cited above have been established. However, similar good seal properties have been measured in the Vedsted-1 well (Mbia et al., 2014), as also noted by Springer et al. (2020) in their review. The cuttings chemistry in the Gassum-1 well appears to be similar to that of the Vedsted-1 well, and it seems reasonable to suggest, as a first approximation, that the Gassum-1 well likely share similar good seal properties as in Vedsted-1 considering their position in the basin with the Gasum-1 being located more centrally at a larger distance to the basin margin (Nielsen 2003, Schovsbo and Petersen 2024).

The clay content in the Vedsted-1 well ranges between 40–45% within the 1350–1745 m interval (7 samples) studied by Mbia et al. (2014). This interval exhibits a Si/Al ratio of 4 and an Al content of about 4000 ppm or slightly higher. Smectite and kaolinite may constitute up to 50% of the clay volume in Vedsted-1, a significant portion of which will go undetected by the GR curve, as these clay types are non-radioactive due to their lack of potassium (K), thorium (Th), and uranium (U) – although smectite might potentially include surface-bound U. A similar K/Al trend, as observed in Vedsted-1, can also be seen in the Gassum-1 well, suggesting that a similar clay mineral assemblage is likely present here (Schovsbo and Petersen 2024). Similar clay mineral assemblages are anticipated in the Thorning structure as this location is considered situated in an even more distal position than the Gassum-1 and Vedsted-1 sites during deposition of the Fjerritslev Formation.

Recommendations for further studies on seal capacity

Site-specific studies on the seal capacity are needed for all structures to be matured towards CO₂ storage. For the Thorning structure, no site-specific studies exist for the sealing units and the need for establishing fundamental knowledge of the local seal properties is thus high. For the Fjerritslev Formation we can draw parallels to the better-known Fjerritslev Formation in the Stenlille area and the Vedsted-1 sample set as a basis for the evaluation. However, due to the distances to these data sets and the related uncertainties of correlations, it is recommended to generate a local data set for thorough evaluation.

In Figure 7.2.4, a workflow to establish the fundamental seal information is outlined. In this workflow, the studies that ideally should be conducted from all potential seal units in the Thorning structure, on both cuttings samples and core material. HH-XRF, cuttings imaging, and TOC and Rock Eval analysis, form only part of the screening data that needs to be gathered. Other important high-volume samples include porosity, surface area determination, mineralogy, and clay type determination combined with grain size analysis. Once established, selection for more costly but crucial analyses such as pore size distribution and capillary entry pressures, as well as petrographic and microfacies descriptions, is advised.

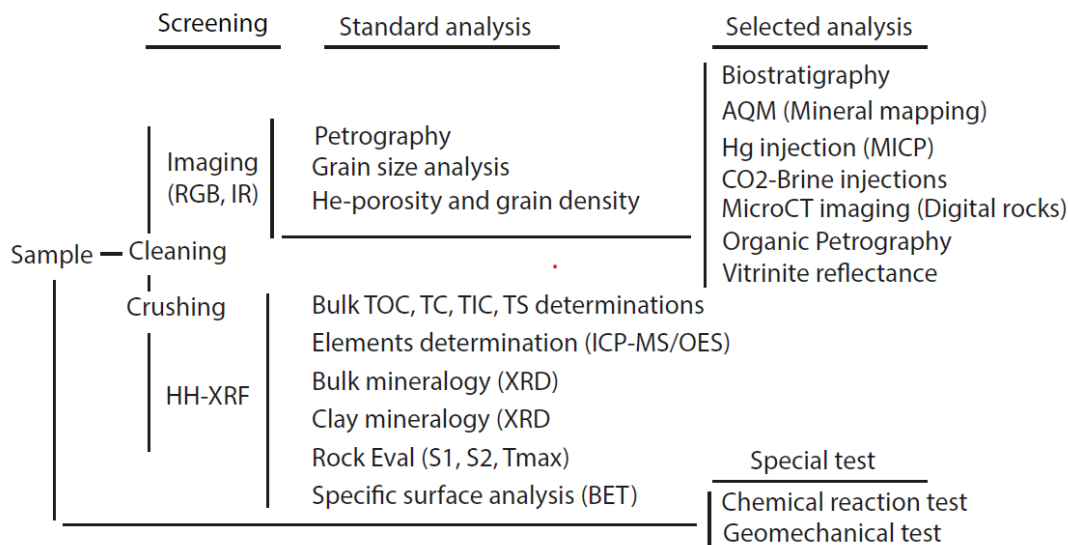


Figure 7.2.4 Workflow for seal characterisation. Based on Schovsbo & Petersen (2024).

The Børglum Formation Secondary seal of the Gassum Formation:

The Børglum Formation may represent an additional or secondary seal unit to the Gassum Formation. In the surrounding wells to the Thorning structure the Børglum Formation is 5–47 m thick and of Oxfordian–Kimmeridgian in age (Appendix B, Biostratigraphic charts), indicating an unconformable lower boundary to the Lower Jurassic Fjerritslev Formation.

Based on the surrounding wells the Børglum Formation comprise a relatively condensed interval, considering the expanded age span covered. The formation represents generally offshore muddy depositional environments and interdigitates in the upper part with shallow marine sandstones of the Frederikshavn Formation towards the North and Northeast (Michelsen et al 2003). Towards the SW near the Ringkøbing–Fyn High the formation is conformably overlain by marine mudstones of the Vedsted Formation. In Gassum-1, the Børglum Formation is 20 m thick and is dominated by dark grey, sandy mudstones, with bands of light grey and greenish-grey sandstones in the basal part. The core 31 from 1193–1189 m is represented by hard, greenish grey claystones with shining, conchoidal fractures. Irregular patches of deep red and purple colours may indicate a subaerial induced weathering horizon (Fig. 7.2.3D, Norwood et al. 1951, Larsen 1966). In Gassum-1, the upper boundary of the Børglum Formation is potentially conformable overlain by sandstones of the Frederikshavn Formation of Kimmeridgian–Valanginian age (Dybkjær 1991, Appendix B). The Thorning area probably represent a more distal setting than the Gassum area and the upper boundary relation thus remains highly speculative. No data exists on seal performance and integrity of the Børglum Formation onshore Denmark (Mathiesen et al 2022).

Seals of the Frederikshavn Formation: The Vedsted Formation, Rødby Formation and lower part of the Chalk Group

Sealing units to reservoir sandstones of the Frederikshavn Formation (uppermost Jurassic–Lower Cretaceous) in the Thorning area comprise overlying mudstones of the Vedsted Formation and in some areas; mudstones, marls and carbonates of the Rødby Formation and tight carbonates in lower part of the Chalk Group (Fig. 7.2.1, Mathiesen et al. 2022). The marine mudstones of the Vedsted Formation are considered as the main sealing unit with a thickness of 40–200 m recorded in wells in the area. The formation is general thickest towards the north and thinnest towards the south. The thinnest Vedsted Formation is encountered in the two wells Nøvling-1 and Løve-1 southwest of the Thorning structure. The overlying Rødby Formation may also be present with thickness of up to 24 m (Fig. 7.1.1, Table 7.2.2). The Rødby Formation is not present in the eastern wells surrounding the Thorning structure. The seismic mapping indicates that the composite thickness of the Vedsted Formation and Rødby Formation (Top Fjerritslev Formation to Base Chalk) in the Thorning structure is uneven c. 40–80 m thick, (Fig. 6.2.3B). The overlying Chalk Group is 900–1100 m thick in the area but only the lower part of the group is considered as part of the potential sealing (i.e. deeper than 800 m below terrain). The Chalk Group is overlain by Cenozoic sediments that are up to several hundred meters thick. The seal performance of the seals to the Frederikshavn Formation reservoir onshore Denmark is essentially unknown (Mathiesen et al. 2022).

Stratigraphic framework

The Vedsted Formation in the Danish Basin spans the Valanginian to Albian. The lower boundary coincides with the transition from marine silty claystones of the Børglum Formation to less silty claystones of the Vedsted Formation in the central part of the Danish Basin (e.g. in Hyllebjerg-1, Michelsen et al. 2003, Larsen 1966). In the northern and more proximal parts of the basin, the Vedsted Formation conformably overlies the sandy shallow marine deposits of the Frederikshavn Formation. The Rødby Formation, which overlies or in some places are lateral transitional to the upper part of the Vedsted Formation, consists of marine red marlstones and marly chalks. Its base is suggested to be late Aptian or early Albian in age in the Danish Basin based on foraminifers and ammonites (Sorgenfrei and Buch 1964) and its upper boundary with the Late Cretaceous Chalk Group is late Albian to early Cenomanian in age (Lauridsen et al. 2022; Jensen et al. 1986). Mudstones and carbonate beds forming the upper part of the Vedsted Formation, and the overlying Rødby Formation were deposited in mixed siliciclastic-calcareous depositional systems. Lowstands were represented by deposition of marly chalk and marl, and highstands were in general represented by deposition of more pure chalk (Ineson 1993; Ineson et al. 1997, 2022). Onset of pelagic carbonate production started in the late Early Cretaceous (Late Albian) and dominated the depositional environment in the Danish Basin from the Early Cenomanian. The Lavø-1 well reveals that the siliciclastic sedimentation continued into the Early Cenomanian. The lower part of the Upper Cretaceous Chalk Group is characterised by white, hard chalk intercalated with marly beds. Several unconformities are potentially present in this succession linked with a tectonic active period causing erosional events in response to large regressions in the Late Cenomanian to Early Turonian (Scotese et al. 2024).

The Lower Cretaceous Vedsted Formation varies in thickness from a maximum of 700 meters in the Fjerritslev Trough in the northern central part of the Danish Basin to around 50

meters or less towards the south at basin marginal positions along the Ringkøbing–Fyn High, e.g. 49.3 m in Nøvling-1 and 40 m in Løve-1 (Table 7.2.2). A recent core study on parts of the Vedsted Formation in the Vinding-1 well, drilled c. 40 km west of the Thorning structure, presents the vertical lithological variation in the formation and a revised biostratigraphic breakdown of the Lower Cretaceous. The study indicates the presence of several unconformities and condensed intervals in the sedimentary record (Lauridsen et al. 2022).

The boundary above the Vedsted – Rødby formations to the Upper Cretaceous Chalk Group is considered to be transitional in the deeper part of the Danish Basin and associated with an unconformity in more proximal parts. The lower part of the Chalk Group is characterised by dense chalk and abundant marl layers in the lower 200–300 meters.

The Vedsted Formation

The Vedsted Formation varies from 40–200 m in thickness in the wells surrounding the Thorning structure (Table 7.2.3) (Fig. 7.1.1). The Vedsted Formation is represented by cores 25–28 in Vinding-1, cores 17 and 18 in Gassum-1 and in sidewall cores from the Mejrup-1, Kvols-1, Hobro-1, and Voldum-1 wells (Table 7.2.2).

The seismic mapping indicates that the composite thickness of the Vedsted Formation and Rødby Formation (Top Fjerritslev Formation to Base Chalk) in the Thorning structure is uneven c. 40–80 m thick, (Fig. 6.2.3B). The unit is thinnest at the top of the structure at top Frederikshavn Formation level. A thickness increase to >150 m is recorded in the small graben SW of the Thorning structure (Fig. 6.1.4).

The lower part of the Vedsted Formation is present in cores 17 and 18 from the Gassum-1 well (Fig. 7.2.5). Core 18 comprises grey to dark grey, medium hard to hard, sandy, and calcareous mudstones with fossil remains of bivalves, gastropods, belemnites and fish scales. Core 17 represents the upper part of the formation and comprises homogenous, calcareous, dark, pyrite rich, hard mudstones. Fossil remains include ammonites, gastropods, bivalve and fish debris. This upper part was previously dated as Aptian but is revised to the middle Barremian (Zone BC15) based on nannofossil biostratigraphy (Keiding et al. 2024). The carbonate content of the Vedsted Formation generally increases upwards.

In Mejrup-1, the Vedsted Formation is 194.4 m thick and dominated by mudstones. Abundant thin beds of sandstones and siltstones occur in certain intervals in the lower, middle and upper part of the formation. In Kvols-1 the formation is 120 m thick and represented by mudstones.

New data from the Vinding-1 cores are presented in Lauridsen et al. (2022); but no petrophysical logs exist from this well. The Vedsted Formation is here estimated to be 75 m thick and comprises Valanginian–lower Hauterivian siltstones and sandy mudstones, upper Hauterivian glauconitic marlstones, lower Barremian marly chalk, and Aptian marly chalk, slightly marly chalk and marl representing overall marine pelagic deposition of mixed siliciclastic and carbonates. A major unconformity is recorded between the Lower Barremian marly chalk and lower Aptian marlstone (Lauridsen et al. 2022).



Figure 7.2.5 Core photos of the Vested Fm, Gassum-1 well. A. Lower Hauterivian, grey–dark grey calcareous mudstones Core 18, 3490–3501' (c. 1064–1067 m). B. Middle Barremian highly calcareous grey mudstones. Core 17, 3305–3325' (c. 1007–1013 m). Note the general poor core condition, core diameter 8.5 cm.

Table 7.2.2 Available sample material from the Lower and Upper Cretaceous in the Thorning area; cores, sidewall cores (SWC) and ditch cuttings samples (grey shade).

	Upper Cretaceous (Turonian to Maastrichtian)	Upper Cretaceous (Turonian to Maastrichtian)	Rødby Fm	Vedsted Fm
Løve-1				
Nøvling-1				
Vinding-1	Cores 10 (?) to 23	Core 24 (?)	Core 24 (?)	Cores 25–28
Mejrup-1				SWC
Kvols-1				SWC
Hobro-1		SWC		SWC
Gassum-1	Cores 1 to 15	Core 16		Cores 17, 18
Voldum-1				SWC
Rønde-1				
Horsens-1	Core 1 (Coniacian)			



 No cores, but ditch samples
 SWC Sidewall cores

Table 7.2.3 Lower Cretaceous units of the Vedsted Formation and Rødby Formation and Upper Cretaceous Chalk Group - depths and thicknesses in the nearest wells to the Thorning structure. Location of wells relative to the Thorning structure is seen in Fig. 3.1.

	Løve-1		Nøvling-1		Vinding-1		Mejrup-1		Kvols-1		Hobro-1		Gassum-1		Voldum-1		Rønde-1		Horsens-1	
	Depth (m)	Thickn. (m)	Depth (m)	Thickn. (m)	Depth (m)	Thickn. (m)	Depth (m)	Thickn. (m)	Depth (m)	Thickn. (m)	Depth (m)	Thickn. (m)	Depth (m)	Thickn. (m)	Depth (m)	Thickn. (m)	Depth (m)	Thickn. (m)	Depth (m)	Thickn. (m)
Top Chalk Group	340		515.4		552		543		253		73		28.3		27		128		224	
Top Danian	340	752	515.4	812.6	552	720.5	543	886.5	253	1488	73	1542.4		973.6	1220		128	1855	224	944
Top Cretaceous	425		622		537		768		537		159		28.3		27		317		472	
Top Rødby Fm	1092	4	1328	17.7	1272.5	24.4	1429.5	18.3	1741	14	1615.4	4.4	1001.9	0	1247	0	1983	0	1168	5
Top Vedsted Fm	1096	40	1345.7	49.3	1296.9	75.1	1447.8	200.3	1755	120	1619.8	153.2	1001.9	76.5	1247	66	1983	73	1173	52

The Rødby Formation

The Rødby Formation is in general poorly known in the wells surrounding the Thorning area and a revision of the lithostratigraphy and biostratigraphy is highly needed (Lauridsen et al. 2022, Keiding et al. 2024). Petrophysical logs and vintage biostratigraphy of cutting samples in completion reports suggest the presence of the Rødby Formation in the wells north, west and south of the Thorning structure (Figure 7.1.1, Table 7.2.3). The Rødby Formation is thus suggested to be 4 m thick in Løve-1 and 24.4 m thick in Vinding-1 and is therefore considered to be below seismic resolution. In the Hobro-1 and Kvols-1 wells the formation is described as dark grey, green, red, black calcareous mudstones. In Mejrup-1 the formation is dominated by marly chalks and marlstones. In Vinding-1, core 24 comprises marly chalk. The revision of Vinding-1 showed no presence of the Rødby Formation in the interval previously suggested and underlined that the colours of the facies are not useful in identifying the Rødby Formation lithology (Lauridsen et al. 2022). The Rødby Formation has been characterized as marine red marlstones and marly chalks (Sorgenfrei & Buch 1964).

The Rødby Formation is not identified with certainty in the Gassum-1 well, since vintage biostratigraphy (based on foraminifera) from the Lower–Upper Cretaceous was inconclusive. The geological completion report from the Gassum-1 well suggests that the upper boundary of Lower Cretaceous is represented by an unconformity while biostratigraphic notes within that report suggest a transitional boundary. In Kvols-1 and Voldum-1 an unconformity at the upper boundary of Lower Cretaceous is also suggested based on both geological observations and biostratigraphy. In other parts of the Danish Basin, the upper boundary of the Rødby Formation is transitional, based on petrophysical log data indicating an upward decrease in the gamma ray signal reflecting general increasing carbonate content.

The Chalk Group

The Chalk Group in the Thorning area spans the Cenomanian–Danian (Table 7.2.3). The base of the Chalk Group is situated at roughly 1100 m below mean sea level at the apex of the Thorning structure based on the seismic depth conversion (Chapter 6). The group has a thickness of 900–1100 m, thinnest at the apex, and is overlain by Cenozoic deposits. Basic subdivisions of the Chalk Group, where chronostratigraphic subdivision is based on biostratigraphy or final well reports, are shown in stratigraphic summary charts for selected wells (Appendix B). The lower part of the Chalk Group might be considered relevant as a potential seal when situated deeper than 800 m below terrain. A few cored sections of the Chalk Group exist in the deep relevant part of the succession, e.g. in Gassum-1, Vinding-1 and Horsens-1, and side wall cores are available from Kvols-1, that can be studied in detail. New biostratigraphic datings from Gassum-1 cores show that the stratigraphic framework of the Chalk Group in the region needs major revision that is relevant for the addressing the lateral distribution of potential sealing units in the lower part of the Chalk Group (Keiding et al. 2024). Schematic logs of cores 11–16 from the Gassum-1 well are presented in Figure 7.2.6, where the revised ages of the lower part of the Chalk Group and main facies are also shown.

The lower part of the Chalk Group is Cenomanian in age and locally consists of hard to microcrystalline chalk. This significant hard, lithified chalk likely causes locally increased seismic velocities in the lowermost part of the Chalk Group (Japsen 2000, 2018, Nielsen et al. 2011). On the density logs from the Hobro-1, Kvols-1 wells, a downwards slightly increase in density towards the base of the Chalk that indicates this hard, lithified chalk (Appendix A).

In the basal part of the Cenomanian of the Hobro-1 well, a glauconitic calcareous silt- to mudstone bed is present. In Kvols-1 white to light grey soft to firm chalk is present in a SWC drilled at the base of the Upper Cretaceous.

Core 16 in Gassum-1 is taken about 10 m above the base of the Chalk Group and it is dated as Late Cenomanian nannofossil subzones UC2c to UC3b. The core was previously dated as Santonian in the completion report (DAPCO 1951). The core consists of greyish, bioturbated marly chalk (facies 1) intercalated in a cyclic manner by thin, dark, marly laminated beds (facies 2) with marly beds appearing for each 30 to 50 cm (Fig. 7.2.6). Bioturbation related to the marl beds is not recorded. Some of the marly chalk beds have a coarse-grained fraction of fossil fragments, predominantly bivalves. Flaser bedding and solution seams reflecting chemical dissolution during burial diagenesis are common. Flint is not present. Core 15 is taken 55 m above the base of the Chalk Group, and it is dated as Late Turonian nannofossil subzone UC8ab. The core comprises clean white chalk with a few thin, marly, slightly laminated beds (facies 3). Core 14 is taken 100 m above the base of the Chalk Group, and it is dated as mid Campanian nannofossil subzones UC14d–15d. The core comprises clean

white chalk with a few thin, marly, slightly laminated beds (facies 3). Cores 13–12 are situated 180 m and 200 m, above the base Chalk Group, respectively, and are dated as mid Campanian subzone UC15d. The cores consist of marly chalk (facies 4), which is also reflected in slightly higher GR values. Core 11 is taken 250 m above the base of the Chalk Group at ca 750 meters. It is dated as mid Campanian nannofossil subzones UC15c-d and comprises cyclic marly chalk alternating with thin marl beds (facies 1). The remaining cores 1–10 from the Chalk Group are from shallower depths than 750 m.

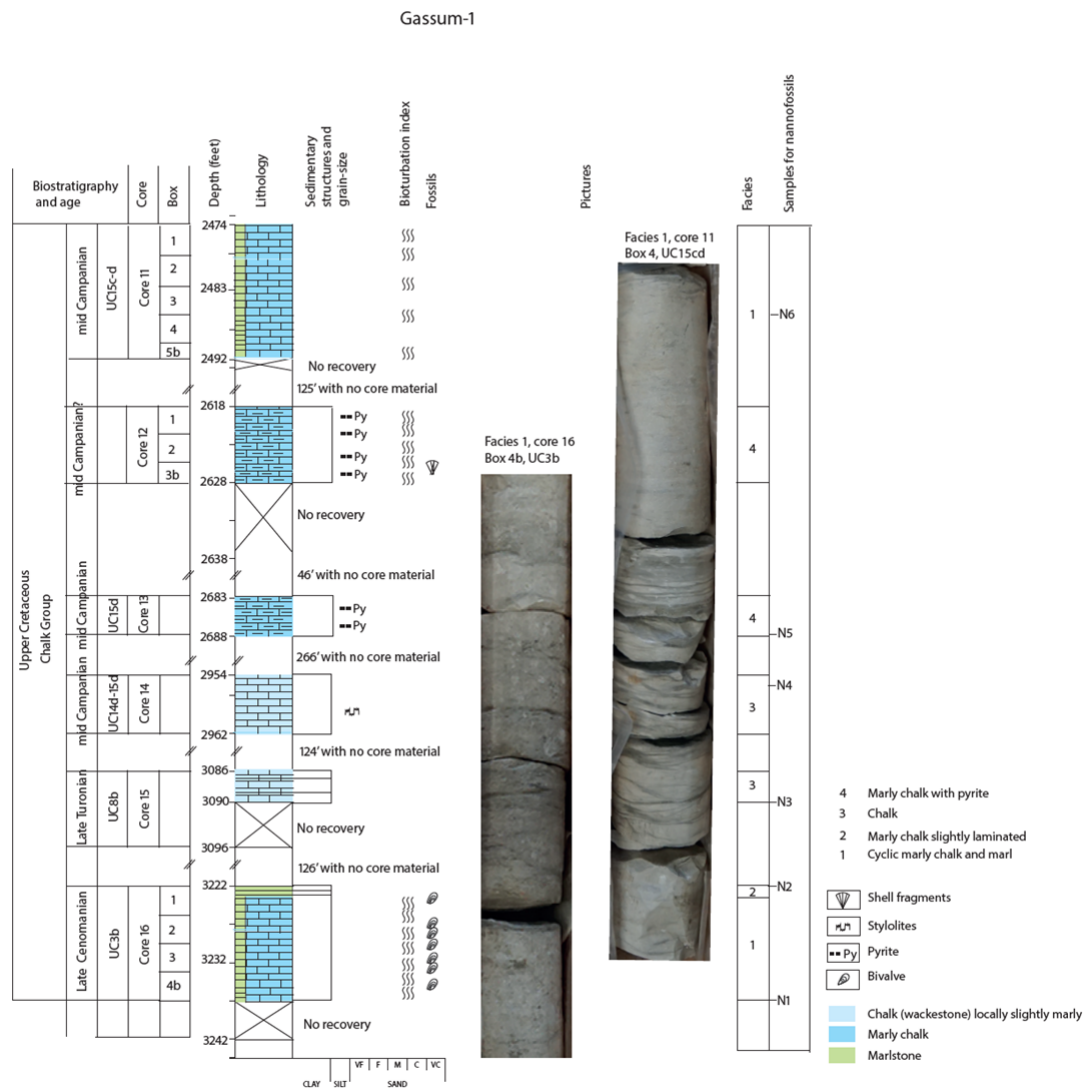


Figure 7.2.6. Upper Cretaceous cores in the lower part of the Chalk Group in the Gassum-1 well, with biostratigraphic ages and main facies. Note the highly heterogeneous facies composition of the chalk group relevant for addressing the sealing capacity.

Porosity and permeability data of the lower part of the Chalk Group

Porous chalk reservoir is tested as CO₂ reservoir in its own rights (Yu et al. 2023), in contrast the possibility for low porous chalk to act as seal for CO₂ migration of super critical scCO₂ from below has been less studied.

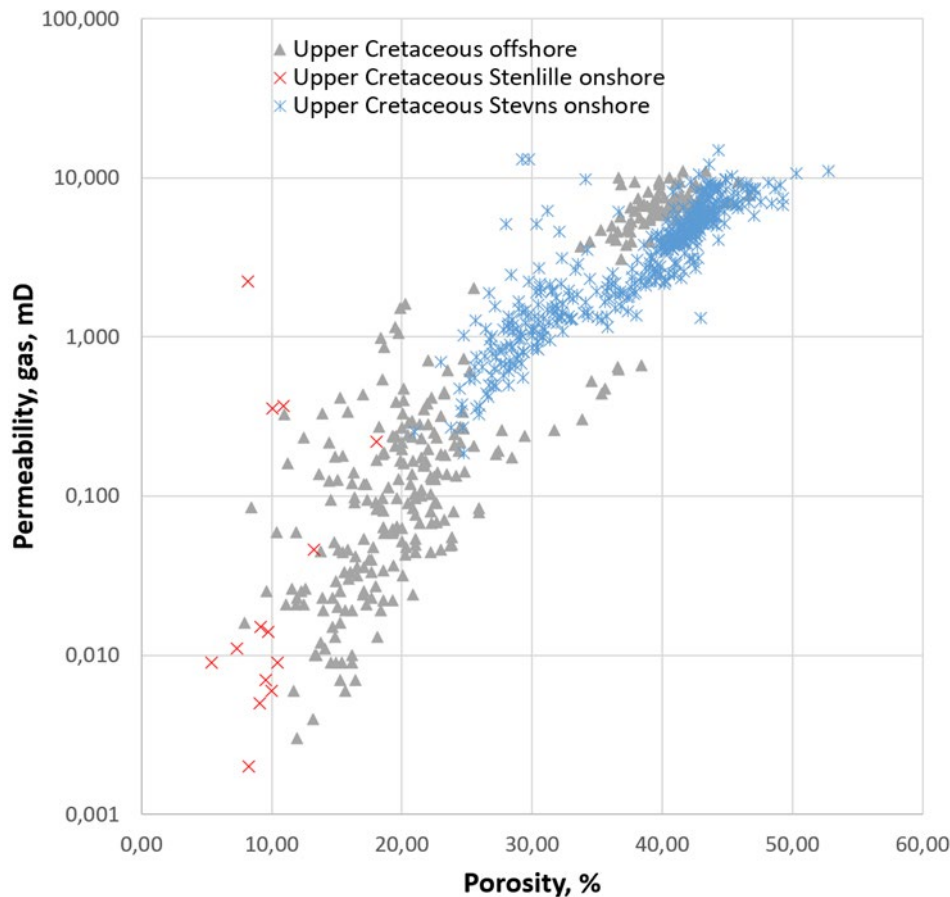


Figure 7.2.7. Porosity and permeability plot of Upper Cretaceous chalks from onshore wells Stenlille-5 core, Stevns-1 core and from offshore wells in the Danish Central Graben (GEUS inhouse data).

There are no porosity and permeability data from the Chalk Group in the Gassum-1 well. However, porosity and permeability data from the Upper Cretaceous of the Stevns-1 and Stenlille-5 wells onshore Denmark and from Danish offshore wells are plotted in Figure 7.2.7. It is evident that the Coniacian chalks in the Stenlille-5 well have the lowest porosity and permeability values (Gregersen et al. 2022). The relatively high porosity and permeability values from the Upper Campanian to Maastrichtian from the Stevns-1 well can be explained by the relatively shallow burial history of this location, with maximal burial of 450 to 600 m (Nielsen et al. 2011). Burial depths for the offshore chalks of the Danish Central Graben often exceed 3000 m, but these chalk reservoirs have preserved a relatively high porosity due to retarded compaction caused by regional overpressure of the formations and the presence of oil and gas (e.g. Japsen 1998). The Stenlille data show a normal burial compaction with no overpressure.

The non-reservoir chalks (low porosity and permeability) of the Central Graben have been investigated with respect to understanding their capability as a pressure seal (Mallon & Swarbrick 2002, 2008). Non-reservoir chalks have permeabilities which are similar to those of siliciclastic mudstones. These studies show that both in clean and argillaceous chalks, diagenetic alterations resulted in low permeability. Furthermore, the diversity of rock types that exhibit low permeabilities suggests that seals are pervasive throughout the Chalk Group.

Non-reservoir chalks such as those presumably present in the Thorning area can therefore potentially act as significant barriers to fluid flow and as significant pressure seals to formations beneath the Chalk Group.

Summary remarks on the seal of the Frederikshavn Formation

The seals of the Frederikshavn Formation in the Thorning area comprise the overlying Lower Cretaceous Vedsted and Rødby Formations and the lower part of the Upper Cretaceous Chalk Group. As these formations have not been the main target for coring in the nearest wells to the Thorning structure, this report summarizes the present knowledge of these units based on vintage data.

The Vedsted Formation is considered as the main sealing unit of Frederikshavn Formation in the Thorning area with thickness variations of 52–194 m in the surrounding wells. The seismic data suggest that the formation is uneven, 40–80 m thick across the Thorning structure (Fig. 6.2.3B). The formation consists of relatively homogenous mudstones with slight variations in silt content and with upwards increasing carbonate content, and potential carbonate units in the upper part as indicated on the well logs. The Vedsted Formation possibly contains several unconformities related to erosion and non-deposition, but more biostratigraphic dating is needed to confirm this. E.g. in the Gassum-1 well, lower Hauterivian to middle Barremian deposits are present, but the presence of upper Barremian and Lower to middle Aptian strata is not confirmed. In Vinding-1, Lower Hauterivian to Aptian and Upper Albian deposits is confirmed.

The overlying Rødby Formation is 0–24 m thick in the area with most prominent thickness towards the west and north and probably wedging out eastwards. The formation is generally described as dark grey, green, red, black calcareous shale- and claystone. It is suggested that the upper boundary of the Lower Cretaceous represents an unconformity in at least the Gassum-1, Kvols-1 and Voldum-1 wells (Appendix B). There exists no analytical seal characterisation data (Fig. 7.2.4) on the Vedsted Formation and Rødby Formation and their seal performance is therefore essentially unknown (Mathiesen et al. 2022).

The Chalk Group in the Gassum area spans the Cenomanian–Danian, the uppermost part of the Maastrichtian–Danian part is however missing in Gassum-1. The Cenomanian part cored in the Gassum-1 well is represented by greyish, completely bioturbated, marly chalk intercalated in a cyclic manner by thin, dark, marly laminated beds. The marly chalk is very hard and is indicated by increasing sonic velocities in other wells closest to the Gassum structure. The cored Turonian part in Gassum-1 comprises clean, soft, white chalk with few thin marly beds and stylolites. The cored mid Campanian part comprises an increasing marly upward succession going from clean chalk via marly chalk to and cyclic marly chalk with thin marl beds.

The porosity and permeability data for the Chalk Group in Denmark is listed in this report (Fig. 7.2.7). Porosity and permeability values of the lower part of the Chalk Group are generally very low when compared with other onshore data from the Danish Basin (e.g. Stevns-1). The porosity and permeability data from the lower part of the Chalk Group in the Stenlille-5 well reveal an ordinary burial compaction with no overpressure. There are however no data from Gassum-1 cores or from the nearest wells to the Thorning structure.

The properties of the lower part of the Chalk Group and its potential capacity as a secondary seal, can be compared with studies from the Danish Central Graben (Mallon & Swarbrick 2002, 2008, Amour et al 2022). It is possible that the lower part of the Chalk Group will act

as a seal to upwards fluid flow and high-pressure propagation from the underlying formations in the Thorning area. However, this can be further investigated when core material from Vinding-1 and Gassum-1 and material from new wells are analysed. Sidewall core material from Kvals-1 can also be very useful and relevant to study in more detail regarding the sealing capacity of the lower part of the Chalk Group.

Seals for the Skagerrak Formation/Bunter Sandstone Formation: The Ørslev Formation and Falster Formation

As discussed earlier, the presence of reservoir sandstones of the Bunter Sandstone or Skagerrak formations in the Thorning structure is uncertain. However, for reasons of completeness their sealing units are briefly described here. These are the lower to middle Triassic Ørslev Formation and Falster Formation that are present in the Løve-1, Nøvling-1, Gassum-1 and Rønde-1 wells (Fig. 7.1.18). It should be noted that the lithostratigraphic subdivision of the above-mentioned units needs a revision.

The Ørslev Formation is 314.9 m thick in Gassum-1 (measured depths of 2432.3–2747.2 m) and is represented by cores 100–111. The formation comprises brown to dark brown argillaceous sandstones and shales with minor anhydrite and gypsum units representing mainly lacustrine–distal fluvial plain depositional environments. The lithology derived from the petrophysical logs show a lower unit, 65 m thick, of alternating mudstone and siltstones with thin sandstones, a middle mudstone-dominated unit, 150 m thick, and an upper unit, 100 m thick, of mudstones and minor amounts of thin siltstone and sandstone beds (Fig. 7.1.18). Only a few other wells reach the Ørslev Formation and Skagerrak Formation in the region, e.g. Rønde-1 to the east (70 km) where the Ørslev Formation is 235 m thick and has significantly high amounts of sand in the lower part. The Ørslev Formation is only 83 m thick in Nøvling-1, situated 30 km towards the west of the Thorning structure and here the formation consists of mudstones with minor amounts of dolomites in the middle part.

The seismic mapping of the Thorning area shows the Ørslev Formation c. 100–200 m thick (Fig. 6.2.3.L).

The overlying Falster Formation and lower part of the Tønder Formation form a composite mudstone dominated succession, nearly 300 m thick, in Gassum-1 and may serve as an additional seal unit. Selected cored intervals are represented by cores 99–93 in Gassum-1 (Appendix B). In Nøvling-1, the Falster Formation and Tønder Formation are represented by a succession of mudstones and thin siltstones, 383 m thick. The Falster Formation is 122 m thick in Rønde-1 and comprises mudstones and dolostones. The overlying Tønder Formation is 241 m thick and forms an overall coarsening upward succession from mudstones to sandstones.

The seismic mapping of the Thorning area shows a relative even thick Falster Formation N–S above the Thorning structure (c. 250 m), and a prominent thickness increase towards the Brande Trough to >450 m to the west of the Thorning Structure (Fig. 6.2.3.K).

A number of vintage reservoir property measurements exist from the Ørslev Formation in the Gassum-1 well (Michelsen et al. 1981). These data show a wide range of porosity and permeability values, but they are not related to detailed geological descriptions. Associated analyses of grain sizes by sieving are achieved for 7 samples in the lower part of the Ørslev Formation. These show a grain size range between 0.02 mm and 0.15 mm. Analysis of other

20 samples did not provide any results on average grain size due to fine-grained nature of the mudstones. No data are available regarding bulk mineralogy, clay mineralogy and other specialized analyses relevant for addressing the seal performance of the Ørslev Formation and Falster Formation.

Seals of the Tønder Formation: The Oddesund Formation

The Tønder Formation is in general dominated by mudstones but may in places contain potential reservoir sandstones, e.g. in Løve-1 (Fig. 7.1.18). Where containing reservoir sandstones, the overlying Oddesund Formation may form the seal. In Løve-1, the Oddesund Formation is only 59 m thick and represented by mudstones. It thickens dramatically towards the north and east in the central part of the Danish Basin where it may be more than 1000 m thick and comprise a fivefold subdivision with three mudstone units intercalated with two evaporite units of mainly halite. In Gassum-1, the formation is 375 m thick, the evaporite units are 30 m and 22 m thick, respectively. In Rønde-1, it is 633 m thick and here the evaporite units are 60 m and 190 m thick, respectively. In the Thorning structure the combined Oddesund Formation and overlying Vinding Formation has a thickness of 250–400 m (Fig. 6.2.3I). The succession is thin along the top of the Thorning structure in a N-S orientation and shows a moderate thickness increase towards the north. The succession thickens to > 650 m westwards in the Brande Trough and also in an eastward direction. The seismic signature e.g. in profile P7 has mainly low amplitude parallel reflectivity in the southern part of and more variable and diffuse reflectivity in the northern part. The site of the Thorning structure represents a southwards more marginal position compared to the site of the Gassum structure during deposition of the Oddesund Formation and therefore probably contain less amounts of evaporites. Synsedimentary faulting is recorded in the SV part the structure with formation of small SW-dipping halfgrabens during deposition of the Oddesund Formation (Figs 6.2.3I, 6.2.5.G).

8. Discussion of storage and potential risks

8.1 Volumetrics and Storage Capacity

Primary input for the estimation of potential CO₂ storage capacity has been the seismic reinterpretation of primary Gassum Formation reservoir within the current older 2D-Survey lines combined with extended interpretation across the newly acquired 2D seismic data, GEUS2023-THORNING (see also Section 4.1). Sandstone reservoirs in the Frederikshavn Formation may also possess a considerable reservoir potential level. But the storage potential of this reservoir units has not been evaluated in this study (see also Section 7.1). The same applies for the deeper Skagerrak Formation and Tønder Formation. Combined, these units may provide a significant upside to the storage capacity of the Thorning structure. The detailed well analysis and a crucial element of revising the depth conversion impacts the understanding of the reservoirs and their geometry in this well-defined relief structure (see Fig. 8.1.1).

The method used for the storage capacity estimation is described in Chapter 5.1. The reservoir characteristics within the Thorning structure are interpreted based on the data from the Gassum-1 and Nøvling-1 wells which represent a more proximal and distal depositional setting, respectively, compared to the site of the Thorning structure. Scenario 3 is used as input parameters for the storage capacity estimation assuming a seismic thickness of c. 95 m around the structural top point with an excellent lower 54 m and presence of sandstone layers in the upper Gassum Formation (Section 7.1). The petrophysical and geological understanding of thicknesses and average net to gross reservoir ratio across the entire GRV in the nearest wells are transformed into structure-specific geological-based average values for the storage capacity estimation simplifying the spatial distribution of sandstone facies within the Gross Rock Volume (GRV).

The GRV is calculated as a total volume between the top and base reservoir depth surfaces and is confined by the upper and lower boundaries of the gross reservoir, where outline area of the structure is defined by the top point depth and deepest closing contour constrained by the spill point depth (see Figs 8.1.1. and 8.1.3.). Average reservoir thickness (or the net sand thickness) is not just equal to the isochore thickness (or the relief) between top and base depth surfaces, why the gross thickness is corrected with the N/G ratio to get a more realistic reservoir sand thickness for the GRV. Preferably, the estimation could also incorporate potential thin sandstone wedges between the top point depth and the closing contour depth on the flanks of the structure.

For the storage capacity estimation of the Thorning structure, the Gassum Formation have been evaluated as a structural three-way dip closure with faults in the southern part of the structure confining the GRV (Fig. 8.1.1). The estimated values can be compared to CO₂ capacities of other structures across Denmark (e.g. Gregersen et. al. 2023 and Hjelm et al. 2022).

The physical properties of the Gassum reservoir unit are described in Section 7.1. At a later stage the reservoir unit and possible influence of the faults must be assessed in more detail

by dynamic 3D reservoir simulation models to ensure optimal development, injection and filling of the reservoir unit of the structure, and to ensure less uncertainty on storage capacity.

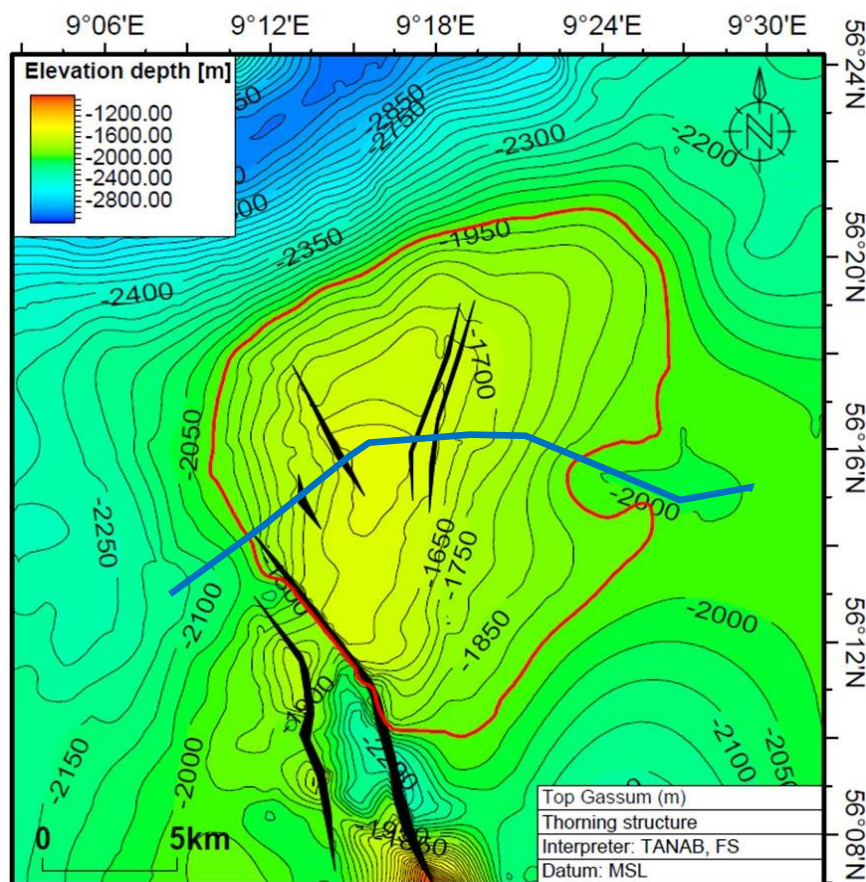


Figure 8.1.1. The top Gassum depth structure map in meters (m) (generated in Petrel®, tied to nearest wells located outside the map area and gridded by 100x100 meter) provides the primary input to the capacity assessment. Notice the NNW–SSE orientated fault system located south of Thorning structure constraining the extent of the GRV. The structural top point is located at c. 1520 m b.msl. and the deepest closing contour at 1950 m b.msl. (marked in red) with an area within the spill point of c. 235 km². See also Section 6.1.1. for fault analyses and map location. A schematic W–E profile across the structure is shown in Figure 8.1.3 (blue line).

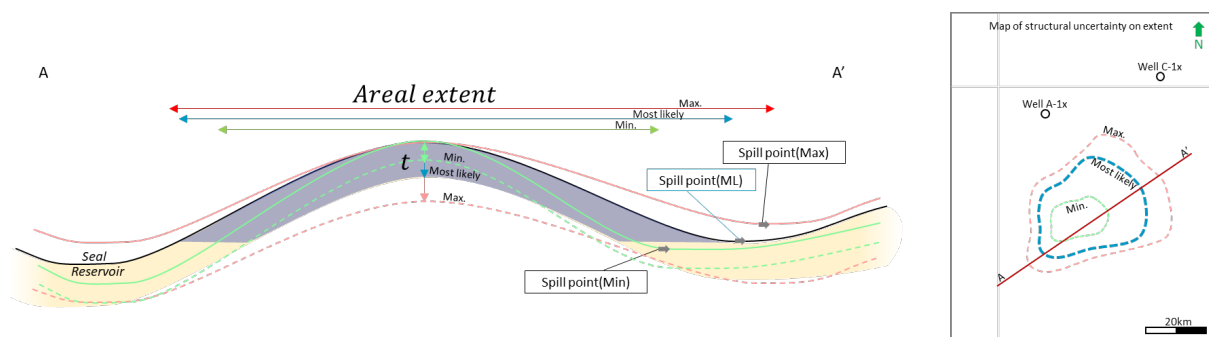


Figure 8.1.2. Conceptual profile (A-A') across a potential structure. The uncertainty in mapping the structure results in the hypothetically minimum (Min.) and maximum (Max.) scenarios looking very different from the most likely mapped scenario. Variance in area and in gross

thickness (t) will affect the Gross Rock Volume (GRV) of the structure. The uncertainty is addressed by applying uncertainty on the resulting GRV and other parameters and by conducting simple Monte Carlo simulation to calculate P90, P50 and P10.

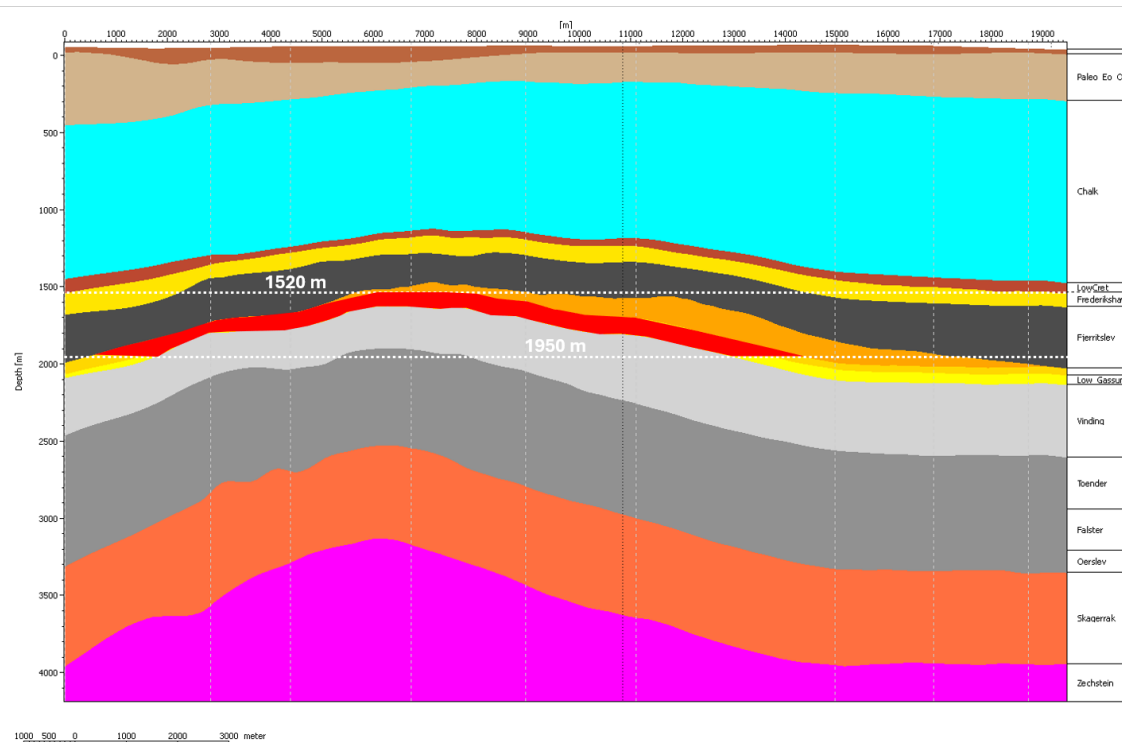


Figure 8.1.3. W–E schematic cross section of the Thorning structure showing the location of the top and spill depth surfaces for the Gassum Fm at the c. 1520 m and 1950 m contour depth used for a GRV estimation (marked with red polygon above 1950 m). For the Gassum Fm, the GRV is calculated in Petrel as the volume between the top Gassum and base Gassum depth surfaces. Near the top of the Thorning structure the Gassum Fm has a depth converted thickness of c. 95 based on the new interpretation and depth conversion (see Section 7.1 and Fig. 6.2.2F). Notice that the profile is located north of the fault zone located in the southern part of the Thorning structure (see Fig. 8.1.1 for location of the section and the fault zone). The influence of other faults on the estimated storage capacity is not considered in this study.

8.2 Volumetric input parameters

Evaluation and maturation of a CO₂ storage site includes several steps. The maturation phase, carried out by GEUS, includes static calculation of theoretical storage capacity - primarily based on Gross Rock Volume (GRV), net/sand thickness, average effective porosity and density of the CO₂ (see also Section 5.1 and Section 7.1). The primary input parameters are derived from Table 7.1.2, Scenario 3.

The current maturation phase does not provide dynamic capacity estimates of the potential CO₂ structures but focus on identifying and assessing extent and quality of reservoir aquifers. Furthermore, no attempts are made to address e.g. dynamic pressure build-up, fault leakage, fault reactivation, solubility of CO₂ in brine, the effect of high concentration of salt etc.

To do detailed CO₂ storage capacity evaluation, it is important to assess aquifer quality and connectivity, i.e. to identify potential distribution of thick, high permeable sandstone aquifers

with high connectivity with no major faults. This will require dynamic reservoir simulation, that may result in different storage capacity than static estimations and will normally be the next step for potential license holders.

Gross rock volume

The Gross Rock Volumes (GRV) of the Thorning structure was original based on the Area and Thickness vs. Depth methodology (described by e.g. James et al. 2013). The calculated GRV is in this study estimated from the seismic mapped and depth converted top and base reservoir surfaces, where the base surface is constrained by the spill point surface (Figs 8.1.2. and 8.1.3.).

The GRV is calculated in Petrel as the volume between the seismic top and base Gassum reservoir surfaces, giving a depth converted Grassum Formation thickness of c. 95 m (see Table 7.1.2, Scenario 3). The expected reservoir sand thickness is calculated by multiplying GRV with the net/gross ratio estimated from petrophysical analysis based on the nearest wells (see Section 7.1). Calculating reservoir sand thickness this way provides greater accuracy and flexibility compared to previous introduced correction factors for geometries with overestimated wedge volumes (e.g. Hjelm et al. 2022). This is because it allows for uncertainty ranges on GRV and reservoir sand thickness to be modeled independently. Furthermore, the method allows for a rapid GRV calculation, which can be used in a Monte Carlo simulation, to establish an unbiased estimated range of GRV.

To evaluate the uncertainty on the GRV across the Thorning structure, a minimum and maximum case was also estimated as illustrated in Figure 8.1.2. by assigned a min., mode, and max. uncertainty range, where mode is the data value that occurs most often in the dataset. This variation in GRV was inferred to cover uncertainty in interpretations, seismic well ties, mapping and depth conversion. To reflect this uncertainty, a distribution for the average GRV was constructed by defining the min. and max. of the distribution based on surrounding wells and supplied by c. $\pm 10\%$ (Table 8.2.1.). It is assumed that the GRV distribution follows a Pert distribution defined by the min., mode, and max. values. The Pert distribution is believed to give suitable representation for naturally occurring events following the subjective input estimates (Clark, 1962).

Table 8.2.1. Assessment of important parameters for the Gassum reservoir in Thorning structure, where only the resulting Gross Rock Volume (GRV) min, mode and max estimates are used for the capacity estimation in Table 8.2.3. The mode gross thickness (i.e. the seismic gross sand thickness) is taken from Section 7.1 and Fig. 6.2.2F.

Reservoir	Apex (m, TVDSS)	Spill point (m, TVDSS)	Area (km ²)	Gross Sand TCK (m)			GRV (km ²)		
				Min.	Mode	Max.	Min.	Mode	Max.
Gassum Fm	1520	1950	235	85.5	95	104.5	21.1	23.5	25,9

For the reservoir unit, the other input parameters are also given as min., mode, and max. values - Net/Gross, porosity, CO₂ reservoir density and the storage efficiency factor, where also assumed to follow a Pert distribution.

Net to Gross ratio

The Net to Gross (N/G) ratios estimated from the petrophysical analysis of especially the Gassum-1 and Nøvling-1 wells are evaluated and reasonable average N/G-ratios across the entire structure is defined as the mode of the distribution (see also Section 7.1). Some variance is expected due to lateral variation of the lithologies owing to differences in facies distribution, depositional environment, diagenesis and poor quality of the Gassum-1 and Nøvling-1 logs. To reflect this uncertainty, a distribution for the average N/G ratio was constructed by defining the min. and max. of the distribution as c. $\pm 20\%$ with minor adjustments. A Pert distribution has been applied.

Porosity

The porosity (ϕ) was estimated from petrophysical analysis of the Gassum-1, Nøvling-1 and surrounding wells as described in Section 7.1. The well-derived estimates are considered as reasonable average effective porosity across the entire structure (i.e. set as mode). Some lateral and depth variations are expected and the poor quality of the Gassum-1 logs also add uncertainty to the estimates. To reflect this, an average effective porosity distribution has been constructed defining the min. and max. of the distribution as c. $\pm 20\%$ with minor adjustments. A Pert distribution for this element has been applied.

CO₂ density

The average in-situ density of CO₂ was estimated using the 'Calculation of thermodynamic state variables of carbon dioxide' web-tool essentially based on Span and Wagner (1996) [http://www.peacesoftware.de/einigewerte/co2_e.html]. The average reservoir pressure was calculated on the assumption that the reservoir is under hydrostatic pressure and a single pressure point midway between apex and max spill point was selected representing the entire reservoir.

Temperature for this midway point was calculated assuming a surface temperature of 8°C and a geothermal gradient of 28 C°/km based on the Gassum-1 well, which is slightly higher than the typical onshore gradient of c. 27 C°/km estimated by Fuchs et al. (2020). Assumptions and calculated densities for the individual reservoir units are tabulated in Table 8.2.2. For a quick estimation of the uncertainty on CO₂ density, various P-T scenarios were tested and in general terms a -5% (min.) and +10% (max.) variation from the calculated mode was applied for building a Pert distribution. All calculations showed that CO₂ would be in super-critical state.

Table 8.2.2. CO₂ fluid parameter assumption and estimated values.

Reservoir	Apex depth (TVDSS, m)	Spill point depth (TVDSS, m)	Structural relief (m)	Pressure HydroS. (MPa)	GeoThermal grad. (°C/km)	Mid Res. Temp. (°C)	CO ₂ density (kg/m ³)
Gassum Fm	1520	1950	430	17.02	28	56.6	679.4

8.3 Storage efficiency

Storage efficiency is heavily influenced by local geological subsurface factors such as confinement, reservoir performance, compartmentalisation etc. together with well and injection configuration and operation (i.e. financial controlled factors) (e.g. *Wang et al. 2013*). A sufficient analogue storage efficiency database is not available to this study and accurate storage efficiency factor-ranges lacks at this early stage of maturation. This emphasises the need for further investigations of the subsurface and development of scenarios and dynamic reservoir simulation to better understand the potential storage efficiency ranges. In this evaluation, a range from 5% to 20% with a mode of 10% is used as a possible range. The use of a storage efficiency factor value of 0.1 assumes that the Gassum reservoir in the Thorning structure have good reservoir characteristics based on Scenario 3 in Table 7.1.2. The uncertainty caused by the identification of faults in the southern part of can have influence in the estimation of the storage capacity and requires further analysis (Fig. 8.1.1. and Section 6.1.1). A Pert distribution for this element has also been applied.

8.4 Summary of input factors

In Tables 8.4.1, input parameter distributions are listed (all selected to follow Pert distributions defined by min, mode and max). Input parameter distributions for the Gassum reservoir is displayed in Figure 8.4.1.

Table 8.4.1. *Input parameters for the Thorning structure – Gassum Fm*

Parameter	Assumption		
	Min	Mode	Max
GRV (km ³)	21.2	23.5	25.9
Net/Gross	0.22	0.28	0.34
Porosity	0.20	0.256	0.31
Storage eff.	0.05	0.1	0.2
<i>In situ</i> CO₂ density (kg/m³)	645.5	679.4	747.4

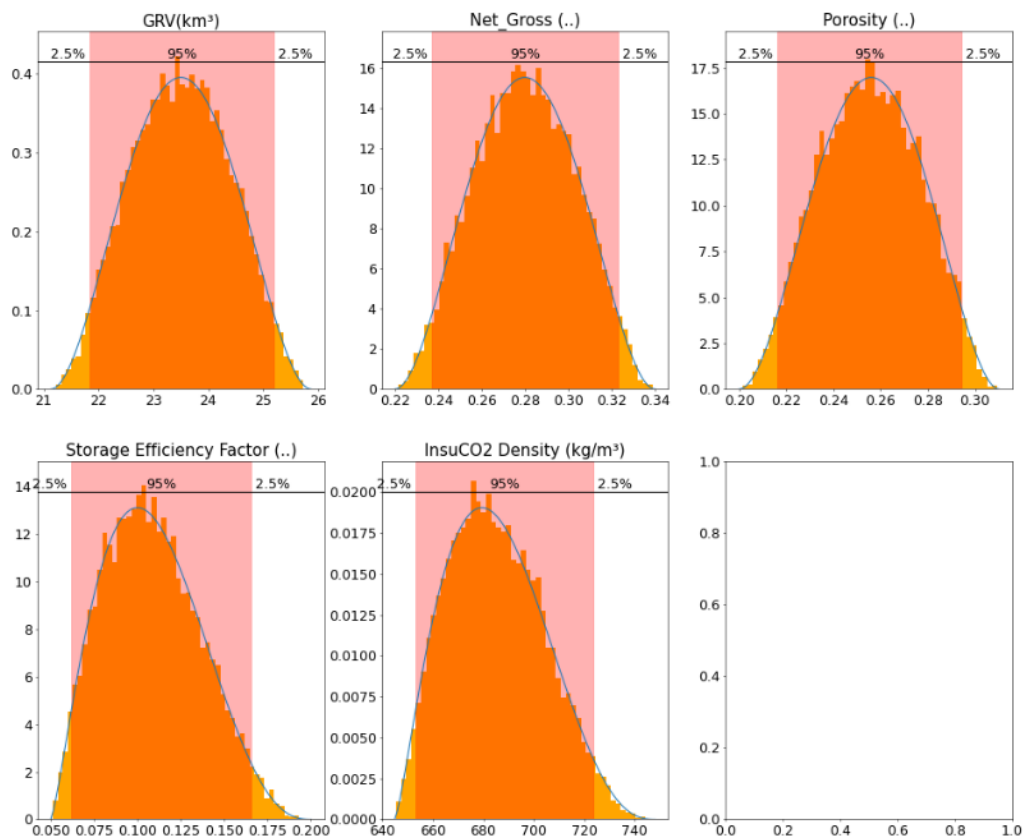


Figure 8.4.1. *Example of some of the distribution shapes (Pert distributions) for the 5 input parameters for the Gassum reservoir. The last input distribution plot is empty and not used.*

8.5 Storage capacity results

The modelled volumetrics was made on the assumption of the presence of an efficient reservoir/seal pair capable of retaining CO₂ in the reservoir. This basic assumption needs to be tested by new 3D seismic data and further geological investigation. In Tables 8.5.1, the results of the Monte Carlo simulations are tabulated. The tables indicate both the pore volume available within the trap (full potential above structural spill), the effective volume accessible for CO₂ storage (applying the Storage efficiency factor to pore volume) and mass of CO₂ in mega-tons (Mt) that can be stored. The tables present the 90%, 50% and 10% percentiles (P90, P50 and P10) corresponding to the chance for a given storage volume scenario to exceed the given storage capacity value. Mean values of the resultant outcome distribution are also tabulated and is considered the “best” single value representation for the entire distribution.

Without addressing the influence of the faults located south of the top point of the Thorning structure the increase in a mean unrisks static storage capacity of c. 125 Mt CO₂ is calculated for the Gassum Formation, Scenario 3 with a range between c. 81 Mt CO₂ (P90) and c. 174 Mt CO₂ (P10) and a P50 of c. 122 Mt CO₂ (Fig. 8.5.1). Due to the variability-ranges of the behind-lying factors, the modelled storage capacity has a significant range. As illustrated in Figure 8.5.2, the storage capacity uncertainty is linked with the uncertainty of the storage efficiency factor. In comparison, CO₂ density at reservoir conditions, is believed to be of minor concern.

Table 8.5.1. *Thorning structure – Gassum Fm storage capacity potential*

Results	P90	P50	P10	Mean
Buoyant trapping pore volume (km ³)	1.4254	1.6727	1.9531	1.6811
Buoyant eff. storage volume (km ³)	0.1186	0.1778	0.2533	0.1824
Buoyant storage capacity (Mt CO ₂)	81.3	121.5	173.6	124.9

Notice that the storage efficiency factor is here assumed to be 0.1 (compared to the previously used 0.4; (Hjelm et al. 2022)), thus reducing the overall CO₂ storage capacity compared to previously studies. This estimation of CO₂ storage capacity must be investigated further by e.g., reservoirs simulation modelling to ensure optimal development and filling of the Thorning structure, and to ensure less uncertainty.

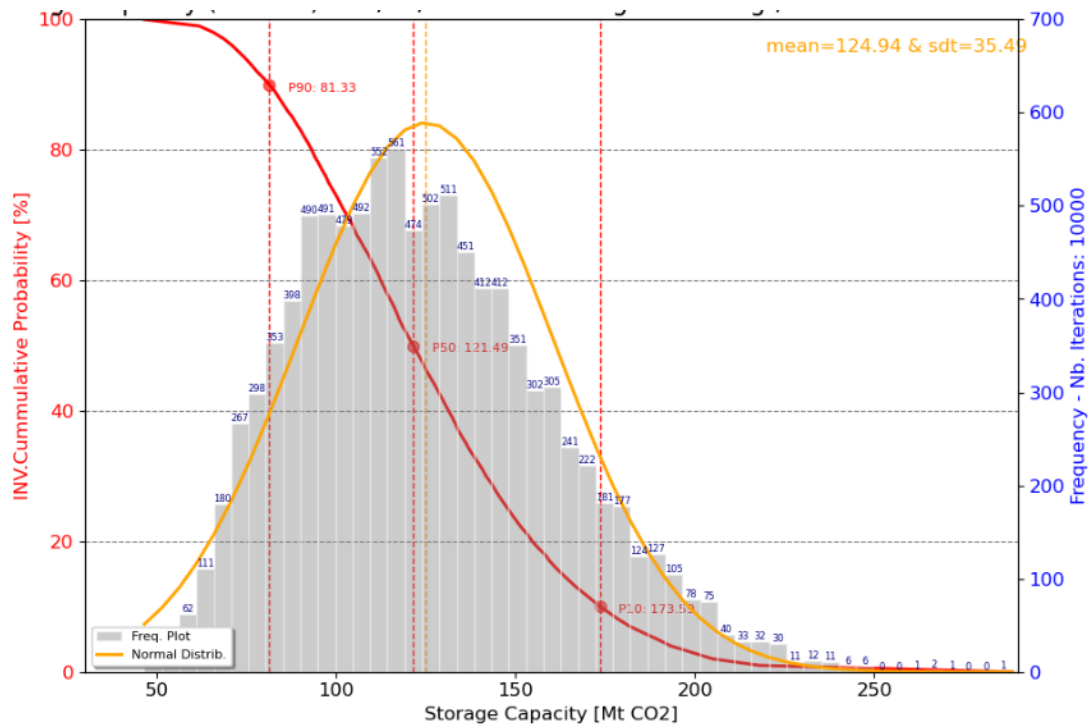


Figure 8.5.1. Modelled statistical distribution of the combined storage capacity potential for the Gassum reservoir in the Thorning structure.

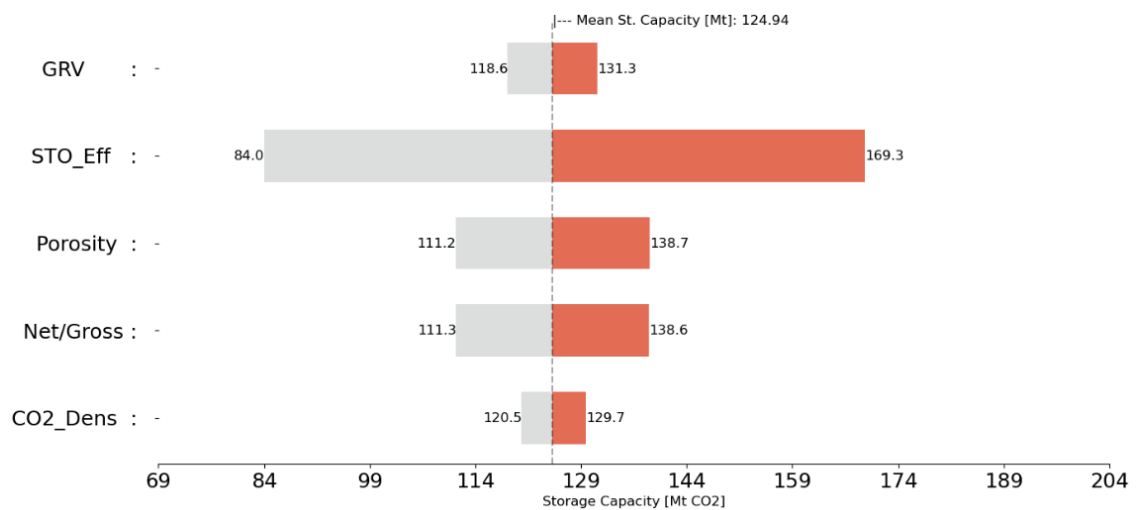


Figure 8.5.2. Sensitivity or Tornado plot to how the various input parameters affect the estimate mean of storage capacity (c. 125 Mt CO₂) of the Gassum reservoir. The horizontal bars for each parameter indicate change in storage capacity given that only that parameter is changed leaving all other constant (end levels being P90 and P10, respectively, in the parameter input range). The colours show the symmetric representation of the parameters on both sides of the mean storage capacity.

8.6 Potential risks

The present report provides an updated geological evaluation describing reservoir-seal couples, the extent, thickness, closure, reservoir quality and volume of the primary reservoir formation, as well as larger faults, but does not comprise a dedicated study of risks or risk assessment of the structure for potential storage of CO₂. Thus, the report provides a geological characterization and maturation of these identified elements and points out geological related potential risk issues, that are recommended to be included for further evaluation and maturation, e.g., in risk assessment studies. Risks treated here are primary geological parameters incompletely understood, that may negatively affect the CO₂ storage potential.

Not all risks can be identified at this early stage due to lack of dense seismic coverage and well information, while other risks identified at this stage will be mitigated by collection of new geophysical and geological data and further investigations. The risks described below are not considered a full list, but rather emphasizes important points that needs further attention in future studies and data collections.

Faults

Leakage along existing faults and compartmentalization of the reservoir due to faults in of the Gassum–Fjerritslev Formations reservoir-seal pair is considered the primary risks at the current level of understanding.

The NW-SE striking fault zone, c. 5 km wide, forms a graben structure along the southwestern part of the Thorning structure and closure (Fig. 6.1.5). The faults offset the entire Triassic section including the Gassum Formation reservoir. The corresponding effective seal interval of the Fjerritslev Formation along the boundary fault to the closure has been estimated to be less than 100 m based on the depth converted thickness maps (Fig. 6.1.5). Furthermore, the northward extension of the fault is poorly defined due to poor seismic data coverage. The risk associated with potential leakage along this bounding fault zone should be addressed by additional seismic coverage and a thorough assessment of the seal integrity of the fault zone (Fig. 6.1.5).

Minor extensional faults are observed at both the eastern and western rim of the domal structure to the north (Figs 6.1.2, 6.1.3). The faults are W-dipping, oriented NNE–SSW and NNW–SSE respectively, and they are only observed on E–W striking profiles in the new GEUS lines P2 and P8. The faults offset the Top Gassum Formation horizon with throws up-to c. 20–25 ms TWT corresponding to 30–37 m offset. The faults may terminate in the overlying seal of the Fjerritslev Formation or may be linked with similar faults systems recorded above at Base Chalk Group level.

By analogy, faults are also present in the Stenlille structure, where the mapped faults are typically minor in both lateral extension (up to few km) and vertical throws (typical up to 10–15 milliseconds) and located kilometres apart (Gregersen et al., 2023). Despite the presence of faults in the Stenlille structure, there are not registered any leakage or natural escape of gas, which has been stored in the Stenlille structure since 1989 (Laier and Øbro, 2009). It is not known whether the faults in the Thorning structure could act as migration pathways for CO₂, hence, at this point the faults should be considered as a potential risk of vertical leakage from storage in the Gassum Formation, that needs to be addressed when maturing the structure further.

Faults could also be a challenge to lateral distribution of the injected CO₂ by causing compartmentalization of the reservoir, such as known from the Gassum Formation in the Stenlille structure. Compartmentalization due to faults may reduce internal reservoir communication, and thus lower the storage efficiency and increase the number of injection wells required to fill the structure.

Furthermore, near surface-faults could also control and impact the location of incised glacial valleys that carved into the pre-Quaternary surface, as supported by the study of Sandersen and Jørgensen (2016), who mapped glacial buried valleys in the Thorning study area using SkyTEM electromagnetic data and documented a possible correlation between the NW–SE orientation of the deep-seated faults and lineaments with glacial valleys (WNW–ESE). Several profiles from the new 2023 GEUS_THORNING2D survey show incised valleys with an NW–SE orientation that extends deep and almost intersects the Top Chalk surface. Hence, the location and lateral extend of near-surface structures should be closely mapped and investigated to secure the successions above the top seals and other potential risks of migration routes or leakage through the glacial deposits.

Earthquake hazard

Denmark is a low risk area for earthquakes though small earthquakes do occur (Fig. 8.6.1). Earthquake hazard for Denmark can be found in Voss al. (2015), where also lists of felt and damaging earthquakes can be found. The largest earthquakes in or near Denmark have occurred offshore Thy and in Kattegat. Large earthquakes have occurred in Kattegat, with a M 4.7 event in 1985 in the Swedish part of Kattegat (Arvidsson et al., 1991), and another large earthquake in 1759 in northern Kattegat (Wood, 1988). The largest instrumentally recorded earthquake offshore Thy occurred in 2010 and had a M 4.3 (Fig. 8.6.2). The depths of the earthquakes are very uncertain, but they are located within Earth's crust.

For comparison, a monitoring study was carried out around Gas Storage Denmark gas storage facility close to Stenlille. Six seismic stations were in operation for almost three years during 2018–2021, i.e. during a period with seasonal injection and withdrawal of natural gas, but 30 years after the start of the gas storage operation. The detection limit within the storage area was calculated to be at least ML 0.0. No local events were detected within the survey period (Dahl-Jensen et al. 2021). Based on the permanent seismic network, only few, small earthquakes have been recorded near the Thorning structure and the seismic hazard of the area is low (Fig. 8.6.2).

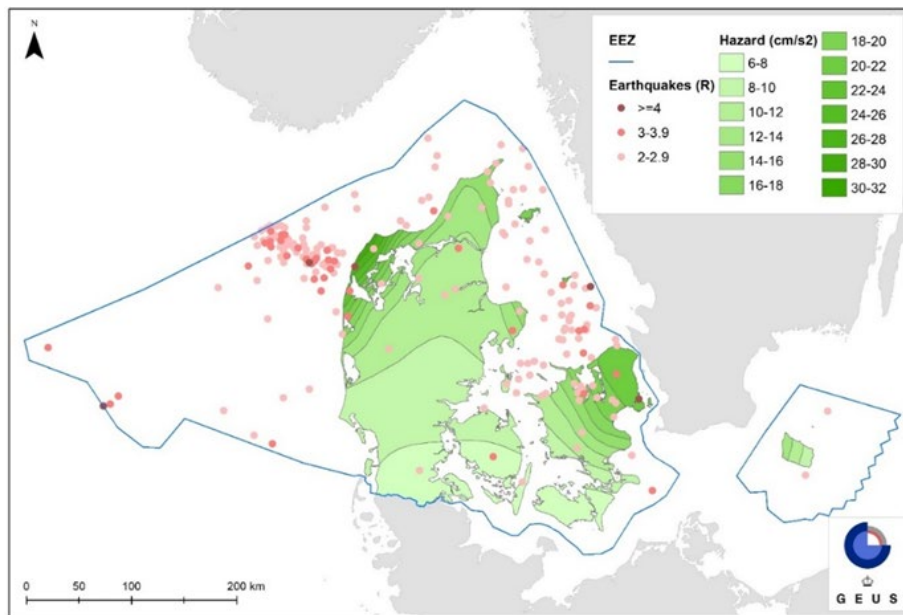


Figure 8.6.1. The coloured contours are redrawn onshore from Voss et al. (2015) and show the estimated hazards given by the peak ground accelerations [cm/s²] for a return period of 475 years. This corresponds to a 90% non-exceedance probability in 50 years. Given values are only valid onshore Denmark. The contours are based on a validated catalogue of earthquakes over Magnitude 3 from 1960 to 2013. As the attenuation of earthquakes (ground motion prediction) has not been determined specifically for Denmark, the global reference model by Spudich et al. (1997) that describes attenuation from normal faults in hard-rock conditions was used.

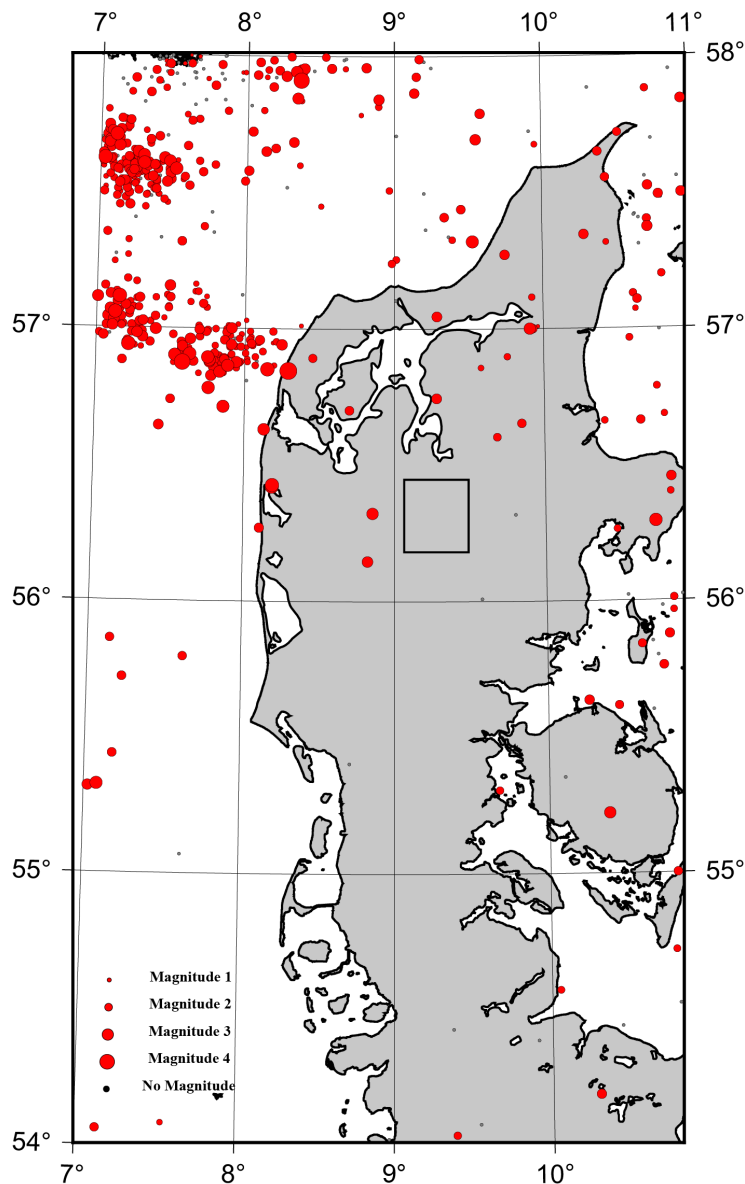


Figure 8.6.2. All known earthquakes until 2024, located since 1930 within the shown area. The magnitude (shown by the size of the red dots) varies from ML 4.0 and down. All known and assumed explosions have been removed, but some may remain, mainly offshore. The Thorning study area of this report is marked with a black rectangle. The two earthquakes shown west of the study area were ML3.1 in July 2024 (North), and ML 2.9 in April 1988 (South). Based on the permanent seismic network, only few, small earthquakes have been recorded near the Thorning structure.

9. Conclusions

This study shows that the Thorning structure forms a well-defined structural anticlinal dome, with a three-way dip closure at Top Gassum Formation level and bounded by a fault zone towards the southwest. The structure is cored by a Zechstein salt pillow that is overlain by a thick Triassic – Lower Jurassic successions and younger strata. The structure is covered by both vintage seismic data, as well as the c. 133 km new seismic lines acquired during August to October 2023 to increase the seismic data coverage of the structure.

Deep wells are not present in the Thorning structure which leads to major uncertainty as to the presence and quality of potential reservoirs. The primary reservoir is considered to be the sandstones of the Upper Triassic Gassum Formation, with a thick mudstone succession of the uppermost Triassic – Lower Jurassic Fjerritslev Formation as the primary seal. Both formations are well-known from wells in the area surrounding the Thorning structure. Secondary sandstone reservoirs may potentially be present in the structure: The deeper situated Triassic Bunter Sandstone Formation / Skagerrak Formation with the Ørslev Formation mudstones as a seal, the Tønder Formation with the Oddesund Formation as a seal, and the shallower Upper Jurassic – Lower Cretaceous Frederikshavn Formation with the Lower Cretaceous claystone-dominated Vedsted Formation as a seal. Both the Bunter Sandstone Formation / Skagerrak Formation and the Frederikshavn Formation have large closure areas but the presence of potential good reservoir intervals in these formations is essentially unknown in the Thorning structure.

Estimation of reservoir quality of the Gassum Formation in the Thorning structure is calculated in three scenarios by interpolation of the data from the Gassum-1 and Nøvling-1 well using core descriptions and core measurements and petrophysical log interpretations and stratigraphic interpretation of seismic data. The main reservoir interval is interpreted as between Base Gassum Formation and to intra Gassum Formation transgressive surface TS5 and the modelled net reservoir sand thickness is between 20.5–35 m, and good reservoir properties are expected. The top of the primary reservoir of the Gassum Formation is located at roughly 1520 m b.sl. and 1580 m below terrain at the apex of the structure, the estimated salinity reaches approximately 111 mg/l Cl⁻ at median depth. At the expected depth of the Bunter Sandstone / Skagerrak Formation sandstone reservoir, at medium depth of around 2880 meters below terrain, salinity is estimated to be approximately 198 mg/l Cl⁻, indicating that it is nearing saturation with respect to halite. The shallower secondary reservoir of the Frederikshavn Fm is situated at a depth of 1187 m below main sea level and 1247 m below terrain and have an estimated salinity of 99 mg/l Cl⁻.

The mudstone dominated Fjerritslev Formation is known to have good seal properties. The thickness of the Fjerritslev Formation is 100–350 m in the Thorning structure based on the seismic data. The convex upward structure in the lower part of the Fjerritslev Formation which is located in the eastern part of the Thorning structure may contain an additional reservoir interval and is thereby reducing the seal interval accordingly with up to 150 m in this area. The effective seal thickness remains 100–300 m thick except along the boundary fault zone of the Top Gassum Fm closure to the southwest, where the effective seal interval may decrease to less than 100 m along the fault. The sealing capacity of the Fjerritslev Formation is clearly demonstrated in the Stenlille structure where the marine claystones and mudstones of the Fjerritslev Formation forms an effectively seal for the seasonal storage of natural gas in the Gassum Formation. Compared to the Stenlille area, the Fjerritslev Formation in the

Thorning structure is expected to be more fine-grained and contains less siltstone and sandstone layers.

Faults are interpreted and described from the 2D seismic data with focus on their occurrence in the Gassum and Fjerritslev Formations.

The three-way closure of the Thorning structure is bounded towards southwest by a c. 5 km wide significant fault zone with a small graben, observed on two of the new seismic profiles, (P4 and P5). The graben structure probably formed as a mini-basin due to salt withdrawal and collapse resulting in a marked thickening of the Fjerritslev Formation in the fault zone. The large throws at the Top Gassum to Top Falster horizons indicate faulting during deposition of the Fjerritslev Formation. The northern continuation of the fault zone is poorly constrained due to lack of seismic coverage. Extensional faults are recorded at the northeastern crest of the structure on profiles P2 and P8 that demonstrate west-dipping, normal faults which are offsetting the top Gassum Fm horizon with throws up-to 21–23 msec TWT, corresponding to 34–35 m offset. The faults are associated with formation of the salt pillow resulting in stretching of the overlying layers.

As faults may act as migration pathways or result in mechanical weakening of the seal or compartmentalization of the reservoir, it is recommended to investigate this further by additional data acquisition and analyses.

The areal extent of the Gassum reservoir in the Thorning structure is estimated to c. 235 km², which is slightly more than mapped in the previous regional study (210 km² in Hjelm et al. 2022), based on vintage seismic data and velocity data. The structural relief is increased significantly from 360 m to 430 m due to a much better constrained depth conversion applying data from the new seismic survey. Without addressing the influence of the faults located in the central part of the Thorning structure the increase in the rock volume of the structure, together with an assumed storage efficiency factor of 10% compared to the previously assumed 40%, the estimated storage capacity is updated to a unrisken mean of 125 Mt CO₂ or between c. 81–174 Mt CO₂ for Scenario 3, compared to the previous estimate of 297 Mt CO₂ in Hjelm et al. (2022). The estimations are based on a static assessment of the storage capacity and must be investigated further by more site-specific assessments and reservoir simulation modelling.

The main cause of the discrepancy between the previous and new estimates of storage capacity is the larger GRV and furthermore, due to choosing a lower and more realistic value for the assumed storage efficiency factor of 10% compared to the previously assumed 40%, which only is valid in a well-constrained system with good well control etc., such as the Stenlille area. The efficiency factor is the most widely ranging parameter in the storage calculation in deep saline aquifers. In the literature, the efficiency factor varies between 0.01% and 40% but the processes underlying its derivation are not always clear as presented by Ehlig-Economides and Economides (2010).

10. Recommendations for further work

New 2D seismic data has been acquired over the Thorning structure and has improved the database with eight new seismic sections. The new data together with the existing data provided a comprehensive database for the present maturation efforts including updated mapping and analyses of the size, spill-point, volume, details of reservoir- and seal successions, and faults of the Thorning structure. However, it is recommended, that a further evaluation of the structure should include new seismic acquisition, a drilling program, and a risk assessment with seal integrity study, including analysis of leakage risk at faults. Faults can lead to compartmentalization of the reservoir and weaken the seal, which may pose significant risks to CO₂ storage projects. Such a supplementary exploration program can help to understand the faults' impact on reservoir connectivity and seal integrity, allowing the future operator of the Thorning site to plan CO₂ injection pathways that avoid fault zones and prevent potential leakage or migration of CO₂.

New 3D seismic acquisition over the potential injection and storage sites is recommended, for more detailed interpretation prior to CO₂ injection. Acquisition of 3D seismic data over the structure can add important new data towards mitigating the fault related risks, develop scenarios to evaluate optimal well design, as well as provide data for modelling studies of CO₂ migration.

The lack of deep wells in the Thorning structure poses an uncertainty on the thickness and quality of the assumed primary reservoir of the Gassum Formation. The geological interpretation of the Thorning structure suggests a potential major upside to the storage capacity if reservoir intervals are present in the mapped Frederikshavn Formation, the Bunter Sandstone Formation / Skagerrak Formation and the Tønder Formation. The storage capacity should thus be reevaluated once future wells are drilled on the structure with associated modern electrical log suites and coring programs.

Later if the Thorning license should be awarded and hereafter matured from an exploration and assessment phase to a development and CO₂ injection ("production") phase, repeated seismic surveys in same area can contribute to monitor the extent of the CO₂ migration, together with other monitoring (e.g., sampling in monitoring wells, seismometers, and other instrumentation). Such data will also enable a more precise definition of trap closures and reservoir outline, which again will feed into a refined storage volume calculation. The modelled storage capacity is associated with variability-ranges and uncertainty, which e.g., are dependent on volume and closure definition.

The geometry of the structure on the mapped surface of the Top Gassum Formation and the relief from the deepest closure (spill-point) to the top structure is sensitive to mapping and depth conversion constraints despite the much-improved database. Thus, it is recommended to further improve the database and conduct a careful mapping and time-to-depth models.

A further key element for the quantification of the storage potential of the structure is the understanding of the storage efficiency. The storage efficiency factor is mostly dependent on reservoir architecture and performance and thus potential heterogeneity, permeability, and compartmentalization, but also by economic aspects such as well density, well layout and injection design. Better understanding of the reservoir and dynamic simulation of reservoir flow could constrain storage efficiency better and thus narrow the estimated final capacity range.

The study documents the existence of faults at the southwest flank and near the top of the Thorning structure. The risk of leakage, fault reactivation and compartmentalization should be addressed in geomechanical and reservoir modelling studies. Possible CO₂ injection in the Gassum Formation should be away from faults and the lowermost contour and saddle-point (spill-point) of the structure. Besides the potential storage of CO₂ within the structure as considered here, potential effects from injection and storage on reservoir and seal at the specific site(s) should also be considered, including mineral solubility, mineral trapping, pressure and stress effects, etc.

New necessary data acquisition and sampling, analyses and evaluations should be carried out for further maturation, including risk analyses, to cover geological and other technical uncertainties and risks.

Site-specific studies on the seal capacity are needed for all structures to be matured towards CO₂ storage. For the Thorning structure, no site-specific studies exist for the sealing units and the need to establish fundamental knowledge of the seal properties is very high. For the Fjerritslev Formation we can draw parallels to the better-known Fjerritslev Formation in the Stenlille area and the Vedsted-1 sample set as a basis for the evaluation, but we cannot safely rely on its representation. For the younger and older secondary sealing units in the Thorning structure no analytical data exist on the seal capacity.

11. Acknowledgement – The new seismic data

GEUS appreciates the excellent collaboration with Professor Alireza Malehmir and his researcher team from Uppsala University, including Jolanta Putnaite, Tatiana Pertuz, Michael Westgate, Emmanouil Konstantinidis, Kristina Kucinskaite, Samuel Zappalá, Grzegorz Paletko, Myrto Papadopoulou, and Lea Gyger on the planning, and acquisition and completion of the GEUS2023-THORNING seismic survey.

We also acknowledge the work by Geopartner Geofizyka on the operation of the seismic sources and the great field assistance from all the students from the University of Copenhagen and University of Aarhus. Furthermore, the good cooperation with COWI on permits, logistics and communication with local citizens during the acquisition is highly appreciated.

The good cooperation with the geophysics company Realtimeseismic during reprocessing of the 2D survey is also appreciated.

12. References

- Abramovitz, T., Vosgerau, H., Gregersen, U., Smit, F.W.H., Bjerager, M., Jusri, T.A., Mathiesen, A., Mørk, F., Schovsbo, N.H., Petersen, H.I., Nielsen, L.H., Laghari, S., Rasmussen, L.M. and Keiding, M. 2024. CCS2022-2024 WP1: The Rødbby structure. Seismic data and interpretation to mature potential geological storage of CO₂. Danmarks og Grønlands Geologiske Undersøgelse Rapport 2024/18. <https://doi.org/10.22008/gpub/34739>
- Amour, F., Hajiabadi, M.R., Hosseinzadehsadati, S. and Nick, H.M. 2022. Impacts of CO₂ injection on the compaction behaviour of chalk reservoirs. Proceedings of the 16th Greenhouse Gas Control Technologies Conference (GHGT-16). <https://dx.doi.org/10.2139/ssrn.4286144>
- Anthonsen, K.L., Aagaard, P., Bergmo, P.E.S., Gislason, S.R., Lothe, A.E., Mortensen, G.M. and Snæbjörnsdóttir, S.Ó. 2014. Characterisation and selection of the most prospective CO₂ storage sites in the Nordic region. Energy Procedia 63, 4884–4896. <https://doi.org/10.1016/j.egypro.2014.11.519>
- Arvidsson, R., Gregersen, S., Kulhánek, O. and Wahlström, R. 1991. Recent Kattegat earthquakes - evidence of active intraplate tectonics in southern Scandinavia. Physics of the Earth and Planetary Interiors 67 (3-4), 275–287. [https://doi.org/10.1016/0031-9201\(91\)90024-C](https://doi.org/10.1016/0031-9201(91)90024-C)
- Beckel, R.A. and Juhlin, C. 2019. The cross-dip correction as a tool to improve imaging of crooked-line seismic data: a case study from the post-glacial Burtrask fault, Sweden. Solid Earth 10 (2), 581–598. <https://doi.org/10.5194/se-10-581-2019>
- Bertelsen, F. 1978. The Upper Triassic – Lower Jurassic Vinding and Gassum Formations of the Norwegian–Danish Basin. Danmarks Geologiske Undersøgelse Serie B, Vol. 3, 26 pp. <https://geusjournals.org/index.php/serieb/issue/view/927>
- Bertelsen, F. 1980. Lithostratigraphy and depositional history of the Danish Triassic. Danmarks Geologiske Undersøgelse Serie B, Vol. 4, 59 pp. <https://geusjournals.org/index.php/serieb/issue/view/928>
- Bull, S., Cartwright, J. and Huuse, M. 2009. A review of kinematic indicators from mass-transport complexes using 3D seismic data. Marine and Petroleum Geology, 26, 1132–1151, <https://doi.org/10.1016/j.marpetgeo.2008.09.011>
- Catuneanu, O. 2019. Model-independent sequence stratigraphy. Earth-Science Reviews 188, 312–388. <https://doi.org/10.1016/j.earscirev.2018.09.017>
- Chadwick, R.A., Zweigel, P., Gregersen, U., Kirby, G.A., Holloway, S. and Johannesen, P.N. 2004. Geological reservoir characterization of a CO₂ storage site: The Utsira Sand, Sleipner, northern North Sea. Energy 29 (9–10), 1371–1381. <https://doi.org/10.1016/j.energy.2004.03.071>
- Clark D. E., Oelkers E. H., Gunnarsson I., Sigfússon B., Snæbjörnsdóttir S. Ó., Aradóttir E. S. and Gislason S. R. 2020. CO₂ and H₂S mineralization during 3.5 years of continuous injection into basaltic rocks at more than 250°C. Geochim. Cosmochim. Acta 279, 45–66.
- Clausen O.R. and Pedersen P.K. 1999. Late Triassic evolution of the southern margin of the Ringkøbing-Fyn High. Marine Petroleum Geology 16, 653–665.

- Dahl-Jensen, T., Jakobsen, R., Bech, T.B., Nielsen, C.M., Albers, C.N., Voss, P.H. and Larsen, T.B. 2021. Monitoring for seismological and geochemical groundwater effects of high-volume pumping of natural gas at the Stenlille underground gas storage facility, Denmark. GEUS Bulletin 47, 5552. <https://doi.org/10.34194/geusb.v47.5552>
- Danish American Prospecting Co 1951. Gassum-1, Completion report (Compiled March 1993).
- Dybkjær, K. 1988. Palynological zonation and stratigraphy of the Jurassic section in the Gassum No. 1-borehole, Denmark. Danmarks Geologiske Undersøgelse Serie A, Vol. 21, 73 pp. <https://geusjournals.org/index.php/seriea/article/view/7040>
- Dybkjær, K. 1991. Palynological zonation and palynofacies investigation of the Fjerritslev Formation (Lower Jurassic - basal Middle Jurassic) in the Danish Subbasin. Danmarks Geologiske Undersøgelse Serie A, Vol. 30, 150 pp. <https://doi.org/10.34194/seriea.v30.7050>
- Ehlig-Economides, C. and Economides, M.J. 2010. Sequestering carbon dioxide in a closed underground volume. Journal of Petroleum Science and Engineering 70 (1–2), 123–130. <https://doi.org/10.1016/j.petrol.2009.11.002>
- Fam, H.J.A., Naghizadeh, M., Smith, R., Yilmaz, Ö., Cheraghi, S. and Rubingh, K. 2023. High-resolution 2.5D multifocusing imaging of a crooked seismic profile in a crystalline rock environment: Results from the Larder Lake area, Ontario, Canada. Geophysical Prospecting 71 (7), 1152–1180. <http://dx.doi.org/10.1111/1365-2478.13285>
- Fuchs, S., Balling, N. and Mathiesen, A. 2020. Deep basin temperature and heat-flow field in Denmark – New insights from borehole analysis and 3D geothermal modelling. Geothermics, 83, 101722. <http://doi.org/10.1016/j.geothermics.2019.101722>
- Global CCS Institute 2022. Global status of CCS 2022. URL: <https://status22.globalccsinstitute.com>
- Goodman, A., Hakala, A., Bromhal, G., Deel, D., Rodosta, T., Frailey, S., Small, M., Allen, D., Romanov, V., Fazio, J., Huerta, N., McIntyre, D., Kutchko, B. and Guthrie, G. 2011. U.S. DOE methodology for the development of geologic storage potential for carbon dioxide at the national and regional scale, International Journal of Greenhouse Gas Control 5 (4), 952–965. <https://doi.org/10.1016/j.ijggc.2011.03.010>
- Gorecki, C.D., Holubnyak, Y.I., Ayash, S.C., Bremer, J.M., Sorensen, J.A., Steadman, E.N. and Harju, J.A. 2009. A new classification system for evaluating CO₂ storage resource/capacity estimates. SPE International Conference on CO₂ Capture, Storage, and Utilization, San Diego, California, USA. <https://doi.org/10.2118/126421-MS>
- Gregersen, U. and Smit, F.W.H. 2003. Two-way Time (TWT) grids from the Havnsø project. GEUS Dataverse V2, Geological Survey of Denmark and Greenland. Link to published data: <https://doi.org/10.22008/FK2/ADIJKG>
- Gregersen, U., Vosgerau, H., Laghari, S., Bredesen, K., Rasmussen, R. and Mathiesen, A. 2020. Capture, Storage and Use of CO₂ (CCUS): Seismic interpretation of existing 2D and 3D seismic data around the Havnsø structure (Part of work package 5 in the CCUS project). Danmarks og Grønlands Geologiske Undersøgelse Rapport 2020/33; GEUS. 60 pp. <https://doi.org/10.22008/gpub/34530>
- Gregersen, U., Smit, F.W.H., Lorentzen, M., Vosgerau, H., Bredesen, K., Hjelm, L., Mathiesen, A. and Laghari, S. 2022. Tectonostratigraphy and Structural Evolution of the Stenlille Structure in Zealand, Denmark – a Site for Natural Gas and CO₂ Storage. GHGT

16 Conference Proceedings (2022); SSRN Electronic Journal Nov. 2022 & Geophysics eJournal 4 (85) Dec. 2022, 12 pp. SSRN: <http://dx.doi.org/10.2139/ssrn.4275875>

Gregersen, U., Hjelm, L., Vosgerau, H., Smit, F.W.H., Nielsen, C.M., Rasmussen, R., Bredesen, K., Lorentzen, M., Mørk, F., Lauridsen, B.W., Pedersen, G.K., Nielsen, L.H., Mathiesen, A., Laghari, S., Kristensen, L., Sheldon, E., Dahl-Jensen, T., Dybkjær, K., Hidalgo, C.A. and Rasmussen, L.M. 2023. CCS2022-2024 WP1: The Stenlille structure - Seismic data and interpretation to mature potential geological storage of CO₂. Danmarks og Grønlands Geologiske Undersøgelse Rapport 2022/26. 164 pp. <https://doi.org/10.22008/gpub/34661>

Gregersen, U., Vosgerau, H., Smit, F.W.H., Lauridsen, B.W., Mathiesen, A., Mørk, F., Nielsen, L.H., Rasmussen, R., Funck, T., Dybkjær, K., Sheldon, E., Pedersen, G.K., Nielsen, C.M., Bredesen, K., Laghari, S., Olsen, M.L. and Rasmussen, L.M. 2023. CCS2022-2024 WP1: The Havnsø structure. Seismic data and interpretation to mature potential geological storage of CO₂. Danmarks og Grønlands Geologiske Undersøgelse Rapport 2023/38. 200 pp. <https://doi.org/10.22008/gpub/34705>

Gulf Oil Company Denmark 1967, Nøvling-1, Completion Report.

Hall, G. 2008. Carbon Storage Atlas of the United States and Canada, 2014-07-01. <https://edx.netl.doe.gov/dataset/2008-carbon-storage-atlas-of-the-united-states-and-canada>

Hamberg, L. and Nielsen, L.H. 2000. Shingled, sharp-based shoreface sandstones: depositional response to stepwise forced regression in a shallow basin, Upper Triassic Gassum Formation, Denmark. In: Hunt, D. and Gawthorpe, R.L. (eds): Sedimentary Responses to Forced Regressions. Geological Society, London, Special Publications 172, 69–89. <https://doi.org/10.1144/GSL.SP.2000.172.01.04>

Hjelm L., Anthonsen K.L., Dideriksen K., Nielsen C.M., Nielsen L.H. and Mathiesen A. 2022. Capture, Storage and Use of CO₂ (CCUS). Evaluation of the CO₂ storage potential in Denmark. Vol.1: Report & Vol 2: Appendix A and B [Published as two separate volumes both with Series number 2020/46]. Danmarks og Grønlands Geologiske Undersøgelse Rapport 2020/46, 141 pp. <https://doi.org/10.22008/gpub/34543>

Holmslykke, H.D., Schovsbo, N.H., Kristensen, L., Weibel, R. and Nielsen, L.H. 2019. Characterising brines in deep Mesozoic sandstone reservoirs, Denmark. GEUS Bulletin 43. <https://doi.org/10.34194/GEUSB-201943-01-04> IPCC (Intergovernmental Panel on Climate Change) 2022. Climate Change 2022: Mitigation of Climate Change. Working Group III contribution to the Sixth Assessment Report of the Intergovernmental Panel on Climate Change. UN, New York. 2913 pp.

Ineson, J.R. 1993. The Lower Cretaceous chalk play in the Danish Central Trough. Geological Society, London, Petroleum Geology Conference Series 4, 175–183. <https://doi.org/10.1144/00401>

Ineson, J.R., Jutson, D.J. and Schiøler, P. 1997. Mid-Cretaceous sequence stratigraphy in the Danish Central Trough. Danmarks og Grønlands Geologiske Undersøgelse Rapport 1997/109, 60 pp. <https://doi.org/10.22008/gpub/14675>

Ineson, J.R., Petersen, H.I., Andersen, C., Bjerager, M., Jakobsen, F.C., Kristensen, L., Mørk, F. and Sheldon, E. 2022. Early Cretaceous stratigraphic and basinal evolution of the Danish Central Graben: a review. Bulletin of the Geological Society of Denmark 71, 75–98. <https://doi.org/10.37570/bgsgd-2022-71-05>

- James, B., Grundy, A.T. and Sykes, M.A. 2013. The Depth-Area-Thickness (DAT) method for calculating gross rock volume: a better way to model hydrocarbon contact uncertainty. AAPG International Conference & Exhibition, Cartagena, Colombia.
- Japsen, P. 1998. Regional velocity–depth anomalies, North Sea chalk: a record of overpressure and Neogene uplift and erosion. AAPG Bulletin 82, 2031–2074.
- Japsen, P. 2000. Investigation of multi-phase erosion using reconstructed shale trends based on sonic data. Sole Pit axis, North Sea. Global and Planetary Change 24, 189–210.
- Japsen, P. 2018. Sonic velocity of chalk, sandstone and marine shale controlled by effective stress: Velocity-depth anomalies as a proxy for vertical movements. Gondwana Research 53, 145–158.
- Japsen, P. and Bidstrup, T. 1999. Quantification of late Cenozoic erosion in Denmark based on sonic data and basin modelling. Bulletin of the Geological Society of Denmark 46, 79–99. <https://doi.org/10.37570/bgds-1999-46-08>
- Japsen, P., Green, P.F., Nielsen, L.H., Rasmussen, E.S. and Bidstrup, T. 2007. Mesozoic–Cenozoic exhumation events in the eastern North Sea Basin: a multi-disciplinary study based on palaeothermal, palaeoburial, stratigraphic and seismic data. Basin Research 19 (4), 451–490. <https://doi.org/10.1111/j.1365-2117.2007.00329.x>
- Jensen, E.F. 2023. Towards inferring elastic moduli for argillaceous sandstones: clay content estimation in drill core utilizing hyperspectral imaging. Master thesis. University of Copenhagen. https://pub.geus.dk/files/40976670/EFJ_THESIS.pdf
- Jensen, T.F., Holm, L., Frandsen, N. and Michelsen, O. 1986. Jurassic-Lower Cretaceous Lithostratigraphic Nomenclature for the Danish Central Trough. Danmarks Geologiske Undersøgelse Serie A, Vol. 12, 65 pp. <https://doi.org/10.34194/seriea.v12.7031>
- Keiding, M., Vosgerau, H., Gregersen, U., Rasmussen, E. S., Smit, F.W.H., Bjerager, M., Mathiesen, A., Mørk, F., Fyhn, M.B.W., Jusri, T.A., Laghari, S., Schovsbo, N.H., Petersen, H.I., Nielsen, L.H., Sheldon, E., Dybkjær, K., Lauridsen, B.W., Rasmussen, R., Abramovitz, T. and Rasmussen, L.M. 2024. CCS2022-2024 WP1: The Gassum structure. Seismic data and interpretation to mature potential geological storage of CO₂. GEUS. Danmarks og Grønlands Geologiske Undersøgelse Rapport Vol. 2024 No. 25. <https://doi.org/10.22008/gpub/34746>
- Laier, T. 2002. Vurdering af udfældningsrisici ved geotermisk produktion fra Margretheholmboringen MAH-1A. Beregning af mætningsindeks for mineraler i saltvand fra Danmarks dybere undergrund. Danmarks og Grønlands Geologiske Undersøgelse Rapport 2002/95, 48 pp. https://data.geus.dk/pure-pdf/18501_GEUS_R_2002_95_opt.pdf
- Laier, T. 2008. Chemistry of Danish saline formation waters relevant for core fluid experiments: fluid chemistry data for lab experiments related to CO₂ storage in deep aquifers. Danmarks og Grønlands Geologiske Undersøgelse Rapport 2008/48. 10 pp. https://data.geus.dk/pure-pdf/27171_GEUS-R_2008_48_opt.pdf
- Laier, T. and Øbro, H. 2009. Environmental and safety monitoring of the natural gas underground storage at Stenlille, Denmark. Geological Society, London, Special Publications 313, 81–92. <https://doi.org/10.1144/SP313.6>
- Larner, K.L., Gibson, B.R., Chambers, R. and Wiggins, R.A. 1979. Simultaneous estimation of residual static and cross-dip corrections. Geophysics 44 (7), 1175–1192. <https://doi.org/10.1190/1.1441001>

- Larsen, G. 1966. Rhaetic–Jurassic– Lower Cretaceous sediments un the Danish Embayment (A heavy-mineral study). Danmarks Geologiske Undersøgelse II. Række, Vol. 91, 127 pp. <https://doi.org/10.34194/raekke2.v91.6882>
- Larsen, M., Bidstrup, T. and Dalhoff F. 2003. Mapping of deep saline aquifers in Denmark with potential for future CO₂ storage. Danmarks og Grønlands Geologiske Undersøgelse Rapport 2003/39, 83 pp. <https://doi.org/10.22008/gpub/19006>
- Larsen, T.B., Gregersen, S., Voss, P.H., Bidstrup, T. and Orozova-Bekkevold, V. 2008. The earthquake that shook central Sjælland, Denmark, November 6, 2001. Bulletin of the Geological Society of Denmark 56, 26–37. <https://doi.org/10.37570/bgds-2008-56-03>
- Lauridsen, B.W., Lode, S., Sheldon, E., Frykman, P., Anderskov, K. and Ineson, J. 2022. Lower Cretaceous (Hauterivian–Aptian) pelagic carbonates in the Danish Basin: new data from the Vinding-1 well, central Jylland, Denmark. Bulletin of the Geological Society of Denmark 71, 7–29. <https://doi.org/10.37570/bgds-2022-71-02>
- Lindström, S., Pedersen, G.K., Vosgerau, H., Hovikoski, J., Dybkjær, K. and Nielsen, L.H. 2023. Palynology of the Triassic–Jurassic transition of the Danish Basin (Denmark): a palynostratigraphic zonation of the Gassum–lower Fjerritslev formations, Palynology 47 (4), 1–34. <https://doi.org/10.1080/01916122.2023.2241068>
- Malehmir, A. and Papadopoulou, M. 2022. Innovative land seismic data acquisition for geological CO₂ storage in Stenlille, Denmark. Final Acquisition and Processing Report of the GEUS2022-STENLILLE survey. Uppsala University, July 2022, 42 pp. Data and report available via GEUS: Processing summary sheet (geus.dk)
- Mallon, A.J. and Swarbrick, R.E. 2008. Diagenetic characteristics of low permeability, non-reservoir chalk from the Central North Sea, Marine and Petroleum Geology 25 (10), 1097–1108. <https://doi.org/10.1016/j.marpetgeo.2007.12.001>
- Mancuso, C. and Naghizadeh, M. 2021. Generalized cross dip moveout correction of crooked 2D seismic surveys. Geophysics 86 (4), 1–61. <https://doi.org/10.1190/geo2020-0278.1>
- Mathiesen, A., Dam, G., Fyhn, M.B.W., Kristensen, L., Mørk, F., Petersen, H.I. and Schovsbo, N.H. 2022. Foreløbig evaluering af CO₂ lagringspotentiale af de saline akviferer i Nordsøen. Danmarks og Grønlands Geologiske Undersøgelse Rapport 2022/15, 151 pp. <https://doi.org/10.22008/gpub/34650>
- Maystrenko, Y., Bayer, U., Brink, H.-J. & Littke, R. 2008: The central European Basin system – an overview. In R. Littke, U. Bayer, D. Gajewski & S. Nelskamp (eds.): *Dynamics of Complex Intracontinental Basins, the Central European Basin System*, 17–34. Springer Verlag, Berlin, Heidelberg.
- Mbia, E.N., Fabricius, I.L., Krogsbøll, A., Frykman, P. and Dalhoff, F. 2014: Permeability, compressibility and porosity of Jurassic shale from the Norwegian-Danish Basin. Petroleum Geoscience 20, 257–281. <https://doi.org/10.1144/petgeo2013-035>
- McBride, E.F. 1963. A classification of common sandstones. Journal of Sedimentary Research 33, 664–669.
- Michelsen, O. 1975a. Lower Jurassic biostratigraphy and ostracods of the Danish Embayment. Danmarks Geologiske Undersøgelse II. Række, Vol. 104, 1–287. <https://doi.org/10.34194/raekke2.v104.6895>

- Michelsen, O., 1975b. Foreløbig stratigrafisk inddeling baseret på ostracoder. Unpublished DGU report. 3 pp and 1 enclosure.
- Michelsen, O. 1978. Stratigraphy and distribution of Jurassic deposits of the Norwegian–Danish Basin. Danmarks Geologiske Undersøgelse Serie B, Vol. 2, 28 pp. <https://doi.org/10.34194/serieb.v2.7057>
- Michelsen, O. 1989a. Revision of the Jurassic lithostratigraphy of the Danish Subbasin. Danmarks Geologiske Undersøgelse Serie A, Vol. 24, 22 pp. <https://doi.org/10.34194/seriea.v24.7044>
- Michelsen, O. 1989b. Log-sequence analysis and environmental aspects of the Lower Jurassic Fjerritslev Formation in the Danish Subbasin. Danmarks Geologiske Undersøgelse Serie A, Vol. 25, 23 pp. <https://doi.org/10.34194/seriea.v25.7045>
- Michelsen, O. and Bertelsen, F. 1979. Geotermiske reservoirinformationer i den danske lagserie. Danmarks Geologiske Undersøgelse, Årbog 1978, 151–163. https://data.geus.dk/pure-pdf/1979_Michelsen_Geotermiske_reservoirinformationer.pdf
- Michelsen O. and Nielsen, L.H. 1991. Well records on the Phanerozoic stratigraphy in the Fennoscandian Border Zone, Denmark: Hans-1, Sæby-1, and Terne-1 wells. Danmarks Geologiske Undersøgelse Serie A, Vol. 29. 37 pp. <https://doi.org/10.34194/seriea.v29.7049>
- Michelsen, O., Saxov, S. Leth, J.A., Andersen, C., Balling, N., Breiner, N., Holm, L., Jensen, K., Kristensen, J.I., Laier, T., Nygaard, E., Olsen, J.C., Poulsen, K.D., Priisholm, S., Raade, T.B., Sørensen, T.R. and Würtz, J. 1981. Kortlægning af potentielle geotermiske reservoirer i Danmark. Danmarks Geologiske Undersøgelse Serie B, Vol. 5, 96 pp.
- Michelsen, O., Nielsen, L.H., Johannessen, P.N., Andsbjerg, J. and Surlyk, F. 2003. Jurassic lithostratigraphy and stratigraphic development onshore and offshore Denmark. In: Ineson, J.R. and Surlyk, F. (eds): The Jurassic of Denmark and Greenland. GEUS Bulletin 1, 145–216. <https://doi.org/10.34194/geusb.v1.4651>
- Nedimović, M.R. and West, G.F. 2003. Crooked-line 2D seismic reflection imaging in crystalline terrains: Part 1, data processing. Geophysics 68 (1), 274–285. <https://doi.org/10.1190/1.1543213>
- Nielsen, L.H. 2003. Late Triassic – Jurassic development of the Danish Basin and the Fennoscandian Border Zone, southern Scandinavia. In: Ineson, J.R. and Surlyk, F. (eds): The Jurassic of Denmark and Greenland. GEUS Bulletin 1, 459–526. <https://doi.org/10.34194/geusb.v1.4681>
- Nielsen, L.H. and Japsen, P. 1991. Deep wells in Denmark 1935-1990. Lithostratigraphic subdivision. Danmarks Geologiske Undersøgelse, Danmarks Geologiske Undersøgelse Serie A, Vol. 31, 179 pp. <https://doi.org/10.34194/seriea.v31.7051>
- Nielsen, L., Boldreel, L.O., Hansen, T.M., Lykke-Andersen, H., Stemmerik, L., Surlyk, F. and Thybo, H. 2011. Integrated seismic analysis of the Chalk Group in eastern Denmark – Implications for estimates of maximum palaeo-burial in southwest Scandinavia. Tectonophysics 511 (1–2), 14–26. <https://doi.org/10.1016/j.tecto.2011.08.010>
- Norwood, J.A., Norvang, A. and von Elm, C. 1951. Final Report on Gassum No. 1. Danmarks Geologiske Undersøgelse (unpublished report). 134 pp.

- Olivarius, M., Friis, H., Kokfelt, T.F., Wilson, J.R., 2015. Proterozoic basement and Paleozoic sediments in the Ringkøbing-Fyn High characterized by zircon U–Pb ages and heavy minerals from Danish onshore wells. *Bulletin Geological Society of Denmark*. 63, 29–44.
- Olivarius, M., Vosgerau, H., Nielsen, L.H., Weibel, R., Malkki, S.N., Heredia, B.D. and Thomsen, T.B. 2022. Maturity Matters in Provenance Analysis: Mineralogical differences explained by sediment transport from Fennoscandian and Variscian sources. *Geosciences* 2022, 12 (8), 308, 24 pp. <https://doi.org/10.3390/geosciences12080308>
- Olsen, H. 1988. Sandy braid plan deposits from the Triassic Skagerrak Formation in the Thisted-2 well, Denmark. *Geological Survey of Denmark Serie B*, Vol. 11, 26 pp.
- Palmer, D. 1980. The generalized reciprocal method of seismic refraction interpretation. *Society of Exploration Geophysicists*. <https://doi.org/10.1190/1.9781560802426>
- Payton, C.E. 1977. Seismic Stratigraphy – applications to hydrocarbon exploration. *The American Association of Petroleum Geologists – AAPG Memoir* 26, 516 pp. <https://doi.org/10.1306/M26490>
- Peacock, D. C. P. & Banks, G. J. 2020: Basement highs: definitions, characterisation and origins. *Basin Research* **32**, 1685–1710.
- Pedersen, G.K. 1986. Changes in the bivalve assemblage of an early Jurassic mudstone sequence (the Fjerritslev Formation in the Gassum 1 Well, Denmark). *Palaeogeography, Palaeoclimatology, Palaeoecology* 53 (2–4), 139–168. [https://doi.org/10.1016/0031-0182\(86\)90042-8](https://doi.org/10.1016/0031-0182(86)90042-8)
- Pedersen, G.K. and Andersen, P.R. 1980. Depositional environments, diagenetic history and source areas of some Bunter Sandstones in northern Jutland. *Danmarks Geologiske Undersøgelse, Årbog* 1979, 69–93. https://data.geus.dk/pure-pdf/1980_Pedersen_Depositional_environments.pdf
- Petersen, H. I., Nielsen, L. H., Bojesen-Koefoed, J. A., Mathiesen, A., Kristensen, L. and Dalhoff, F. 2008. Evaluation of the quality, thermal maturity and distribution of potential source rocks in the Danish part of the Norwegian–Danish Basin. *GEUS Bulletin* 16, 66 pp. <https://doi.org/10.34194/geusb.v16.4989>
- Poulsen, N.E. 1996. Dinoflagellate cysts from marine Jurassic deposits of Denmark and Poland (No. 31). *American Association of Stratigraphic Palynologists contribution series* 31, 227 pp.
- Poulsen, N.E. and Riding, J.B. 2003. The Jurassic dinoflagellate cyst zonation of Subboreal Northwest Europe. *GEUS Bulletin* 1, 115–144. <https://doi.org/10.34194/geusb.v1.4650>
- Putnaite, J and Malehmir, A. 2024. GEUS2023-THORNING seismic survey: Acquisition, processing and results, Final Report (June 2024), 22 pp. Data and report available via GEUS: Processing summary sheet (geus.dk)
- Rasmussen, E.S. and Nielsen, A.T. 2020. *Danmarks Geologi – En kort introduktion. Junior Geologerne*. https://junior-geologerne.dk/wp-content/uploads/2020/06/Junior-Geologerne_Danmarks_geologi.pdf
- Sandersen, P. B. E., & Jørgensen, F. (2016). Kortlægning af begravede dale i Danmark. Opdatering 2010-2015. Bind 1: Hovedrapport. De Nationale Geologiske Undersøgelser for Danmark og Grønland. Særudgivelse

- https://www.begravededale.dk/PDF_2015/091116_Rapport_Begravede_dale_BIND_1_Endelig_udgave_Low_res.pdf
- Schmelzbach, C., Juhlin, C., Carbonell, R. and Simancas, J.F. 2007. Prestack and poststack migration of crooked-line seismic reflection data: a case study from the South Portuguese Zone fold belt, southwestern Iberia. *Geophysics* 72 (2), B9–B18. <https://doi.org/10.1190/1.2407267>
- Schonewille, M., Klaedtke, A., Vigner, A., Brittan, J. and Martin, T. 2009. Seismic data regularization with the anti-alias anti-leakage Fourier transform. *First Break* 27 (9). <https://doi.org/10.3997/1365-2397.27.1304.32570>
- Schovsbo, N.H. and Petersen, H.I. 2024. Analysis of the applicability of cuttings samples to test seal integrity, examples from the Triassic to Jurassic interval in 8 wells in Eastern Denmark. *Danmarks og Grønlands Geologiske Undersøgelse Rapport* 2024/10, 67 pp. <https://doi.org/10.22008/gpub/34731>
- Schovsbo, N., Holmslykke, H., Mathiesen, A. and Møller Nielsen, C. submitted. Assessment of brine salinity in selected CO₂ storage sites, Eastern Denmark.
- Sorgenfrei, T. and Buch, A. 1964. Deep Tests in Denmark 1935–1959. *Danmarks Geologiske Undersøgelse III. Række*, Vol. 36, 146 pp. <https://doi.org/10.34194/raekke3.v36.6941>
- Span, R. and Wagner, W. 1996. A new equation of state for carbon dioxide covering the fluid region from the triple-point temperature to 1100K at pressures up to 800 MPa, *J. Phys. Chem. Ref. Data.*, 25, 1509–1596. http://www.peacesoftware.de/einigewerte/co2_e.html.
- Springer, N., Didriksen, K., Holmslykke, H.D., Kjøller, C., Olivarius, M. and Schovsbo, N. 2020. Capture, Storage and Use of CO₂ (CCUS): Seal capacity and geochemical modelling (Part of work package 5 in the CCUS project). *Danmarks og Grønlands Geologiske Undersøgelse Rapport* 2020/30, 42 pp. <https://doi.org/10.22008/gpub/34527>
- Spudich, P., Fletcher, J.B., Hellweg, M., Boatwright, J., Sullivan, C., Joyner, W.B., Hanks, T.C., Boore, D.M., McGarr, A., Baker, L.M. and Lindh, A.G. 1997. SEA96 – A New Predictive Relation for Earthquake Ground Motions in Extensional Tectonic Regimes. *Seismological Research Letters* 68 (1), 190–198. <https://doi.org/10.1785/gssrl.68.1.190>
- Thybo, H. 1997. Geophysical characteristics of the Tornquist fan area, northwest trans-European suture zone: indication of late carboniferous to early Permian dextral transtension. *Geological Magazine* 134, 597–606, <https://doi.org/10.1017/S0016756897007267>.
- Thybo, H. 2001. Crustal structure along the EGT profile across the Tornquist fan interpreted from seismic, gravity and magnetic data. *Tectonophysics* 334, 155–190.
- Vejbæk O.V. 1997. Dybe strukturer i danske sedimentære bassiner. *Geologisk Tidsskrift* 1997/4, 1–31. <https://2dggf.dk/xpdf/gt1997-4-1-31.pdf>
- Vejbæk, O.V. and Britze, P. 1994. Geological map of Denmark 1:750.000. Top pre-Zechstein. *Danmarks Geologiske Undersøgelse Map series* 45, 9 pp.
- Vosgerau, H., Gregersen, U., Hjuler, M.L., Holmslykke, H.D., Kristensen, L., Lindström, S., Mathiesen, A., Nielsen, C.M., Olivarius, M., Pedersen, G.K. and Nielsen, L.H. 2016. Reservoir prognosis of the Gassum Formation and the Karlebo Member within two areas of interest in northern Copenhagen. The EUDP project “Geothermal pilot well, phase 1b”. *Danmarks og Grønlands Geologiske Undersøgelse Rapport* 2016/56. 138 pp + app 1–5. <https://doi.org/10.22008/gpub/32477>

- Wang, Y., Zhangb, K. and Wua, N. 2013. Numerical investigation of the storage efficiency factor for CO₂ geological sequestration in saline formations. *Energy Procedia* 37, 5267–5274. <https://doi.org/10.1016/j.egypro.2013.06.443>
- Weibel, R., Olivarius, M., Kjøller, C., Kristensen, L., Hjuler, M.L., Friis, H., Pedersen, P.K., Boyce, A., Andersen, M.S., Kamla, E., Boldreel, L.O., Mathiesen, A. and Nielsen, L.H. 2017. The influence of climate on early and burial diagenesis in Triassic and Jurassic sand stones from the Norwegian–Danish Basin. *The Depositional Record* 3 (1), 60–91. <https://doi.org/10.1002/dep2.27>
- Weibel, R., Olivarius, M., Vosgerau, H., Mathiesen, A., Kristensen, L., Nielsen, C. M. and Nielsen, L.H. 2020. Overview of potential geothermal reservoirs in Denmark. *Netherlands Journal of Geosciences*, 99, e3, 14 pp. <https://doi.org/10.1017/njg.2020.5>
- Voss; P., Dahl-Jensen, T. and Larsen, T.B. 2015. Earthquake hazard in Denmark. *Danmarks og Grønlands Geologiske Undersøgelse Rapport 2015/24*, 54 pp. <https://doi.org/10.22008/gpub/30674>
- Wu, J. 1996. Potential pitfalls of crooked-line seismic reflection surveys. *Geophysics* 61 (1), 277–281. <https://doi.org/10.1190/1.1443949>
- Yilmaz, Ö. 2001. *Seismic Data Analysis: Processing, Inversion, and Interpretation of Seismic Data*. Society of Exploration Geophysicists. 2065 pp.
- Yu, T., Gholami, R., Raza, A., Vorland K.A.N. and Mamoud M. 2023. CO₂ storage in chalks: What are we afraid of? *International Journal of Greenhouse Gas Control* 123, 103832. <https://doi.org/10.1016/j.ijggc.2023.103832>
- Zhang, J. and Toksöz, M.N. 1998. Nonlinear refraction traveltimes tomography. *Geophysics* 63 (5), 1726–1737. <https://doi.org/10.1190/1.1444468>
- Zhu, X., Sixta, D.P. and Angstman, B.G. 1992. Tomostatics: turning-ray tomography + static corrections. *The Leading Edge* 11 (12), 15–23. <https://doi.org/10.1190/1.1436864>

13. Appendix – Digital version only

Appendix A – Well-log interpretation

- Gassum-1
- Grindsted-1
- Hobro-1
- Horsens-1
- Kvols-1
- Løve-1
- Mejrup-1
- Nøvling-1
- Rønde-1
- Skive-1
- Voldum-1

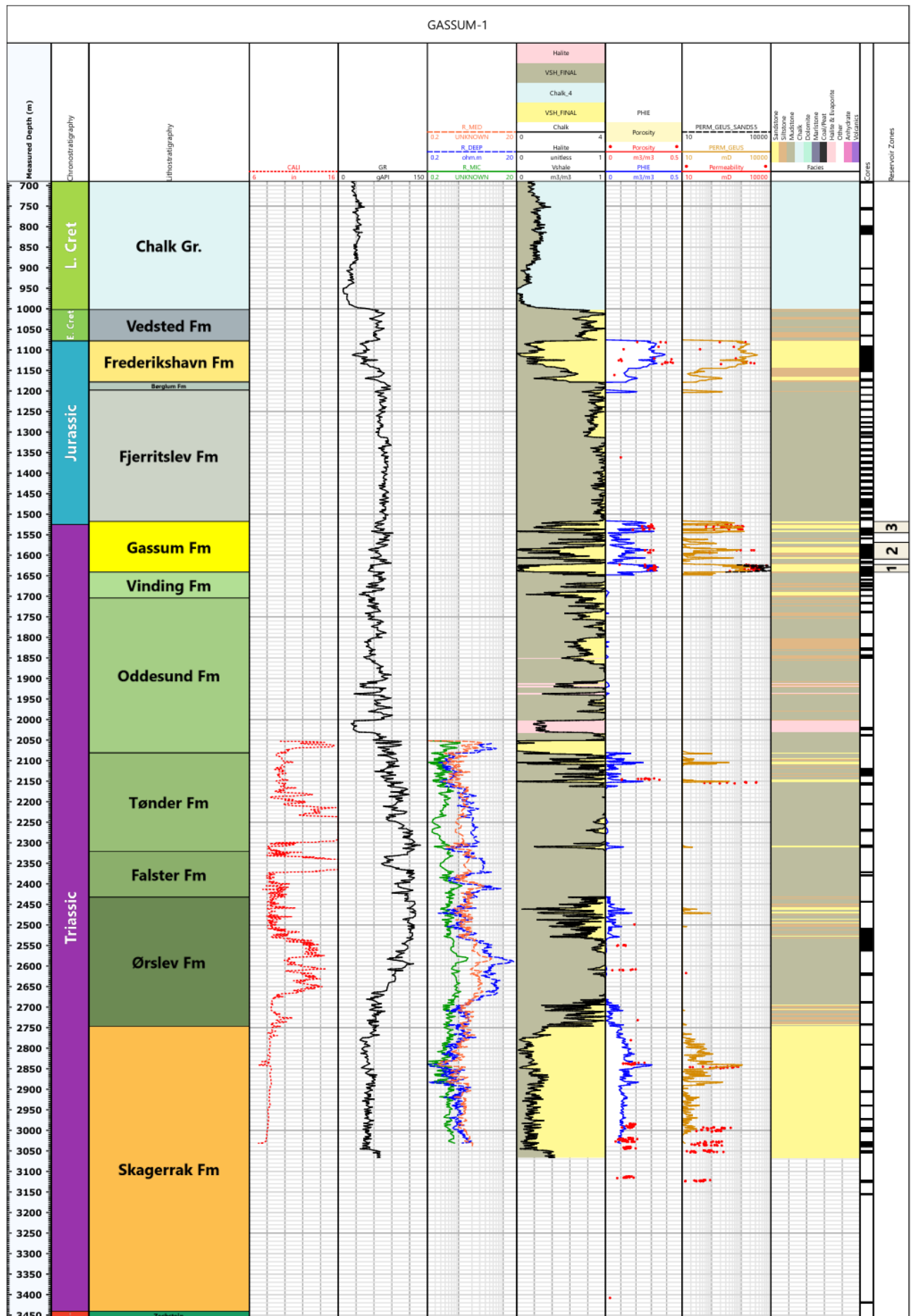
Appendix B – Stratigraphic charts

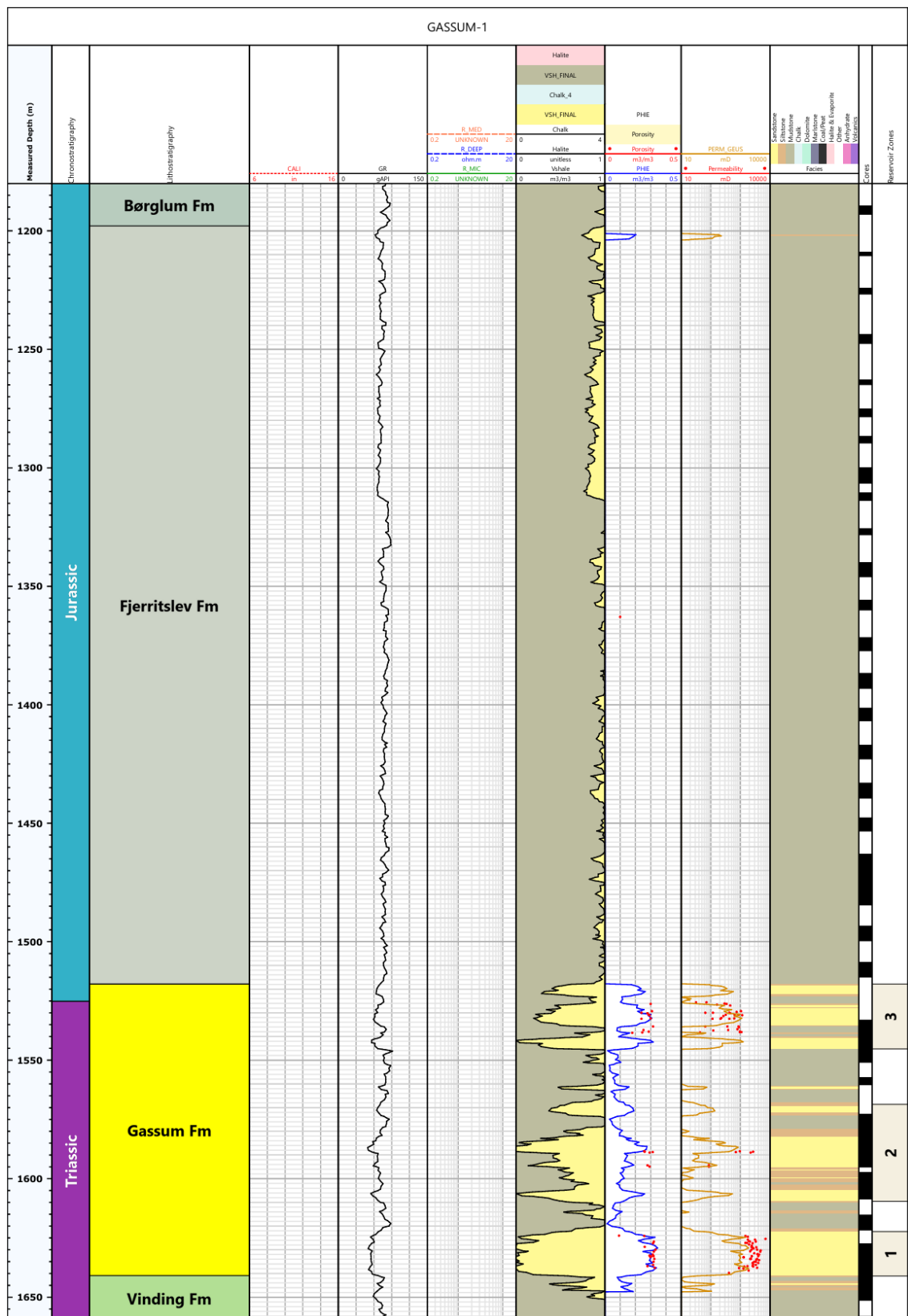
- Gassum-1
- Grindsted-1
- Hobro-1
- Horsens-1
- Kvols-1
- Løve-1
- Mejrup-1
- Nøvling-1
- Skive-1
- Vinding-1
- Voldum-1

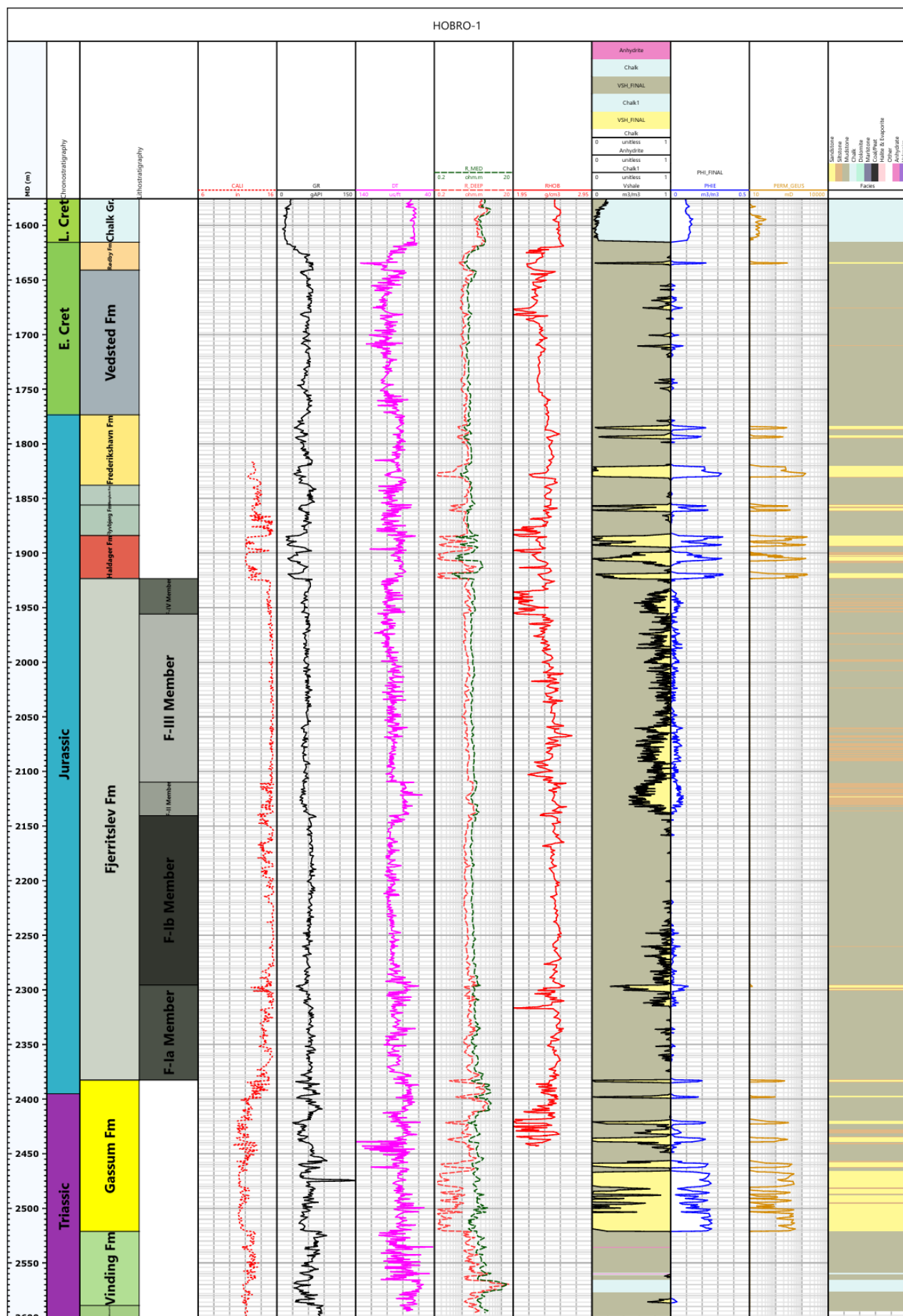
Appendix A – Well-log interpretation

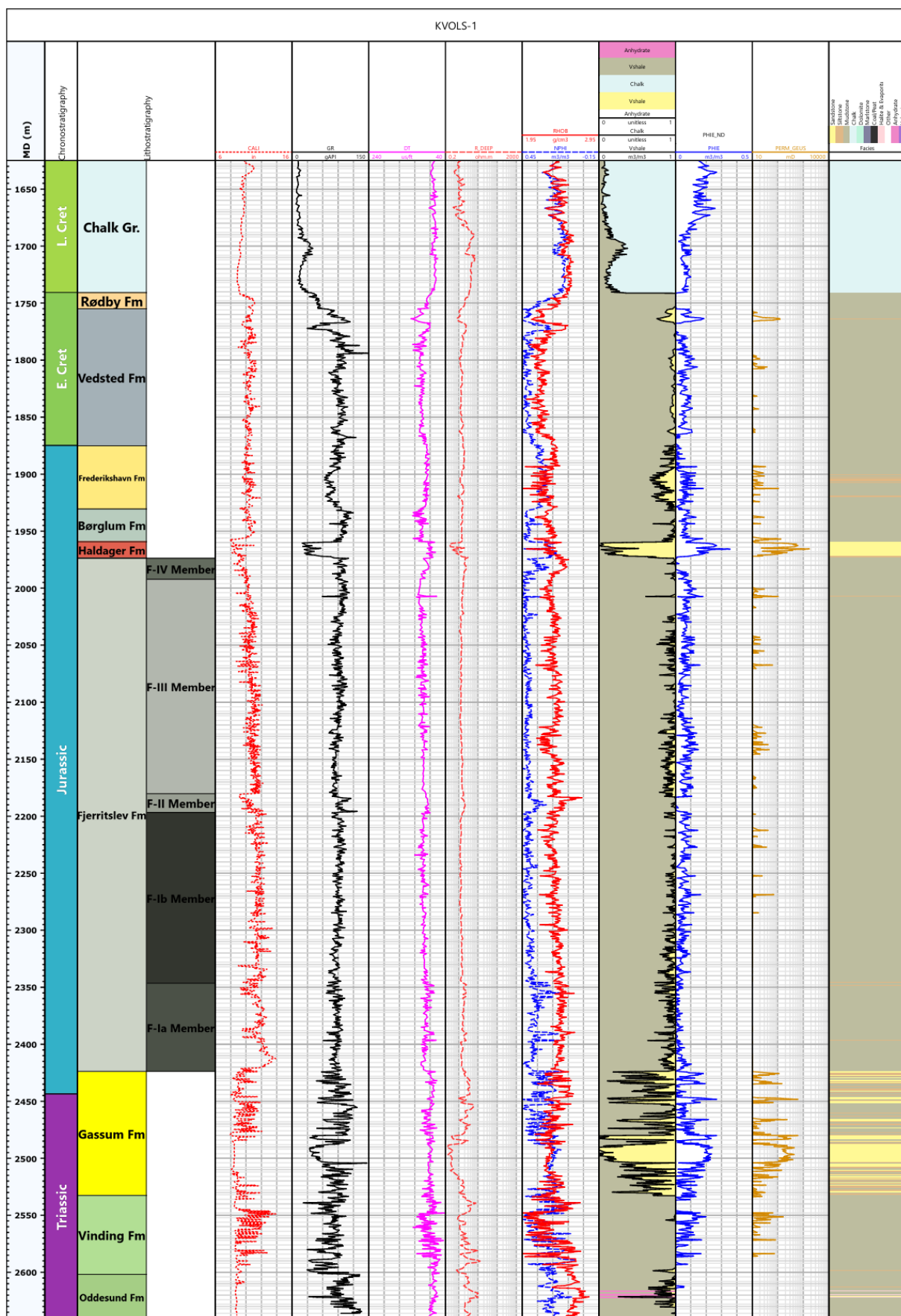
Links to well-log interpretations

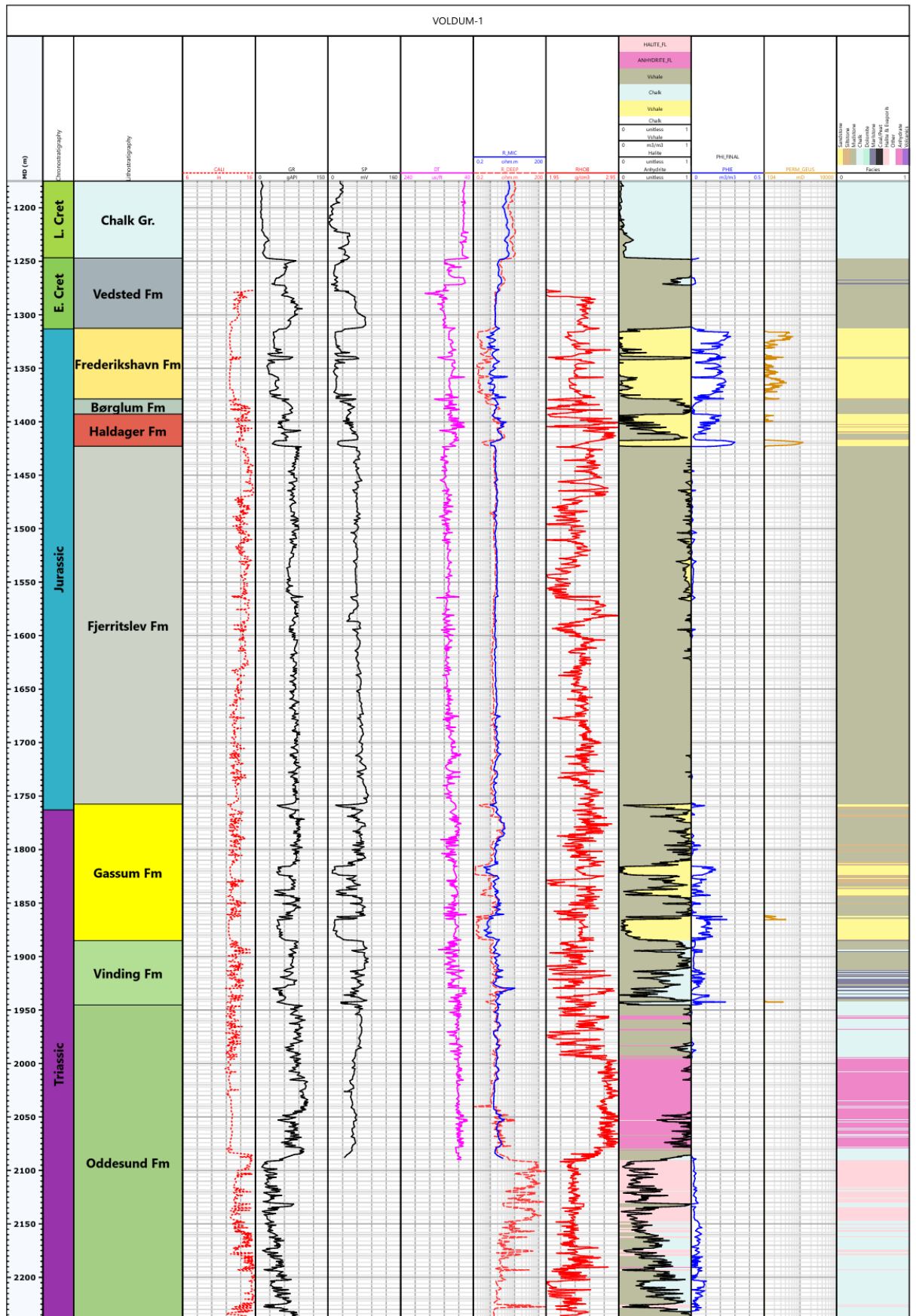
- [Gassum-1](#)
- [Grindsted-1](#)
- [Hobro-1](#)
- [Horsens-1](#)
- [Kvols-1](#)
- [Løve-1](#)
- [Mejrup-1](#)
- [Nøvling-1](#)
- [Rønde-1](#)
- [Skive-1](#)
- [Voldum-1](#)



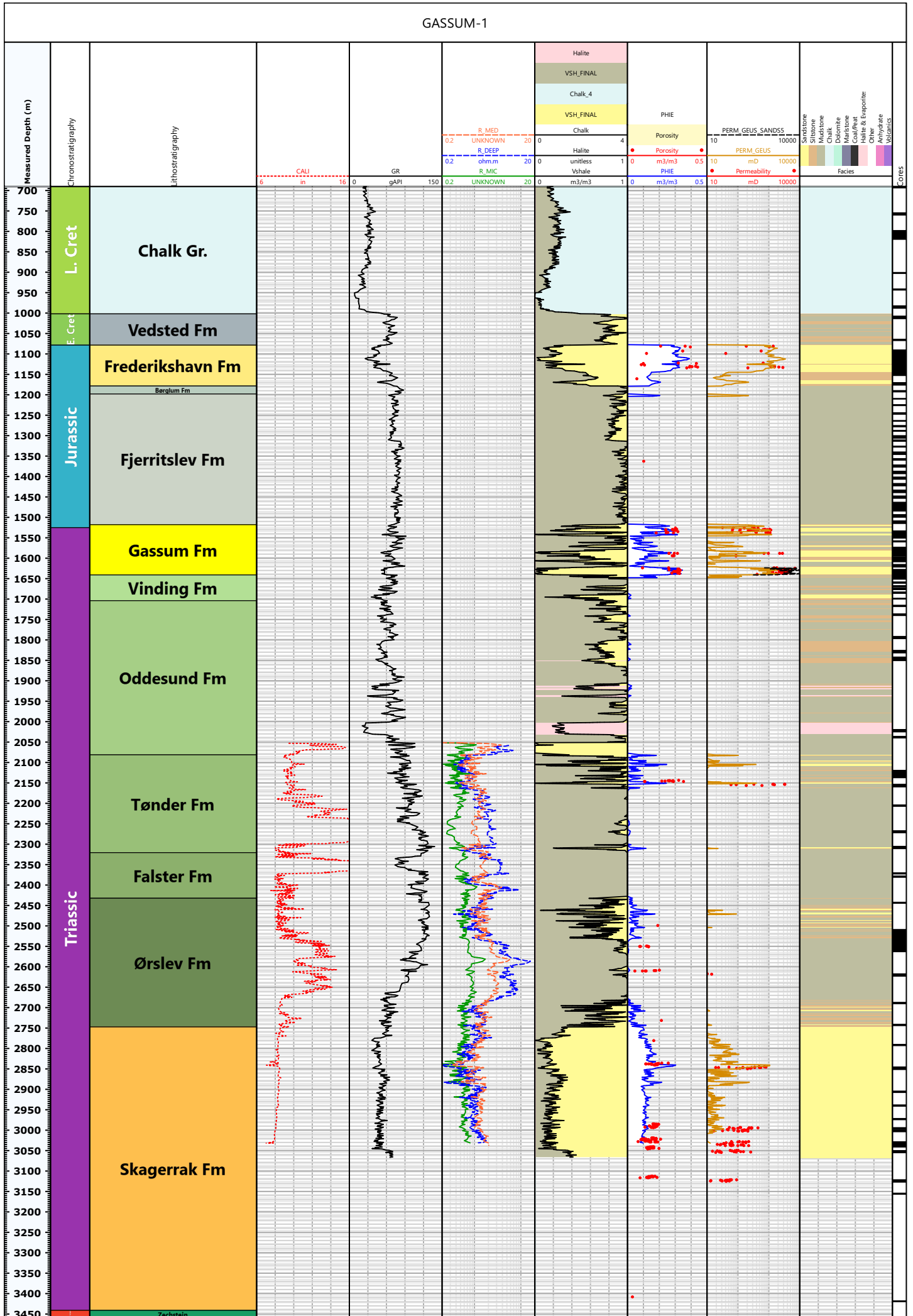




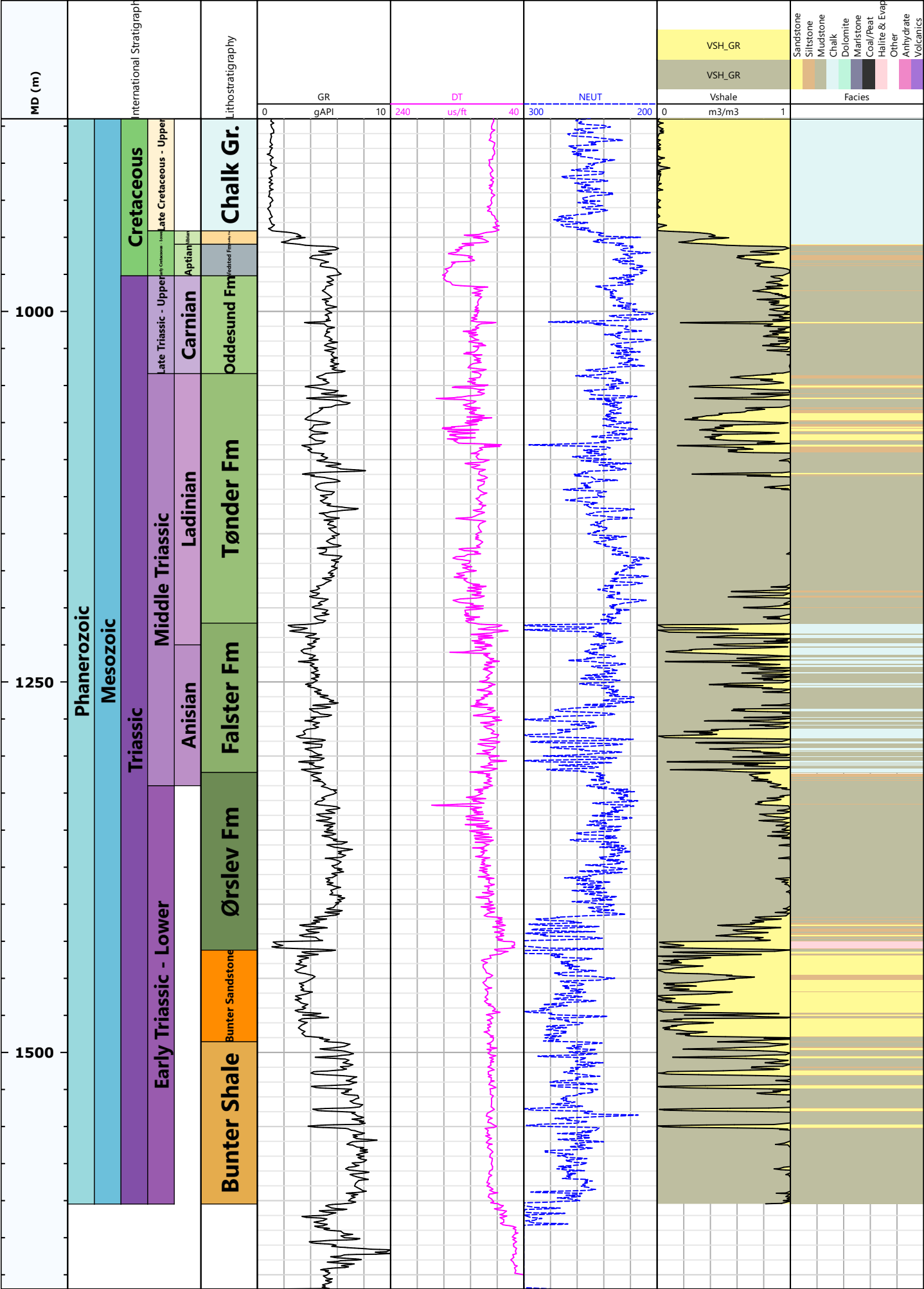




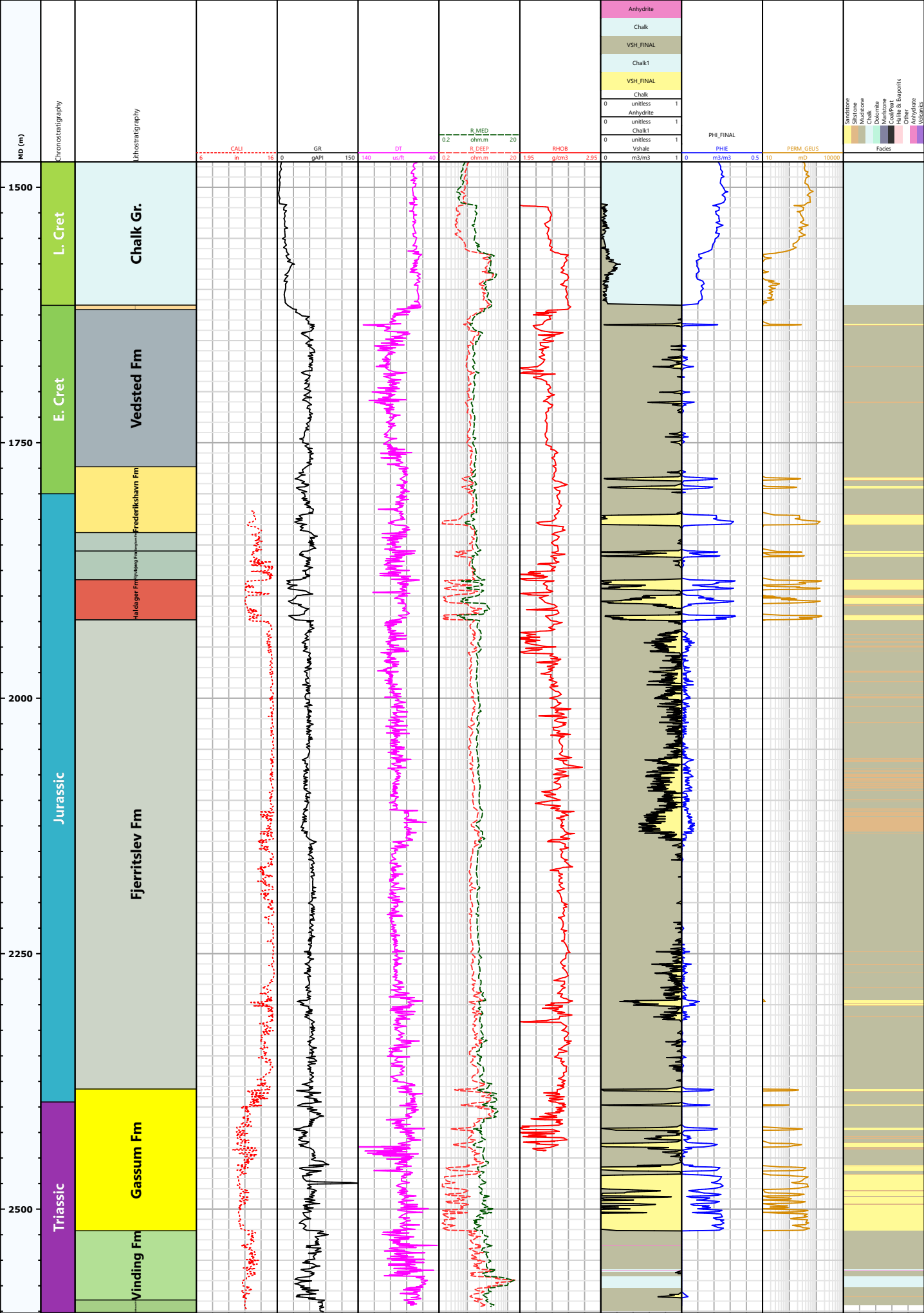
GASSUM-1



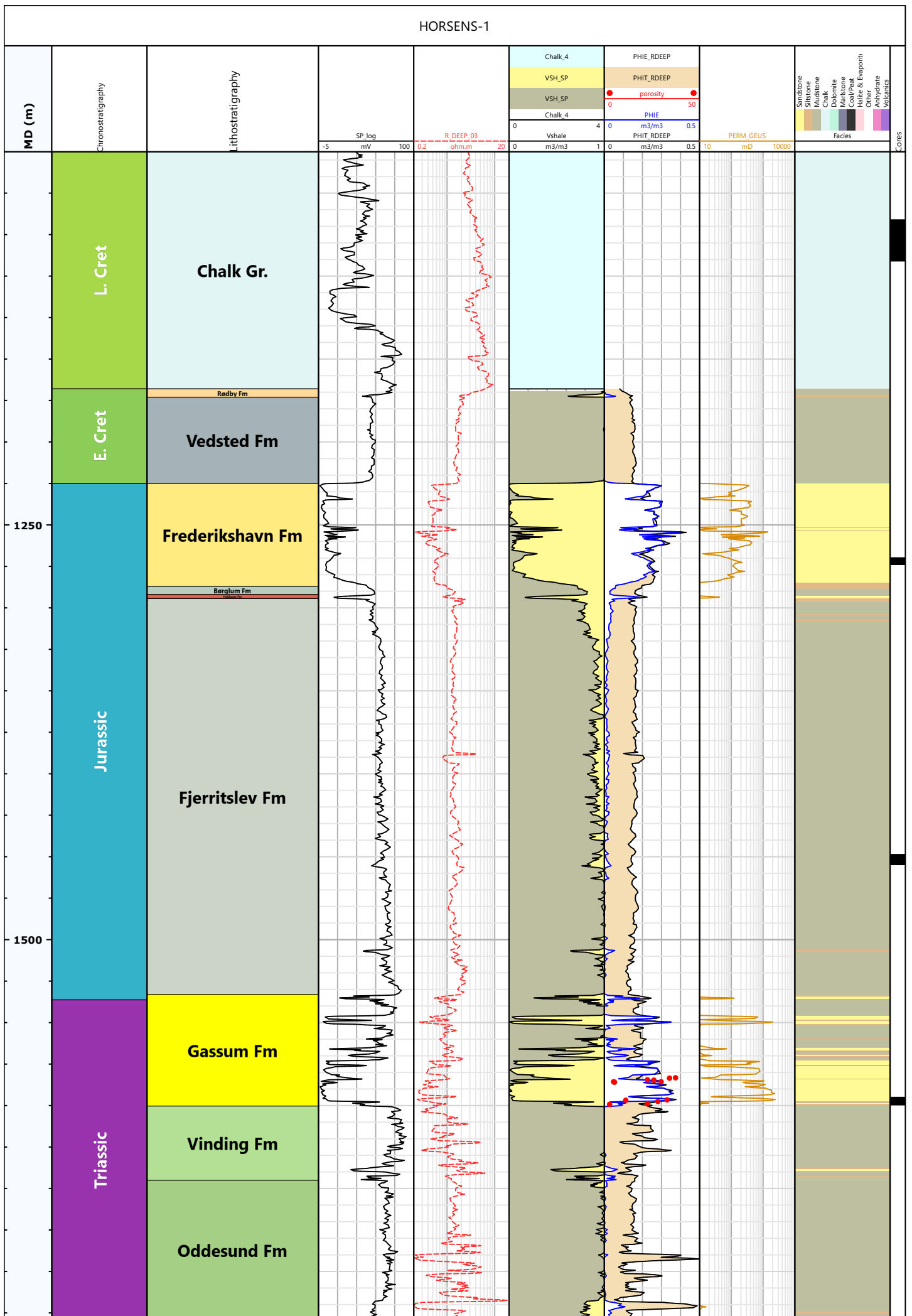
GRINDSTED-1

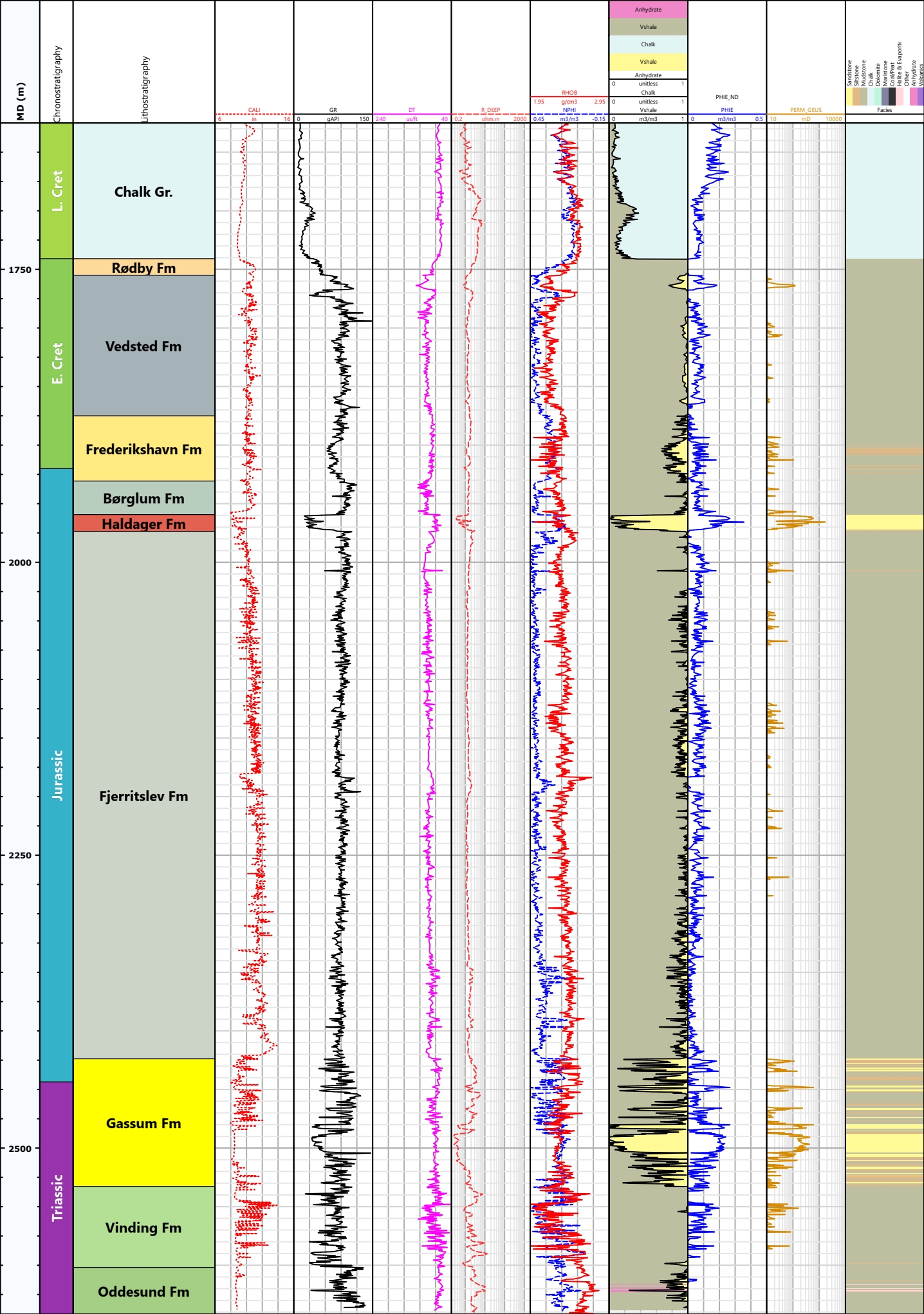


HOBRO-1

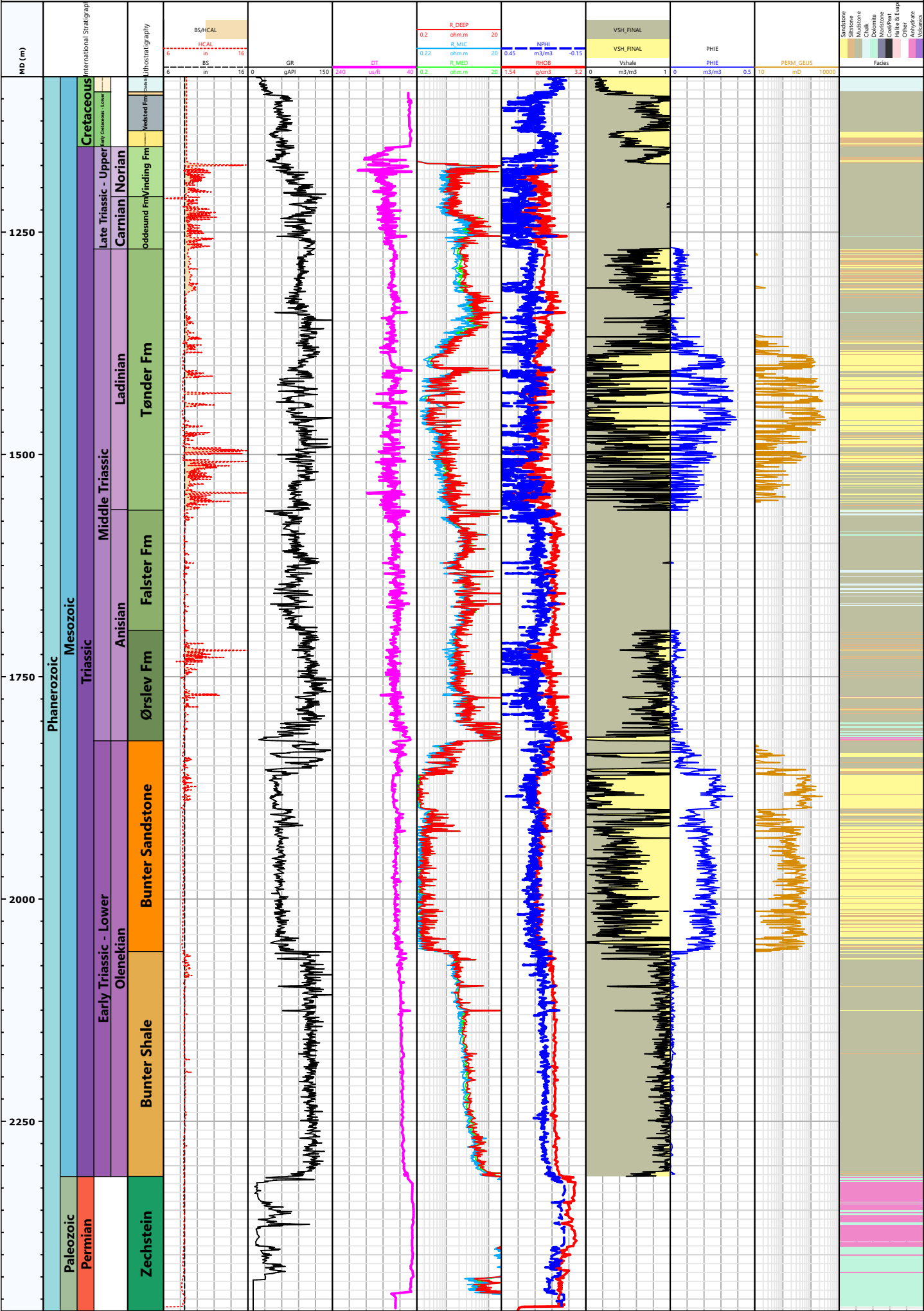


HORSENS-1

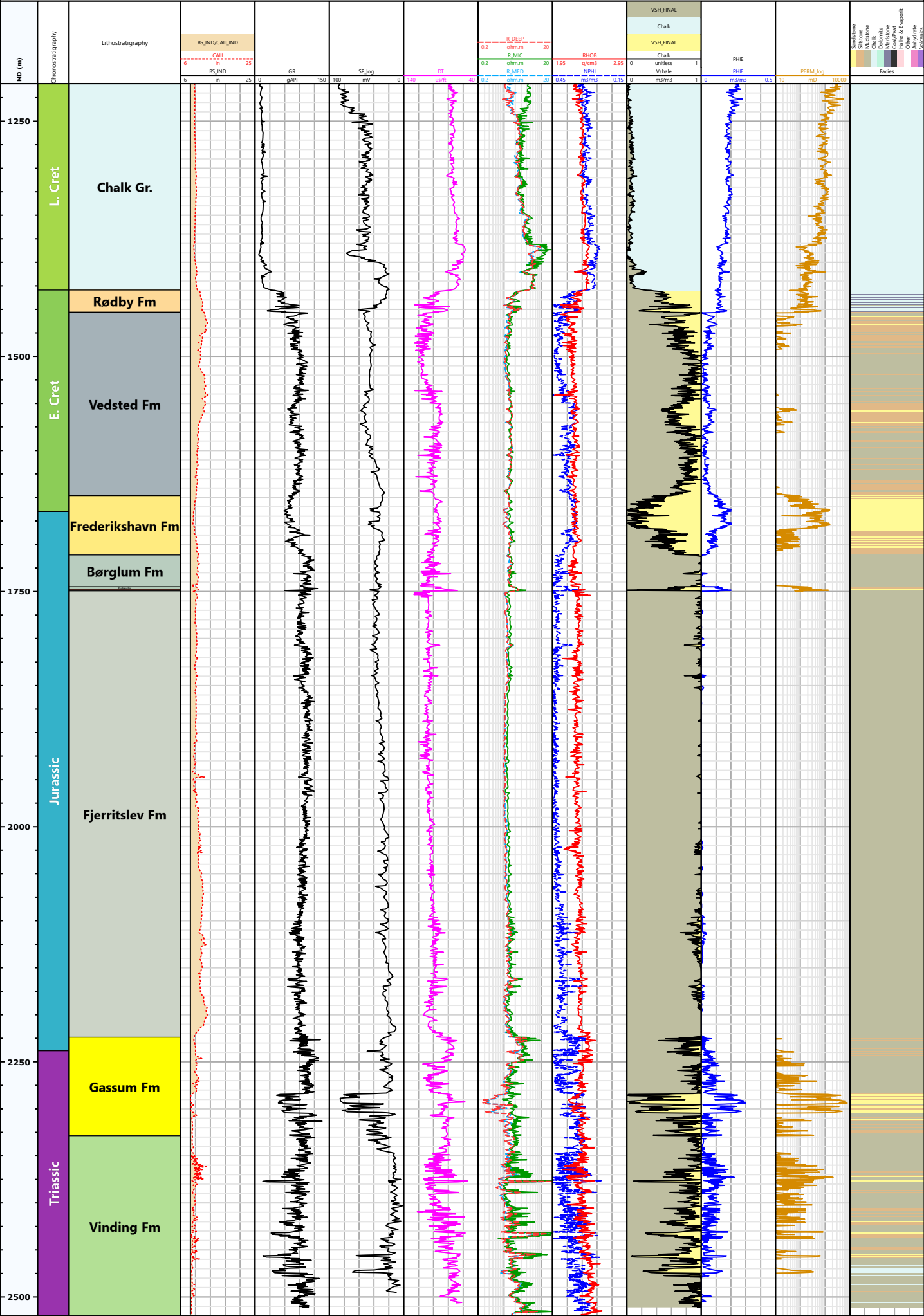




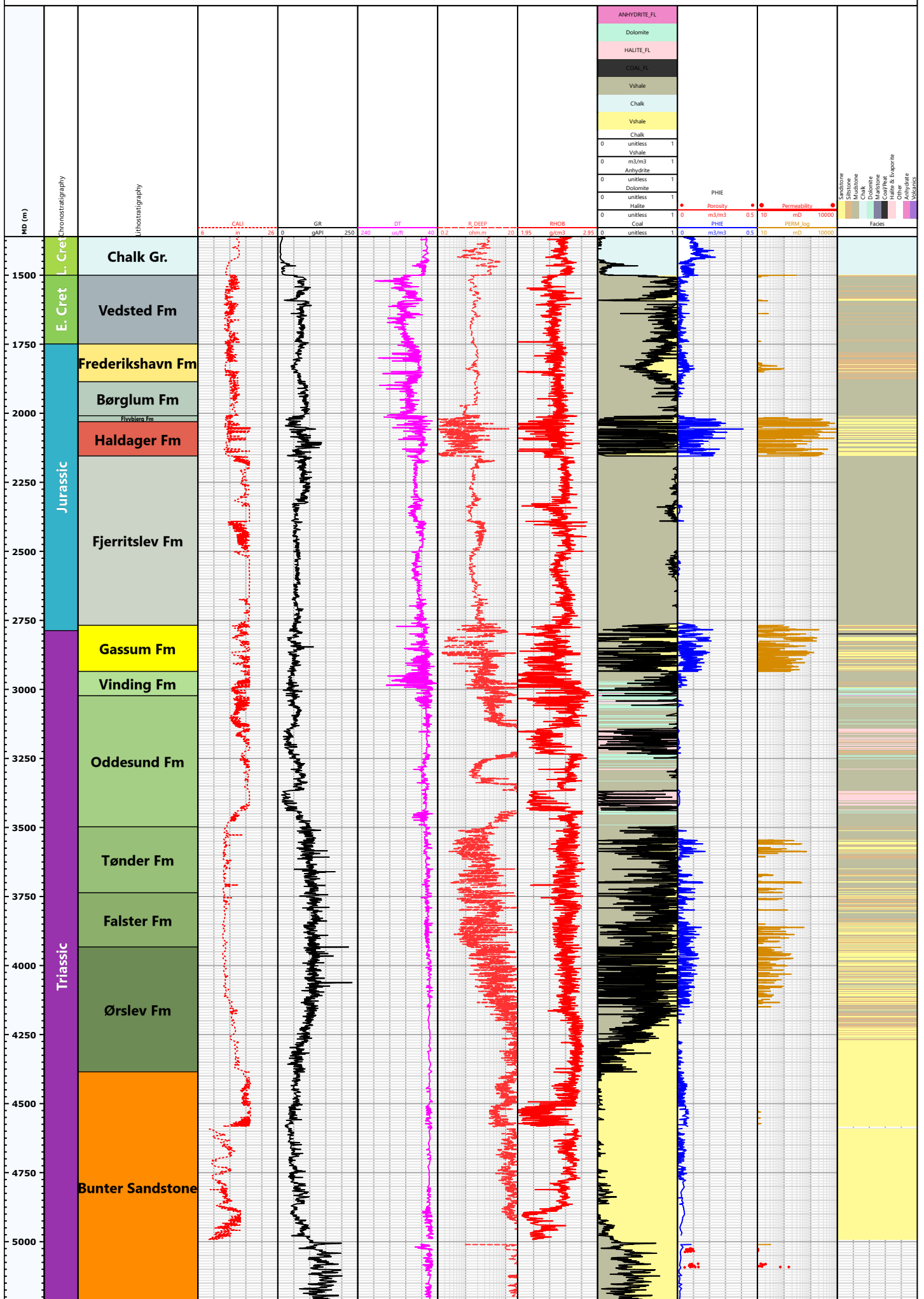
LOEVE-1



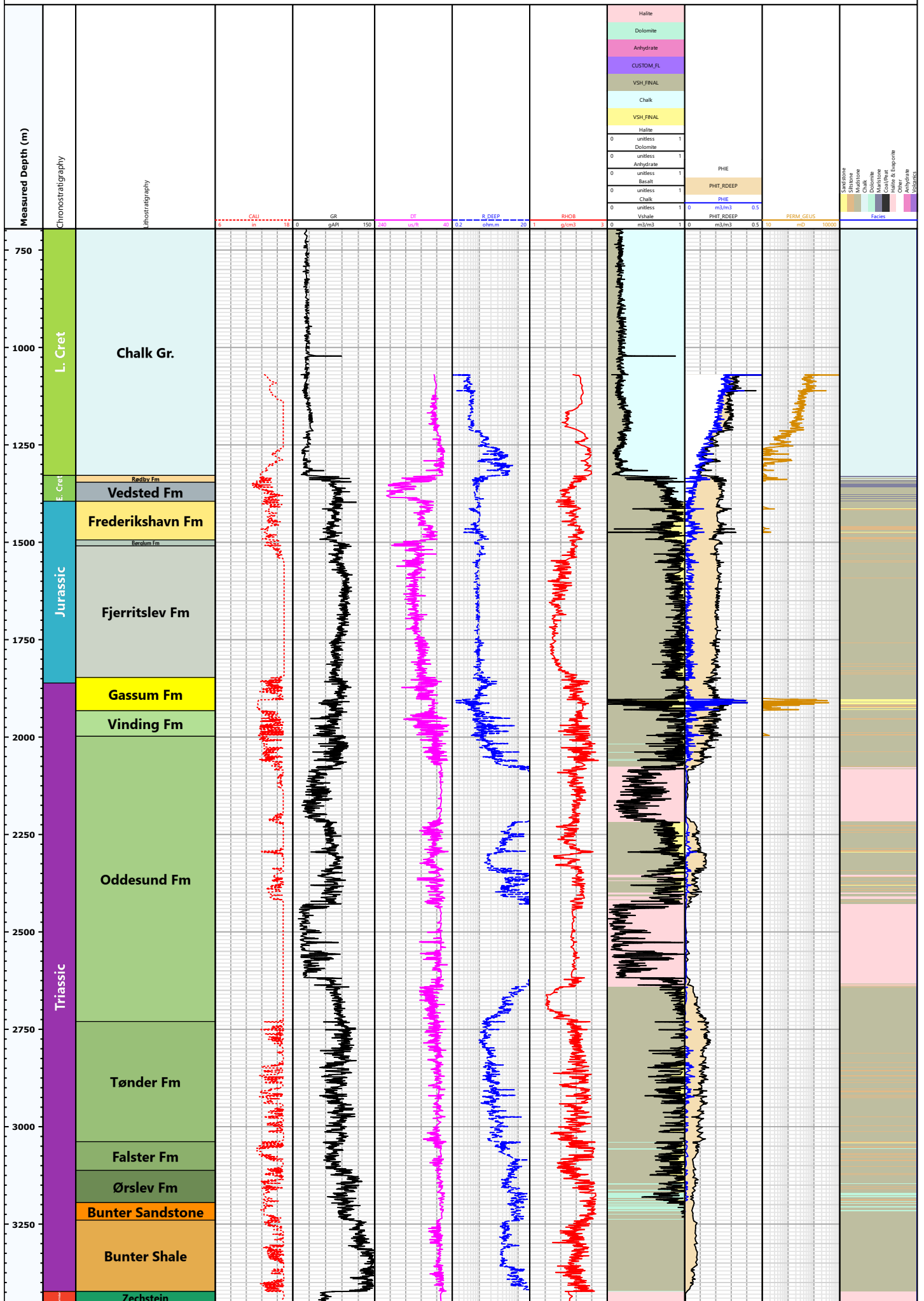
MEJRUP-1



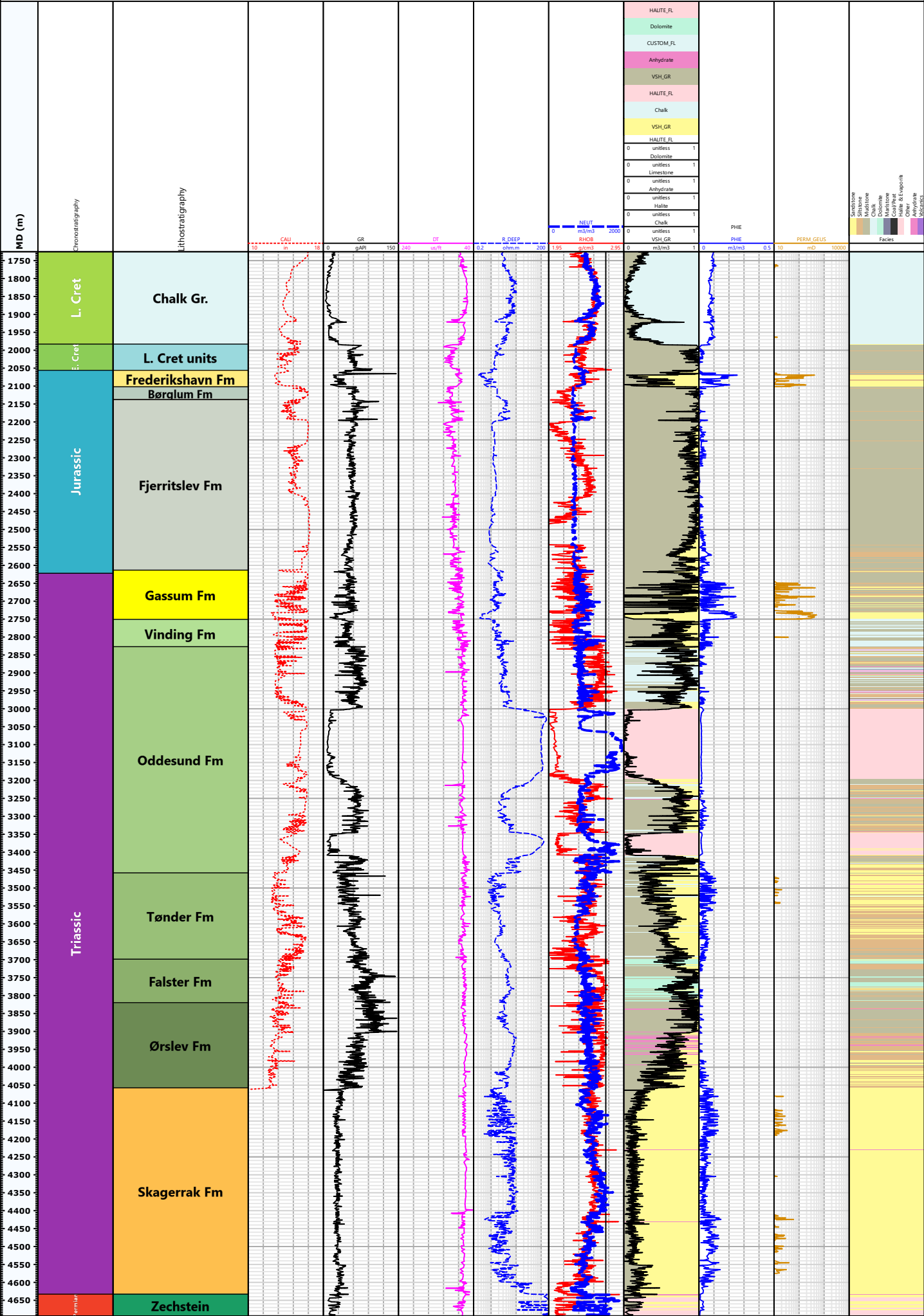
MORS-1

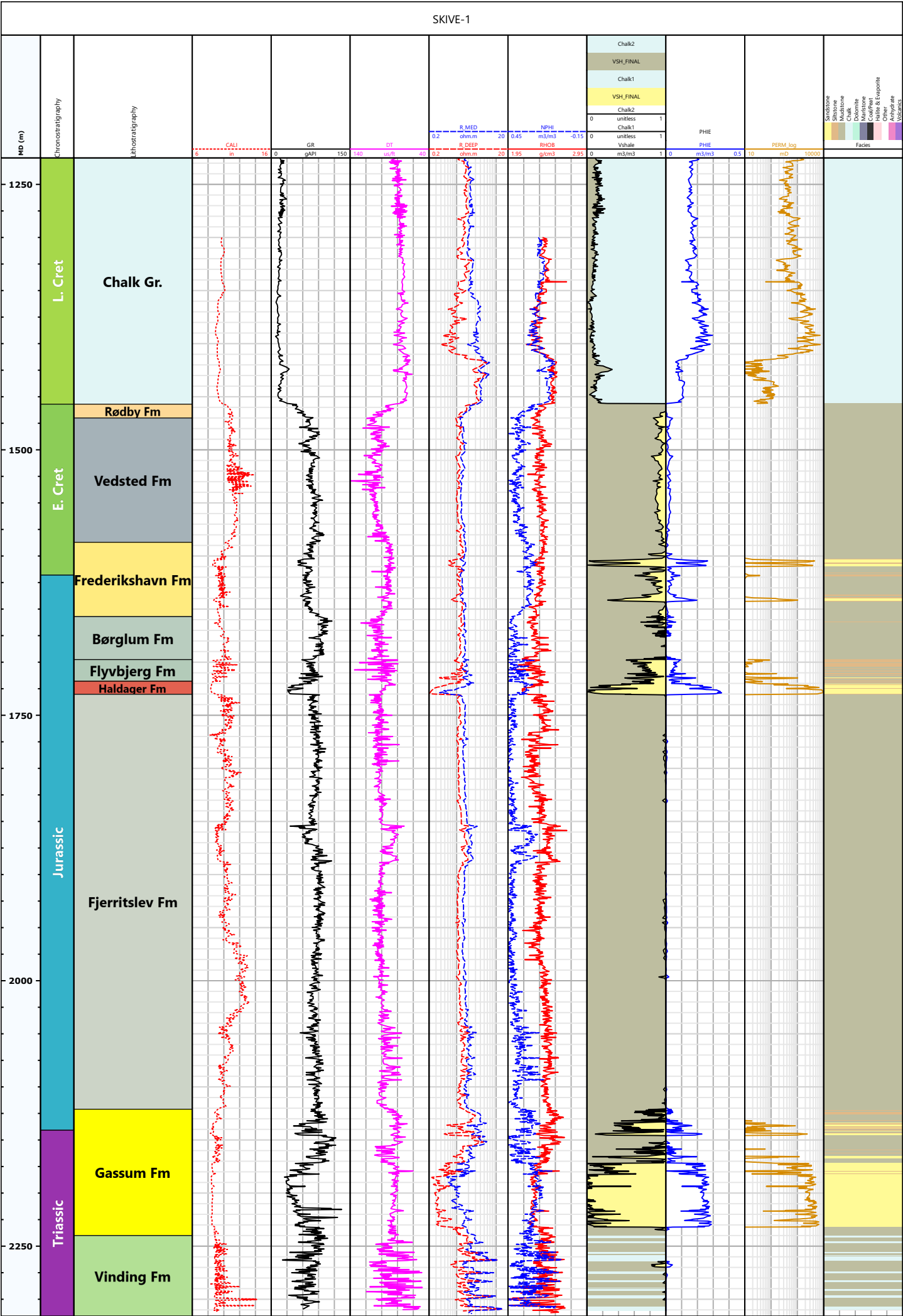


NOEVLING-1

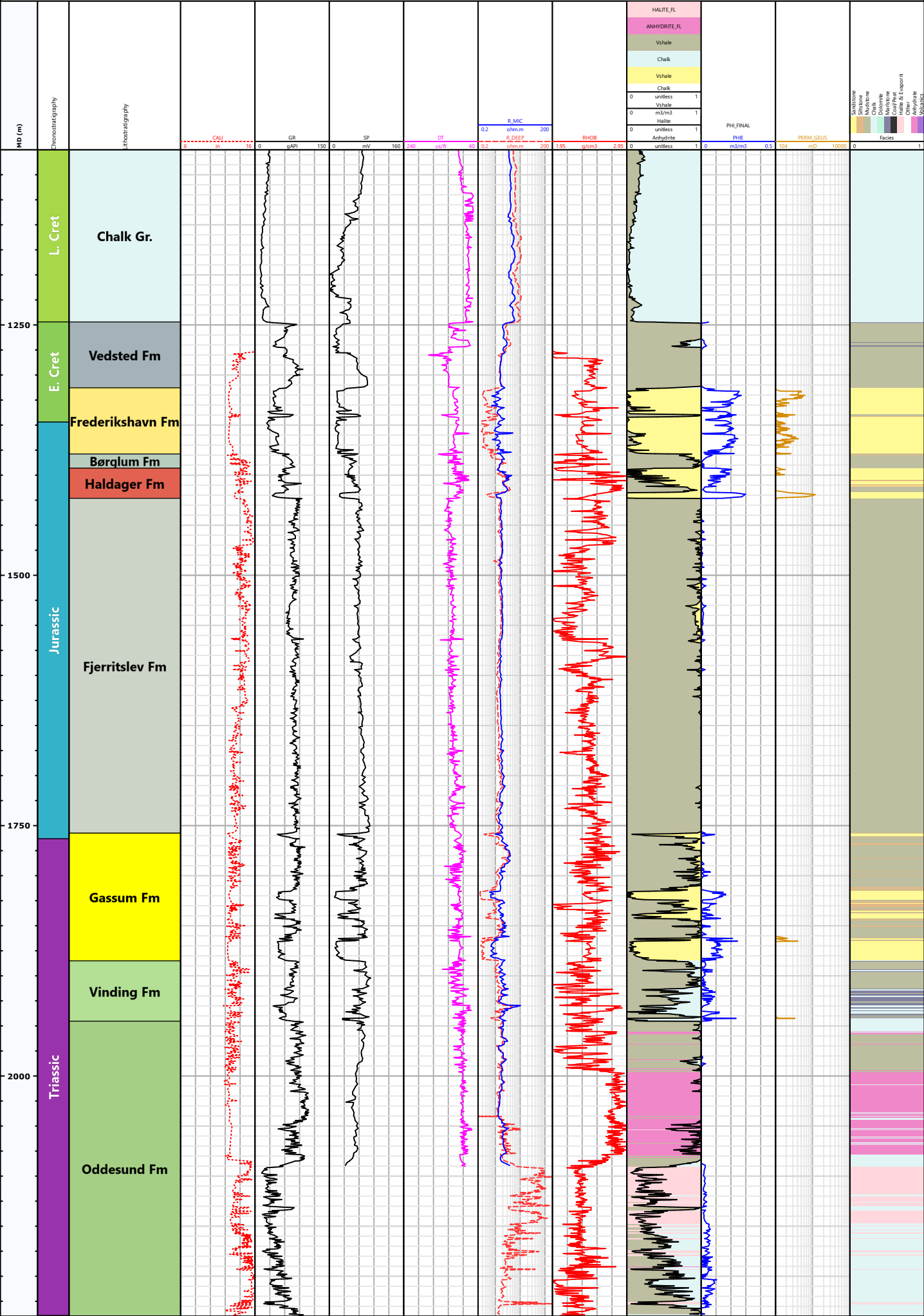


ROENDE-1





VOLDUM-1



Appendix B – Biostratigraphy (See Chapter 7)

Links to stratigraphic charts

- Gassum-1
- Grindsted-1
- Hobro-1
- Horsens-1
- Kvols-1
- Løve-1
- Mejrup-1
- Nøvling-1
- Skive-1
- Vinding-1
- Voldum-1

Introduction

No wells penetrate the Thorning structure. Therefore, the stratigraphy presented in the present report is based on data from a number of wells in a larger area surrounding the structure, including Gassum-1, Grindsted-1, Hobro-1, Horsens-1, Kvols-1, Løve-1, Mejrup-1, Nøvling-1, Skive-1, Vinding-1 and Voldum-1.

The present summary of the biostratigraphy in these 11 wells is mainly focused on the time interval represented by the Gassum- and Fjerritslev formations, but also the Cretaceous succession has been evaluated. The biostratigraphic subdivisions for these intervals in the studied wells are partly based on published data and reports from the GEUS archive and partly from new analysis performed by GEUS biostratigraphers. The biostratigraphy has been used to guide the sequence stratigraphic and lithostratigraphic framework for each well and for the correlations between the wells.

For each well a link is given to two different digital stratigraphic summary charts as these contain too many details to be seen in a printed version. One chart focuses on the Gassum- and Fjerritslev formations and combines the chronostratigraphy, lithostratigraphy, biostratigraphy and sequence stratigraphy and further include the bio-events and biozonations for the succession representing these two formations and their lower and upper boundaries. Another chart shows the overall stratigraphy for the full well, combining the biostratigraphy, chronostratigraphy, lithostratigraphy and sequence stratigraphy.

Provenance data (Olivarius et al. 2022) are included in the summary charts from those wells from which such analysis have been made.

Zonations

The biostratigraphic zonations used include the ostracod zonation of Michelsen (1975a), the dinocyst zonation of Poulsen & Riding (2003) and a combination of the spore-pollen zonations of Lund (1977), Dybkjær (1991) and Lindström et al. (2023).

Biostratigraphic summary for each of the key-wells

The biostratigraphy summarised here for each well is based on data from reports and publications combined with new data from some of the wells.

Gassum-1

The succession in the Gassum-1 well referred to the Gassum- and Fjerritslev formations is represented by a close series of cores and the biostratigraphic data from this interval are based on these cores. The data comprise analysis of spores, pollen, dinoflagellate cysts (Nielsen 1983; Dybkjær 1988, 1991; Poulsen 1996) and ostracods (Michelsen 1975a).

The biostratigraphic data strongly support the lithostratigraphic subdivision for the Gassum-1 well presented in Nielsen & Japsen (1991). The boundary between the Gassum- and Fjerritslev formations is located in the lowermost Hettangian. The upper part of the Fjerritslev Formation (uppermost part of F-III Member and F-IV Member) is missing. The Fjerritslev

Formation is unconformably overlain by Upper Jurassic deposits referred to the Børglum Formation.

Grindsted-1

No deposits from the Gassum- and Fjerritslev formations have been penetrated in this well. There is an unconformity from the Carnian (Upper Triassic) to the Lower Cretaceous. The precise age of the Lower Cretaceous deposits overlying the Triassic are not known. According to the Completion Report (1958) these deposits may even be of Jurassic age. Very few biostratigraphic data exists from this well and these are included in the Completion Report.

Hobro-1

A series of sidewall-cores through the interval from the lower Frederikshavn Formation down to the lower part of the Gassum Formation were analysed for their content of spores, pollen and dinoflagellate cysts by Bertelsen (FB) (Lyngsø et al. 1974).

Michelsen (OM) (in Lyngsø et al. 1974) studied ostracods from a very dense series of ditch cuttings samples from the Haldager Sand Formation down to the basal part of the Gassum Formation. The samples in the Haldager Sand Formation and the upper part of the Fjerritslev Formation were barren of ostracods. Except for one species recorded in the lowermost part of the formation, all the ostracods recorded from the Gassum Formation were interpreted as being caved from younger parts of the succession.

The results of these analysis strongly support the lithostratigraphic subdivision by Nielsen & Japsen (1991) of the succession referred to the Gassum- and Fjerritslev formations. The boundary between the Gassum- and Fjerritslev formations is located in the lowermost Hettangian. The uppermost part of the F-IV Member of the Fjerritslev Formation is missing, and the formation is unconformably overlain by the Middle Jurassic Haldager Sand Formation.

Horsens-1

Poulsen (1996) analysed a single core sample from the lower part of the Fjerritslev Formation for its content of dinocysts and dated it as early Sinemurian.

Michelsen (1975a) studied the ostracods in the interval referred to the Fjerritslev Formation and dated the interval to Hettangian – Upper Pliensbachian.

There is an inconsistency in the location of the top of the Gassum Formation from Nielsen & Japsen (1991) and the present study. Nielsen & Japsen suggested that the top of the formation should be located at 1506 m, while the top in the present study is located at 1533.7 m. The biostratigraphy cannot solve this issue.

The top of the Fjerritslev Formation is late Pliensbachian in age indicating that the youngest part of the formation has been removed by erosion. It is unconformably overlain by the Middle Jurassic Haldager Sand Formation.

Kvols-1

Based on a mixture of ditch cuttings samples and sidewall core samples a series of palyno-events was presented by Robertson Research (1976a, 1983a) from the Lower Cretaceous down to the base of the well.

Ostracod data exists only from the upper part of the Fjerritslev Formation (Michelsen 1989).

The results of these analysis strongly support the lithostratigraphic subdivision by Nielsen & Japsen (1991) of the succession referred to the Gassum- and Fjerritslev formations. The boundary between the Gassum- and Fjerritslev formations is located in the Hettangian. The uppermost part of the F-IV Member of the Fjerritslev Formation is missing, and the formation is unconformably overlain by the Middle Jurassic Haldager Sand Formation.

The biostratigraphy in the Kvols-1 wells indicate a different correlation of sequence stratigraphic surfaces with e.g. the Gassum-1 well at several stratigraphic levels within the Fjerritslev Formation than the correlations presented in the present study, which mainly is based on log-correlations and sequence stratigraphy. A new, more detailed, biostratigraphic study in the Kvols-1 well is therefore suggested.

Løve-1

No deposits from the Gassum- and Fjerritslev formations have been penetrated in this well. Only 3 samples have been analysed for biostratigraphy (palynology) from this well (unpublished GEUS data). The results from these samples supported the overall interpretation indicating that there is an unconformity from the lower Rhaetian (Upper Triassic) to the Lower Cretaceous. The precise age of the Lower Cretaceous deposits overlying the Triassic are not known, but they are interpreted to belong to the Frederikshavn Formation.

Mejrup-1

Based on a mixture of ditch cuttings samples and sidewall core samples a series of palyno-events was presented by Robertson Research (1987). A supplementary study on a few samples from the Vinding and Gassum formations was made by Koppelhus - the results of which are presented in Nielsen (1995).

The results of the biostratigraphic studies strongly support the lithostratigraphic subdivision by Nielsen & Japsen (1991) of the succession referred to the Gassum- and Fjerritslev formations. The boundary between the Gassum- and Fjerritslev formations is located in the lower Hettangian. Most of the F-III Member and all of the F-IV Member of the Fjerritslev Formation are missing, and the formation is unconformably overlain by the Middle Jurassic Haldager Sand Formation.

Nøvling-1

A series of palyno-event was presented by Robertson Research (1982; 1983b) based on ditch cuttings samples. However, it was not a very detailed study and therefore supplementary analysis were made for the present study. A study of the ostracods present in ditch cuttings samples from the Fjerritslev Formation was presented by Michelsen (1975).

The boundary between the Gassum- and Fjerritslev formations is located in the lower Hettangian. Most of the F-III Member and all of the F-IV Member of the Fjerritslev Formation are missing, and the formation is unconformably overlain by the Upper Jurassic Børglum Formation.

There is generally a good correspondence between the biostratigraphic data and the lithostratigraphic subdivision by Nielsen & Japsen (1991). However, in contrast to the interpretation shown here (partly based on the biostratigraphic data and partly on the sequence stratigraphy) suggesting that the lower part of the F-III Member is present, Nielsen & Japsen (1991) suggested that all of the F-III Member is missing in this well.

Skive-1

Based on sidewall-core samples, a series of palyno-events was presented by Robertson Research (1976b) from the Lower Cretaceous down to the base of the well.

The results of these analysis strongly support the lithostratigraphic subdivision by Nielsen & Japsen (1991) of the succession referred to the Gassum- and Fjerritslev formations. The boundary between the Gassum- and Fjerritslev formations is located in the Hettangian. The F-IV Member of the Fjerritslev Formation is missing, and the formation is unconformably overlain by the Middle Jurassic Haldager Sand Formation.

Vinding-1

Based on a combination of core samples and ditch cuttings samples, Michelsen (1975a) subdivided the Fjerritslev Formation into ostracod zones. In addition, Poulsen (1996) analysed a few core samples for dinocysts.

As there is no biostratigraphic data from the lower part of the Fjerritslev Formation and downwards, and furthermore no geophysical logs from this well, the location of the upper boundary of the Gassum Formation is based on lithology of ditch cuttings samples analysed while drilling the well.

An unconformity is suggested to be present on top of the Upper Sinemurian, but due to missing data it is not possible to state what is overlying the Sinemurian. The only information is that there is Lower Ryazanian present further up section.

Voldum-1

A few sidewall-core samples have been analysed palynologically by Bertelsen (1974). Only one sample represents the Gassum Formation, three the Fjerritslev Formation while six samples represent the overlying Middle Jurassic – Lower Cretaceous units. All these samples

were also examined for the present study in order to try to identify additional stratigraphically important taxa.

Michelsen (1975b) analysed ostracods in a series of ditch cuttings samples covering the Vinding, Gassum and Fjerritslev formations. The resulting data are rather sparse as several of the samples were either barren or characterised by caved material. However, three ostracod zones were identified.

The results of these analysis generally support the lithostratigraphic subdivision of the succession referred to the Gassum- and Fjerritslev formations. The upper boundary of the Gassum Formation is located within the lower Hettangian. The upper part of the F-III Member and the F-IV Member of the Fjerritslev Formation are missing, and the formation is unconformably overlain by the Middle Jurassic Haldager Sand Formation.

References

- Bertelsen, F., 1974: Voldum-1 - Datering af side wall core prøver. Unpublished DGU report.
- Danish American Prospection Company (1958): Grindsted-1, Completion report.
- Dybkjær, K. 1988. Palynological zonation and stratigraphy of the Jurassic section in the Gassum No.1-borehole, Denmark. DGU Serie A, 21, 72pp.
- Dybkjær, K. 1998. Datering og palynofacies-analyse af 6 udvalgte prøver fra Stenlille – boringerne. Danmarks og Grønlands Geologiske Undersøgelse Rapport 1998/75.
- Dybkjær, K. 1991: Palynological zonation and palynofacies investigation of the Fjerritslev Formation (Lower Jurassic – basal Middle Jurassic) in the Danish Subbasin. Danmarks Geologiske Undersøgelse Serie A 30, 1–150.
- Gassum-1, Completion report (1951). Compiled March 1993.
- Ineson, J.R. 1993. The Lower Cretaceous chalk play in the Danish Central Trough. Geological Society, London, Petroleum Geology Conference series, 4, 175–183.
- Ineson, J.R., Jutson, D.J. and Schiøler, P. 1997. Mid-Cretaceous sequence stratigraphy in the Danish Central Trough. Danmarks og Grønlands Geologiske Undersøgelser Rapport 1997/109, 60 pp.
- Japsen, P. 1998. Regional velocity–depth anomalies, North Sea chalk: a record of overpressure and Neogene uplift and erosion. AAPG Bull., 82, 2031–2074.
- Jensen, T.F, Holm, L., Frandsen, N. and Michelsen, O. 1986. Jurassic-Lower Cretaceous Lithostratigraphic Nomenclature for the Danish Central Trough. Danmarks Geologiske Undersøgelse Serie A 12, 65 pp. <https://doi.org/10.34194/seriea.v12.7031>
- Koppelhus, E.B. and Nielsen, L.H. 1994. Palynostratigraphy and palaeoenvironments of the Lower to Middle Jurassic Bagå Formation of Bornholm, Denmark. Palynology 18(1), 139–194.
- Larsen, G. 1966. Rhaetic–Jurassic– Lower Cretaceous sediments un the Danish Embayment (A heavy-mineral study). Geological Survey of Denmark, II Series, No. 91, 127 p. plus plates. <https://doi.org/10.34194/raekke2.v91.6882>
- Lauridsen, B.W., Lode, S., Sheldon, E., Frykman, P., Anderskov, K and Ineson, J. 2022. Lower Cretaceous (Hauterivian–Aptian) pelagic carbonates in the Danish Basin: new data

from the Vinding-1 well, central Jylland, Danmark. Bulletin of the Geological Society of Denmark, 71, 7–29. <https://doi.org/10.37570/bgsd-2022-71-02>

Lindström, S., Pedersen, G.K., Vosgerau, H., Hovikoski, J., Dybkjær, K. and Nielsen, L.H., 2023. Palynology of the Triassic–Jurassic transition of the Danish Basin (Denmark): a palynostratigraphic zonation of the Gassum – lower Fjerritslev formations. Palynology, DOI: 10.1080/01916122.2023.2241068

Lyngsø, F., Dinesen, A., Bang, I., Buch, A., Christensen, O.B., Bertelsen, F. and Michelsen, O. 1974. Hobro-1. The lithostratigraphical and biostratigraphical zonation – based upon well-site observations, studies of the logs run by “Dresser atlas” and micropaleontology. DGU report. 3pp. and 7 enclosures.

Mallon, A.J. and Swarbrick, R.E. 2002. A compaction trend for non-reservoir North Sea Chalk, Marine and Petroleum Geology, 19, 10, 527–539.

Mallon, A.J. and Swarbrick, R.E. 2008. Diagenetic characteristics of low permeability, non-reservoir chalk from the Central North Sea, Marine and Petroleum Geology, 25, 10, 1097–1108. <https://doi.org/10.1016/j.marpetgeo.2007.12.001>

Michelsen, O., 1975a. Lower Jurassic ostracods of the Danish Embayment. Danmarks Geologiske Undersøgelse, II Række, nr. 104. 287pp.

Michelsen, O., 1975b. Foreløbig stratigrafisk inddeling baseret på ostracoder. Unpublished DGU report.

Michelsen, O. 1989. Revision of the Jurassic lithostratigraphy of the Danish Subbasin. DGU Serie A 24, 21pp.

Michelsen, O., Nielsen, L.H., Johannessen, P.N., Andsbjerg, J. and Surlyk, F. 2003. Jurassic lithostratigraphy and stratigraphic development onshore and offshore Denmark. In: Ineson, J.R. and Surlyk, F. (eds): The Jurassic of Denmark and Greenland. Geological Survey of Denmark and Greenland Bulletin 1, p. 145–216. <https://doi.org/10.34194/geusb.v1.4651>

Nielsen, L.H. 1995. Genetic stratigraphy of the Upper Triassic – Middle Jurassic deposits of the Danish Basin and Fennoscandian Border Zone. Ph.D. Thesis, part 4.

Nielsen, L.H., 2003. Late Triassic – Jurassic development of the Danish Basin and the Fennoscandian Border Zone, southern Scandinavia. Geological Survey of Denmark and Greenland Bulletin 1, 459–526.

Nielsen, L.H. and Japsen, P. 1991. Deep wells in Denmark 1935-1990. Lithostratigraphic subdivision. Danmarks Geologiske Undersøgelse, DGU Serie A, No. 31, 177 pp.

Nielsen, L., Boldreel, L.O., Hansen, T.M., Lykke-Andersen, H., Stemmerik, L., Surlyk, F. and Thybo, H. 2011. Integrated seismic analysis of the Chalk Group in eastern Denmark – Implications for estimates of maximum palaeo-burial in southwest Scandinavia. Tectonophysics, 511, 14-26. doi:10.1016/j.tecto.2011.08.010

Nielsen, M.V. 1983. Palynologisk undersøgelse af Øvre Trias i Gassum-1 boringen, Volume 1+2. Master thesis, University of Aarhus.

Olivarius, M., Vosgerau, H., Nielsen, L.H., Weibel, R., Malkki, S.N., Heredia, B.D. and Thomsen, T.B. 2022. Maturity matters in provenance analysis: Mineralogical differences explained

by sediment transport from Fennoscandian and Variscan sources. *Geosciences* 12, 308, 24 pp.

Poulsen, N.E., 1996. Dinoflagellate cysts from marine Jurassic deposits of Denmark and Poland. *AASP contribution series* 31, 227pp.

Poulsen, N.E., Riding, J.B. 2003. The Jurassic dinoflagellate cyst zonation of Subboreal Northwest Europe. *Geological Survey of Denmark and Greenland Bulletin* 1, 115–144.

Robertson Research International Ltd., 1976a: Kvols-1, The Biostratigraphy of the interval 60'-8660'.

Robertson Research International Ltd., 1976b: Skive-1, The biostratigraphy of the interval 70'-7600'.

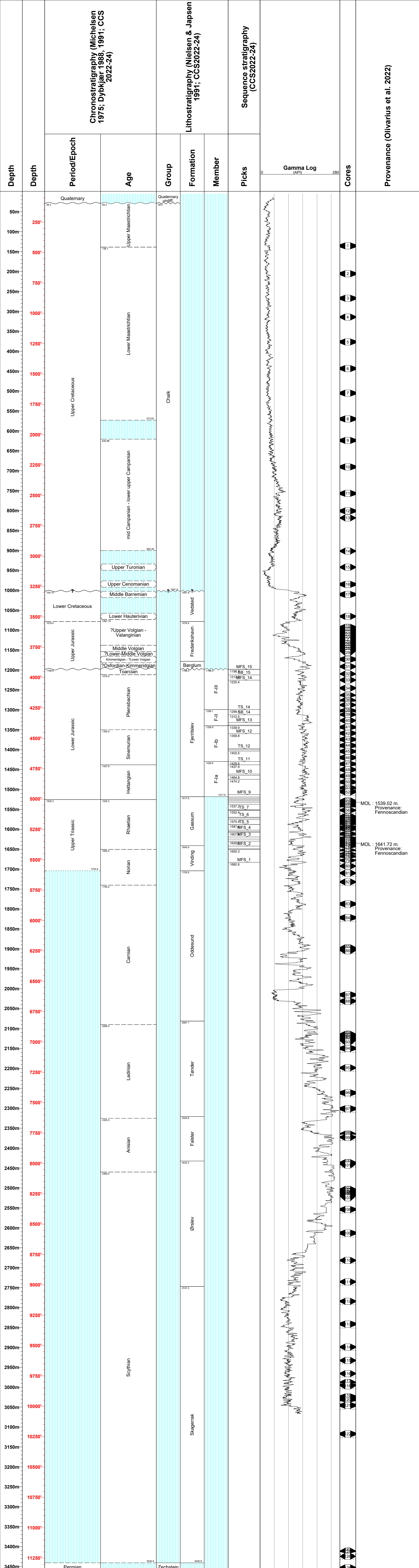
Robertson Research International Ltd., 1982: Preliminary biostratigraphic breakdowns of Nøvling-1, B/11-1, B/11-2, C/15-1 and D/18-1 wells - Preliminary reports B25 to B29.

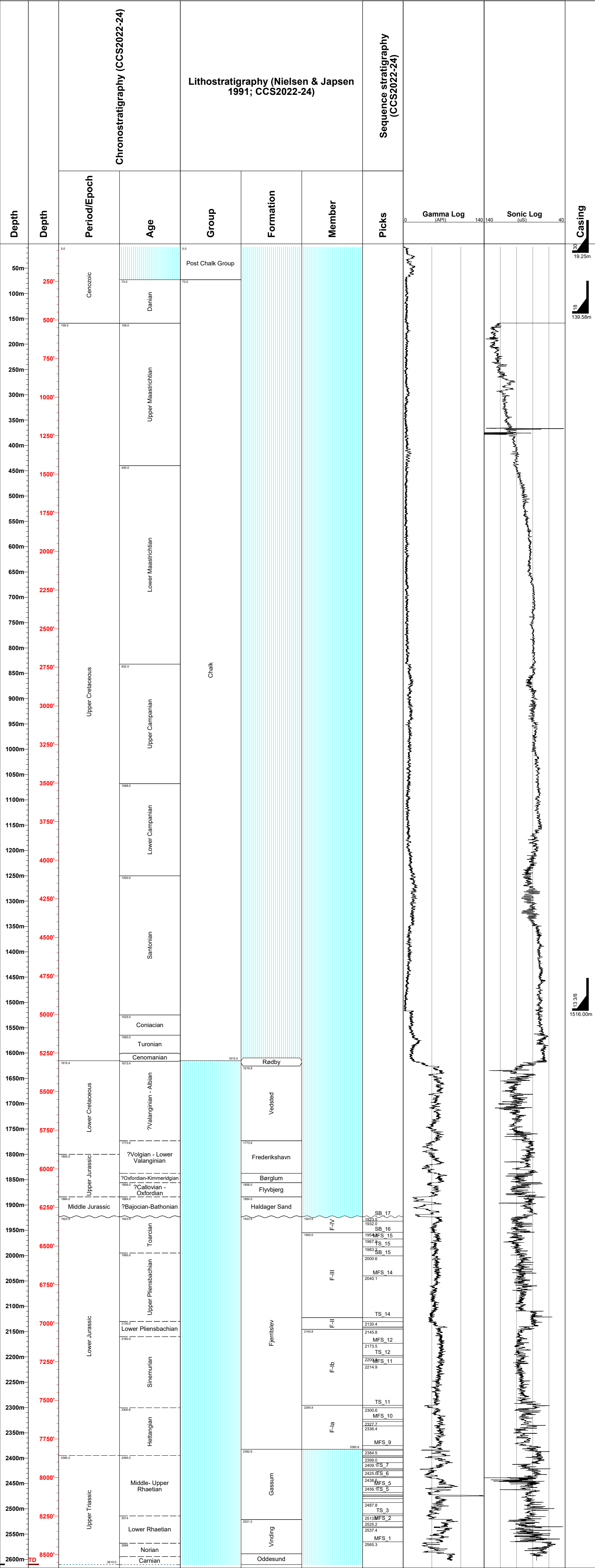
Robertson Research International Ltd., 1983a: Preliminary petroleum geochemistry results of L-1, R-1, S-1 and U-1 wells - Preliminary reports G19 to G22, and preliminary biostratigraphic breakdowns of W-1 and Kvols-1 wells (B22 to B23).

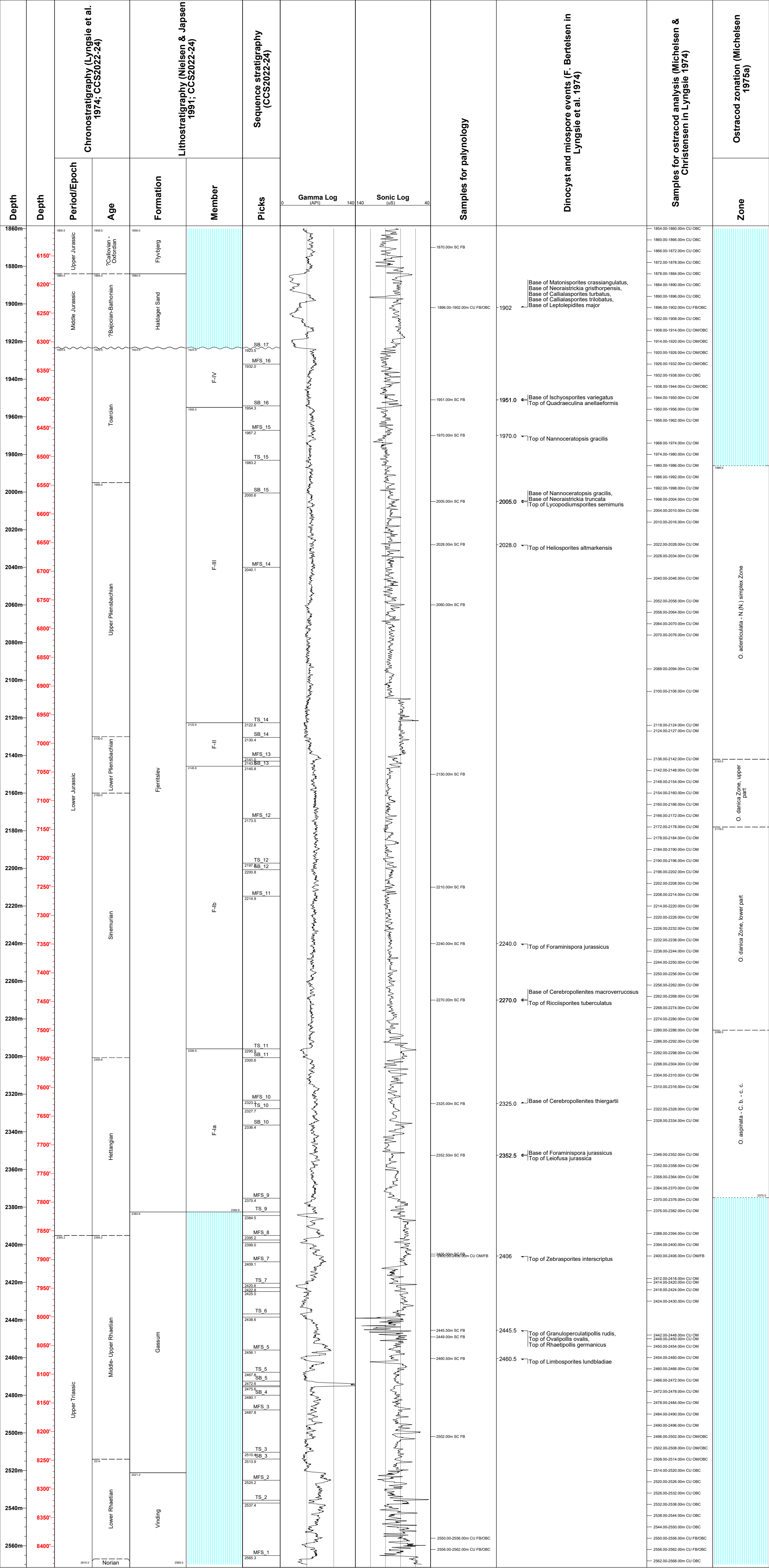
Robertson Research International Ltd., 1983b: The Danish North Sea area: The stratigraphy and petroleum geochemistry of the Jurassic to Tertiary sediments, Volume 1,2,4,6.

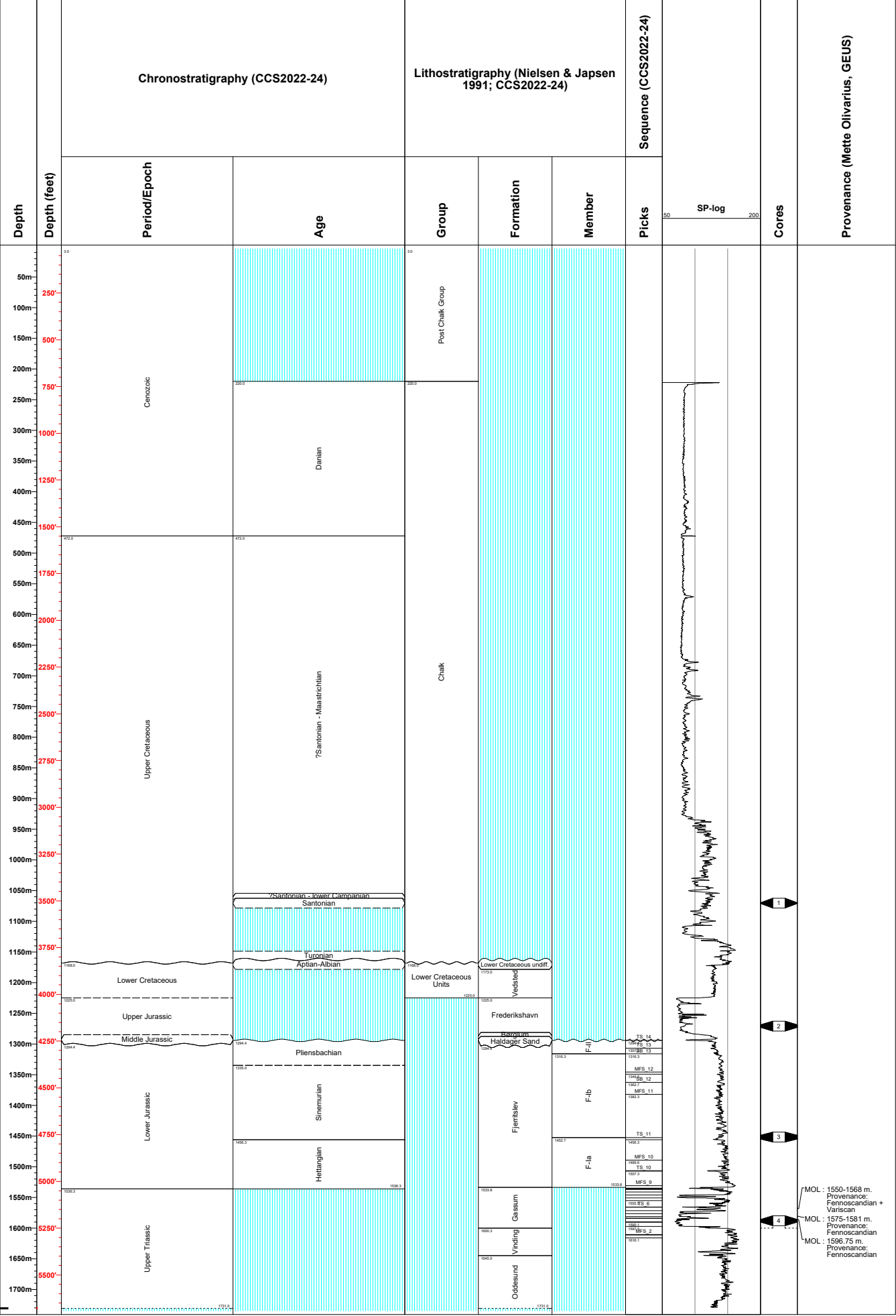
Robertson Research International Ltd., 1987: Biostratigraphy of the interval 120'-8308' TD Mejrups-1.

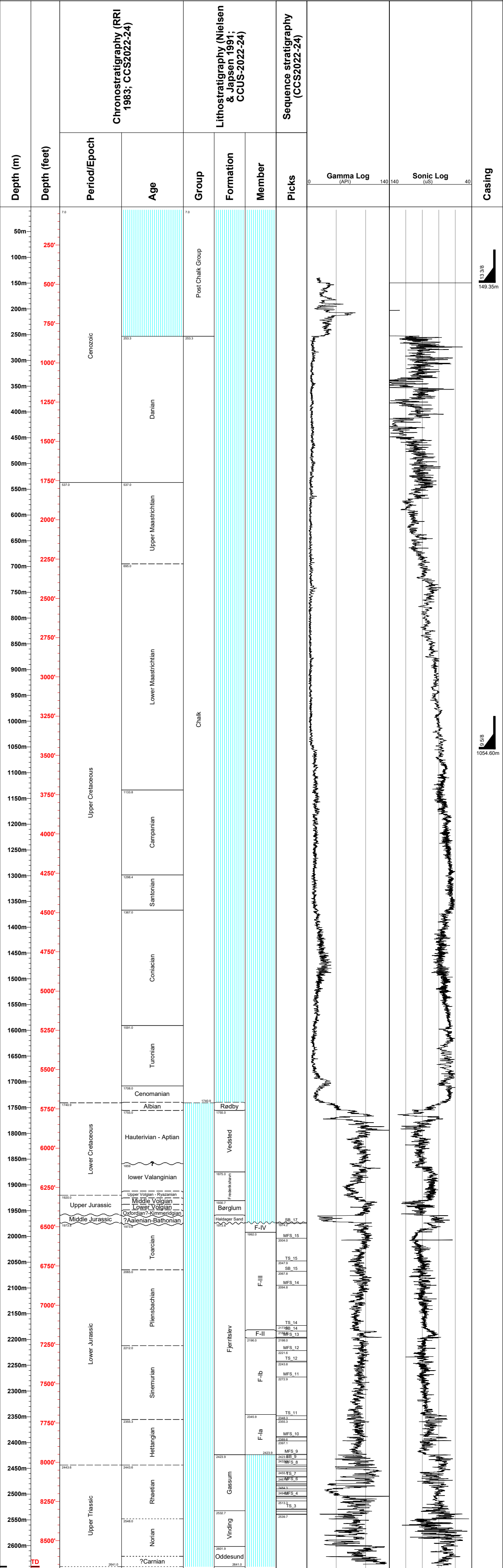
Sorgenfrei, T. and Buch, A. 1964. Deep Tests in Denmark 1935–1959. *Danmarks Geologiske Undersøgelse, Række III, Nr. 36*, 146 pp. <https://doi.org/10.34194/raekke3.v36.6941>

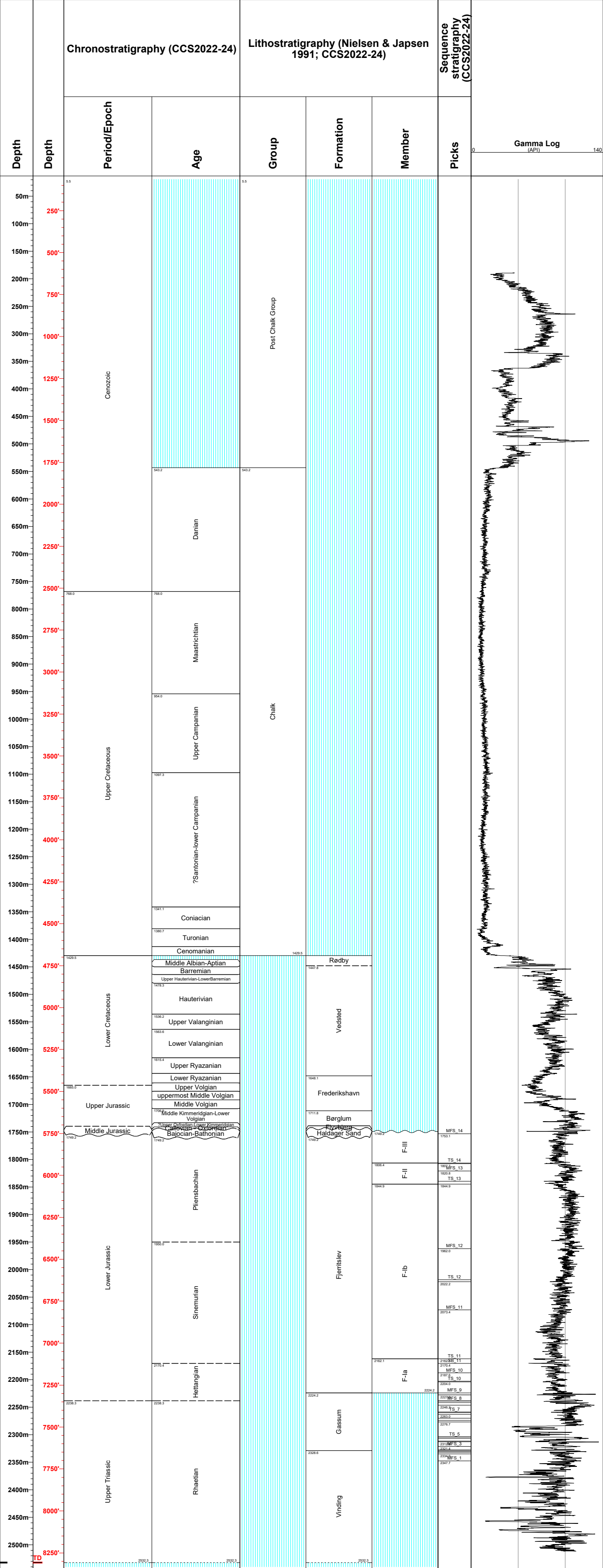


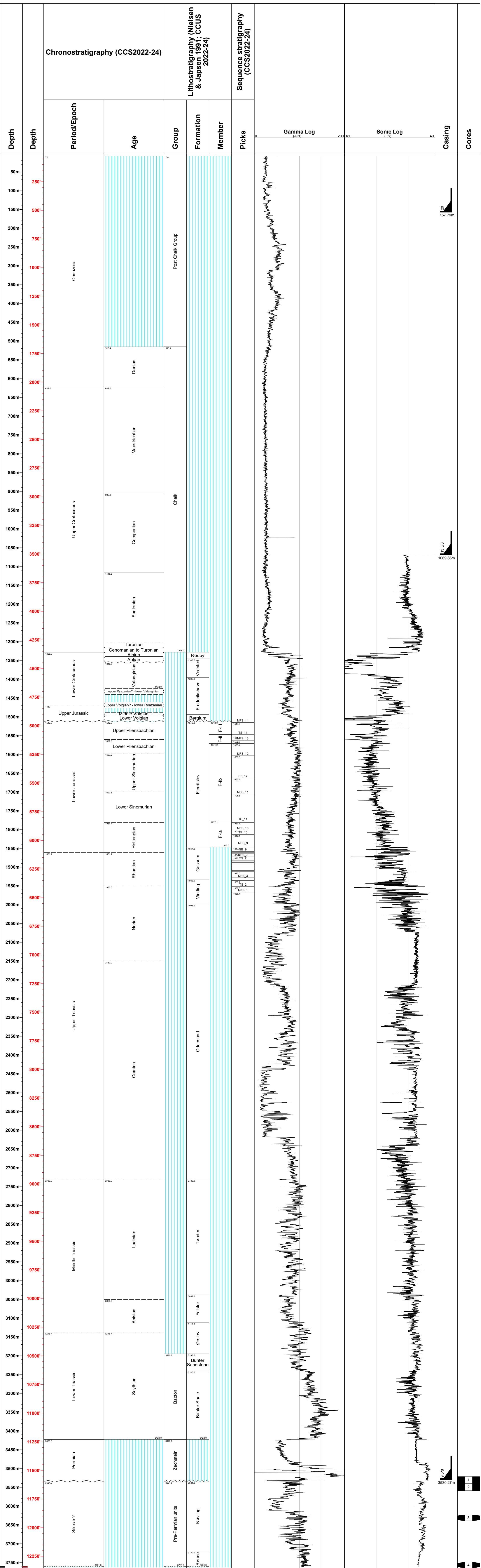


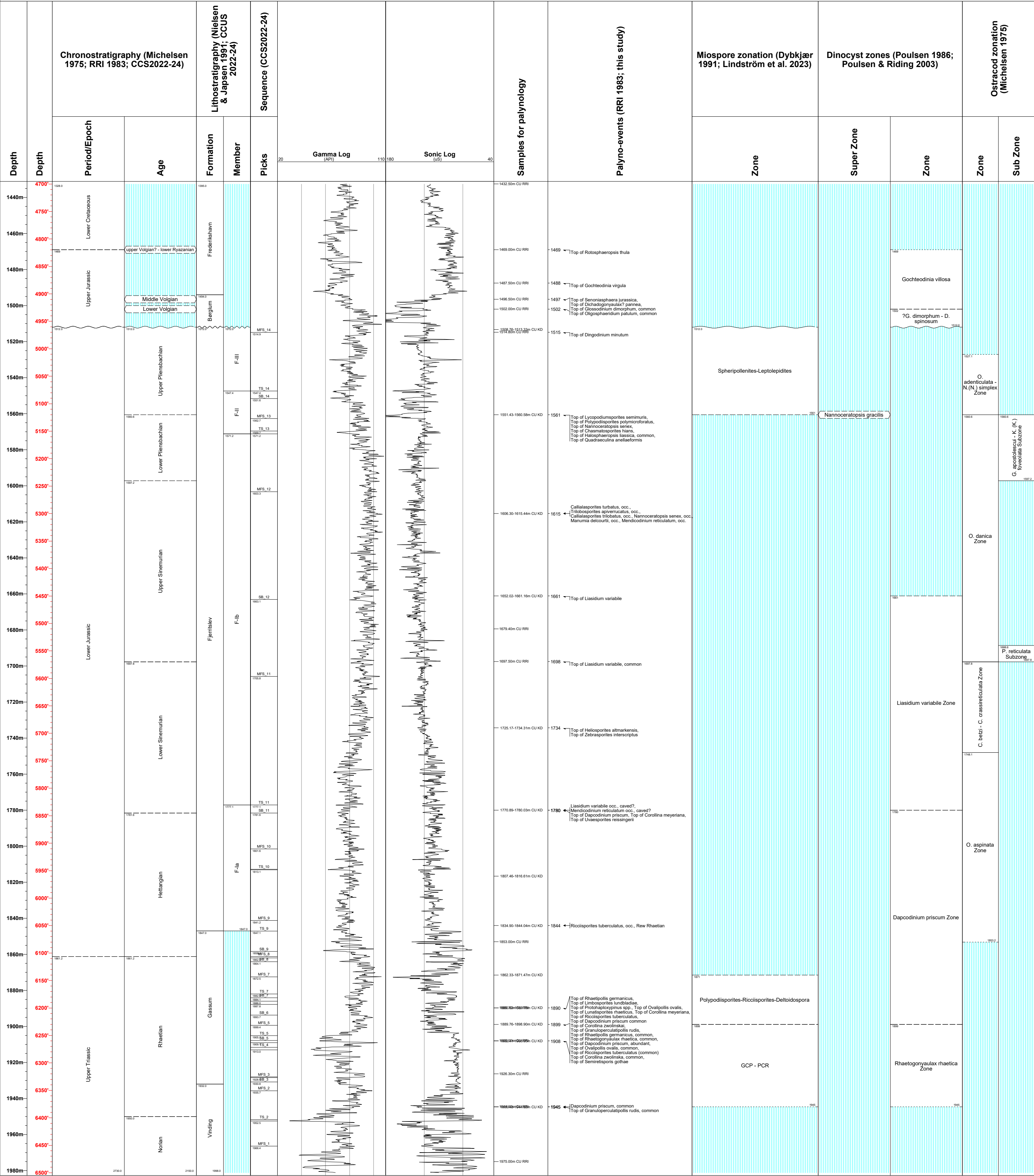


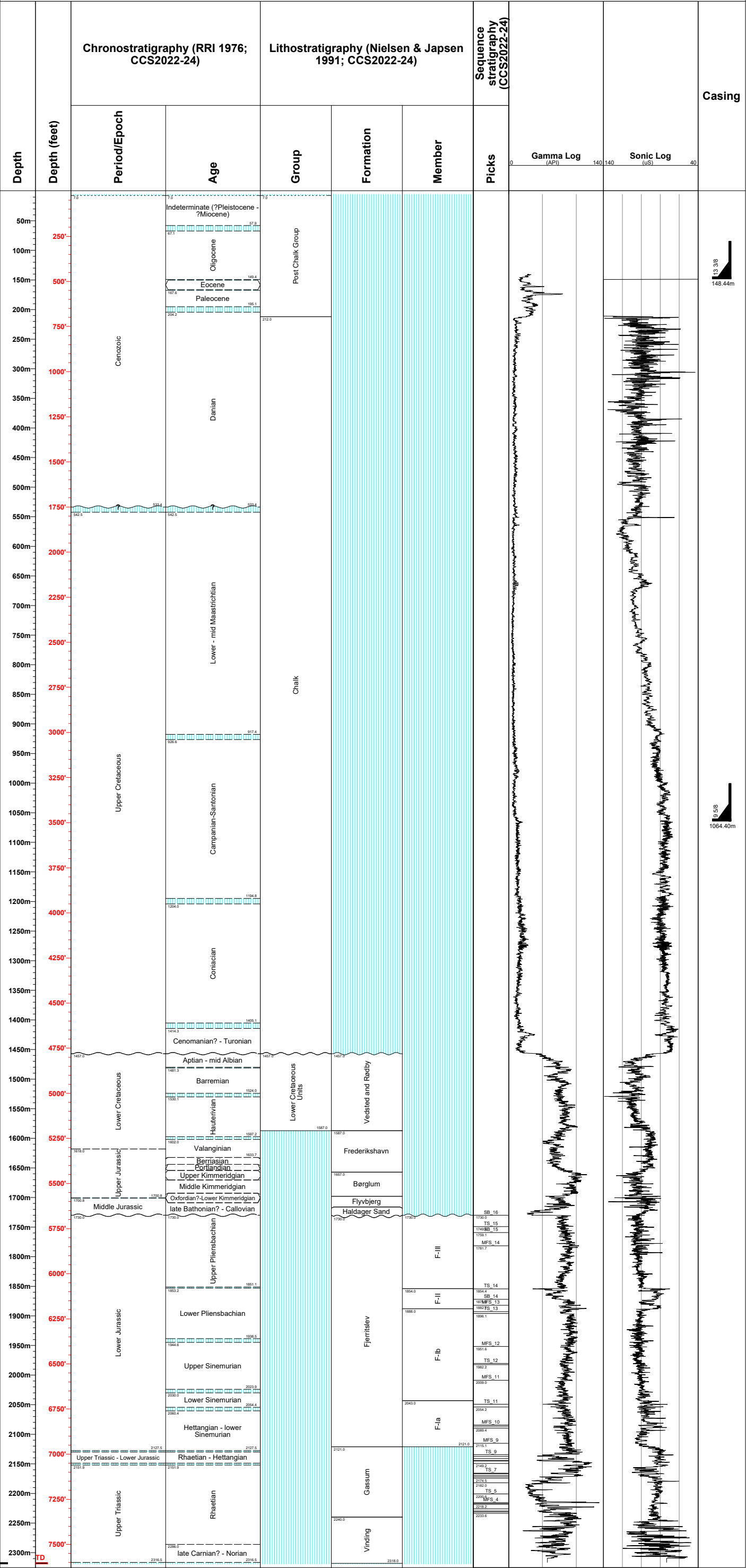






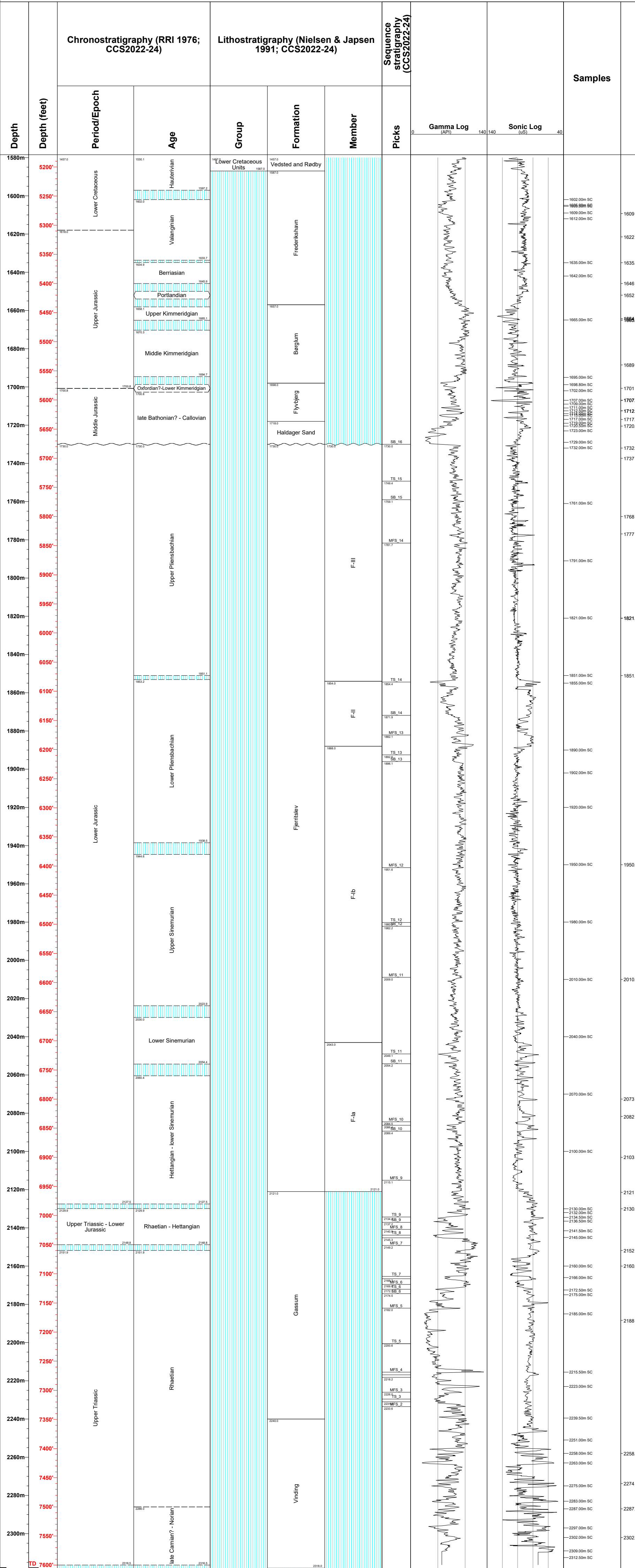


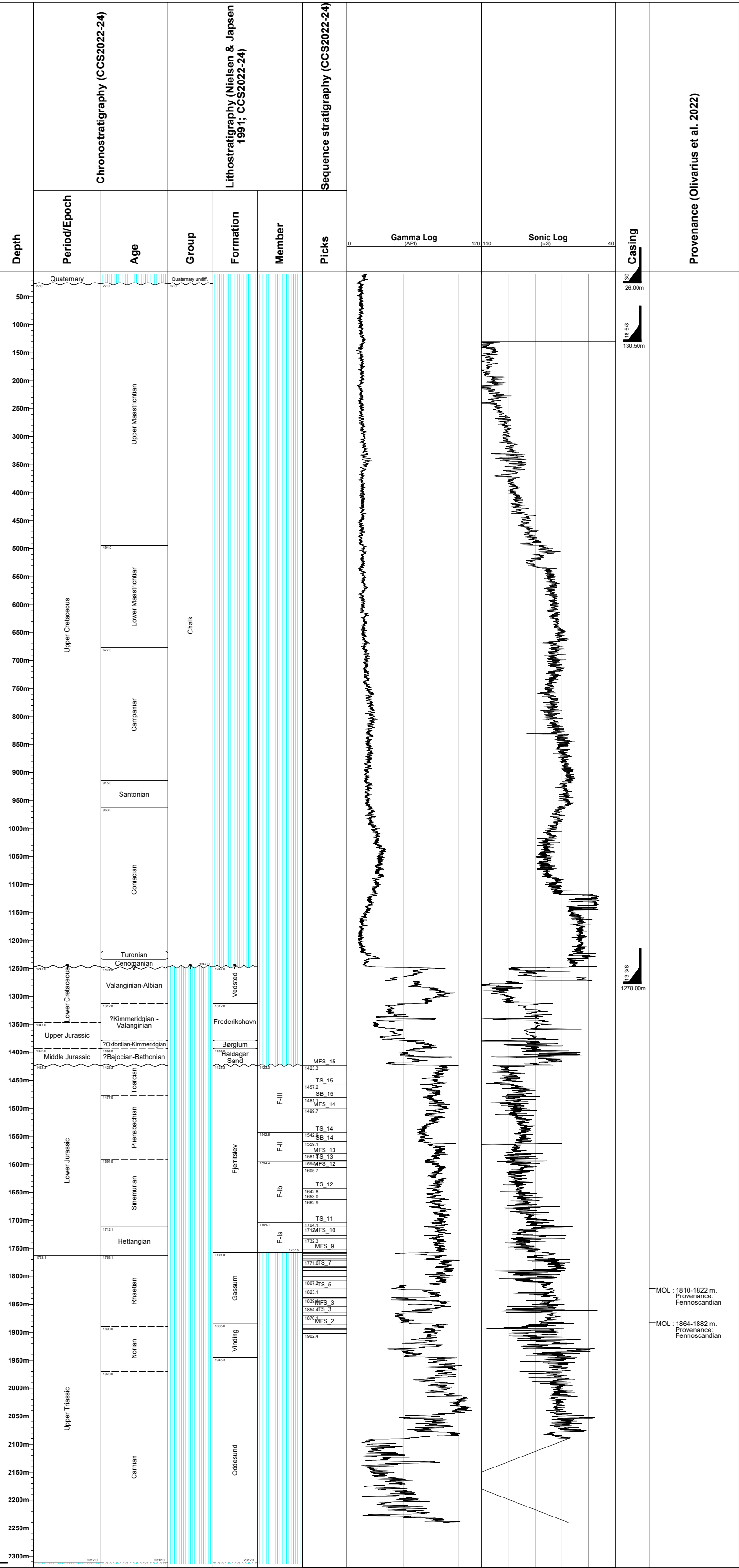




Well Name : Skive-1

Interval : Various
Scale : 1:1000
Chart date : 15 October 2024





1930: